



College of Engineering, Mathematics and Physical Sciences

**A Simulation-Optimization Model to Study the Control of  
Seawater Intrusion in Coastal Aquifers**

Submitted by

**Hany Farhat Abd-Elhamid**

To the University of Exeter as a thesis for the degree of

Doctor of Philosophy in Water Engineering

**December 2010**

This thesis is available for library use on the understanding that it is copyright material and that no quotation from the thesis may be published without proper acknowledgement.

I certify that all material in this thesis which is not my own work has been identified and that no material has previously been submitted and approved for the award of a degree by this or any other university.

*Hany F. Abd-Elhamid*

Dedicated to my family

**A Simulation-Optimization Model to Study the Control of  
Seawater Intrusion in Coastal Aquifers**

Ph.D. in Water Engineering

**University of Exeter**

December 2010



**Advanced Technologies Research Institute**

**Prize for the Best PhD Student at the  
Final Stage 2008/2009**

**Hany Farhat Abdel Hamid**

*In recognition of the best overall PhD student at the final  
stage awarded by the Advanced Technologies Research  
Institute*

Professor K E Evans CEng CPhys  
Head of School

A handwritten signature in black ink, appearing to read "K E Evans", written over a horizontal line.

School of Engineering, Mathematics and Physical Sciences

## ACKNOWLEDGEMENTS

Firstly, I thank my God for giving me the strength and endurance to complete this research.

I would like to express my profound gratitude to my supervisor Dr. Akbar Javadi for his great support, invaluable guidance, continuous encouragement, unlimited help and great efforts he presented to achieve this research project.

Many thanks to all the members of Computational Geomechanics Group for their help and support during my study. Also, I would like to thank all the staff at the College of Engineering, Mathematics and Physical Sciences in Exeter University to all their help during my time in Exeter University.

I also want to thank all the staff of Water and Water Structure Engineering Department, Faculty of Engineering, Zagazig University, Zagazig, Egypt to all their help and support before and during my scholarship and for funding this research.

I wish to express my gratitude to all members of my family (my Mum, brothers and sister) who supported me and encouraged me to continue my work. I am also deeply grateful to my wife for her love, support, prayers, patience, and encouragement during my study. I also want to thank my friends in Egypt for their prayers and their continuous encourage pursuing my goals.

## ***ABSTRACT***

Groundwater contamination is a very serious problem as it leads to the depletion of water resources. Seawater intrusion is a special category of groundwater contamination that threatens the health and possibly lives of many people living in coastal areas. The focus of this work is to develop a numerical model to study seawater intrusion and its effects on groundwater quality and develop a control method to effectively control seawater intrusion. Two major approaches are used in this study: the first approach is the development of a finite element model to simulate seawater intrusion; the second is the development of a simulation-optimization model to study the control of seawater intrusion in coastal aquifers using different management scenarios. The simulation-optimization model is based on the integration of a genetic algorithm optimization technique with the transient density-dependent finite element model developed in this research.

The finite element model considers the coupled flow of air and water and solute transport in saturated and unsaturated soils. The governing differential equations include two mass balance equations of water and air phases and the energy balance equation for heat transfer, together with a balance equation for miscible solute transport. The nonlinear governing differential equations are solved using the finite element method in the space domain and a finite difference scheme in the time domain. A two dimensional finite element model is developed to solve the governing equations and provide values of solute concentration, pore water pressure, pore air pressure and temperature at different points within the region at different times. The mathematical formulation and numerical implementation of the model are presented. The numerical model is validated by application to standard examples from literature followed by application to a number of case studies involving seawater intrusion problems. The results show good agreement with previous results reported in the literature. The model is then used to predict seawater intrusion for a number of real world case studies. The developed model is capable of predicting, with a good accuracy, the intrusion of seawater in coastal aquifers.

In the second approach, a simulation-optimization model is developed to study the control of seawater intrusion using three management scenarios: abstraction of brackish water, recharge of fresh water and combination of abstraction and recharge. The objectives of these management scenarios include minimizing the total costs for construction and operation, minimizing salt concentrations in the aquifer and determining the optimal depths, locations and abstraction/recharge rates for the wells. Also, a new methodology is presented to control seawater intrusion in coastal aquifers. In the proposed methodology ADR (abstraction, desalination and recharge), seawater intrusion is controlled by abstracting brackish water, desalinating it using a small scale reverse osmosis plant and recharging to the aquifer. The simulation-optimization model is applied to a number of case studies. The efficiencies of three different scenarios are examined and compared. Results show that all the three scenarios could be effective in controlling seawater intrusion. However, ADR methodology can result in the lowest cost and salt concentration in aquifers and maximum movement of the transition zone towards the sea. The results also show that for the case studies considered in this work, the amount of abstracted and treated water is about three times the amount required for recharge; therefore the remaining treated water can be used directly for different proposes. The application of ADR methodology is shown to be more efficient and more practical, since it is a cost-effective method to control seawater intrusion in coastal aquifers. This technology can be used for sustainable development of water resources in coastal areas where it provides a new source of treated water. The developed method is regard as an effective tool to control seawater intrusion in coastal aquifers and can be applied in areas where there is a risk of seawater intrusion.

Finally, the developed FE model is applied to study the effects of likely climate change and sea level rise on seawater intrusion in coastal aquifers. The results show that the developed model is capable of predicting the movement of the transition zone considering the effects of sea level rise and over-abstraction. The results also indicate that the change of water level in the sea side has a significant effect on the position of the transition zone especially if the effect of sea level rise is combined with the effect of increasing abstraction from the aquifer.

# TABLE OF CONTENTS

ACKNOWLEDGEMENTS.....	i
ABSTRACT.....	ii
TABLE OF CONTENTS.....	iv
LIST OF FIGURES.....	x
LIST OF TABLES.....	xiii
LIST OF PUBLICATIONS.....	xiv
LIST OF ABBREVIATIONS.....	xvi
LIST OF SYMBOLS .....	xvii
<b>Chapter 1: INTRODUCTION.....</b>	<b>1</b>
1.1 General.....	1
1.2 Groundwater contamination .....	2
1.3 Saltwater intrusion problem.....	4
1.4 Saltwater intrusion control methods.....	5
1.5 Proposed methodology to control saltwater intrusion .....	6
1.6 Effects of climate change and sea level rise on saltwater intrusion .....	7
1.7 Objectives of the study .....	8
1.8 Outline of the thesis .....	9
<b>Chapter 2: SALTWATER INTRUSION INVESTIGATION AND CONTROL</b>	
<b>METHODS.....</b>	<b>11</b>
2.1 Introduction.....	11
2.2 Main causes of saltwater intrusion in coastal aquifers .....	12
2.3 Saltwater intrusion investigation methods.....	13
2.3.1 Geophysical investigations.....	13
2.3.2 Geochemical investigations .....	16
2.3.3 Experimental studies .....	17
2.3.4 Mathematical methods .....	18



2.4 History of saltwater intrusion modelling .....	19
2.4.1 Sharp-interface or diffusive interface models .....	20
2.4.1.1 Sharp-interface models .....	20
2.4.1.2 Diffusive interface models .....	22
2.4.2 Steady-state and transient flow models .....	26
2.4.3 Saturated and unsaturated flow models .....	27
2.4.4 Recent computer codes to simulate saltwater intrusion .....	28
2.5 Saltwater intrusion control methods .....	31
2.5.1 Reduction of pumping rates .....	32
2.5.2 Relocation of pumping wells .....	33
2.5.3 Subsurface barriers .....	35
2.5.4 Natural recharge .....	36
2.5.5 Artificial recharge .....	37
2.5.6 Abstraction of saline water .....	41
2.5.7 Combination techniques .....	42
2.6 A new methodology to control saltwater intrusion (ADR) .....	44
2.6.1 The benefits of ADR methodology .....	45
2.6.2 Desalination of brackish groundwater using RO.....	46
<b>Chapter 3: GOVERNING EQUATIONS OF COUPLED FLUID FLOW AND</b>	
<b>        SOLUTE TRANSPORT .....</b>	<b>50</b>
3.1 Introduction.....	50
3.2 History of coupled fluid flow and solute transport .....	51
3.2.1 Fluid flow in saturated/unsaturated soils .....	51
3.2.2 Energy transport .....	54
3.2.3 Solute transport in saturated/unsaturated soils .....	55
3.2.4 Coupling mechanisms .....	59
3.3 The governing equation for the moisture transfer .....	61
3.3.1 Water flow .....	63
3.3.2 Water vapour flow.....	66
3.3.3 Mass balance equation for the moisture transfer.....	72

3.4 The governing equation for air transfer .....	75
3.5 The governing equation for heat transfer .....	81
3.6 The governing equation for solute transport .....	87
3.6.1 Net rate of solute inflow the control volume .....	88
3.6.1.1 Advection .....	89
3.6.1.2 Diffusion .....	89
3.6.1.3 Mechanical Dispersion .....	90
3.6.2 Net rate of solute production within the control volume .....	92
3.6.3 Governing equation of solute transport in saturated soil .....	94
3.6.4 Governing equation of solute transport in unsaturated soil .....	95
3.7 The governing differential equations .....	98
<b>Chapter 4: NUMERICAL SOLUTION OF GOVERNING EQUATIONS OF COUPLED FLUID FLOW AND SOLUTE TRANSPORT .....</b>	<b>99</b>
4.1 Introduction.....	99
4.2 Solution methods for differential equations .....	99
4.2.1 Analytical methods .....	100
4.2.2 Numerical methods .....	101
4.2.2.1 Finite difference method .....	101
4.2.2.2 Finite element method .....	101
4.3 Numerical solution of the governing equations .....	103
4.3.1 Spatial discretization of the moisture transfer governing equation.....	104
4.3.2 Spatial discretization of the air transfer governing equation.....	110
4.3.3 Spatial discretization of the heat transfer governing equation.....	114
4.3.4 Spatial discretization of the solute transport governing equation.....	119
4.3.4.1 Solute transport in saturated soils .....	119
4.3.4.2 Solute transport in unsaturated soils .....	123
4.3.5 Temporal discretization of the coupled fluid flow and heat transfer .....	127
4.3.6 Temporal discretisation of solute transport .....	129
4.4 Coupling of fluid flow and solute transport equations .....	131

<b>Chapter 5: VALIDATION AND APPLICATION OF THE SIMULATION MODEL.....</b>	<b>133</b>
5.1 Introduction.....	133
5.2 Calibration, validation, and verification of the model. ....	133
5.3 Numerical results. ....	136
5.3.1 Example (1): Transient groundwater flow .....	136
5.3.2 Example (2): Transient solute transport .....	138
5.3.3 Example (3): Saltwater intrusion in confined aquifer (Henry’s problem)...	141
5.3.3.1 Steady-state constant dispersion .....	143
5.3.3.2 Steady-state variable dispersion .....	145
5.3.3.3 Transient constant dispersion .....	146
5.3.3.4 Transient variable dispersion .....	147
5.3.3.5 Effect of variability in dispersion and density of SWI.....	147
5.4 Case studies. ....	149
5.4.1 Case (1): A hypothetical case study .....	149
5.4.2 Case (2): Madras aquifer, India .....	152
5.4.3 Case (3): Biscayne aquifer, Florida, USA .....	154
5.4.4 Case (4): Gaza Aquifer, Palestine .....	157
5.5 Summary. ....	164
<b>Chapter 6: DEVELOPMENT AND APPLICATION OF SIMULATION-OPTIMIZATION MODEL.....</b>	<b>165</b>
6.1 Introduction.....	165
6.2 Optimization techniques .....	166
6.3 Genetic algorithm (GA). ....	168
6.3.1 GA in groundwater management .....	168
6.3.2 GA in water resources management .....	169
6.3.3 GA in seawater intrusion management .....	169
6.4 Simulation-Optimization model .....	173
6.4.1 Simulation model .....	175
6.4.2 Genetic Algorithm Optimization model .....	177

6.4.3 Integration of the simulation and optimization models .....	178
6.5 Formulation of the management models .....	181
6.5.1 Management model 1: (Abstraction wells) .....	182
6.5.2 Management model 2: (Recharge wells) .....	184
6.5.3 Management model 3: (Abstraction and Recharge wells).....	185
6.6 Application of the simulation-optimization model .....	186
6.6.1 A hypothetical case study (Henry’s problem) .....	186
6.6.1.1 Application of management model 1 .....	189
6.6.1.2 Application of management model 2 .....	190
6.6.1.3 Application of management model 3 .....	190
6.6.1.4 Discussion .....	192
6.6.2 Real world case study (Biscayne aquifer, Florida, USA) .....	194
6.6.2.1 Application of management model 1 .....	197
6.6.2.2 Application of management model 2 .....	197
6.6.2.3 Application of management model 3 .....	197
6.6.2.4 Discussion .....	199
6.7 Summary .....	200
<b>Chapter 7: EFFECT OF CLIMATE CHANGE AND SEA LEVEL RISE ON</b>	
<b>    SALTWATER INTRUSION .....</b>	<b>202</b>
7.1 Introduction.....	202
7.2 Climate change. ....	203
7.3 Sea level rise. ....	205
7.3.1 Effects of sea level rise on coastal areas.....	206
7.3.1.1 Erosion and inundation .....	208
7.3.1.2 Saltwater intrusion .....	209
7.3.2 Methods of controlling the effects of sea level rise on coastal areas .....	210
7.3.2.1 Control of erosion and inundation .....	210
7.3.2.2 Control of saltwater intrusion .....	211
7.4 Simulation of saltwater intrusion considering sea level rise .....	212
7.5 Application of SUFT to investigate the effect of sea level rise .....	213
7.5.1 Case (1): A hypothetical case study .....	213

7.5.2 Case (2): Biscayne aquifer, Florida, USA .....	216
7.5.3 Case (3): Gaza Aquifer, Palestine .....	219
7.6 Summary .....	222
<b>Chapter 8: CONCLUSIONS AND RECOMMENDATIONS .....</b>	<b>223</b>
8.1 Conclusions.....	223
8.2 Recommendations for future work .....	225
<b>REFERENCES .....</b>	<b>226</b>

## LIST OF FIGURES

<b>Figure 1.1</b>	Schematic diagram of hydrologic cycle.....	1
<b>Figure 1.2</b>	Main groundwater contaminant pathways and sources.....	3
<b>Figure 1.3</b>	A cross section with interface under natural conditions.....	4
<b>Figure 1.4</b>	The proposed methodology (ADR) to control saltwater intrusion.....	6
<b>Figure 2.1</b>	Hydrostatic equilibrium between fresh and saline water.....	21
<b>Figure 2.2</b>	Location of transition zone.....	23
<b>Figure 2.3</b>	Sketch for subsurface barrier.....	35
<b>Figure 2.4</b>	Sketch for natural recharge process.....	36
<b>Figure 2.5</b>	Sketch of recharge and abstraction wells.....	38
<b>Figure 2.6</b>	Sketch of the new methodology ADR .....	44
<b>Figure 2.7</b>	Schematic sketch layout of RO desalination plant.....	48
<b>Figure 3.1</b>	Control volume of solute transport through porous media.....	88
<b>Figure 4.1</b>	Summary of the solution methods for differential equations.....	100
<b>Figure 5.1</b>	Boundary and initial conditions of example (1) .....	137
<b>Figure 5.2</b>	Head distribution at different times in the reservoir.....	137
<b>Figure 5.3</b>	Comparison between the current model and Wang and Anderson results for head distribution in the reservoir.....	138
<b>Figure 5.4</b>	Boundary and initial conditions of example (2) .....	139
<b>Figure 5.5</b>	Solute concentrations distribution at different times in the reservoir.....	139
<b>Figure 5.6</b>	Comparison between the current model and Wang and Anderson results for solute concentrations distribution in the reservoir.....	140
<b>Figure 5.7</b>	Boundary conditions of Henry's problem.....	141
<b>Figure 5.8</b>	0.5 Isochlor for steady-state constant dispersion ( $D = 6.6 \times 10^{-6}$ ) .....	144
<b>Figure 5.9</b>	0.5 Isochlor for steady-state constant dispersion ( $D = 2.31 \times 10^{-6}$ ) .....	144
<b>Figure 5.10</b>	0.5 Isochlor for steady-state variable dispersion.....	145
<b>Figure 5.11</b>	0.5 Isochlor for transient constant dispersion.....	146
<b>Figure 5.12</b>	0.5 Isochlor for transient variable dispersion.....	147
<b>Figure 5.13</b>	0.5 Isochlor for constant and variable dispersion coefficient.....	148

<b>Figure 5.14</b> 0.5 Isochlor for constant and variable density.....	148
<b>Figure 5.15</b> Problem description of unconfined coastal aquifer with fresh water channel at land side.....	150
<b>Figure 5.16</b> Boundary conditions of the hypothetical case.....	151
<b>Figure 5.17</b> 0.5, 0.25, 0.1, 0.05 and 0.005 Isochlor contours of the hypothetical case....	151
<b>Figure 5.18</b> Boundary conditions of Madras aquifer.....	153
<b>Figure 5.19</b> 35, 17.5, 10, 5 and 2.0 equi-concentration lines in Madras aquifer.....	154
<b>Figure 5.20</b> Schematic sketch and boundary conditions of Biscayne aquifer, Florida....	155
<b>Figure 5.21</b> 1, 0.75, 0.5 and 0.25 isochlor counters in Biscayne aquifer, Florida.....	156
<b>Figure 5.22</b> Location map of Gaza strip.....	157
<b>Figure 5.23</b> Isolines of TDS concentration ( $\text{kg/m}^3$ ) calculated by (SUFT) along Jabalya .....	160
<b>Figure 5.24</b> Isolines of TDS concentration ( $\text{kg/m}^3$ ) calculated by (SUFT) along Wadi Gaza.....	160
<b>Figure 5.25</b> Isolines of TDS concentration ( $\text{kg/m}^3$ ) calculated by (SUFT) along Khan Yunis .....	161
<b>Figure 5.26</b> Isolines of TDS concentration ( $\text{kg/m}^3$ ) calculated by SEAWAT along Khan Yunis (Qahman and Larabi, 2006).....	162
<b>Figure 5.27</b> Isolines of TDS concentration ( $\text{kg/m}^3$ ) calculated by SEAWAT along Jabalya (Qahman and Larabi, 2006) .....	162
<b>Figure 5.28</b> Extant of TDS concentration calculated by SEAWAT (Qahman and Larabi, 2006).....	163
<b>Figure 6.1</b> Flow chart of the solution algorithm.....	176
<b>Figure 6.2</b> Flowchart for the genetic algorithm.....	179
<b>Figure 6.3</b> Flow chart of the schematic steps of the simulation-optimization model.....	180
<b>Figure 6.4</b> Schematic sketch for potential locations and depths for the abstraction and recharge wells.....	181
<b>Figure 6.5</b> 0.5 isochlor for the hypothetical case study.....	187
<b>Figure 6.6</b> Schematic sketch for potential locations and depths for the abstraction and recharge wells of the hypothetical case study.....	187
<b>Figure 6.7</b> 0.5 isochlor distribution from simulation-optimization models for the hypothetical case.....	191

<b>Figure 6.8</b> Comparison between total costs of model 1, 2 and 3 for the hypothetical case study.....	193
<b>Figure 6.9</b> Comparison between total salt concentrations remaining in the aquifer of model 1, 2 and 3 for the hypothetical case study.....	193
<b>Figure 6.10</b> Comparison between total abstraction/recharge rates of model 1, 2 and 3 for the hypothetical case study.....	194
<b>Figure 6.11</b> Isochlor counters in Biscayne aquifer, Florida.....	195
<b>Figure 6.12</b> Schematic sketch for potential locations and depths for the abstraction and recharge wells of Biscayne aquifer, Florida.....	195
<b>Figure 6.13</b> 0.5 isochlor distribution from simulation-optimization models for Biscayne aquifer, Florida.....	198
<b>Figure 6.14</b> Comparison between total costs of model 1, 2 and 3 for Biscayne aquifer, Florida.....	199
<b>Figure 6.15</b> Comparison between total salt concentrations remaining in the aquifer of model 1, 2 and 3 for Biscayne aquifer, Florida.....	199
<b>Figure 6.16</b> Comparison between total abstraction/recharge rates of model 1, 2 and 3 for Biscayne aquifer, Florida.....	200
<b>Figure 7.1</b> Scenarios for estimating average global temperature of earth (IPCC, 2001)...	204
<b>Figure 7.2</b> Scenarios for estimating global average sea level rise (IPCC, 2001).....	206
<b>Figure 7.3</b> Effect of sea level rise on abstraction wells.....	207
<b>Figure 7.4</b> The relationship between sea level rise and saltwater intrusion.....	210
<b>Figure 7.5</b> 0.5 isochlor for the hypothetical case study (no SLR) .....	214
<b>Figure 7.6</b> 0.5 isochlor for the hypothetical case study (with SLR) .....	215
<b>Figure 7.7</b> Isochlor contours in Biscayne aquifer, Florida (no SLR) .....	216
<b>Figure 7.8</b> Isochlor contours in Biscayne aquifer, Florida (with SLR, 50, 100 year).....	217
<b>Figure 7.9</b> 0.5 Isochlor contours in Biscayne aquifer, Florida using three scenarios.....	218
<b>Figure 7.10</b> Isolines of TDS concentration ( $\text{kg}/\text{m}^3$ ) along Jabalya (no SLR).....	219
<b>Figure 7.11</b> Isolines of TDS concentration ( $\text{kg}/\text{m}^3$ ) along Jabalya (Scenario 1).....	220
<b>Figure 7.12</b> Isolines of TDS concentration ( $\text{kg}/\text{m}^3$ ) along Jabalya (Scenario 2).....	221
<b>Figure 7.13</b> Isolines of TDS concentration ( $\text{kg}/\text{m}^3$ ) along Jabalya (Scenario 3).....	221



## LIST OF TABLES

<b>Table 2.1</b> The water type based on TDS content .....	13
<b>Table 5.1</b> The parameters used in Henry’s problem.....	142
<b>Table 6.1</b> Summary of the upper and lower constraints for the hypothetical case study..	188
<b>Table 6.2</b> Summary of the values of cost.....	189
<b>Table 6.3</b> Summary of the results obtained from the simulation-optimization models for the hypothetical case study.....	191
<b>Table 6.4</b> Summary of the upper and lower of constraints for Biscayne aquifer, Florida .....	196
<b>Table 6.5</b> Summary of the results obtained from the simulation-optimization models for Biscayne aquifer, Florida.....	198

## LIST OF PUBLICATIONS

These publications were completed during the author's period of registration to the higher degree program.

### **Refereed Journals**

- H. F. Abd-Elhamid and A. A. Javadi (2010). "A Cost-effective Method to Control Seawater Intrusion in Coastal Aquifers", *Journal of Water Resources Management* (in press).
- A.A. Javadi, H. F. Abd-Elhamid and R. Farmani (2010). "A Simulation-Optimization Model to Control Seawater Intrusion in Coastal Aquifers Using Abstraction/Recharge Wells", *International Journal for Numerical and Analytical Methods in Geomechanics* (in press).
- H. F. Abd-Elhamid and A. A. Javadi (2010). "Impact of Sea Level Rise and Over-pumping on Seawater Intrusion in Coastal Aquifers", *Journal of Water and Climate Change* (in press).
- H. F. Abd-Elhamid and A. A. Javadi (2010). "A Density-Dependant Finite Element Model for Analysis of Saltwater Intrusion in Coastal Aquifers", *Journal of Hydrology* (in press).
- H. F. Abd-Elhamid and A. A. Javadi (2009). "Effects of climate change and saltwater on coastal cities", *Climate change, Barcelona Metropolis, Spain, No.75*, pp: 78-80.

## **Refereed Conferences**

- A.A. Javadi and H.F. Abd-Elhamid (2010). “Optimal Management of Groundwater Resources in Coastal Aquifers Subjected to Seawater Intrusion”, Proceeding of (ISMAR7), Oct 9-13 Abu Dubai, UAE.
- H.F. Abd-Elhamid and A.A. Javadi (2010). “A Simulation-Optimization Model to Study the Control of Seawater Intrusion in Coastal Aquifers Using ADR Methodology”, Proceeding of 21<sup>st</sup> SWIM, June 21-26, 2010, Azores, Prtugal.
- H.F. Abd-Elhamid and A.A. Javadi (2008b). “An investigation into control of saltwater intrusion considering the effects of climate change and sea level rise”, Proceeding of 20<sup>th</sup> SWIM, June 23-27, 2008, Naples, Florida, USA.
- A.A. Javadi and H.F. Abd-Elhamid (2008). “A New Methodology to Control Saltwater Intrusion into Coastal Aquifers” Proceeding of first national seminar of geotechnical problems of irrigation and drainage networks, May 2008, Tehran, Iran.
- H.F. Abd-Elhamid and A.A. Javadi (2008a). “Mathematical models to control saltwater intrusion in coastal aquifer”, Proceeding of GeoCongress 2008, March 9-12, 2008, New Orleans, Louisiana, USA.

## LIST OF ABBREVIATIONS

ADR	Abstraction, Desalination and Recharge
ANN	Artificial Neural Network
FE	Finite Element
FED	Finite Difference Method
FEM	Finite Element Method
FVUM	Finite Volume Unstructured Mesh
GA	Genetic Algorithm
GIS	Geographic Information System
IPCC	Intergovernmental Panel on Climate Change
NE	Number of Elements
NN	Number of Nodes
RO	Reverse Osmosis
SEWAT	Simulation of Three-Dimensional Variable-Density Ground-Water Flow and Transport
S/O	Simulation/Optimization
SLR	Sea Level Rise
SUFT	Saturated/Unsaturated Fluid flow and solute Transport
SUTRA	Saturated-Unsaturated Variable-Density Ground-Water Flow with Solute or Energy Transport
SWI	Saltwater Intrusion
TDS	Total Dissolved Solids

## LIST OF SYMBOLS

$c$	Solute Concentration
$C_r$	Courant number
$C_{ps}$	Specific heat capacities of solid particles
$C_{pw}$	Specific heat capacities of water
$C_{pv}$	Specific heat capacities of vapour
$C_{pda}$	Specific heat capacities of dry air
$C_A$	Cost of abstraction
$C_T$	Cost of treatment
$C_{DW}$	Cost of installation/drilling of well
$C_R$	Cost of recharge
$C_{PW}$	Price of water
$D_{atms}$	Molecular diffusivity of vapour through air
$D_m$	Molecular diffusion coefficient in the porous medium
$D_{m_a}$	Coefficient of air molecular diffusion
$D_{mo}$	Molecular diffusion coefficient in aqueous solution
$D_A$	Depth of abstraction well
$D_R$	Depth of recharge well
$e$	Void ratio
$F$	Source or sink term
$f$	Objective function
$g$	Gravitational acceleration
$H$	Henry's constant
$H_a$	Henry's volumetric coefficient of solubility
$H_c$	Heat capacity of the soil at the reference temperature
$h$	Relative humidity
$h_w$	Hydraulic head

$h_s$	Depth of interface below mean sea level
$h_f$	Height of the potentiometric surface above the mean sea level
$i$	Iteration number
$K_w$	Hydraulic conductivity of water
$K_a$	Unsaturated conductivity of air
$k_a$	Effective permeability of air
$k_w$	Effective permeability of water
$k_f$	Constant for the forward reaction
$k_r$	Constant for reverse reaction
$k_d$	Equilibrium distribution coefficient
$L$	Latent heat of vaporisation
$N$	Shape function
$n$	Porosity
$P_e$	Peclet Number
$Q$	Heat flux per unit area
$Q_A$	Abstraction rate
$Q_R$	Recharge rate
$R$	Retardation factor
$R_v$	Specific gas constant for water vapour
$R_{\Omega w}$	Residual error introduced by the approximation functions
$R_{\Omega a}$	Residual errors introduced by the approximation functions
$R_{\Omega T}$	Residual error introduced by the approximation functions
$R_{\Omega c}$	Residual errors introduced by the approximation function
$R_{da}$	Specific gas constant of dry air
$S$	Salinity
$s$	Suction
$S_a$	Degree of air saturation in unsaturated soil
$S_w$	Degree of water saturation in unsaturated soil

List of symbols

---

$s_r$	Suction at the reference temperature
$T$	Absolute temperature
$T_r$	Reference temperature
$t$	Time step
$u_w$	Pore water pressure
$u_a$	Pore air pressure
$u_v$	Pore water vapour pressure
$u_{da}$	Pore dry air pressure
$v_w$	Velocity of water
$v_a$	Velocity of the air
$v_v$	Velocity of the water vapour
$\bar{v}_{w_x}$	Component of the pore water velocity in x direction
$\bar{v}_{w_y}$	Component of the pore water velocity in y direction
$ v $	Magnitude of the water velocity
$\bar{v}_{a_x}$	Component of the pore air velocity in x direction
$\bar{v}_{a_y}$	Component of the pore air velocity in y direction
$ v $	Magnitude of the air velocity
$\hat{v}_{wn}$	Approximation of water velocity normal to the boundary surface
$\hat{v}_{vd}$	Approximation of diffusive vapour velocity normal to the boundary surface
$\hat{v}_{va}$	Approximation of pressure vapour velocity normal to the boundary surface
$\hat{v}_{fn}$	Approximation of velocity of free dry air
$\hat{v}_{an}$	Approximation of velocity of dissolved dry air
$V_v$	Mass flow factor
$z$	Elevation above the datum (positive upwards)
$\nabla z$	The unit normal oriented downwards in the direction of the force of gravity
$\rho_s$	Saltwater density
$\rho_f$	Freshwater density

$\rho_w$	Density of water
$\rho_a$	Density of air
$\rho_v$	Density of water vapour
$\nabla\rho_v$	Vapour density gradient
$\rho_b$	Bulk density of the porous media
$\rho_0$	Saturated soil vapour density
$\rho_{da}$	Density of dry air
$\rho_s$	Density of solid particles
$\gamma_w$	Unit weight of water
$\mu_w$	Dynamic viscosity of water
$\mu_a$	Absolute viscosity of air
$\theta$	Volumetric moisture content in unsaturated soil
$\theta_w$	Volumetric water content
$\theta_a$	Volumetric air content
$\theta_v$	Volumetric vapour content
$\theta_s$	Saturated volumetric water content
$\xi_r$	Surface energy at the reference temperature
$\xi$	Surface energy at the given temperature $T$
$\alpha_{T_w}$	Transverse dispersivity for water phase
$\alpha_{L_w}$	Longitudinal dispersivity for water phase
$\alpha_{T_a}$	Transverse dispersivity for air phase
$\alpha_{L_a}$	Longitudinal dispersivity for air phase
$\chi_w$	The thermal conductivity of water
$\chi_a$	Thermal conductivity of air
$\chi_v$	Thermal conductivity of vapour
$\chi_T$	Intrinsic thermal conductivity of soil
$\tau_v$	Vapour tortuosity factor



*List of symbols*

---

$\psi$	Capillary potential
$\Omega$	Domain region
$\Omega^e$	Element domain
$\omega$	An empirical correction factor
$\lambda$	Decay constant for the solute
$\Gamma^e$	Element boundary surface

## Introduction

### 1.1 General

Groundwater is a far more important resource than is often realized. It represents about 22 percent of all fresh water on the earth; polar ice represents 77 percent while other freshwater in rivers and lakes represent about 0.3 percent (Bear et al., 1999). Groundwater constitutes an important water resource, supplying water for domestic, industry and agriculture. One-third of the world's drinking water is provided by groundwater. But as it is often the case with critical resources, groundwater is not always available when and where needed, especially in water-short areas where heavy use has depleted underground reserves. Groundwater or subsurface water is a term used to denote all the waters found beneath the surface of the ground and is considered as part of the hydrologic cycle (Figure 1.1).

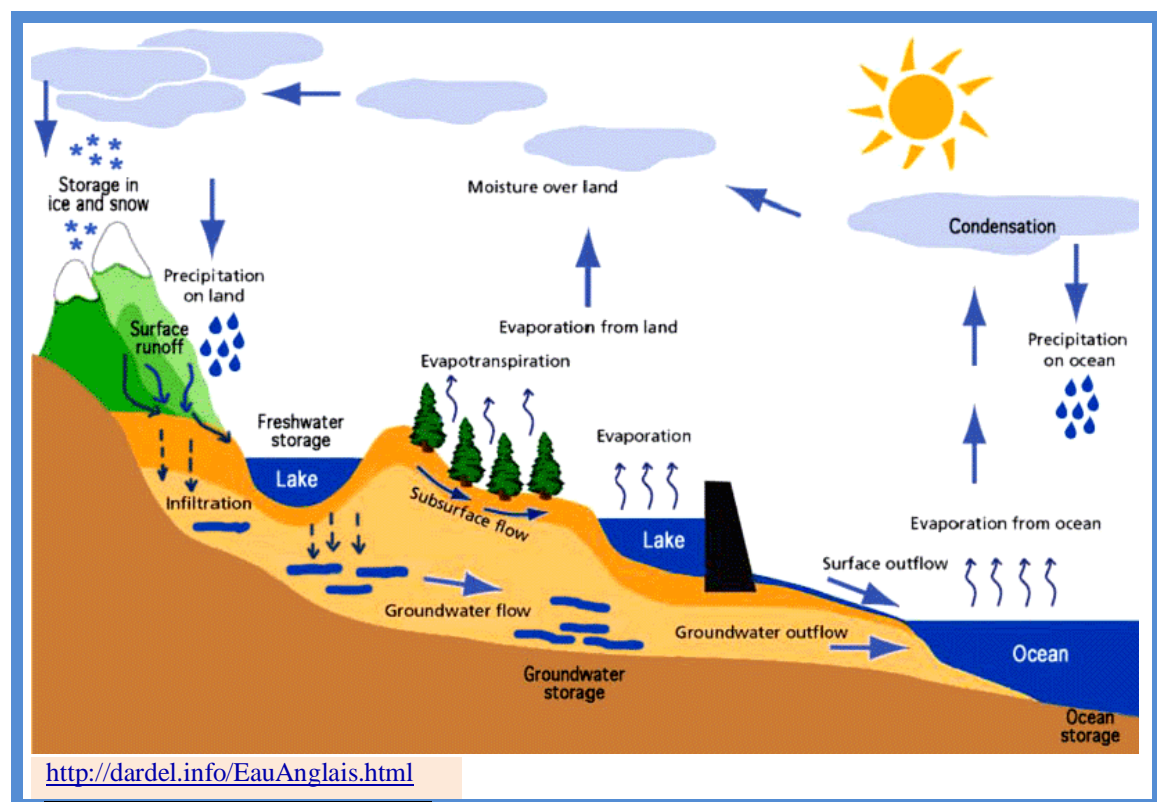


Figure 1.1 Schematic diagram of hydrologic cycle

Population growth and continuous development require large quantities of water. It is a great challenge to secure water demand, while the available water resources are nearly constant. This requires protecting available resources from pollution including saltwater intrusion and other contaminants, which deplete the current resources. The concentrations of people in the coastal regions and the increased related activities have led to an increase in the abstraction of groundwater reserves. Over-abstraction from coastal aquifers has led to the movement of saltwater toward aquifers and increased the salinity of groundwater. High salinity of groundwater limits its usage for irrigation and drinking purposes unless desalinated or mixed with lower salinity water. The protection of groundwater resources becomes an essential matter under the conditions of increasing demands and decreasing the available resources.

## ***1.2 Groundwater contamination***

Groundwater quality is an important issue in the development and management of water resources. In fact, with the increasing demand for water in most parts of the world and with the intensification of water utilization, the quality problem becomes the limiting factor in the development and management of water resources in many parts of the world. The quality of both surface and groundwater resources deteriorates as a result of pollution. Special attention should be devoted to the pollution of aquifers. Although it seems that groundwater is more protected than surface water against pollution, it is still subject to pollution; and when this occurs restoration to the original (non-polluted state) is very difficult and costly. Groundwater pollution is usually traced back to four sources (Bear, 1979):

- 1- ***Environmental***: this type of pollution is due to the characteristics of the environment through which the flow of groundwater takes place. For example, flow through carbonate rock, seawater intrusion and invasion by brackish water from adjacent aquifer.
- 2- ***Domestic***: domestic pollution may be caused by accidental breaking of sewers, percolation from septic tanks, rain infiltrating through sanitary landfills, acid rains, artificial recharge using sewage water after being treated to different levels and biological contaminants (e.g., bacteria and viruses).

- 3- **Industrial:** industrial pollution may come from sewage disposal, which contains heavy metals, non-deteriorating compounds and radioactive materials.
- 4- **Agriculture:** this is due to irrigation water and rain water dissolving and carrying fertilizers, salts, herbicides, pesticides, etc., as they infiltrate through the ground surface and replenish the aquifer.

The main pathways and sources of groundwater pollutants are shown in Figure 1.2.

<http://www.euwfd.com/html/groundwater.html>

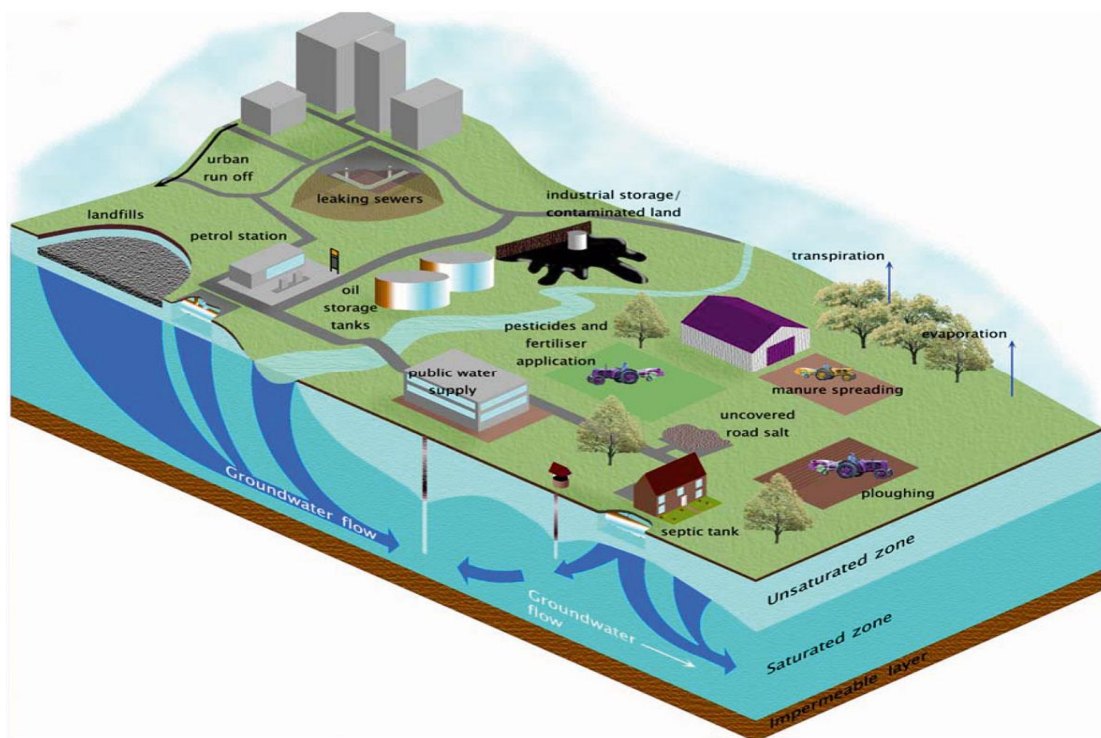


**Figure 1.2** Main groundwater contaminant pathways and sources

Saltwater intrusion is one of the most wide-spread and important processes that degrades groundwater quality by raising salinity to levels exceeding acceptable drinking water and irrigation standards, and endangers future exploitation of coastal aquifers. Salinization of groundwater is considered one of the main sources of pollution. The sources of groundwater salinization include: infiltration of saline wastes, return flow from agriculture, evapotranspiration and seawater intrusion.

### 1.3 Saltwater intrusion problem

Coastal zones are among the most densely populated areas in the world with over 70% of the world's population. These regions face serious hydrological problems such as: scarcity of fresh water, contamination of groundwater and seawater intrusion. The growing in global population and raising standards of living have increased water demands and pumping from aquifers. Excessive pumping has led to a dramatic increase in saltwater intrusion problems. In coastal aquifers a hydraulic gradient exists toward the sea which leads to flow of the excess fresh water to the sea. Owing to the presence of seawater in the aquifer formation under the sea bottom, a zone of contact is formed between the lighter freshwater flowing to the sea and the heavier, underlying, seawater (Figure 1.3). Fresh water and seawater are actually miscible fluids and therefore the zone of contact between them takes the form of a transition zone caused by hydrodynamic dispersion. Across this zone, the density of the mixed water varies between that of fresh water to that of seawater. Under certain conditions the width of this zone is relatively small, when compared with the thickness of the aquifer, so that the boundary can be considered as a sharp interface that separates the two regions occupied by the two fluids, in this case the two fluids are assumed to be immiscible. But, if the transition zone is wide this assumption becomes invalid (Bear, 1979).

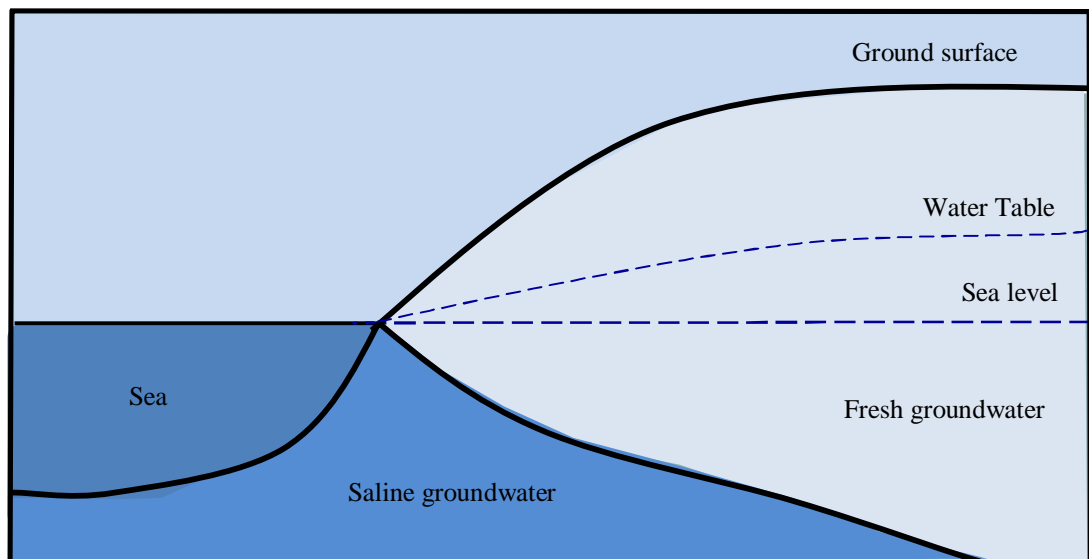


**Figure 1.3** A cross section with interface under natural conditions

Under natural undisturbed conditions in a coastal aquifer, fresh water flows to the sea. By excessive pumping from a coastal aquifer, the water table or piezometric surface could be lowered to the extent that the piezometric head in the fresh water body becomes less than in the adjacent seawater wedge, and the interface could start to advance inland until a new equilibrium is reached. This phenomenon is called seawater intrusion or encroachment. As the interface advances, the transition zone widens. When the interface reaches the inland pumping well, the well becomes contaminated. When the pumping takes place in a well located above the interface, upconing towards the pumping well could occur. Unless the rate of pumping is carefully controlled, seawater will eventually enter the pumped well and the wells may be abandoned. Seawater intrusion leads to the depletion of groundwater resources. Mathematical models can help in understanding the mechanism of saltwater intrusion in coastal aquifers. Coupled fluid flow and solute transport models have been used to simulate saltwater intrusion and to predict the solute concentrations in coastal aquifers. These models can be used to investigate movement and extension of saltwater into coastal aquifers.

#### ***1.4 Saltwater intrusion control methods***

A number of methods have been used to control seawater intrusion to protect groundwater reserves in coastal aquifers. Todd (1974) presented various methods of preventing seawater from contaminating groundwater sources including: reduction of abstraction rates, relocation of abstraction wells, subsurface barriers, natural recharge, artificial recharge, and abstraction of saline water. Extensive research has been carried out to investigate saltwater intrusion in coastal aquifers. However, only few models have been developed to study the control of saltwater intrusion. These models use one or more of the previous measures to study the control of saltwater intrusion. Many limitations of the previous methods have been reported in the literature such as: the source and the cost of fresh water and applicability of such methods (Abd-Elhamid and Javadi, 2008a). Until now there is no complete solution for this problem that can effectively control saltwater intrusion. The main goal of this study is to present a new saltwater intrusion control method that overcomes most, if not all the limitations of previous methods and take into consideration different parameters including: technical, economical and environmental aspects.

### 1.5 Proposed methodology to control saltwater intrusion

In this study a new methodology is proposed to study the control of saltwater intrusion. This methodology aims to overcome the limitations of the previous methods. The proposed methodology ADR (Abstraction, Desalination and Recharge) consists of three steps; abstraction of brackish water from the saline zone, desalination of the abstracted brackish water using reverse osmosis RO treatment process, and recharge of the treated water into the aquifer (Figure 1.4). The main benefits of the ADR methodology are to return the mixing zone into the original status and to reach a dynamic balance between fresh and saline groundwater through two processes; abstraction of brackish groundwater to reduce the volume of saline water and recharge of the treated brackish water to increase the volume of fresh groundwater. The abstraction-recharge process helps to shift fresh water/saltwater interface towards the sea and is considered an efficient method to retard saltwater intrusion (Rastogi et al., 2004 and Mahesha, 1996c). The abstraction-recharge process continues until a state of dynamic equilibrium is reached with respect to the salinity distribution. A suitable quantity of treated brackish water is injected to the aquifer to maintain the balance between fresh and saline groundwater and the excess of the treated brackish water may be used for different purposes or stored in the aquifer.

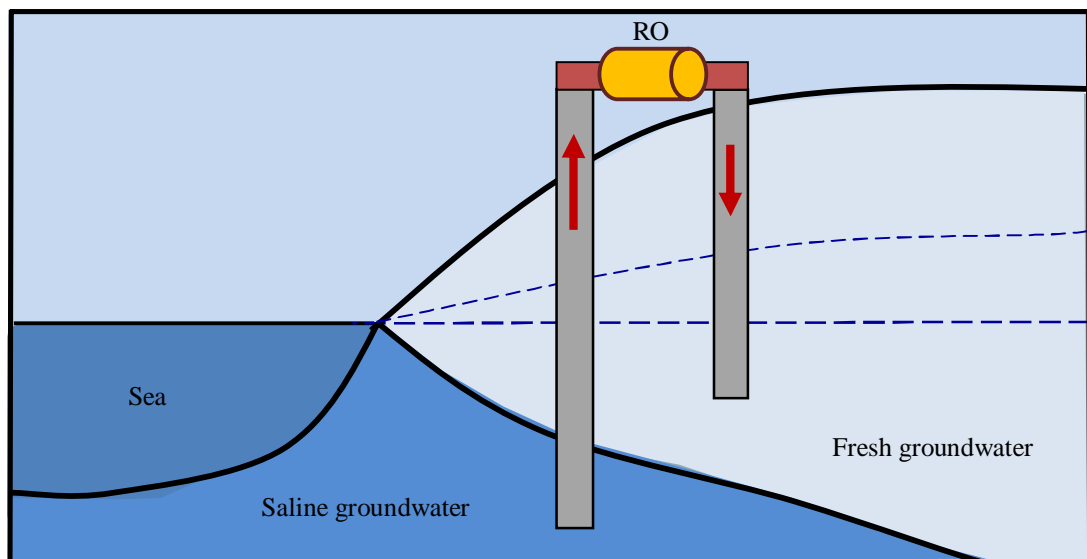


**Figure 1.4** The proposed methodology (ADR) to control saltwater intrusion

The second step of this methodology, desalination of brackish water using the RO treatment process, aims to produce fresh water from the brackish water and use it for recharging the aquifer to overcome the problem of scarcity of water in these areas. It is generally less costly than other sources of freshwater for injection. For example, desalination of seawater has many limitations such as; high cost, pollution (mainly carbon emission), and disposal of the brine. Desalinating brackish water is an efficient alternative to seawater desalination, because the salinity of brackish water is less than one-third of that of seawater. Therefore, brackish water can be desalinated at a significantly lower cost. A simulation-optimization model is developed to study different scenarios to control saltwater intrusion including; abstraction of brackish water, recharge of fresh water and combination of abstraction and recharge with RO desalination through the use of the proposed methodology ADR.

### ***1.6 Effects of climate change and sea level rise on saltwater intrusion***

One of the future challenges is climatic change and the related sea level rise. Climate change is a result of natural and/or man-made activities. Due to climate change the seawater levels might rise for several reasons including thermal expansion of oceans and seas, melting of glaciers and ice caps and melting of Greenland and Antarctic ice sheets. Sea level rise has many effects on coastal regions on the long term such as increase in coastal erosion and seawater intrusion. Climate change has already caused changes in the mean sea level during the last century by 10-20 mm/yr (IPCC, 1996). Future sea-level rise due to climate change is expected to occur at a rate greatly exceeding that of the recent past. It is expected the rise will be between 20–88 mm/yr (IPCC, 2001). The effects of climate change and sea level rise on saltwater intrusion on the long term should be considered in the modeling processes. The majority of the previous studies did not consider this point, while few centimeters rise in sea level could have a great effect on saltwater intrusion. This study considers the effect of increase in sea level due to climate change on the fresh water/saltwater interface with the focus on determining the changes in the position of the interface with time and identifying measures to control such movements. The predicted sea-level rise data by IPCC (2001) will be incorporated into the developed simulation model to investigate the new position of the fresh water/saltwater interface in coastal aquifers considering different scenarios of pumping rates and sea level rise.



## ***1.7 Objectives of the study***

Saltwater intrusion problem is a serious problem that threatens the health and life style of many people living in coastal areas. The problems of saltwater intrusion into groundwater have become a considerable concern in many countries with coastal areas. Development of a simulation-optimization model for the control of saltwater intrusion using different management scenarios is the major aim of the present study. The model is based on the integration of a genetic algorithm optimization technique and a coupled transient density-dependent fluid flow and solute transport model, which has been developed for simulation of seawater intrusion. The objectives of this work are:

- To develop a coupled transient density-dependent FE model of fluid flow and solute transport for computing solute transport in saturated/unsaturated soils. The model includes, coupled water and air flow with energy transport and solute transport.
- To apply the developed model to simulate water flow, air flow, heat transfer and solute transport in saturated/unsaturated soils.
- To apply the developed model to investigate the movement and the extent of saltwater intrusion in coastal aquifers.
- To develop a simulation-optimization model for the control of saltwater intrusion in coastal aquifers using different management scenarios including; abstraction of brackish water, recharge of fresh water and combination of abstraction and recharge. The objectives of these management scenarios include minimizing the total costs for construction and operation, minimizing salt concentrations in the aquifer and determining the optimal depths, locations and abstraction/recharge rates for the wells.
- To apply a new methodology ADR, proposed in this research to control seawater intrusion in real world coastal aquifers by abstracting brackish water, desalinating it using small scale RO plant and recharging to the aquifer.
- To apply the developed model to study the effects of likely climate change and sea level rise on saltwater intrusion in coastal aquifers.

This study has touched on a serious real world problem which has caused considerable concern in coastal regions in many countries throughout the world. The main contributions of this study are (i) the development of a coupled transient variable-density FE model to investigate seawater intrusion and study the effect of climate change and sea level rise on coastal aquifers, (ii) development of management models to control seawater intrusion and (iii) development of a simulation-optimization model to identify optimal arrangements for the proposed control method (ADR). This work presents a new methodology ADR to control saltwater intrusion in coastal aquifers, which is considered a first step in developing a simulation-optimization model to control saltwater intrusion in coastal aquifers using ADR. This methodology is considered to be cost-effective, capable of retarding freshwater/saline water interface toward the sea, and a source of fresh water in coastal regions.

### ***1.8 Outline of the thesis***

To achieve the study objectives, the thesis is organized in eight chapters. The main text of each chapter is intentionally kept as short as possible in favour of easy reading and is written to include only the fundamental concepts and the new ideas.

Chapter 2 presents background of saltwater intrusion investigation and control methods. A review of saltwater intrusion investigation methods, mechanisms and numerical models used for simulating saltwater is presented. The analyses of the numerical models that have been used to control saltwater intrusion using different methods and advantages and disadvantages of each method are presented. Also, a new methodology ADR is presented to control saltwater intrusion.

In chapter 3, the mathematical formulations and governing equations which are used in the development of this model are provided. These equations form a system of highly nonlinear, coupled, partial differential equations. The governing equations can be divided into two sets of equations, one set that describes the fluid flow and another set that describes the solute transport. These equations can rarely be solved analytically for situations of practical importance and so numerical solutions must be developed.

Chapter 4 presents an overview of the different mathematical models that have been used to solve coupled fluid flow and solute transport problem focusing on finite element and finite difference methods. The numerical solution of the governing differential equations of the coupled fluid flow and solute transport model is presented and calibrated.

Chapter 5 presents validation of the developed model through numerous examples and case studies to demonstrate the performance and accuracy of the developed numerical model.

Chapter 6 presents development and application of a simulation-optimization model to control seawater intrusion in coastal aquifers using three management scenarios including; abstraction of brackish water, recharge of fresh water and combination of abstraction and recharge. The objectives of these management scenarios include minimizing the total costs for construction and operation, minimizing salt concentrations in the aquifer and determining the optimal depths, locations and abstraction/recharge rates for the wells.

In chapter 7, the causes of climate change and its effect on coastal areas are presented. In particular, the effect of sea level rise on saltwater intrusion and the methods of control are presented. The application of the developed model to study the effects of likely climate change and sea level rise on saltwater intrusion in coastal aquifers is also presented.

Finally in chapter 8, the main conclusions of this work and recommendations for further studies are presented.

## **Saltwater intrusion investigation and control methods**

### ***2.1 Introduction***

Groundwater is considered the main source of water supply in many coastal regions. Population growth increases the water requirements leading to increase pumping from the aquifers. Over-pumping is considered the main cause of saltwater intrusion; under normal conditions freshwater flows into the sea, but over-abstraction may result in the inversion of the groundwater flow from the sea towards the inland causing saltwater intrusion. Saltwater intrusion can be defined as the inflow of seawater into an aquifer. It is common in coastal aquifers where the aquifers are in hydraulic contact with the sea. Saltwater intrusion leads to an increase in the saline water volume and a decrease in freshwater volume. Salinization of groundwater is considered a special category of pollution because mixing a small quantity of saltwater (2 to 3 percent) with groundwater makes freshwater unsuitable for use and can result in abandonment of freshwater supply wells when salt concentration exceeds drinking water standards. Therefore, saltwater intrusion should be prevented or at least controlled to protect groundwater resources. The key to control saltwater intrusion is to maintain a proper balance between water being pumped from the aquifer and water recharged to the aquifer (Bear et al., 1999).

This chapter presents the background of saltwater intrusion investigation and control methods. The chapter is divided into two main sections. A review of saltwater intrusion investigation methods, mechanisms and numerical models used for simulating saltwater intrusion in coastal aquifers is presented in the first section. The second section presents and analyzes the numerical models that have been used to control saltwater intrusion using different methods and the advantages and disadvantages of each method are highlighted. Also, a new methodology ADR (Abstraction of brackish water, Desalination and Recharge into the aquifer) is presented to control saltwater intrusion. The procedures and advantages of the proposed methodology are presented and discussed.

## ***2.2 Main causes of saltwater intrusion in coastal aquifers***

Coastal aquifers generally lie within some of the most intensively exploited areas of the world. About 70% of the world population lives in such areas. If current levels of population growth and industrial development are not controlled in the near future, the amount of groundwater use will increase dramatically, to the point that the control of seawater intrusion becomes a major challenge to future water resources management engineers. Saltwater intrusion is a serious problem in the coastal regions all over the world. It may occur due to human activities and by natural events such as climate change and sea level rise. The main causes of saltwater intrusion include (Bear et al., 1999):

- 1- Over-abstraction of the aquifers
- 2- Seasonal changes in natural groundwater flow
- 3- Tidal effects
- 4- Barometric pressure
- 5- Seismic waves
- 6- Dispersion
- 7- Climate change – global warming and associated sea level rise

Over-abstraction is considered one of the main causes of saltwater intrusion. Some of the previous causes of saltwater intrusion are periodic (e.g. seasonal changes in natural groundwater flow), some have short term implications (tidal effects and barometric pressure) and others have long term implications (climate changes and artificial influences). Salinization is one of the most widespread forms of groundwater contamination in the world. Saltwater intrusion poses a major limitation to utilization of groundwater resources. The intrusion of seawater should be controlled in order to protect groundwater resources from depletion. In order to take measures to control and prevent seawater intrusion and to get a clear understanding of the relationship between the consumption of groundwater and seawater intrusion, in depth study either from the theoretical point of view or from the numerical analysis and practical point of view is required.

### ***2.3. Saltwater intrusion investigating methods***

The analysis of salinization process in coastal regions requires information on both; geological and hydrochemical characteristics of aquifers. The intrusion of saltwater in coastal aquifers has been investigated by several methods including geophysical and geochemical methods. A number of experimental studies have been presented and different analytical and numerical models have been used to investigate saltwater intrusion in coastal aquifers. These approaches attempted to ascertain the position of freshwater/saltwater interface and predict changes in water levels and salinity. A brief description of the methods that have been used is presented in the following sections.

#### ***2.3.1 Geophysical investigations***

Saltwater intrusion can be distinguished by the movement of water with high total dissolved solids (TDS) content into fresh water. The degree of salinity varies in the transition zone between fresh and saline groundwater. The contour map of TDS is one measure of salinity and the location of the contour of TDS=1000 mg/l marks the area under the influence of seawater intrusion. The description of water type based on TDS content suggested by USGS is shown in Table 2.1.

**Table 2.1** The water type based on TDS content

<b>TDS (ppm) or (mg/l)</b>	<b>Description</b>
< 1000	Fresh water
1000-3000	Slightly saline
3000-10000	Moderately saline
10000-35000	Very saline
>35000	Brine

Geophysical methods measure the spatial distribution of physical properties of the earth, such as bulk conductivity of seismic velocity. Several geophysical methods can be used for hydrogeologic investigations such as (Bear et al., 1999):

### 1- Surface geophysical methods

- Electrical methods, such as: DC resistivity, frequency domain electromagnetic methods, airborne EM, loop-loop EM, time-domain electromagnetic sounding, and very low frequency EM
- Seismic methods, such as: seismic refraction, and seismic reflection
- Ground penetrating radar

### 2- Borehole methods

- Electric logs
- Radiometric logs
- Integrated use of borehole logs

### 3- Integrated geophysical surveys

Numerous researchers used geophysical methods to investigate saltwater intrusion. Melloul and Goldenberg (1997) analysed different methods of monitoring saltwater intrusion in coastal aquifers using direct methods that include measurement of groundwater salinity profiles and groundwater sampling of observation and pumping wells, and indirect methods using geoelectromagnetics and the time domain electromagnetic method. Mulrennan and Woodroffe (1998) examined the pattern and process of saltwater intrusion into the coastal plains of the lower Mary River, northern Territory, Australia, due to the effect of tides. Nowroozi et al. (1999) used the Schlumberger sounding resistivity methods in the investigation of saltwater/freshwater interface in the eastern shore of Virginia. Willert et al. (2001) used coastal aquifer test field (CAT-Field) to build a 3-D numerical model for prediction of saltwater intrusion and water quality and quantity between Bermerhaven and Cuxhaven, Germany, by DC-geoelectric measurements. Thomas et al. (2001) presented a study to evaluate and determine the feasibility of partially replacing the imported water with highly treated wastewater for injection to control saltwater intrusion. Maimone (2001) developed a numerical model to simulate saltwater intrusion and used time domain electromagnetic technique to locate the interface and confirm the accuracy of the model results. Fitterman and Deszcz-Pan (2001) used airborne electromagnetic technique for mapping saltwater intrusion in Everglades National Park, Florida.

Ekwurzel et al. (2001) carried out a hydrogeologic investigation using isotopes to determine the source of salinization in the Souss-Massa Basin, Morocco. Tulipano and Fidelibus (2002) presented the history of saltwater intrusion in the Salento Peninsula Puglia, southern Italy during the last 30 years, and established a methodology to describe and quantify salinization to Karstic aquifer subject to over exploitation. Rao and Rao (2004) investigated the movement of saltwater/freshwater interface in Krishna delta, India. They studied the control of saltwater intrusion using barriers of treated wastewater and industrial effluents. Pina et al. (2004) investigated the island of Santiago to characterize groundwater quality and identify the principal areas in risk of salt water intrusion in order to develop mitigating measures to reduce saltwater intrusion. Lazar et al. (2004) measured and characterized the fresh-saline interface fluctuation by sea tides by measurements of electrical conductivity taken across the interface interval. Bocanegra and Massone (2004) presented the results of analysis of coastal aquifers related to medium and large cities in Latin America and the Caribbean. They also developed a model to prevent migration of salts to protect the coastal aquifers. The study cases were applied to: Cuba, Mexico, Colombia, Brazil and Argentina. Qurtobi et al. (2004) presented an investigation to determine the mechanism of recharge to the aquifer and the region of salinity and its impact on fresh groundwater resources in the Souss-Massa basin in the south west of Morocco using isotopic techniques.

Levi et al. (2010) presented a geophysical study using combined high resolution electrical resistance tomography and accurate time domain electromagnetic measurements to study the relationships between seawater and groundwater via estuarine rivers at two sites along the lower part of the Alexander river in Israel. The objective of the study was to delineate the expected saline water intrusion from estuarine rivers into adjacent aquifers by means of high resolution and accurate geoelectric/geoelectromagnetic methods. Using geophysical techniques, Sherif et al. (2010) presented field investigations and measurements that revealed the nature and extent of the seawater intrusion in the coastal aquifer of Wadi Ham, UAE. They presented a 3D geological and true earth resistivity modelling for the aquifer. They used the results of the earth resistivity imaging surveys and chemical analyses of collected water samples to obtain an empirical relationship between the inferred earth resistivity and the amount of total dissolved solids.



### ***2.3.2 Geochemical investigations***

The distinction of different salinization mechanisms is crucial to the evolution of the origin, pathways, rates and future salinization of coastal aquifers. Several geochemical criteria can be used to identify the origin of salinity in coastal aquifers (Bear et al., 1999):

- 1- Cl-concentration: the Cl-concentration of 200 mg/l in groundwater is used as index of saltwater intrusion.
- 2- Cl/Br ratios: the bromide ion can be considered as a good indicator of saltwater intrusion. The concentration of bromide in fresh water is less than 0.01 mg/l.
- 3- Na/Cl ratios
- 4- Ca/Mg, Ca/(HCO<sub>3</sub>+SO<sub>4</sub>) ratios
- 5- O and H isotopes
- 6- Boron isotopes

A number of researchers used geochemical methods to investigate saltwater intrusion. Zubari (1999) presented a hydrochemical study to identify the sources of aquifer salinization and delineated their area of influence. Edet and Okereke (2001) examined the extent of seawater intrusion using vertical electrical sounding and hydrochemical data into shallow aquifers beneath the coastal plains of south eastern Nigeria. Gaye (2001) presented the necessary roles of using integrated geochemical and isotopic methods to study groundwater salinity problem in terms of its origin and prevention. Vallejos et al. (2004) studied the hydrochemical data with conductivity and water temperature diagrams to assess the process that causes changes in groundwater composition. Demirel (2004) used chemical analysis and electrical conductivity measurements to show the history of saltwater intrusion in time and space. Christensen et al. (2001) presented a study on both the geochemical and physical aspects of saltwater intrusion and their interaction during an intrusion experiment into a shallow aquifer in Shanshage, Denmark. Allen et al. (2001) presented a multidisciplinary study involving hydrochemical sampling and borehole geophysics to study the nature and occurrence of saline groundwater in the gulf islands, British Columbia, Canada.

Sherif et al. (2005) conducted a 2-D earth resistivity survey in Wadi Ham, UAE in the area between Fujairah and Kalba to delineate the seawater intrusion. They used Monitoring wells to measure the horizontal and vertical variations in water salinity and thus to improve the interpretation of earth resistivity imaging data. They used the results of vertical electrical soundings and chemical analyses of collected water samples to obtain an empirical relationship between the inferred earth resistivity and the amount of total dissolved solids. This relationship was used along with the true resistivity sections resulting from the inversion of 2D resistivity data to identify three zones of water-bearing formation (fresh, brackish, and salt-water zones). EL Moujabber et al. (2006) used physico-chemical analysis of water samples to investigate saltwater intrusion in the Choueifat-Rmeyle region, Lebanon.

### ***2.3.3 Experimental studies***

Some researchers presented experimental studies to investigate saltwater intrusion. Koch and Starke (2001) presented an experimental study using a Plexiglass for carrying out 2-D tracer experiment of macrodispersion in density-dependent flow within a stochastic realization of a heterogeneous media. Van Meir et al. (2004) developed an in situ laboratory where an integrated set of tools were developed for characterising the saltwater intrusion process in a hard rock aquifer with an appreciable level of heterogeneity. The final goal of the geophysical and hydraulic investigations was to derive 3-D porosity and permeability models as input for the analysis of specific saltwater intrusion experiments. Mukhopadhyay et al. (2004) presented a laboratory study to investigate the effects of artificial recharge on the aquifer material properties such as; porosity and permeability in group aquifer, Kuwait. Motz (2004) used inactive cells to present the saltwater part of the aquifer and a no-flow boundary along the interface. He performed a series of numerical experiments to investigate how the saltwater-freshwater interface should be approximated in a groundwater flow model to yield accurate values of hydraulic heads in the freshwater zone.

### ***2.3.4 Mathematical models***

Various analytical and numerical models have been developed to investigate saltwater intrusion in coastal aquifers. Some of the important contributions are discussed here after a comprehensive discussion in the following sections. Sherif et al. (1990) developed a finite element model for flow and solute transport to investigate the effect of lowering piezometric head due to excessive pumping on the saline water intrusion. Panday (1995) provided perspectives on the analytical upconing solutions, and numerical solutions as related to the physical system being modelled. Ghafouri and Parsa (1998) developed a finite element model to simulate the hydrodynamics of flow and salt transport in well-mixed estuaries in order to reduce the undesirable impacts of seawater intrusion. Tsutsumi et al. (2001) developed a numerical model with a groundwater module to predict the movement of freshwater/saltwater and the depth of freshwater/saltwater interface in coastal aquifers. Teatini et al. (2001) developed a finite element model to simulate saltwater intrusion in shallow confined aquifers. Qahman and Zhou (2001) applied SUTRA to simulate seawater intrusion in the northern part of the Gaza strip, Palestine. Prieto et al. (2001) applied SUTRA code to analyze the effects of seasonal variation in pumping and artificial and natural recharge on the dynamics of saltwater intrusion in the Nitzamin, Israel.

Zhang (2002) constructed the characteristics finite element alternating-direction schemes which can be divided into three continuous one-dimensional problems. This scheme was used to analyze saltwater intrusion in three dimensions. Oude Essink and Schaars (2002) developed a model to simulate density-dependent groundwater flow, heat and salinity distribution, and seepage and salt load flux to the surface water system, using MOCDENS3D code. The model was used to assess the effect of future development such as climate changes, sea level rise, land subsidence as well as human activities on qualitative and quantitative aspects of the groundwater system. Isikh and Karahanoglu (2004) used a quasi three dimensional finite element model to simulate seawater intrusion into a coastal aquifer below sea level mining operation. Vazquez et al. (2004) developed a numerical model to investigate saltwater transport in Llobregat delta aquifer, Barcelona, Spain. Lee (2004) investigated the effects of dewatering using SUTRA code to predict the movement of seawater inland under various scenarios of recharge in the coastal plain.

## ***2.4 History of saltwater intrusion modelling***

Mathematical models help to understand the relevant processes that cause saltwater intrusion in coastal aquifers (Bear et al., 1999). Over the years, a large number of analytical and numerical models have been used to predict the location and movement of the saltwater/freshwater interface. The numerical models can be categorized as sharp interface models or diffusive (dispersive) interface models. The first attempt to model seawater intrusion was made by Ghyben (1889) and Herzberg (1901). This simple model is known as Ghyben- Herzberg model which assumes that saltwater and freshwater are immiscible and separated by a sharp interface. Hubbert (1940) and Henry (1959) presented numerical solutions of steady saltwater intrusion into coastal aquifer based on the assumption of sharp interface.

This assumption treats the interface between saltwater and freshwater as sharp and well defined interface. However, in practice the interface is not sharp and the saltwater merges gradually with the freshwater by the process of mechanical dispersion. The width of the dispersion zone depends on the characteristics of the aquifer and the movement of water particles due to tides or the fluctuation due to recharge (Cooper, 1959). The assumption of sharp interface can be applied in some field conditions to obtain a first approximation to the freshwater pattern if the transition zone is relatively narrow otherwise the dispersion process should be taken into account and the entrainment of saltwater by the moving freshwater is necessary to describe the phenomena (Kohout, 1960). Over the years, several mathematical models have been developed to predict the interface or transition zone between freshwater and saltwater. Rifai et al. (1956) and Ogata (1959) indicated that the dispersion coefficient is proportional to the velocity and it is much greater in the direction of the velocity than in the lateral direction. Henry (1964) developed the first analytical solution including the effect of dispersion in confined coastal aquifer under steady-state conditions. Henry's problem was later solved by Lee and Cheng (1974) in terms of stream functions. Segol et al. (1975) developed the first transient solution based on a velocity-dependant dispersion coefficient, using Galerkin finite element method. Numerous other researchers, such as Pinder and Cooper (1970), Frind (1982) and Huyakorn et al. (1987),

employed numerical models in the simulation of saltwater intrusion problem using the diffusive interface approach.

Extensive research is being carried out in many parts of the world with the objectives of understanding the mechanism of seawater intrusion and improving the methods to control it in order to protect groundwater resources in coastal aquifers. The developed numerical models are based on different concepts and can be categorized as:

- 1- Sharp-interface or diffusive interface (density-dependent) models.
- 2- Saturated or unsaturated flow models.
- 3- Transient or steady flow models.

### ***2.4.1 Sharp-interface or diffusive interface models***

A number of mathematical models have been developed to simulate saltwater intrusion based on sharp interface assumption. Recently, researchers have been focusing more on diffusive interface (density-dependent) models which are more realistic.

#### ***2.4.1.1 Sharp-interface models***

Modelling of seawater intrusion in coastal aquifers is not a new subject. The initial model was developed independently by Ghyben (1988) and Herzberg (1901). This simple model is known as Ghyben-Herzberg model and is based on the hydrostatic equilibrium between fresh and saline water as shown in Figure 2.1, and is described by Ghyben-Herzberg equation as;

$$h_s = \left(\frac{\rho_f}{\rho_s - \rho_f}\right)h_f \quad (2.1)$$

where:

$\rho_s$  : is the saltwater density

$\rho_f$  : is the freshwater density

$h_s$  : is the depth of interface below mean sea level

$h_f$  : is the height of the potentiometric surface above the mean sea level

According to Ghyben-Herzberg equation, if the saltwater density is  $1025 \text{ kg/m}^3$  and freshwater density is  $1000 \text{ kg/m}^3$ , this gives  $h_s = 40 h_f$ .

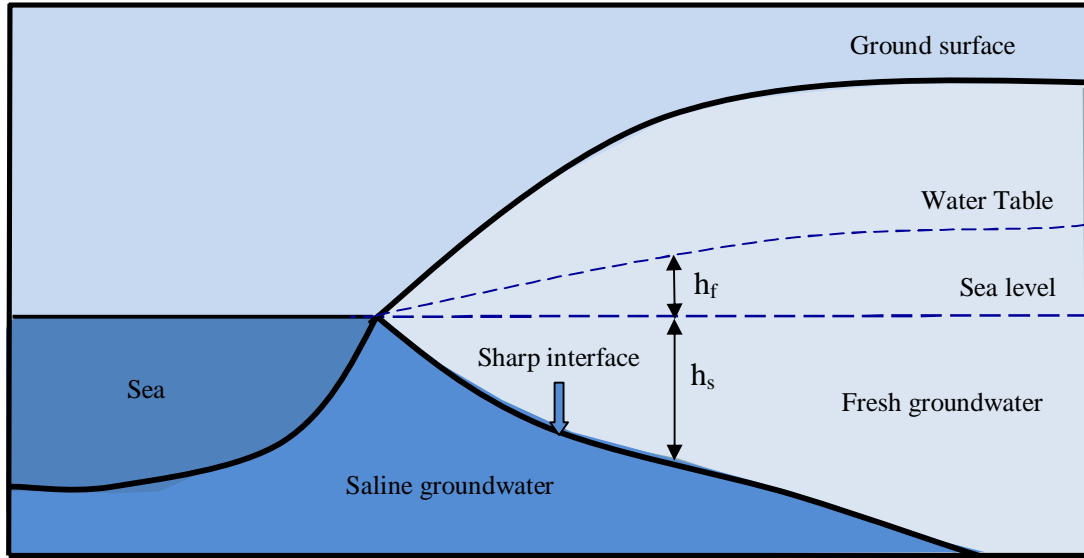


**Figure 2.1** Hydrostatic equilibrium between fresh and saline water

Several mathematical and numerical models were developed to simulate saltwater intrusion based on sharp interface assumption. Sbai et al. (1998) used the finite element method for the prediction of saltwater intrusion under steady state and transient conditions based on a sharp interface model assuming the fresh water and saltwater to be immiscible. Izuka and Gingerich (1998) presented a method to calculate vertical head gradients using water head measurements taken during drilling of a partially penetrating well. The gradient was then used to estimate interface depth based of Ghyben-Herzberg relation. Naji et al. (1998) used an optimization technique to determine the location of sharp interface between saltwater and freshwater. The algorithm used was based on the combination of nonlinear programming and h-adaptive boundary element method. Bower et al. (1999) presented an analytical model for saltwater upconing in a leaky confined aquifer. The model assumed the existence of a sharp interface between freshwater and saltwater.

Fitzgerald et al. (2001) presented a series of inter-related codes that together can address the issues related to effective management of coastal aquifer systems. This set of tools included groundwater flow, solute transport, sharp interface and coupled flow and transport modelling codes. All of these codes are 3-D and linked by common database (input/output) files. Groundwater flow in the multi-aquifer system could be simulated and management practices such as aquifer storage and retrieval, injection barrier wells, optimization of pumping location and depths could be evaluated using these codes. Brunke and Schelkes (2001) developed a program SIM-COAST to simulate the time-dependent behaviour in coastal aquifers. In this approach the interface between freshwater and saltwater was simplified to a line. Marin et al. (2001) used a quasi-three dimensional finite-difference model, in which freshwater and saltwater flow were separated by a sharp interface, to simulate groundwater flow in Karstic aquifer of northwestern Yucatan, Mexico. Aharmouch and Larabi (2001) presented a numerical model, based on the sharp interface assumption, to predict the location, shape and extent of the interface that occur in coastal aquifer due to groundwater pumping. El Fleet and Baird (2001) developed a 2D-2 layer sharp interface model to predict the impact of over-abstraction from the coastal aquifer on saltwater intrusion, and applied the model to the coastal aquifer in Tripoli, Libya. Taylor et al. (2001) presented a comparison between results of different codes applied to Henry's problem and analyzed the sensitivity of each code to changes in the parameters.

#### ***2.4.1.2 Diffusive interface models***

Saltwater and fresh groundwater are separated by either a sharp interface or a transition zone. Hydrodynamic dispersion and diffusion tend to mix the two fluids forming a transition zone at the interface as shown in Figure 2.2. The transition zone depends on the extent of seawater intrusion and aquifer properties. This transition zone is a result of hydrodynamic dispersion of the dissolved matter and could be wide or narrow according to the aquifer depth. Steady flow minimizes the transition zone thickness, whereas pumping, recharge, tides and other excitations increase its thickness. The thickness of transition zones could range from a few meters to several kilometres in over-pumped aquifers. The thickness of a transition zone depends on (Todd (1974):

- 1- structure of the aquifer,
- 2- extraction from the aquifer,
- 3- variability of recharge,
- 4- tides, and
- 5- climate change.

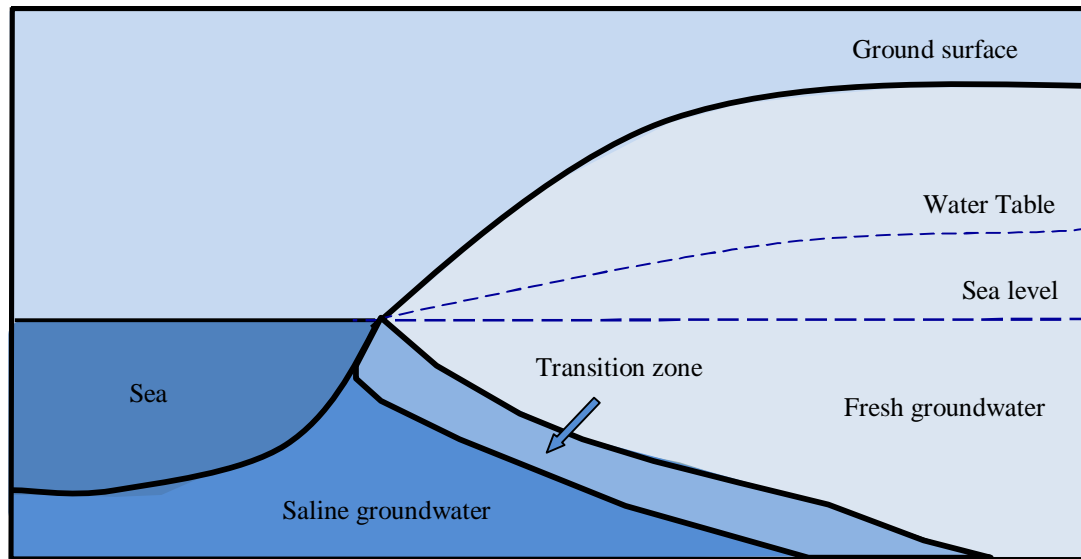


**Figure 2.2** Location of transition zone

A number of mathematical models have been developed to simulate saltwater intrusion based on diffusive interface. Tasi and Kou (1998) developed a two dimensional finite element code, considering density-dependant flow and transport. The model was used to simulate saltwater intrusion and to evaluate the major effects of hydrological and geological parameters, including hydraulic conductivity, hydraulic gradient on saltwater intrusion. Benson et al. (1998) studied the effect of velocity gradient on solute transport. The study showed that in case of saltwater intrusion, the velocity is so high and hence affects the solute transport. Other numerical models assume approximate value of the velocity due to its low value. Cheng et al. (1998) developed a 2-D finite element model for density-dependant flow and solute transport through saturated and unsaturated soils. Sakr (1999) presented a finite element model to simulate density-dependent solute transport. He used the model to investigate the limitation of the sharp interface approach in coastal aquifers for both steady and unsteady states.



Some researchers used computer codes to simulate saltwater intrusion. Paniconi et al. (2001) used the CODESA-3D code that treats density-dependant variably saturated flow and miscible solute transport to investigate the occurrence of seawater intrusion in the Korba plain in northern Tunisia. Oude Essink (2001a,b) used MOCDENS3D for density-dependant groundwater flow in three dimensions to simulate saltwater intrusion in the island of Texel and also Noord-Holland Netherland. In addition, a relative sea level rise of 0.5 meter per century was considered. Payne et al. (2001) used SUTRA to predict the effects of various pumping scenarios on groundwater supplies, in the context of management of groundwater resources in coastal Georgia.

Bear et al. (2001) developed a 3-D finite element model that took into account the development of a transition zone and variation of fluid density with time. The model was used to analyze seawater intrusion induced by pumping wells in the upper section of the coastal aquifer in Israel. Oswald et al. (2001) developed a 3-D model for variable density flow to study the effect of several pumping scenarios on water quality in an island aquifer, in China. Moe et al. (2001) presented a 3-D coupled density-dependent flow and transport model for simulating seawater intrusion, migration of brine, and transport of brackish water in the Gaza strip, Palestine. Lecca et al. (2001) presented a three-dimensional density-dependent finite element model to simulate saltwater intrusion in the Sahel region of the Atlantic coast, Morocco. Sabi et al. (2001) developed finite element model to predict the interface in steady and transient conditions. The model was applied to the coastal aquifer of Martil in Morocco to study the aquifer response to change in recharge and total rate of pumping water and their effects on saltwater intrusion.

A numerical model to study density-dependent groundwater flow and solute transport in unsaturated soil was developed by Jung et al. (2002). Gingerich and Voss (2002) expanded a cross-sectional 2-D model developed by (Voss, 1984) to 3-D. The developed model showed the effect of variable-density flow and solute transport on groundwater flow, freshwater/saltwater zone and salinity distribution. Abarca et al. (2002) studied the effect of aquifer bottom topography on seawater intrusion, using a three dimensional density-dependant groundwater flow and transport model. Lecca et al. (2004) used a 3-D density-

dependant flow and contaminant transport code to improve the understanding of groundwater degradation mechanism within the complex hydrodynamic system in the coastal plain, Muravera, Italy.

Hamza (2004) presented a numerical model considering the dispersion zone between freshwater and saltwater. The model was used to predict the effect of saltwater upconing on the salinity of pumped water from a pumping well. He considered the effect of velocity-dependent, hydrodynamic dispersion and density-dependant flow. The study was conducted to determine the most important parameters that affect the quality of pumped water. Stuyfzand et al. (2004) used salinization potential for water resources (SAPORE) index to assess the use of brackish groundwater for drinking on the upconing of saline water. They used reverse osmosis to treat brackish groundwater. Voudouris et al. (2004) described the methods of the salinity distribution by seawater intrusion based on chemical analysis of samples collected from the aquifer of Greece. Bakkar et al. (2004) developed a package for modelling of regional seawater intrusion with MODFLOW, and used it to simulate the evolution of the three-dimensional salinity distribution through the time considering the effects of variation in density.

Lakfifi et al. (2004) developed a numerical model based on the SEWAT code to study groundwater flow and saltwater intrusion in the coastal aquifer of Chaouia Morocco. SEWAT code was used to simulate the spatial and temporal distribution of hydraulic head and solute concentration. Doulgieris and Zissis (2005) developed a 3-D finite element model for the simulation of saltwater intrusion in coastal confined aquifers by considering the development of a transition zone between fresh water and seawater and thus density-dependant flow and transport. Shalabey et al. (2006) presented a numerical model of advective and dispersive saltwater transport below a partially penetrating pumping well. The numerical solution included a solution of the coupled flow and solute transport equations. Canot et al. (2006) developed a 2-D numerical model for solution of transient density driven flow in porous media.

### ***2.4.2 Steady-state and transient flow models***

Numerous models have been presented to study coupled fluid flow and solute transport in porous media. Several researchers assumed steady-state solution for simplicity and avoided the transient simulation because of high computational requirements.

Bixio et al. (1998) developed a fully coupled steady-state flow and solute transport finite element model for the prediction of the maximum extent of saltwater intrusion in a vertical section in the Venice aquifer, Italy. Sadeg and Karahannoglu (2001) developed a two-stage finite element simulation model. In the first atage, an areal 2-D model was formulated to perform a steady-state calibration for the physical parameters and boundary conditions of the hydrostatic system. In the second stage, seawater intrusion was analysed using cross-sectional finite element model.

Sbai et al. (1998) developed a finite element model for prediction of saltwater intrusion under steady-state and transient flow conditions. Sakr (1999) developed a 2-D finite element model to simulate density-dependent solute transport to investigate the limitation of the sharp interface approach in coastal aquifers for both steady-state and unsteady state conditions. Liu et al. (2001) presented a 2-D finite volume model to simulate saltwater intrusion in coastal aquifers, the flow was considered transient and the variability of fluid density was taken into account. Bear et al. (2001) developed a 3-D model using the finite element framework. The model took into account the development of a transition zone and variation of fluid density with time. Shalabey et al. (2006) developed a numerical model of advective and dispersive saltwater transport below partially penetrating pumping wells. They presented a solution of the coupled flow and solute transport equations that permits estimation of salt concentration in the aquifer and water pumped from wells in time and space.

### ***2.4.3 Saturated and unsaturated flow models***

Various models were developed to simulate solute transport in saturated soil. However, few models were developed to simulate solute transport in unsaturated zone.

Teatini et al. (2001) developed a finite element model for saturated flow and transport to simulate saltwater intrusion in shallow confined aquifers. Cau et al. (2002) developed a 3-D model supported by GIS to investigate the causes of saltwater intrusion, using coupled flow and solute transport in saturated porous media. The model was used to predict the movement of the freshwater-saltwater mixing zone under different future scenarios.

Jung et al. (2002) presented a 3-D numerical model to investigate density-dependent groundwater flow and solute transport in unsaturated soil. Cheng et al. (1998) developed a 2-D finite element model for density-dependant flow and solute transport through saturated/unsaturated porous media to simulate saltwater intrusion. Paniconi et al. (2001) developed a numerical model that treats density-dependant flow and miscible salt transport. The developed model was used to investigate the occurrence of seawater intrusion in the Korba plain in northern Tunisia. They also examined the effect and interplay between pumping, artificial recharge, soil, aquifer properties and the unsaturated zone. A three dimensional saturated-unsaturated finite element code, CODESA-3D was used in this study. Voss (1984) employed a 2-D hybrid finite element model integrated with the finite difference technique to simulate the flow of density-dependent fluid and solute transport in saturated and unsaturated soil. Voss and Provost (2001) used the 3-D SUTRA code to simulate variable-density flow and saltwater intrusion in coastal aquifers, which was applied to study the intrusion of seawater in a number of real cases studies. Gingerich and Voss (2002) expanded a cross-sectional 2-D model analysis (Voss, 1984) to 3-D using GIS. This 3-D model produced the overall behaviour of groundwater flow and the salinity distribution depending on variable-density flow and solute transport.

#### ***2.4.4 Recent computer codes to simulate saltwater intrusion***

Over the years, a large number of models and computer codes have been developed and used to study saltwater intrusion in coastal aquifers. These include analytical and numerical models. Finite difference and finite element were widely used in this field. A number of computer codes have been used to model coupled flow and solute transport and saltwater intrusion in coastal aquifers. Summary of the common computer codes used to investigate saltwater intrusion in coastal aquifers is presented below.

##### ***SUTRA***

SUTRA is a 2-D and 3-D finite element code. SUTRA can simulate density-dependent groundwater flow with energy transport or solute transport (Voss, 1984). This code has been widely used to simulate variable-density groundwater flow. Gotovac et al. (2001) used SUTRA to examine the effects of geologic heterogeneity upon the development of the transition zone in coastal aquifer subject to seawater intrusion. The results indicated that heterogeneity plays an important role in the displacement of the transition zone and the variability of salt concentration. Gurdu et al. (2001) used SUTRA to simulate saltwater intrusion in the Goksu delta at Silifke, Turkey. Narayan et al. (2002) used SUTRA to define the current and potential extent of saltwater intrusion in the Burdekin delta aquifer under various pumping and recharge conditions. A 2-D vertical cross-section model was developed for the area, which accounted for groundwater pumping and artificial recharge schemes. The results addressed the effects of seasonal variation in pumping rate and artificial and natural recharge rates on the dynamics of saltwater intrusion. Alf et al. (2002) presented a combination of SUTRA and hydrochemical investigations to investigate saltwater intrusion in coastal aquifers. Ojeda et al. (2004) modelled the saline interface of the Yucatan peninsula aquifer using SUTRA. The results showed that the interface position is very sensitive to head changes.

##### ***SEWAT***

SEWAT is a combination of MODFLOW and MT3DMS. It is designed to simulate 3-D variable density groundwater flow and solute transport (Zheng and Wang 1999). This code was used by a number of researchers to simulate different cases of saltwater intrusion. Rao

and Rao (2004) developed a simulation-optimization approach to control saltwater intrusion through a series of extraction wells. SEAWAT was used to simulate the dynamics of saltwater intrusion and the simulated annealing algorithm was used to solve the optimization problem. Tiruneh and Motz (2004) investigated the effect of sea level rise on the freshwater-saltwater interface, using SEWAT. Lakfifi et al. (2004) applied SEWAT to study groundwater flow and saltwater intrusion in the coastal aquifer of Chaouia in Morocco. Qahman and Larabi (2004) used SEAWAT code for simulating the spatial and temporal evolution of hydraulic heads and solute concentrations of groundwater in the Gaza aquifer (Palestine). The results showed that seawater intrusion would become more severe in the aquifer if the current rates of groundwater pumping continued.

### ***CODESA-3D***

CODESA-3D is a 3-D finite element model that can simulate saltwater interface in saturated and variably saturated porous media by solving the convective-dispersive transport equation. Barrocu et al. (2004) used CODESA 3-D with GIS to study the migration of contaminant and the impact of land management using different groundwater abstraction schemes and artificial recharge in Sardinia, Italy. Paniconi et al. (2001) used CODESA-3D to investigate the occurrence of seawater intrusion in the Korba plain in northern Tunisia. They examined the effect and interplay between pumping, artificial recharges, soil/aquifer properties and the unsaturated zone.

### ***SWIFT***

SWIFT is a 3-D code to simulate groundwater flow, heat transfer and brine and radio nuclide transport in porous and fractured media (Ward and Benegar 1998 and Ward 1991). Ma et al. (1997) used SWIFT to simulate saltwater upconing and its effect on the salinity of pumped water.

### ***MOCDENS3D***

MOCDENS3D is a 3-D code to simulate density-dependant groundwater flow and solute transport (Oude Essink, 1998). Oude Essink (2001c) used the code to model the movement of freshwater, brackish and saline groundwater in coastal aquifers including advection and dispersion.

***SHARP***

Barreto et al. (2001) used a finite difference model (SHARP) to simulate groundwater flow in aquifers and established a relationship between the pumping flow, the location of the wells, the number of the wells, the drop of freshwater heads, and the movement of interface.

***Quasi-three-dimensional finite element***

Zhou et al. (2003) used a quasi-three-dimensional finite element to simulate the spatial and temporal distribution of groundwater levels in the three-aquifer system. Mahesha (1996c) used a quasi-three-dimensional finite element to examine the efficiency of battery of injection wells in controlling saltwater intrusion.

***SHEMAT***

Scholze et al. (2002) applied SHEMAT to simulate saltwater intrusion in the coastal aquifers of Metro Cebu.

Some other codes have been used to simulate saltwater intrusion in coastal aquifers (e.g., FEFLOW; HST3D; FAST-C (2D/3D) and MOC DENSE), (Beer et al., 1999).

## ***2.5 Saltwater intrusion control methods***

Considerable attention has been recently focused on models to study the control of saltwater intrusion in order to protect groundwater resources. The control of saltwater intrusion representing a continues challenge because groundwater provides about one-third of the total freshwater consumption in the world especially in the coastal areas where 70 % of the world population lives (Bear et al., 1999). The key to control saltwater intrusion is to maintain a proper balance between water being pumped from the aquifer and water recharged to the aquifer. Over the years, a number of methods have been used to control saltwater intrusion in coastal aquifers. Not all the solutions are economically feasible because they are considered long term solutions, and the time to reach the state of dynamic equilibrium between freshwater and brackish water may takes tens of years (Bear et al., 1999).

Different measures have been presented to control saltwater intrusion in coastal aquifers. Todd (1974) presented various methods of preventing saltwater from contaminating groundwater sources including:

- 1- reduction of pumping rates
- 2- relocation of pumping wells
- 3- use of subsurface barriers
- 4- natural recharge
- 5- artificial recharge
- 6- abstraction of saline water
- 7- combination techniques

Numerical models have been developed and used to help understanding the relevant process that causes saltwater intrusion in coastal aquifers and identify suitable methods of control. Extensive research has been carried out to investigate saltwater intrusion in coastal aquifers. However, only limited amount of research has been directed to study the control of saltwater intrusion. The following sections present the previous methods that have been used to control saltwater intrusion in different locations. Also, the advantages and disadvantages of each one are discussed (Abd-Elhamid and Javadi, 2008a).



### ***2.5.1 Reduction of pumping rates***

The natural balance between freshwater and saltwater in coastal aquifers is disturbed by abstraction and other human activities that lower groundwater levels, reduce the amount of fresh groundwater flowing to the sea, and ultimately cause saltwater to intrude coastal aquifer. Increasing pumping rate is considered the main cause of saltwater intrusion along the coasts. Other parameters that cause saltwater intrusion have smaller impact in comparison with pumping. Population growth in coastal areas has increased water demand which has in turn resulted in increase in abstraction from aquifers. The reduction of pumping rates aims to achieve the sustainable yield and use other water resources to supply adequate water demand. This can be achieved by a number of measures including;

- 1- increase in public awareness of the necessity of water to save water,
- 2- reduction of losses from the water transportation and distribution systems,
- 3- reduction of water requirement in irrigation by changing the crop pattern and using new methods for irrigation such as drip irrigation, canal lining, etc,
- 4- recycling of water for industrial uses, after appropriate treatment,
- 5- reuse of treated waste water in cooling, irrigation and recharge of groundwater, and
- 6- desalination of seawater.

A number of models have been developed to control saltwater intrusion by reducing pumping rates from the aquifer or using optimization models to optimize the abstraction and control the intrusion of saline water. Scholze et al. (2002) used the SHEMAT code to simulate saltwater intrusion in coastal aquifer of Metro Cebu. They applied different scenarios of abstraction and decrease in water consumption, to protect groundwater resources and avoid saltwater intrusion. Zhou et al. (2003) used a quasi-three-dimensional finite element model to simulate the spatial and temporal distribution of groundwater levels. The objective of the model was to maximize the total groundwater pumping from the confined aquifer and control saltwater intrusion by relocating the wells. Amaziane et al. (2004) coupled the boundary element method and a genetic algorithm for the optimization of pumping rates to prevent saltwater intrusion.

Qahman and Larabi (2004) investigated the problem of extensive saltwater intrusion in Gaza aquifer, Palestine using the SEWAT code. Different scenarios were considered to predict the extension of saltwater intrusion with different pumping rate over the time. Bhattacharjya and Datta (2004) used an artificial neural network as a simulator for flow and solute transport in coastal aquifer to predict salt concentrations of the pumped water. A linked simulation-optimization model was formulated to link the trained ANN with a GA based optimization model to solve saltwater management problems. The objective of the management model was to maximize the permissible optimal abstraction of groundwater from the coastal aquifer for beneficial use, while maintaining salt concentration in the pumped water under specific permissible limits.

**Advantages:** Reduction of abstraction rates and use of other water resources help to increase the volume of freshwater which retards the intrusion of saltwater.

**Disadvantages:** Control of saltwater intrusion using this method has some limitations. The control of abstraction rates cannot be fully achieved especially from private stakeholders. Also the alternatives proposed for facing the shortage of water and the increased demands may be very costly, especially when freshwater is not available and requires transportation. Desalination of seawater as an alternative has also a lot of disadvantages; it is still very expensive, is a source of pollution and requires a large area of land. The treated waste water is also costly. Furthermore, this can only be a temporary solution because it does not prevent saltwater intrusion but it attempts to reduce it, but with the population growth and increasing demands the problem will not be controlled (Abd-Elhamid and Javadi, 2008a).

### ***2.5.2 Relocation of pumping wells***

Changing the location of pumping wells by moving the wells to more inland positions aims to raise the groundwater level and maintain the groundwater storage. This is because in the inland direction the thickness of the freshwater lens increases and the risk of upconing of saltwater decreases accordingly.

Ofelia et al. (2004) used a mathematical model to identify saltwater volume interred the fresh groundwater in Santa Fe, Argentina. The study examined a management model to protect the fresh groundwater system. Several pumping wells were removed from services and a new pimping field was designed and implemented. Hong et al. (2004) developed an optimal pumping model to evaluate optimal groundwater withdrawal and the optimal location of pumping wells in steady-state condition while minimizing adverse effects such as water quality in the pumping well, drawdown, saltwater intrusion and upconing. The study involved experimental verification of the optimal pumping model to develop sustainable water resources in the coastal areas.

Ojeda et al. (2004) modeled the saline interface of the Yucatan peninsula aquifer using SUTRA assuming an equivalent porous medium with laminar flow and two dimensional flow. The models showed that the interface position is very sensitive to head changes and a simple groundwater abstraction scheme was presented which was based on the well depth and the distance from the coast. Maimone and Fitzgerald (2001) applied three dimensional groundwater flow models, dual phase sharp interface intrusion model, radial upconing model, and single phase contaminant transport model to develop a coastal aquifer management plan. Two techniques were used; one based on developing new well locations inland from the coast and the other one on use of RO treatment for desalinating brackish water and using it for domestic purposes. Sherif et al. (2001) used two models to simulate the problem of saltwater intrusion in the Nile Delta aquifer in Egypt in the vertical and horizontal directions. The two models were 2D-FED and SUTRA. The 2D-FED model was employed to simulate the current condition and predict the effect of the seawater level rise in the Mediterranean Sea under the condition of global warming. SUTRA was used to define the best location of additional groundwater pumping wells from the Nile Delta aquifer and to assess the effect of various pumping scenarios on the intrusion process.

**Advantages:** Moving pumping wells further inland helps to decrease the occurrence of upconing of saltwater (Abd-Elhamid and Javadi, 2008a).

**Disadvantages:** Control of saltwater intrusion by this method is costly and may face some obstructions such as, buildings or the size of the aquifer may not allow such movment. It is also a temporary solution and does not prevent the intrusion of saline water into the aquifer.

### 2.5.3 Subsurface barriers

This method involves establishment of a subsurface barrier to reduce the permeability of the aquifer to prevent the inflow of seawater into the basin. Construction of barriers could be achieved using sheet piling, cement grout, or chemical grout. Figure 2.3 shows a sketch of a subsurface barrier to control saltwater intrusion.

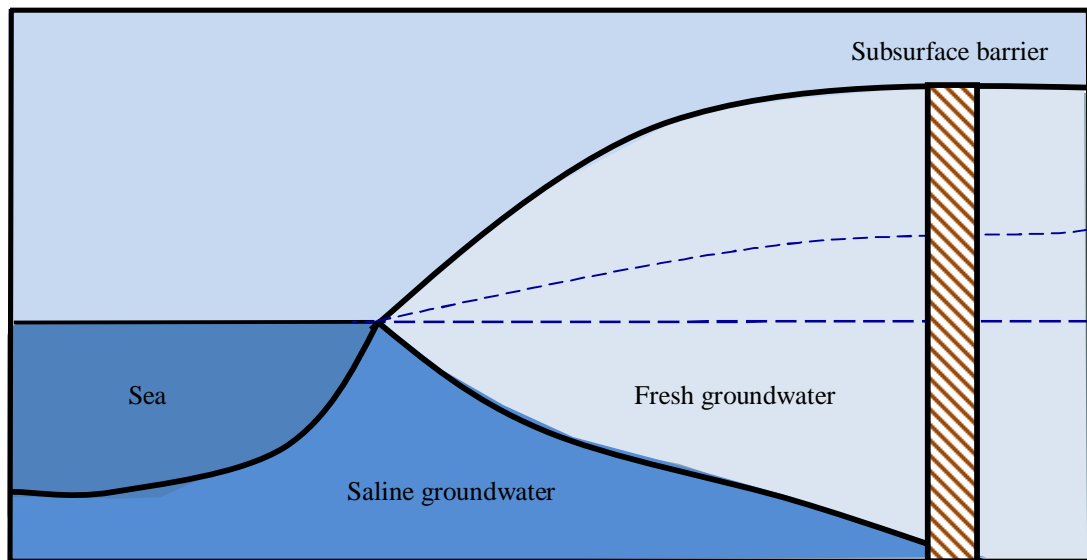


**Figure 2.3** Sketch of a subsurface barrier

Barsi (2001) developed two methods for optimal design of subsurface barriers to control seawater intrusion through the development of implicit and explicit simulation-optimization models. The main objective was to find the optimal design of subsurface barrier to minimize the total construction cost through the selection of the width and location of the barrier. Harne et al. (2006) presented a 2-D sub-surface transport model of saltwater considering the soil to be homogenous and isotropic under the influence of constant seepage velocity. They used the finite difference method to solve the transport equation. The model examined the efficiency of subsurface barrier to control saltwater intrusion. James et al. (2001) developed a process for selectively plugging permeable strata with microbial biofilm. These biofilm barriers can aid the prevention of saltwater intrusion by reducing the subsurface hydraulic conductivity. The main advantage offered by the biofilm

barrier technology is that biofilm barrier construction can be achieved without excavation and therefore will be economic.

**Advantages:** Using subsurface barriers helps to reduce the intrusion of saline water.

**Disadvantages:** Control of saltwater intrusion using subsurface barriers could be costly in terms of construction, operation, maintenance and monitoring. It is also not efficient for deep aquifers (Abd-Elhamid and Javadi, 2008a).

#### 2.5.4 Natural recharge

This method aims to feed aquifers with additional surface water by constructing dams and weirs to prevent the runoff from flowing to the sea. This method can also be used for flood protection. The retained water infiltrates into the soil and increases the volume of groundwater storage. Figure 2.4 shows a sketch of the natural recharge process.

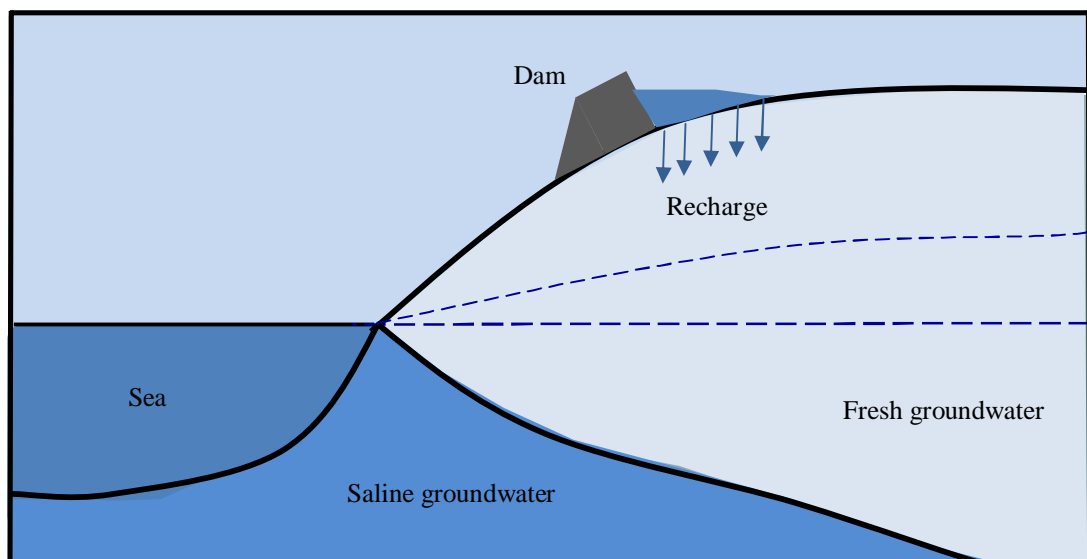


**Figure 2.4** Sketch of the natural recharge process

This method could be efficient for unconfined aquifers but it could take a long time to recharge the aquifer depending on its properties. Ru et al. (2001) used a quasi three-dimensional model to simulate the movement of the interface between seawater and freshwater and evaluate the effect of constructing a dam to protect groundwater resources.

The function of the subsurface dam was to collect the rainfall water and recharge the aquifer to increase the groundwater storage and retard saltwater intrusion. Bajjali (2005) applied geostatistical techniques of GPI, IDW with GIS, to examine the effect of recharge dam on groundwater quality. The infiltrated water below the dam increases the aquifer storage of freshwater and pushes the saline water toward the sea.

**Advantages:** This method helps to prevent the runoff to flow directly to the sea and uses it to increase the groundwater storage in the aquifer and prevent the intrusion of saline water.

**Disadvantages:** Natural recharge depends on the soil properties and requires high permeability soil. Depending on the soil permeability, the recharge process could take a long time. The cost of construction of dams and weirs and their maintenance is very high. This solution is unsuitable for confined and deep aquifers.

### ***2.5.5 Artificial recharge***

Artificial recharge aims to increase the groundwater levels, using surface spread for unconfined aquifers and recharge wells for confined aquifers. The potential sources of water for injection may be from surface water, pumped groundwater, treated wastewater, desalinated seawater, or desalted brackish water. Surface water can be taken from rivers or canals through pipelines. Figure 2.5 shows a sketch of a recharge well.

A number of researchers used this method to control saltwater intrusion in coastal aquifers. Narayan et al. (2006) used SUTRA to define the current and potential extent of saltwater intrusion in the Burdekin Delta aquifer under various pumping and recharge conditions. A 2-D vertical cross-section model was developed for the area, which accounted for groundwater pumping and artificial recharge schemes. The results addressed the effects of seasonal variation in pumping rate and artificial and natural recharge rates on the dynamic of saltwater intrusion. The simulation was carried out for a range of recharge, pumping rates and hydraulic conductivity. Papadopoulou et al. (2005) developed a 3-D finite element-finite difference groundwater flow simulation model. The extension of the saltwater front along the coastal zone was calculated only hydraulically because his model did not consider diffusion due to different densities of saltwater and freshwater. Artificial

recharge was presented using different scenarios including different well locations and different injection rates. The source of water used for recharge was the effluent of the waste water treatment plant of the industrial zone after tertiary treatment.

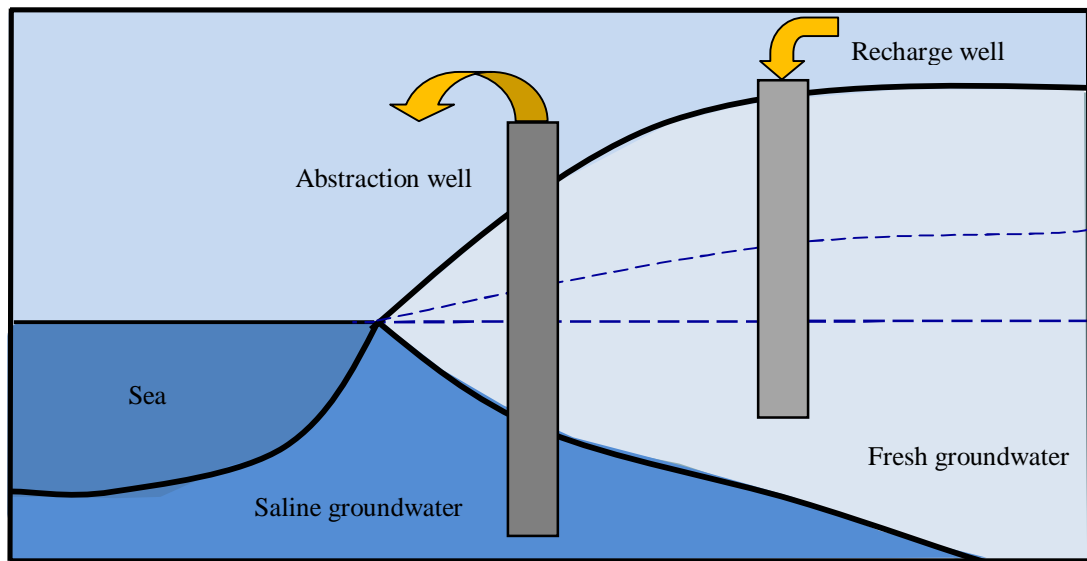


**Figure 2.5** Sketch of recharge and abstraction wells

Kashef (1976) studied the effect of recharge wells of different patterns on the degree of saltwater retardation in confined coastal aquifers. The batteries (recharge wells) were located at various distances parallel to the shoreline; each battery consisting of equally spaced recharge wells of a certain number. It was found that, the optimum location of the batteries should lie between  $0.7L$  and  $L$ , where  $L$  is initial length of the intruded saltwater wedge. Mahesha (1996a) studied the effect of battery of injection wells on seawater intrusion in confined coastal aquifers. He used a quasi three-dimensional areal finite element model considering a sharp interface. He studied various conditions by changing the well spacing and intensity and duration of fresh water injection. He concluded that, spacing between wells, injection rate and duration of injection control the repulsion of the saline wedge.

Mahesha (1996b) presented steady state solutions for the movement of the fresh water/seawater interface due to a series of injection wells in a confined aquifer using a sharp interface finite element model. The model was used to perform parametric studies on

the effect of location of the series of injection wells, spacing of the wells and fresh water injection rate on the seawater intrusion. It was found that reduction of seawater intrusion (of up to 60-90 %) could be achieved through proper selection of injection rate and spacing between the wells. Also, he studied the effect of double series of injection wells and compared with the single series. He found that a double series performs slightly better than single series. Also, it was found that the staggered system of wells in the series is slightly better than the straight well system for long spacing. Lopez-Ramirez et al. (2006) presented a study to define the optimum conditions for physiochemical pre-treatment of secondary effluents for successful reverse osmosis operation for groundwater recharge. They also examined the suitability of treated waste water for groundwater recharge and concluded that high quality reclaimed wastewater can be safely used in groundwater recharge. Paniconi et al. (2001) developed a numerical model that treats density-dependant variably saturated flow and miscible salt transport to investigate the occurrence of seawater intrusion in the Korba plain in northern Tunisia. They examined the effect and interplay between pumping, artificial recharge, soil/aquifer properties and the unsaturated zone.

A quasi three-dimensional groundwater flow model was developed using MODFLOW to simulate groundwater basin flow characteristics in response to pumping and recharge scenarios by Johnson et al. (2001). Three major steps were taken to control saltwater intrusion; construction of saltwater barriers, basin adjudication to set a limit on groundwater extraction and artificial recharge. Liles et al. (2001) developed a groundwater model using MODFLOW with the objective of forecasting injection quantities and well locations needed to prevent saltwater intrusion. They used highly treated wastewater in injection into Orange County aquifers to prevent saltwater intrusion. Tompson et al. (2001) applied integrated isotopic characterization and numerical modelling techniques to assess the migration of reclaimed water that was used for artificial recharge in the coastal aquifer underlying Orange County, California to characterize the age of groundwater recharged in order to determine the distance between the recharge and production wells. It was shown that the recharged reclaimed wastewater must reside below the surface for at least one year before it could be produced for drinking water. This would present a technical challenge to the commercial and public sector hydrologic community.



Paniconi et al. (2001) used CODESA-3D to investigate the occurrence of seawater intrusion in eastern Cap-Bon, Tunisia. The model examined the interplay between pumping regime and recharge scenarios and its effect on controlling the saline water intrusion. Fitzgerald et al. (2001) presented a series of inter-related codes that together addressed the issues related to effective management of coastal aquifer systems. This set of tools included groundwater flow, solute transport and coupled flow and transport modeling codes. All of these codes were 3-D and linked by common database (input/output) files. Groundwater flow in a multi-aquifer system was simulated. Management practices such as aquifer storage and retrieval, injection barrier wells, optimization of pumping location and depths were evaluated.

Mukhopadhyay (2004) presented a laboratory study to investigate the effects of artificial recharge on the aquifer properties; porosity and hydraulic permeability. Recharged water may be groundwater-desalinated seawater mixed with 10% - treated waste water. Barrocu et al. (2004) implemented the CODESA-3D code with GIS to study the migration of contaminant and simulate the impact of land management using different groundwater abstraction schemes and artificial recharge in Sardinia, Italy. Vandenhede et al. (2008) presented a simulation model to study sustainable water management using artificial recharge of fresh water in the dunes of the western Belgian coastal plain by two recharge ponds. The recharged water was produced from secondary treated waste water effluent by the combination of ultra filtration and reverse osmosis.

***Advantages:*** Artificial recharge helps to increase the groundwater storage in the aquifer and prevent the intrusion of saline water.

***Disadvantages:*** The artificial recharge has been discussed in many papers as a solution to control saltwater intrusion. However, some of these models ignored the source of fresh water especially in the areas that suffer from scarcity of water. On the other hand the cost of fresh water in cases where it is not available in these areas and transported from other places has not been taken into consideration. Using desalinated seawater is costly and could be a source of pollution. The treated wastewater was used in many areas for recharge to control saltwater intrusion. This technique is often costly and ineffective in the areas where excessive groundwater pumping occurs (Narayan et al. 2002 and Narayan et al. 2006).

Treated waste water affects the aquifer properties and requires at least one year before abstraction from the aquifer. At present there is a growing opposition against artificial recharge by infiltration at the land surface, because it occupies a large area.

### ***2.5.6 Abstraction of saline water***

This method of control aims to reduce the volume of saltwater by extracting brackish water from the aquifer and returning to the sea. Figure 2.5 shows a sketch of an abstraction well. Sherif and Hamza (2001) developed a finite element model (2D-FED) considering dispersion and variable density flow to simulate the effect of pumping brackish water from the transition zone in order to restore balance between freshwater and saline water in coastal aquifer. The disposal of abstracted saline water was a problem. They proposed different solutions to use abstracted saline water for some purposes such as; cooling, desalting, injection into deep wells, irrigation, or disposal to the sea. Johnson and Sperry (2001) presented different methods to control saltwater intrusion in different states in the USA. In California they extracted saline water and desalinated it using RO treatment process. The treated water was blended with untreated groundwater to produce water suitable for domestic delivery. In Los Angeles injection wells were used to protect the coastal aquifers from saltwater intrusion. Potable and highly treated waste water was injected into the wells.

Maimone and Fitzgerald (2001) applied three dimensional groundwater flow models, dual phase sharp interface intrusion model, radial upconing model and single phase contaminant transport model to develop a coastal aquifer management plan. Two techniques were used; development of new well locations further inland and use of RO treatment for desalinating brackish water and using it for domestic purposes. Sherif and Kacimov (2008) suggested pumping brackish water, encountered between the freshwater and saline water bodies, to reduce the extension of seawater intrusion. They used SUTRA to examine different pumping scenarios in the vertical view and the equiconcentration lines and velocity vectors were identified for the different cases. They concluded that seawater intrusion problems could be controlled through proper pumping of saline groundwater from the coastal zone.

Kacimov et al. (2009) investigated seawater intrusion in coastal unconfined aquifers of Oman, experimentally, analytically and numerically. Water table elevation, capillary fringe, moisture distribution, EC were observed and measured in a pilot site Al-Hail, Oman. Laboratory measurements of conductivity and capillary rise were conducted in repacked columns in the laboratory. Evaporation from a shallow horizontal water table to a dry soil surface was modelled by HYDRUS2D. An analytical Dupuit-Forchheimer model was developed for the planar part of the catchment with explicit expressions for the water table, sharp interface and stored volume of fresh water. SUTRA code is used to study a variable density flow in a leaky aquifer with line sinks modelling fresh water withdrawal and evaporation. Both analytical and numerical models proved that pumping of saline groundwater from coastal aquifers would mitigate the migration of seawater into the aquifer and would contribute to the enhancement of the groundwater quality that is consistent with the findings of Sherif and Hamza (2001).

***Advantages:*** Abstraction of saline water decreases the volume of saline water in the aquifer and protects pumping wells from upconing.

***Disadvantages:*** The main problem in abstraction of brackish water is the disposal of the saline water. Many researchers have attempted to solve this problem but it is still a subject of current research. Brackish water is suitable only for certain types of crops and using it in cooling may cause corrosion to the systems. The disposal of brackish water into the sea could affect the marine life in these areas, fishing and tourism activities. Another problem is that increasing abstraction of saline water could, in some cases, increase the intrusion of saltwater (Abd-Elhamid and Javadi, 2008a).

### ***2.5.7 Combination techniques***

Combination between two or more of the above methods can help to eliminate the disadvantages of these methods and give better control of saltwater intrusion. Zhou et al. (2003) and Hong et al. (2004) used a combination of reduction in pumping rates and relocation of pumping wells to control saltwater intrusion. Maimone and Fitzgerald (2001) used development of new well locations further inland and use of RO treatment for desalinating brackish water and using it for domestic consumption to reduce the abstraction

from the aquifer. Narayan et al. (2006), Paniconi et al. (2001) and Barrocu et al. (2004) used reduction of pumping rates and recharge of freshwater to the aquifer. Johnson et al. (2001) used a combination of three techniques: subsurface barriers, reduction of abstraction rates and recharge of freshwater. Fitzgerald et al. (2001) used change of well locations, reduction of pumping rates and recharge of freshwater.

Combination of injection of freshwater and extraction of saline water can reduce the volume of saltwater and increase the volume of freshwater. Only few models have been developed for this technique. Georgpoulou et al. (2001) developed a decision aid tool to investigate the feasibility and applicability of a strategy involving the use of desalinated brackish groundwater, pumped from the aquifers, coupled with recharge of aquifers by reclaimed wastewater to control saltwater intrusion.

Mahesha (1996c) studied the control of seawater intrusion by a series of abstraction wells for saline water alone and also in combination with freshwater injection wells in a confined aquifer using a vertically integrated two dimensional sharp interface model under steady state conditions. It was found that the combination of injection wells with extraction wells produced excellent results to the individual cases for larger well spacing and small rates of injection. Rastogi et al. (2004) developed a two-dimensional steady state numerical model to study seawater intrusion problem involving hydrodynamic dispersion in synthetic multi-layered confined coastal aquifer. The model was used to investigate the efficiency of seawater control measures involving two scenarios; (i) freshwater recharge, and (ii) combination of freshwater recharge and saltwater discharge wells. The study found that depth, location and head of recharge wells are important parameters that can control saltwater intrusion. The model confirmed that combined recharge and discharge system is more effective in controlling seawater intrusion.

## 2.6 A new methodology to control saltwater intrusion (ADR)

This work presents a new methodology ADR (abstraction, desalination and recharge) to control saltwater intrusion in coastal aquifers. This method aims to overcome all or at least most of the limitations of the previous models. This methodology can help to control the saltwater intrusion in coastal aquifers considering different parameters such as; technical, economical and environmental aspects. Figure 2.6 shows a sketch of the new methodology (ADR) (Abd-Elhamid and Javadi, 2008a).

*The proposed methodology ADR consists of three steps:*

**Abstraction:** Abstraction of brackish water from the saline zone using abstraction wells.

**Desalination:** Desalination of the abstracted brackish water using small-scale RO plant.

**Recharge:** Recharge of the treated water using recharge wells into the aquifers.

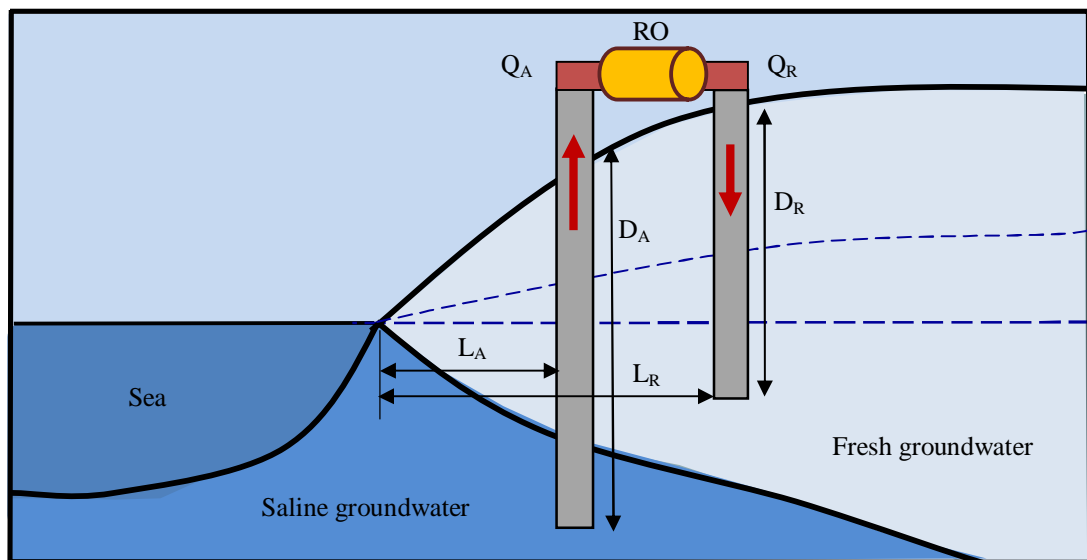


**Figure 2.6** Sketch of the new methodology (ADR)

The proposed methodology considers:

- 1- the relationship between abstraction and recharge rates;  $Q_A$  and  $Q_R$ ,
- 2- the locations of abstraction and recharge wells;  $L_A$  and  $L_R$ ,
- 3- the depths of abstraction and recharge wells;  $D_A$  and  $D_R$ ,
- 4- the aquifer properties,
- 5- construction and operation costs,
- 6- environmental impacts, and
- 7- climate changes, sea level rise and their effects on saltwater intrusion.

### ***2.6.1 The benefits of ADR methodology***

This method is a combination of two methods; abstraction of saline water and recharge of fresh water in addition to desalination of abstracted water and treatment to be ready for recharge or domestic use. It combines the advantages of these three steps as:

***The first step:*** Abstraction of brackish water helps to reduce the saline water volume in the aquifer and reduce the intrusion of saltwater.

***The second step:*** Desalination of abstracted brackish water using RO treatment process aims to produce fresh water from brackish water for recharge. This step is very important to produce freshwater in the areas where freshwater is scarce. The advantages of RO as a desalination method are discussed in details in the next section.

***The third step:*** Recharge of treated water aims to increase the fresh groundwater volume to prevent the intrusion of saltwater.

The combination of abstraction and recharge techniques is considered one of the most efficient methods to control saltwater intrusion. It increases the volume of fresh groundwater and decreases the volume of saltwater. This method is capable of retarding saltwater intrusion. It also has lower energy consumption, lower cost and lower environmental impact. ADR can be used to increase the water resources in coastal regions by increasing the abstraction of saline water and desalination. The excess reclaimed water can be used directly for different purposes or injected into the aquifer to increase the groundwater storage (Abd-Elhamid and Javadi, 2008a).

### ***2.6.2 Desalination of brackish groundwater using RO***

Desalination of seawater and brackish groundwater is considered a non-conventional method to produce freshwater in coastal areas. Desalination of brackish groundwater could increase the water supply in the region since it is technologically feasible and usually will not have much negative environmental impact. Brackish groundwater with an amount of TDS between 1,000 and 10,000 mg/l, can be desalinated at relatively low cost (compared with seawater which contains 35000 mg/l of TDS). Desalination is a process of removal of dissolved minerals (mainly salts) from either seawater or brackish groundwater to produce fresh water of potable water quality. The produced water is divided into two streams, one for potable water with a low TDS and the second for brine which includes high percentage of dissolved salts. Despite the evolution of desalination technologies, desalination has some major problems such as; high cost, environmental effects, carbon emission, land use for plants and noise, and disposal of brine waste which contain high salt concentration. Discharge of brine waste with high salt concentration and high temperature into the environment has many environmental impacts as it affects marine habitats at shores, tourism industry, fishing and fisheries industry, changes in the sea currents, temperature, salinity and density and increased salinity leading to increasing the salinity of groundwater.

The desalination can be accomplished by different techniques that can be classified under three main processes; thermal processes, membrane processes and other processes (Ismail, 2003). Thermal process consists of applying heat to the source of water to change the water phase to vapour and solid, separate salts and collect the condensed water vapour to produce pure water. A number of thermal methods can be used for desalination such as: Multistage Flash distillation, Multiple Effects Distillation and Vapour Compression. Membrane processes aim to separate the components with a membrane and without phase change, as they move in response to an externally applied pressure. Saline solution is pressurized to a point greater than the osmotic pressure of the solution, to separate water from salts. Two main processes of this type are used for desalination: Reverse Osmosis and Electro Dialysis. Other new desalinating processes are also used based on different techniques such as: ion exchange, membrane distillation, freezing separation, solar distillation, nuclear desalination.

The choice of a desalination method is not an easy one. The desalination method can be selected based on three main aspects; technical aspects, environmental aspects and economical aspects (Bakheet, 2006). Power costs in water desalination may account for 30 to 60 % of the operational costs, or about 30% to 50% of the total cost of the produced water depending on the type of energy used. So, if the power costs increase, there is a direct impact on the cost of the desalinated water. The challenge in desalination process is the reduction of energy used to reduce the total cost of the produced water. Several methods can be used for desalinating brackish groundwater but RO has become more attractive because it consumes less energy so it is cheaper and has less carbon emission, requires simple equipments, does not need to be linked to power plant, requires small area of land and produces less noise. In the last decades there has been a rapid progress in the RO desalination technology aiming to decrease the power consumption. A sharp reduction in the cost has occurred; the average price of desalination is one-tenth of what it was twenty years earlier, dropping dramatically from (\$5.50/m<sup>3</sup>) in 1970 to (\$0.55/m<sup>3</sup>) in 1999, including interest, capital recovery and operation and maintenance (Ismail, 2003).

Reverse osmosis is currently one of the fastest-growing techniques in water desalination. RO is a widely used method for desalinating water by using a pressure driven technique. It uses dynamic pressure to overcome the osmotic pressure of the salt solution. Water is forced to flow through small pores under high pressure through semi-impermeable membranes while salt is rejected. The pressure difference must be high enough to overcome the natural tendency of water to move from the low salt concentration side of a membrane to the high concentration side as defined by osmotic pressure. The major energy consumption comes from creating pressure. Small pores require high pressure and consequently more energy. The quality of produced water depends on efficiency of membranes, pressure and degree of salinity. Membranes are sensitive to pH, oxidizers, a wide range of organics, algae, and bacteria and of course particulates and other foulants. Therefore, pretreatment of the feed water is important in order to prevent membrane contamination and fouling where large particles are filtered. Pretreatment can offer a significant impact on the cost reduction of RO. On the other hand, RO post-treatment includes removing dissolved gasses (CO<sub>2</sub>), and stabilizing the pH via the addition of Ca or Na salts. Figure 2.7 shows a schematic sketch layout of a RO plant (Bakheet, 2006).



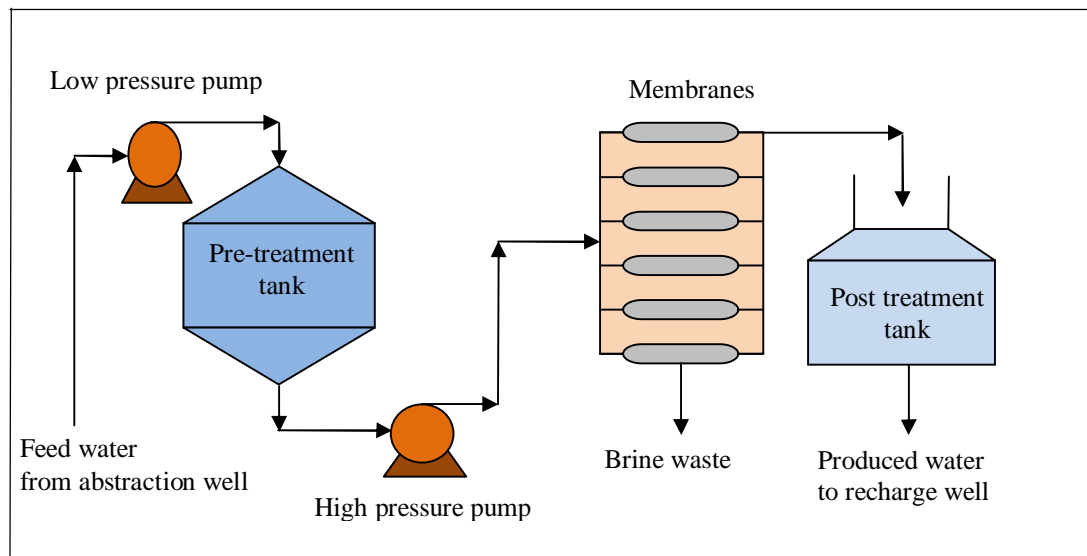


**Figure 2.7** Schematic sketch layout of RO desalination plant

Various models were developed to study the technical and economical feasibility of desalting brackish groundwater using RO. Al-Hadidi (1999) presented an economic feasibility study to desalination of brackish groundwater using RO and its use as a non-convictional water resource for integrated water resources management plan. The problem of the study was the use and disposal of brine waste. Georgpoulou et al. (2001) developed a decision aid tool for the investigation of feasibility and applicability of an alternative water supply strategy involving the use of desalinated brackish groundwater pumped from the aquifers coupled with aquifer recharge by reclaimed wastewater. Abderahman (2001) described the process of desalting brackish water and reuse after blending with freshwater. Shahalam et al. (2002) developed a combining unit process for pre-treatment of RO to improve the quality of feed water at a minimal cost and with minimal effects on succeeding the process.

Ramirez et al. (2003) used physical-chemical pre-treatment for the reverse osmosis unit for reclamation of secondary effluent. The produced water is suitable for injection into a groundwater aquifer to counteract saltwater intrusion. Al-azzan et al. (2003) used RO brine staging for desalination to increase the recovery rate to 97 % in Kuwait. El Sheikh et al. (2003) presented a technical and economical study to the cost and power consumption of reverse osmosis plants in Gaza strip. RO technology can substitute the deficit in domestic

water requirements with comparatively acceptable and affordable cost. Purnama et al. (2003) studied the impact of brine disposal operations on coastal and marine environment. These effects can be avoided by extending the outfalls further offshore to the sea.

Afonso et al. (2004) presented a study to assess the technical-economical feasibility of brackish groundwater treatment by RO for the production of potable water from brackish water in Mediterranean countries. The study proved that RO can produce potable water with low operating cost, and recovery rate of about 75%. Jaber and Ahmed (2004) presented technical and economical aspects of RO brackish water desalination plants in Gaza strip and estimated the quantities of desalinated brackish water over the planning period. Lopez-Ramirez et al. (2006) presented a study to determine the optimum conditions for physiochemical pre-treatment of secondary effluents for successful reverse osmosis operation for groundwater recharge. They concluded that high quality reclaimed wastewater can be used safely in groundwater recharge.

According to the literature, desalination of brackish groundwater has been successfully used as non-conventional source of water in coastal areas. Using RO for the desalination of brackish groundwater is a cost-effective method and is competitive with seawater desalination in terms of technical, economical and environmental aspects. RO produces high quality water which is friendly to the public health and the environment, the soil and the groundwater. The cost of desalinated brackish groundwater is dropping because of improvement in membrane technologies. Therefore, a small-scale RO brackish groundwater desalination plant is selected as a desalination method in the proposed ADR methodology to treat the abstracted brackish water and recharge it again to the aquifer to prevent the intrusion of saltwater. A combination of abstraction and recharge wells in addition to small-scale RO brackish groundwater desalination plant is a cost efficient system to control saltwater intrusion in coastal areas as it produces freshwater from brackish water to recharge the aquifer in order to prevent saltwater intrusion and the produced pure water can be used in domestic, irrigation and industry. A simulation-optimization model has been developed and will be discussed in the following chapters to determine the optimum cost of the ADR system considering the optimal well locations, depths and abstraction/recharge rates.

## Governing equations of coupled fluid flow and solute transport

### 3.1 Introduction

Groundwater is an important natural resource. Many agricultural, domestic and industrial water users rely on groundwater as the sole source because of its low cost and high quality. However, in recent years it has become clear that human activities and climate change have a negative impact on both quantity and quality of groundwater resources. The depletion of groundwater may occur due to excessive pumping and contamination of the groundwater by waste disposal or other activities. Coupled groundwater flow and solute transport models can be used to assess the impact of existing or proposed activities on groundwater quantity and quality (Istok, 1989).

This chapter presents background and theoretical formulation of coupled fluid flow and solute transport in saturated and unsaturated soil. The theoretical equations include the coupling between water flow, air flow, heat transfer and solute transport in saturated and unsaturated soil. The flow of moisture is governed by the liquid transfer and vapour transfer in soil. The flow of air in soil is considered to be a mixture of dry air transfer and water vapour transfer. The governing equations for both moisture flow and air transfer are based on the consideration of conservation of mass. The heat transfer in soil is driven by conduction, liquid convection and latent heat of vaporisation. The governing equation for heat transfer is based on the consideration of conservation of energy. The theoretical formulation of thermal and hydraulic behaviour in unsaturated soil will describe coupled water, air and heat flow in unsaturated soil. The governing equations are obtained in terms of the three primary variables; pore water pressure ( $u_w$ ), pore air pressure ( $u_a$ ) and absolute temperature ( $T$ ). Then, the governing equations that describe solute transport will be given for each phase and the mass transfer processes between phases will be discussed. The effects of different phenomena that govern the process of solute transport such as advection, diffusion, dispersion, adsorption, chemical reaction and biological degradation are also integrated into the model.

### ***3.2 History of coupled fluid flow and solute transport***

The interest in understanding the mechanism and prediction of solute transport through soils has increased in the last decades due to growing evidence and public concern that the quality of the subsurface environment is being adversely affected by industrial, municipal, agricultural activities and climate change. Salinization of groundwater due to saltwater intrusion is a special category of contaminants which should be studied and controlled because it increases the salinity of groundwater and then groundwater may become unsuitable for use. Accurate predictions need to be made regarding the movement of solute and energy transport in aquifers. This process can be divided into three sections: the fluid flow, energy transport and solute transport processes. Once the fluid pressure distribution through the domain is determined, the flow distribution may be obtained. Solute transport in the groundwater is done through different mechanisms such as; advection, diffusion, dispersion, adsorption, chemical reaction, and biological degradation. The transport of energy in the groundwater and solid matrix of the aquifer includes the changes in temperature due to the change in conduction, convection and latent heat transfer (AL-Najjar, 2006). In the following sections a review of fluid flow, energy transport and solute transport and coupling mechanisms is presented.

#### ***3.2.1 Fluid flow in saturated/unsaturated soils***

The fluid flow in soils includes groundwater flow and ground air flow. Groundwater hydrology is very important in evaluating the existing situation and maintaining the development of water resources. The study of groundwater flow has started by Darcy's experimente (Darcy, 1856), which introduced what is known as Darcy's law. Among the early applications of Darcy's law to groundwater, the contributions of Dupuit, Theim, Forchheimer, and Boussinesq were of particular note (Zheng and Bennett, 2002). A number of scientists have contributed to the theory of groundwater flow. Theis (1935) and Jacob (1950) in particular, are widely recognized for providing the basis for much of modern groundwater hydrology.

Over the years, many models have been developed to simulate groundwater flow. Gottardi and Venutlelli (2001) developed a finite element model to simulate water flow in saturated-unsaturated soils. The flow domain can be either in a vertical or in a horizontal plane, or in a 3-D system. Lapen et al. (2005) developed a 2-D steady-state finite element groundwater flow model to simulate groundwater flow and examined the sensitivity of flow system to changes in water recharge and aquifer properties. There have been many studies of movement of water in saturated and unsaturated soils. However, few have focused on the movement of the air phase. Most of these studies have ignored the influence of the water movement on the air phase (Binning, 1994). Green et al. (1970) were among the first to recognize the importance of the air phase in the unsaturated zone and include it in a one dimensional finite difference model of two-phase flow. However, the focus of many of the multiphase flow models of water and air movement in the unsaturated zone has been on the water phase. Recently, there has been a renewed focus on air movement in the unsaturated zone. To date there have only been a limited number of models that consider only the air phase. For example, Johnson et al. (1990) assumed constant moisture content to derive analytical solutions of air movement. Others who followed this approach include Mendoza and Frind (1990), Rathfelder et al. (1991), Benson et al. (1993) and McCarthy and Johnson (1993).

Groundwater flow can be studied in two zones separated by the water table. The region of low saturation values between the ground surface and the water table is called the unsaturated zone and the region that is found below the water table is called saturated zone (Gunduz, 2004). Groundwater flow could either be characterized by a three dimensional or a vertically averaged two dimensional model. A number of modelers have used a three dimensional representation of the groundwater flow (e.g., Frind and Verge, 1978; Huyakom et al. 1986 and McDonald and Harbaugh, 1988). Others such as Aral (1990) have preferred a vertically averaged two dimensional representation. The numerical simulation of the saturated groundwater flow equation is performed by finite element or finite difference method. The finite element method has found wide applications in the field of groundwater modelling and numerous models used the finite element discretisation (Huyakom et al., 1986 and Aral, 1990). McDonalds and Harbaugh (1988) applied the finite difference method.

The movement of moisture in variably saturated soil is often modelled by Richards' equation and closed by constitutive relations to describe the relationship among fluid pressures, saturations and hydraulic conductivities. The unsaturated zone is characterized by spatially and temporally varying levels of water content below saturation and negative capillary pressure heads. Over the years, three different forms of Richards' equation have been widely applied by scientists; pressure head-based equation, moisture content-based equation and mixed form of the equation with both the pressure head and the water content. Pressure-head based and moisture content-based equations were used by a number of researchers (e.g., Huang et al., 1996; Hills et al., 1989; Gottardi and Venutelli, 1993; Pan and Wierenga, 1997). However, these forms of Richards' equations have limitations in application to simulate the saturated conditions (AL-Najjar, 2006).

The mixed-form has been proposed to overcome the difficulties associated with both the pressure-based and the moisture content-based forms of Richards' equation. This method uses both the moisture content and the pressure head as the dependent variables. Celia et al. (1990) solved Richard's equation using a method that employs the mixed form of the equations to guarantee mass conservation. The method has been shown to be robust and accurate, but requires a fine spatial and temporal discretization and so is fairly computationally demanding (Binning, 1994). The mixed form has both the superior mass conservation characteristics of the moisture content-based equation as well as the unlimited applicability to both saturated and unsaturated regions of flow that the pressure-based equation offers (AL-Najjar, 2006). The numerical solution of the mixed form has found wide applicability in the last decade and many researchers used this form to model the flow in variably saturated-unsaturated media (e.g., Tocci et al., 1997; Miller et al., 1998; Williams and Miller, 1999; Zhang and Ewen, 2000 and Zhang et al, 2002). A number of analytical solutions have been developed for transient infiltration under various boundary conditions (e.g., Philip and Knight (1991), Wilson and Gelhar (1981) and Van Genuchten (1980)). Unsaturated drainage of a uniformly wet soil was solved by Sisson et al. (1980) for gravitational flow, whereas more complicated solutions for drainage with capillary suction was derived by Warrick et al., (1990) and Philip (1992).

### **3.2.2 Energy transport**

Energy-transport simulation may be employed to model thermal regimes in aquifers, subsurface heat conduction, aquifer thermal-energy storage systems, geothermal reservoirs, thermal pollution of aquifers, and natural hydrogeologic convection systems (Voss and Provost, 2003). Energy is transported in the water-solid matrix by flow of groundwater and by the thermal conduction from higher to lower temperature through both the fluid and solid. In fact, the average velocity of fluid is affected by variation in temperature because change in temperature leads to the change in density and viscosity and subsequently the fluid velocity. The simulation of energy transport is based on the change of the amount of energy stored in the solid matrix and fluid. The stored energy in a volume may change due to ambient water with different temperature flowing in, well water of a different temperature injected, changes in the total mass of water in the block, thermal conduction (energy diffusion) into or out, and energy production or loss due to nuclear, chemical or biological reactions. The transport of energy in the groundwater and solid matrix of an aquifer includes the changes in temperature due to the change in conduction, convection and latent heat transfer (Voss and Provost, 2003).

Energy transport is simulated through numerical solution of an energy-balance equation. The solid grains of the aquifer matrix and fluid are locally assumed to have equal temperature, and fluid density and viscosity may be affected by the temperature. A number of numerical models have been developed to simulate fluid flow and energy transport in soil. Dakshanamurthy and Fredlund (1981) proposed a one dimensional formulation for coupled heat, mass and air flow in unsaturated soils. Three partial differential equations were employed to describe the three flow phases in an unsaturated soil. The differential equation for air flow was based on Fick's law and the differential equation for fluid and water vapour flow (moisture flow) was based on Darcy's law. Water vapour flow due to diffusion and advection processes was also considered. A Fourier diffusion equation was employed to describe heat flow in unsaturated soils. Heat flow due to conduction and latent heat transfer caused by phase changes were also considered in the heat flow. A finite difference scheme was applied to solve the governing equations and the proposed model was applied to simulate the coupled flow behavior of compacted Regina clay.

### ***3.2.3 Solute transport in saturated/unsaturated soils***

In recent years, great efforts have been directed towards establishing better knowledge of what governs solute transport in soils. Solute transport was considered only in a very limited way in early groundwater investigations. The method of analysis generally applied was advective calculation, in which solutes were assumed to move at the calculated average velocity of the groundwater, and to be unaffected by sorption, kinetic reaction, and other processes. The transport problem in porous media was the subject of extensive research in the chemical engineering field. Within the field of groundwater, it was recognized that the average fluid velocity did not describe the actual motion of individual solute particles, and that advective calculation could therefore never give a full description of solute movement (AL-Najjar, 2006). A number of laboratory and theoretical investigations of dispersion were done by Day (1956) and Rifai et al. (1956). The theory of advective-dispersive transport continued to develop by Bear (1961) and Bachmat (1967). A number of analytical solutions to the advective-dispersive transport equation were developed in this period; several of these are summarized by Ogata (1970).

The modelling of transport in groundwater flow has been done using different analytical and numerical methods. Analytical solutions to selected groundwater flow and solute transport problems are discussed in Bear (1979). Finite element codes have also been used effectively to simulate transport of subsurface contaminants (Bear et al., 1993; Istok, 1989). Numerous mathematical models were developed for simulating groundwater flow and solute transport. Nwaogazie (1986) developed a two dimensional transient finite element code for modelling groundwater flow and transport. Ahuja and Lehman (1983) and Wallach et al. (1989) applied a diffusive transport model to predict the solute transport in soil in the absence of infiltration. Snyder and Woolhiser (1985) conjectured that using a convective-dispersive model of solute transport in soils would be most appropriate when infiltration occur. Their model was used by Wallach and Shabtai (1992) to describe the downward solute movement in soil in the presence of surface water. Zienkiewicz and Codina (1995) applied the characteristic Galerkin method to the advection-diffusion problems and developed an explicit algorithm for these problems.



Smith et al. (1992) developed a non-equilibrium sorption dispersion-advection model that involves a convolution integral of the product of the rate of change of concentration and a time dependent sorption coefficient. Sheng and Smith (2002) presented a two dimensional finite element method for the solution of advection-dispersion transport equation for multi component contaminants. Their analysis was restricted to nonlinear, equilibrium controlled sorption and exchange of soluble inorganic ions. Zhang and Brusseau (2004) presented a distributed domain mathematical model incorporating the primary mass transfer processes that mediate the transport of immiscible organic liquid constituents in water-saturated, locally heterogeneous porous media. Specifically, the impact of grain heterogeneity on immiscible liquid dissolution and sorption and desorption was represented in the model by describing the system as comprising a continuous distribution of mass-transfer domains. Kacur et al. (2004) discussed the numerical approximation schemes for the solution of contaminant transport with adsorption in dual-well flow. Their method was based on time stepping and operator splitting for the transport with adsorption and diffusion. The nonlinear diffusion was solved by a finite volume method and by Newton's type of linearization.

Remesikova (2005) introduced an efficient operator splitting scheme for solving two dimensional convection-diffusion problems with adsorption. He particularly, considered a practical problem of soil parameters identification using dual-well tests by using a general mathematical model including contaminant transport, mechanical dispersion and molecular diffusion and adsorption in both equilibrium and non-equilibrium models. However, due to the transformation, the transport problem (linear or non-linear) was reduced to one dimensional and solved in an analytical form. The dispersion part was solved using standard finite volume method. In spite of all the advances achieved and new techniques developed, there is no single technique that can yield completely satisfactory solutions to the numerical solution of advection-dominated contaminant transport. It remains a difficult problem due to the often contradictory needs to suppress numerical dispersion, avoid artificial oscillation and conserve mass (Gunduz, 2004).

In the recent years, there has been a profusion of studies of the transport equations in the unsaturated zone. The impetus for this rapid development has been the strict regulatory stance on groundwater pollution (Gee et al., 1991). Therefore, research on solute transport in the unsaturated zone has become more important and the studies for developing numerical models have increased. A number of analytical methods were developed to simulate water movement and solute transport in unsaturated zones (Islas and Illangasekare, 1992 and Barry et al., 1993). Smiles et al. (1978) developed a quasi-analytical solution for non-reactive solute flow during unsteady horizontal infiltration under constant concentration boundary conditions which has been discussed by Watson and Jones (1981) particularly in relation to assessing the performance of the solute model. Lessoff and Indelman (2004) presented an analytical model of advective solute transport by unsteady unsaturated gravitational infiltration.

Finite difference techniques are the simplest of the numerical techniques to apply and there are a large number of models using this solution technique. Weeks et al. (1982) were some of the first to use a numerical model to study transport in the unsaturated zone. The finite difference models range from the simple one dimensional model of Rosenbloom et al. (1993) through to the comprehensive model of Sleep and Sykes (1993). The finite difference models have usually used forward (explicit) time stepping. Benson et al. (1993) and Sleep and Sykes (1993) presented a summary of the arguments for the different forms of temporal discretization. The implicit method is more computationally expensive than the explicit method. The implicit time stepping scheme is unconditionally stable, so that large time steps can be taken. However, large time steps may not be advantageous in an implicit scheme as the truncation error increases with time step size leading to a loss of accuracy in the solution. In contrast, the explicit methods do have a limitation on the time step size, so that small time steps must be taken. Accuracy of an explicit scheme increases with increasing time step size.

Another common numerical approach to solving the transport equations has been to use the finite element method. The Galerkin finite element method was applied by Mendoza and Frind (1990) and Culver et al. (1991). The solutions obtained by the method are prone to oscillations. Karkuri and Molenkamp (1997) analyzed the advection-dispersion of non-reactive pollutant movement through a layered porous medium domain under the effect of

transient groundwater flow. The governing partial differential equations of the groundwater flow and advection-dispersion of pollutant together with their integral formulations were based on Galerkin's method and Green's theorem. Li et al. (1999) presented a numerical model to simulate miscible contaminant transport through unsaturated soils to account for the influence of multiple non-equilibrium sources on the contaminant transport. Marshall et al. (2000) developed a general methodology for investigating the effect of short-term temporal variability in infiltration on the long term transport of contaminants in soils. A one dimensional, unsaturated transport model was used to simulate the transport of a sorbing, non-volatile solute, using either steady state or randomly varying infiltration. Islam and Singhal (2002) presented a one dimensional reactive multi-component landfill leachate transport model coupled to three modules (geochemical equilibrium, kinetic biodegradation, and kinetic precipitation–dissolution) to simulate the migration of contaminants in soils under landfills. It was found that, the transport of contaminants through unsaturated soil is influenced by several processes, two of the most important being sorption and transformation.

Worch (2004) presented a solute transport model that describes non-equilibrium adsorption in soil and groundwater systems by mass transfer equations for film and intraparticle diffusion. Furthermore, a sensitivity analysis was performed to illustrate the influence of different process and sorption parameters on the shape of the calculated breakthrough curves. Kacur et al. (2004) described a numerical approximation scheme for the solution of contaminant transport problems with diffusion and adsorption in equilibrium and non-equilibrium modes. Kacur et al. (2004) method was based on time stepping and operator splitting. The non-linear transport was solved semi-analytically via the multiple Riemann problems, the non-linear diffusion by a finite volume method and by Newton's type of linearization. Finally the reaction part, incorporating the non-equilibrium adsorption, was transformed to an integral equation which was solved numerically using time discretization. Several researchers have tried to improve the finite element solution by adding upstream weighting. Upstream weighting was demonstrated to be effective in reducing oscillations in the saturated transport equation by Dick (1983).

### ***3.2.4 Coupling mechanisms***

Over the years, a number of models have been developed for coupling fluid flow, heat transfer and solute transport. Couvillion and Hartley (1985) investigated the movement of thermally induced drying fronts in sandy soils and presented an explicit finite difference solution of three governing equations describing the flow of heat, moisture and air. Geraminegad and Saxena (1986) presented a mathematical model for the flow of heat, moisture and gas in unsaturated porous media. Three linear partial differential equations were derived; one for heat flow based on a modified Philip and de Vries approach, one for liquid flow based on a modified Philip and de Vries approach and one for gas flow based on Darcy's law.

Pollock (1986) developed a mathematical model to describe the coupled transport of energy, liquid water and water vapour, and dry air transport in unsaturated media. Three coupled non-linear partial differential equations were developed, each describing one flow phase. Connell and Bell (1993) developed a numerical model to describe coupled liquid and vapour flow processes in waste dumps under climatic influences. Three governing equations were developed to describe the flow of liquid, air and heat. Thermodynamic equilibrium between liquid and vapour phases was not assumed for this model. Instead, separate relationships were employed for vapour (viscous vapour and diffusive vapour) and liquid phases. Pinder and Abriola (1986) solved the fully coupled three phase problem using an implicit finite difference model with a Newton Raphson non-linear iteration scheme with the assumption of a constant-pressure immobile gas. Zhou and Rowe (2005) analysed a set of fully coupled governing equations expressed in terms of displacement, capillary pressure, air pressure, and temperature increase and solved the equations using the finite element method with a mass conservative numerical scheme. Gawin et al. (2005) described a fully coupled numerical model to simulate the flow transient phenomena involving heat and mass transfer in deforming porous media. The governing differential equations were solved simultaneously in terms of displacements, temperature and capillary pressure using the finite element method.

Thomas and Ferguson (1999) presented a coupled heat and mass transfer numerical model describing the migration of a contaminant gas through unsaturated porous medium. The model treats the migration of liquid water, air, heat and contaminant gas separately with independent system variables of capillary potential, temperature, pore air pressure and concentration of the contaminant gas. Sheng and Smith (2000) presented a characteristic finite element algorithm for modelling contaminant transport problems coupled with nonlinear adsorption. Crowe et al. (2004) developed a numerical model for simulating groundwater-wetland interactions and contaminant transport. The model calculated transient hydraulic head in a two dimensional heterogeneous domain.

Liang et al. (2002) studied the transport mechanism of hydrophobic organic chemicals and the energy change in a soil/solvent system. A soil leaching column chromatographic experiment at an environmental temperature range of 20-40° C was carried out. It was found that the transport process quickens with the increase of column temperature. Gao (2001) presented a model for simulating the transport of chemically reactive components in conjunction with energy transport in saturated and unsaturated groundwater systems. McGrail (2001) developed a numerically based simulator to assist in the interpretation of complex laboratory experiments examining transport processes of chemical and biological contaminants subject to nonlinear adsorption or source terms. Javadi and Al-Najjar (2008) and Javadi et al. (2008) presented a numerical model for the simulation of water and air and contaminant transport through unsaturated soils considering chemical reactions and assuming constant density flow.

Saltwater intrusion in coastal aquifers has been simulated using different methods. Coupled fluid flow and solute transport models can help in understanding the mechanism of saltwater intrusion and can be applied in the prediction of solute concentration in coastal aquifers. A review of fluid flow, solute transport, and coupling mechanisms has been presented. The following sections present the development of coupled fluid flow and solute transport model to simulate saltwater intrusion in coastal aquifers.

### 3.3 The governing equation for the moisture transfer

The moisture transfer in unsaturated soils is composed of two main phase movements: water transfer and water vapour transfer. The volumetric moisture content in unsaturated soil,  $\theta$ , is defined as the sum of volumetric water content,  $\theta_w$ , and volumetric vapour content,  $\theta_v$ :

$$\theta = \theta_w + \theta_v \quad (3.1)$$

The law of conservation of mass for water phase states that the temporal discretisation of the water content must be equal to the spatial discretisation of the water flux and this can be written as (Ramesh, 1996):

$$\rho_w \frac{\partial \theta_w}{\partial t} = -\rho_w \nabla v_w - \rho_w F \quad (3.2)$$

where,

$\rho_w$  : is the density of water  $[M][L]^{-3}$ ,

$t$  : is the time [T],

$v_w$  : is the velocity of water  $[L][T]^{-1}$ ,

$F$  : is the source or sink term.

Similarly, the law of conservation of mass for vapour phase states that the temporal discretisation of the vapour content must be equal to the spatial discretisation of vapour flux and this can be written as (Ramesh, 1996):

$$\rho_v \frac{\partial \theta_v}{\partial t} = -\rho_v \nabla v_v - \nabla(\rho_v v_a) + \rho_w F \quad (3.3)$$

where,

$\rho_v$  : is the density of water vapour  $[M][L]^{-3}$ .

$v_a$  : is the velocity of the air [L][T]<sup>-1</sup>.

$v_v$  : is the velocity of the water vapour [L][T]<sup>-1</sup>.

By substituting equations (3.2) and (3.3) into (3.1), the conservation of mass for moisture transfer can be written as:

$$\frac{\partial(\theta_w \rho_w)}{\partial t} + \frac{\partial(\theta_a \rho_v)}{\partial t} + \nabla(v_w \rho_w) + \nabla(v_v \rho_w) + \nabla(v_a \rho_v) = 0 \quad (3.4)$$

The volumetric water content  $\theta_w$  and the volumetric air content  $\theta_a$  can be expressed in terms of porosity  $n$  and degree of saturation as following:

$$\theta_w = nS_w \quad (3.5)$$

$$\theta_a = nS_a \quad (3.6)$$

$$S_a = 1 - S_w \quad (3.7)$$

where,

$S_w$  : is the degree of water saturation in unsaturated soil and

$S_a$  : is the degree of air saturation in unsaturated soil.

Substituting equations (3.5) and (3.6) into (3.4) the governing equation for the moisture transfer can be expressed as:

$$\frac{\partial(nS_w \rho_w)}{\partial t} + \frac{\partial(nS_a \rho_v)}{\partial t} + \nabla(v_w \rho_w) + \nabla(v_v \rho_w) + \nabla(v_a \rho_v) = 0 \quad (3.8)$$

From equation (3.8) the flow of water is governed by the pressure head gradient and a gradient due to elevations differences and vapour transport is governed by the diffusive and pressure flows. Therefore, the various components of each flow phase and the flow laws of the two phases of moisture transfer, namely, water flow and vapour flow are explained separately in next sections.

### 3.3.1 Water flow

The hydraulic head gradient is defined as the sum of the pressure head and the elevation head gradients, which is considered the potential driving force for water flow (Fredlund and Rahardjo, 1993). According to Darcy's law the velocity of water  $v_w$  can be expressed as (Darcy, 1856):

$$v_w = -K_w \left[ \nabla \left( \frac{u_w}{\gamma_w} \right) + \nabla z \right] \quad (3.9)$$

where,

$K_w$  : is the hydraulic conductivity of water  $[L][T]^{-1}$ .

$u_w$  : is the pore water pressure (hydraulic pressure)  $[M][L]^{-1}[T]^{-2}$ .

$\gamma_w$  : is the unit weight of water  $[M][L]^{-2}[T]^{-2}$ .

$\nabla z$  : is the unit normal oriented downwards in the direction of the force of gravity.

The relation between pore water pressure and hydraulic head can be expressed as (Fredlund and Rahardjo, 1993):

$$h_w = \frac{u_w}{\rho_w g} + z \quad (3.10)$$

where,

$h_w$  : is the hydraulic head [L]

$g$  : is the gravitational acceleration  $[L][T]^{-2}$ .

$z$  : is the elevation above the datum (positive upwards) [L].

The hydraulic conductivity can be expressed as (Fredlund and Rahardjo, 1993):

$$K_w = \frac{\rho_w g k_w}{\mu_w} \quad (3.11)$$



where,

$k_w$  : is the effective permeability of water [L]<sup>2</sup>

$\mu_w$  : is the dynamic viscosity of water [M][L]<sup>-1</sup>[T]<sup>-1</sup>

Kaye and Laby (1973) expressed the dependence of dynamic viscosity of liquid water  $\mu_w$  ( $Ns/m^2$ ) on absolute temperature  $T$  in the form of a relation as:

$$\mu_w(T) = 661.2(T - 229)^{-1.562} * 10^{-3} + 0.5\% \quad (3.12)$$

The hydraulic conductivity of unsaturated soil is influenced by a number of factors such as mineralogical composition, particle sizes and the size distribution, void ratio  $e$  and the fluid characteristics (Mitchell, 1976). Hydraulic conductivity is a function of any two of three possible volume-mass properties (Lloret and Alonso, 1980 and Fredlund, 1981) as following:

$$K_w = K_w(e, S_w) \quad (3.13)$$

$$K_w = K_w(e, \theta_w) \quad (3.14)$$

$$K_w = K_w(\theta_w, S_w) \quad (3.15)$$

In general, the hydraulic conductivity is significantly affected by the combined change in void ratio and degree of saturation of the soil (Fredlund and Rahardjo, 1993). Matyas and Radhakrishna (1968) proposed that the water degree of saturation  $S_w$  could be expressed as stress dependent quantity and initial void ratio, initial degree of saturation and stress parameters, namely, net stress, deviatoric stress, and suction. Alonso et al. (1988) and Fredlund and Rahardjo (1993) pointed out that the effect of changes in stress on the degree of saturation is insignificant and can be negligible. Therefore, the major effect on the degree of saturation comes from the changes in suction. Suction,  $s$ , is defined as the difference between pore air pressure  $u_a$  and pore water pressure  $u_w$  and is mathematically represented as:

$$s = (u_a - u_w) \quad (3.16)$$

The soil suction was referred to as the free energy state of soil water (Edlefsen and Anderson (1943) and Fredlund and Rahardjo (1993)). Thus, for unsaturated soils, suction is dependent on the surface energy  $\xi$ , which is in turn, dependent on absolute temperature  $T$ . Therefore suction  $s$  at any moisture content  $\theta_w$  and temperature  $T$  can be obtained by the following relationship:

$$s(\theta_w, T) = \frac{\xi(T)}{\xi_r(T_r)} s_r(\theta_w, T_r) \quad (3.17)$$

where,

$T_r$  : is the reference temperature.

$s_r$  : is the suction at the reference temperature.

$\xi_r$  : is the surface energy at the reference temperature.

$\xi$  : is the surface energy at the given temperature  $T$ .

Edlefsen and Anderson (1943) proposed a relation between the state surface energy  $\xi$  and the absolute temperature  $T$  as:

$$\xi = 0.1171 - 0.00001516T \quad (3.18)$$

Incorporating the above mentioned variation of suction with temperature, the degree of saturation of water can be expressed as:

$$S_w = S_w(s, T) \quad (3.19)$$

or in differential form as:

$$\frac{\partial S_w}{\partial t} = \frac{\partial S_w}{\partial s} \frac{\partial s}{\partial t} + \frac{\partial S_w}{\partial T} \frac{\partial T}{\partial t} \quad (3.20)$$

By substituting equation (3.16) into equation (3.20)

$$\frac{\partial S_w}{\partial t} = \left[ \frac{\partial S_w}{\partial s} \frac{\partial u_a}{\partial t} - \frac{\partial S_w}{\partial s} \frac{\partial u_w}{\partial t} \right] + \frac{\partial S_w}{\partial T} \frac{\partial T}{\partial t} \quad (3.21)$$

### 3.3.2 Water vapour flow

The vapour transfer in unsaturated soils occurs as a result of diffusive and pressure flows. The air phase is in bulk motion due to free or forced convection (Rohsenow and Choi 1961). This bulk air is considered to be a binary mixture of water vapour and dry air. Soil water content has a significant effect on the air permeability. In general, higher water contents reduce the air-filled porosity, thereby decreasing the connected pores through which air can flow by advection. The part of vapour transferred by the pressure flow is governed by the movement of the air mixture and can be described using the extension of Darcy's law. The part of vapour transferred by diffusion can be interpreted using the theory of Philip and de Vries (1957). Fick's (1855) and Darcy's laws have been commonly used to describe the flow of air through a porous media. According to generalised Darcy's law in unsaturated soil, the velocity of pore air  $v_a$  can be defined as:

$$v_a = -\frac{k_a}{\mu_a} \nabla u_a = -K_a \nabla u_a \quad (3.22)$$

where,

$k_a$  : is the effective permeability of air [L]<sup>2</sup>

$\mu_a$  : is the absolute viscosity of air [M][L]<sup>-1</sup>[T]<sup>-1</sup>

$K_a$  : is the unsaturated conductivity of air [L][T]<sup>-1</sup>, which can be defined as following:

$$K_a = \frac{\rho_a g k_a}{\mu_a} \quad (3.23)$$

where,  $\rho_a$  : is the density of air [M][L]<sup>-3</sup>

The air properties can be considered to be constant and the only properties that affect the conductivity of air are the volume-mass properties such as the degree of saturation and the void ratio (Fredlund and Rahardjo, 1993):

$$K_a = K_a(e, S_a) \quad (3.24)$$

Philip and de Vries (1957) proposed an expression for the vapour velocity  $v_v$  as:

$$v_v = -\frac{D_{atms} V_v \tau_v \theta_a}{\rho_w} \nabla \rho_v \quad (3.25)$$

where,

$D_{atms}$  : is the molecular diffusivity of vapour through air.

$V_v$  : is the mass flow factor.

$\tau_v$  : is the vapour tortuosity factor.

$\nabla \rho_v$  : is the vapour density gradient.

The determination of these parameters which describe the vapour velocity is discussed below.

Philip and de Vries (1957) adopted the approach suggested by Krischer and Rohnlter (1940) to determine the molecular diffusivity  $D_{atms}$  (Ramesh, 1996), where the diffusion due to the temperature gradient was represented by the expression:

$$D_{atms} = 5.893 * 10^{-6} \frac{T^{23}}{u_a} \quad (\text{m}^2/\text{sec}) \quad (3.26)$$

where,  $T$  is the absolute temperature. This equation is valid in the temperature range of (20 – 70  $C^\circ$ , 293 - 343  $K^\circ$ ).

The mass flow factor  $V_v$  is evaluated as suggested by Philip and de Vries (1957). They adopted the expression suggested by Partington (1949), who showed that for steady state diffusion in closed system between evaporating source and a condensing sink, the mass flow factor  $V_v$  can be expressed as:

$$V_v = \frac{u_a - u_v}{u_a} \quad (3.27)$$

where  $u_v$  is the pore water vapour pressure  $[M][L]^{-1}[L]^{-2}$ , which can be calculate as:

$$u_v = \rho_v R_v T \quad (3.28)$$

where,

$R_v$  : is the specific gas constant for water vapour  $[L]^2[T]^{-2}[K]^{-1}$  (461.5J/kg K).

Philip and de Vries, (1957) suggested that expression for mass flow factor in equation (3.27) may not be valid under non-stationary conditions, but the value is quite close to 1 under normal soil temperatures.

Edlefsen and Anderson (1943) proposed a thermodynamic relationship for the density of water vapour  $\rho_v$ , as:

$$\rho_v = \rho_0 h = \rho_0 \exp\left(\frac{\psi g}{R_v T}\right) \quad (3.29)$$

where  $h$  is the relative humidity,  $\psi$  is the capillary potential, which is given by:

$$\psi = \frac{u_w - u_a}{\gamma_w} \quad (3.30)$$

and  $\rho_0$  is the saturated soil vapour density  $[M][L]^{-3}$  and can be calculated by a relationship was given by Ewen and Thomas (1989) as:

$$\frac{1}{\rho_0} = \left[ 194.4 \exp\{-0.06374(T - 273) + 0.1634 * 10^{-3}(T - 273)^2\} \right]^{-1} \quad (3.31)$$

The density of pore vapour  $\rho_v$  is dependent on the saturated soil vapour density  $\rho_0$  (which is dependent on the absolute temperature  $T$ ) and the relative humidity  $h$  (which is dependent on both suction  $s$  and temperature  $T$ ). Thus, the gradient of vapour density  $\nabla\rho_v$  can be represented as:

$$\nabla\rho_v = h\nabla\rho_0 + \rho_0\nabla h \quad (3.32)$$

By expanding the terms

$$\nabla\rho_v = h\left(\frac{\partial\rho_0}{\partial T}\nabla T\right) + \rho_0\left(\frac{\partial h}{\partial\psi}\frac{\partial\psi}{\partial s}\nabla s + \frac{\partial h}{\partial T}\nabla T\right) \quad (3.33)$$

By substituting suction from equation (3.16) into equation (3.33) and rearrange the terms, the gradient of vapour density  $\nabla\rho_v$  can be written as:

$$\nabla\rho_v = \left(\rho_0\frac{\partial h}{\partial\psi}\frac{\partial\psi}{\partial s}\nabla(u_a - u_w)\right) + \left(h\frac{\partial\rho_0}{\partial T} + \rho_0\frac{\partial h}{\partial T}\right)\nabla T \quad (3.34)$$

or,

$$\nabla\rho_v = K_{fw}\nabla u_w + K_{fa}\nabla u_a + K_{fT}\nabla T \quad (3.35)$$

where,

$$K_{fw} = -\rho_0\frac{\partial h}{\partial\psi}\frac{\partial\psi}{\partial s} \quad (3.36)$$

$$K_{fa} = \rho_0\frac{\partial h}{\partial\psi}\frac{\partial\psi}{\partial s} \quad (3.37)$$

$$K_{fT} = h \frac{\partial \rho_0}{\partial T} + \rho_0 \frac{\partial h}{\partial T} \quad (3.38)$$

Substitute equation (3.35) into equation (3.25) the velocity of water vapour can be written as:

$$v_v = \left( -\frac{D_{atms} V_v \tau_v \theta_a}{\rho_w} K_{fa} \nabla u_a - \frac{D_{atms} V_v \tau_v \theta_a}{\rho_w} K_{fw} \nabla u_w - \frac{D_{atms} V_v \tau_v \theta_a}{\rho_w} K_{fT} \nabla T \right) \quad (3.39)$$

Philip and de Vries (1957) indicated that the theory proposed in the equation (3.39) could not satisfactorily predict vapour transfer under a thermal gradient. Two refinements were made to the thermal gradient term (Ramesh, 1996):

- Adding a flow area factor  $f$  in an attempt to reduce the vapour flow with increasing reduction in the available flow area.
- Introducing a pore temperature gradient  $\frac{(\nabla T)_a}{\nabla T}$  which is the ratio of the average temperature gradient in the air filled pores to the overall temperature gradient.

Introducing these two refinements, the expression for vapour velocity in equation (3.39) can be written as:

$$v_v = \left( -\frac{D_{atms} V_v \tau_v \theta_a}{\rho_w} K_{fa} \nabla u_a - \frac{D_{atms} V_v \tau_v \theta_a}{\rho_w} K_{fw} \nabla u_w - f \frac{D_{atms} V_v (\nabla T)_a}{\rho_w \nabla T} K_{fT} \nabla T \right) \quad (3.40)$$

Preece (1975) suggested an expression of pore temperature gradient (Ramesh, 1996) which has been implemented in the present work and is defined as:

$$\frac{(\nabla T)_a}{\nabla T} = \frac{1}{3} \left[ \frac{2}{1+BG} + \frac{1}{1+B(1-2G_v)} \right] \quad (3.41)$$

where,

$$B = \left[ \frac{(\chi_a + \chi_v)}{\chi_w} - 1 \right] \quad (3.42)$$

$$G_V = \left\{ \begin{array}{ll} \frac{0.3333 - 0.325(n - \theta_w)}{n} & 0.09 < \theta_w < n \\ 0.0033 + 11.11\theta_w \left( \frac{0.33 - 0.325(n - 0.09)}{n} \right) & 0 < \theta_w < 0.09 \end{array} \right\} \quad (3.43)$$

where,

$\chi_w$  : is the thermal conductivity of water  $[M][L][T]^{-3}[K]^{-1}$  .

$\chi_a$  : is the thermal conductivity of air  $[M][L][T]^{-3}[K]^{-1}$  .

$\chi_v$  : is the thermal conductivity of vapour  $[M][L][T]^{-3}[K]^{-1}$  which can be expressed as:

$$\chi_v = D_{atms} V_v h L \frac{\partial \rho_0}{\partial t} \quad (3.44)$$

Ewen and Thomas, (1989) suggested two alternatives to extend vapour velocity equation proposed by Philip and de Vries, (1957) these alternatives are:

- The vapour flow area factor  $f$  should be present in both temperature and moisture gradient terms.
- The flow area factor  $(\tau_v \theta_a)$  can be modified to be equal to the porosity to avoid choking occurrence of vapour flow at high moisture contents.

By including these to changes and rewriting the equation (3.40), the vapour velocity can be written as:

$$v_v = \left( -\frac{D_{atms} V_v n}{\rho_w} K_{fa} \nabla u_a - \frac{D_{atms} V_v n}{\rho_w} K_{fw} \nabla u_w - \frac{D_{atms} V_v n (\nabla T)_a}{\rho_w \nabla T} K_{fT} \nabla T \right) \quad (3.45)$$



or,

$$v_v = K_{vw} \nabla u_w + K_{va} \nabla u_a + K_{vT} \nabla T \quad (3.46)$$

where,

$$K_{vw} = -\frac{D_{atms} V_v n}{\rho_w} K_{fw} \quad (3.47)$$

$$K_{va} = -\frac{D_{atms} V_v n}{\rho_w} K_{fa} \quad (3.48)$$

$$K_{vT} = -\frac{D_{atms} V_v n (\nabla T)_a}{\rho_w \nabla T} K_{fT} \quad (3.49)$$

### 3.3.3 Mass balance equation for the moisture transfer

The various components of liquid transfer and vapour transfer have been discussed in the previous sections. These components are used to derive the governing equation for the moisture transfer. Substituting equations (3.7), (3.9), (3.22) and (3.46) into equation (3.8) the mass conservation equation for the moisture flow can be written as:

$$\begin{aligned} & \left[ \frac{\partial(nS_w \rho_w)}{\partial t} + \frac{\partial(n\{1-S_w\} \rho_v)}{\partial t} \right] + \nabla \left( \left\{ -K_w \left[ \nabla \left( \frac{u_w}{\gamma_w} \right) + \nabla z \right] \right\} \rho_w \right) \\ & + \nabla \left( \left\{ - (K_{va} \nabla u_a + K_{vw} \nabla u_w + K_{vT} \nabla T) \right\} \rho_w \right) + \nabla \left( \left\{ -K_a \nabla u_a \right\} \rho_v \right) = 0 \end{aligned} \quad (3.50)$$

Equation (3.50) comprises various terms, Therefore, simplifying each term is necessary in order to make the governing equation of moisture flow written in terms of the three primary variables pore water pressure  $u_w$ , pore air pressure  $u_a$  and absolute temperature  $T$ . The simplification is explained below:

1. Applying product rule of differentiation to the first and second terms of equation (3.50) will yield:

$$\left[ \frac{\partial(nS_w\rho_w)}{\partial t} + \frac{\partial(n\{1-S_w\}\rho_v)}{\partial t} \right] =$$

$$\left[ \frac{\partial n}{\partial t} S_w \rho_w + \frac{\partial S_w}{\partial t} n \rho_w \right] + \left[ \frac{\partial n}{\partial t} (1-S_w) \rho_v + \frac{\partial(1-S_w)}{\partial t} n \rho_v + \frac{\partial \rho_v}{\partial t} n(1-S_w) \right] =$$

$$n(\rho_w - \rho_v) \frac{\partial S_w}{\partial t} + n S_a \frac{\partial \rho_v}{\partial t} + \frac{\partial n}{\partial t} (S_w \rho_w + S_a \rho_v) = n(\rho_w - \rho_v) \frac{\partial S_w}{\partial t} + n S_a \frac{\partial \rho_v}{\partial t}$$

2. The third term of equation (3.50) can be rewritten as:

$$\nabla \left( \left\{ -K_w \left[ \nabla \left( \frac{u_w}{\gamma_w} \right) + \nabla z \right] \right\} \rho_w \right) = -\frac{\rho_w}{\gamma_w} \nabla (K_w \nabla u_w) - \rho_w \nabla (K_w \nabla z)$$

3. The fourth term of equation (3.50) can be rewritten as:

$$\nabla \left( \left\{ -(K_{va} \nabla u_a + K_{vw} \nabla u_w + K_{vT} \nabla T) \right\} \rho_w \right) = -\nabla \rho_w (K_{va} \nabla u_a + K_{vw} \nabla u_w + K_{vT} \nabla T)$$

4. The fifth term of equation (3.50) can be rewritten as:

$$\nabla \left( \left\{ -K_a \nabla u_a \right\} \rho_v \right) = -\nabla (\rho_v K_a \nabla u_a)$$

By substituting the simplified terms into equation (3.50), it can be written as:

$$n(\rho_w - \rho_v) \frac{\partial S_w}{\partial t} + n S_a \frac{\partial \rho_v}{\partial t} - \frac{\rho_w}{\gamma_w} \nabla (K_w \nabla u_w) - \nabla (\rho_v K_a \nabla u_a)$$

$$- \nabla \rho_w (K_{va} \nabla u_a + K_{vw} \nabla u_w + K_{vT} \nabla T) = \rho_w \nabla (K_w \nabla z) \quad (3.51)$$

Substituting equation (3.21) into the first term of equation (3.51) yields:

$$n(\rho_w - \rho_v) \frac{\partial S_w}{\partial t} = n(\rho_w - \rho_v) \left[ \left[ \frac{\partial S_w}{\partial s} \frac{u_a}{\partial t} - \frac{\partial S_w}{\partial s} \frac{\partial u_w}{\partial t} \right] + \frac{\partial S_w}{\partial T} \frac{\partial T}{\partial t} \right]$$

$$= n(\rho_w - \rho_v) \left[ -\frac{\partial S_w}{\partial s} \frac{\partial u_w}{\partial t} + \frac{\partial S_w}{\partial s} \frac{\partial u_a}{\partial t} + \frac{\partial S_w}{\partial T} \frac{\partial T}{\partial t} \right]$$

$$n(\rho_w - \rho_v) \frac{\partial S_w}{\partial t} = C_{fw} \frac{\partial u_w}{\partial t} + C_{fT} \frac{\partial T}{\partial t} + C_{fa} \frac{\partial u_a}{\partial t} \quad (3.52)$$

where,

$$C_{fw} = -n(\rho_w - \rho_v) \frac{\partial S_w}{\partial s} \quad (3.53)$$

$$C_{fT} = n(\rho_w - \rho_v) \frac{\partial S_w}{\partial T} \quad (3.54)$$

$$C_{fa} = n(\rho_w - \rho_v) \frac{\partial S_w}{\partial s} \quad (3.55)$$

Substituting equation (3.35) into the second term of equation (3.51) yields

$$nS_a \frac{\partial \rho_v}{\partial t} = C_{vw} \frac{\partial u_w}{\partial t} + C_{vT} \frac{\partial T}{\partial t} + C_{va} \frac{\partial u_a}{\partial t} \quad (3.56)$$

where,

$$C_{vw} = nS_a K_{fw} \quad (3.57)$$

$$C_{vT} = nS_a K_{fT} \quad (3.58)$$

$$C_{va} = nS_a K_{fa} \quad (3.59)$$

Substituting equation (3.52) and (3.56) into equation (3.51) yields the governing equation of moisture flow written in terms of the three primary variables  $u_w$ ,  $u_a$  and  $T$ :

$$C_{fw} \frac{\partial u_w}{\partial t} + C_{fT} \frac{\partial T}{\partial t} + C_{fa} \frac{\partial u_a}{\partial t} + C_{vw} \frac{\partial u_w}{\partial t} + C_{vT} \frac{\partial T}{\partial t} + C_{va} \frac{\partial u_a}{\partial t} - \frac{\rho_w}{\gamma_w} \nabla(K_w \nabla u_w) - \nabla(\rho_v K_a \nabla u_a) - \nabla \rho_w (K_{va} \nabla u_a + K_{vw} \nabla u_w + K_{vT} \nabla T) = \rho_w \nabla(K_w \nabla z)$$

or

$$C_{ww} \frac{\partial u_w}{\partial t} + C_{wT} \frac{\partial T}{\partial t} + C_{wa} \frac{\partial u_a}{\partial t} = \nabla[K_{ww} \nabla u_w] + \nabla[K_{wT} \nabla T] + \nabla[K_{wa} \nabla u_a] + J_w \quad (3.60)$$

where,

$$C_{ww} = C_{fw} + C_{vw} \quad (3.61)$$

$$C_{wT} = C_{fT} + C_{vT} \quad (3.62)$$

$$C_{wa} = C_{fa} + C_{va} \quad (3.63)$$

$$K_{ww} = \frac{\rho_w K_w}{\gamma_w} + K_{vw} \rho_w \quad (3.64)$$

$$K_{wa} = \rho_v K_a + \rho_w K_{va} \quad (3.65)$$

$$K_{wT} = \rho_w K_{vT} \quad (3.66)$$

$$J_w = \rho_w \nabla (K_w \nabla z) \quad (3.67)$$

### 3.4 The governing equation of air transfer

The transfer of air through the soil is governed by two main effects (Alonso et al., 1988): the bulk air flow due the pressure gradient, which can be determined by the use of Darcy's law and the dissolved air transfer within pore-liquid, which can be determined by the use of Henry's law. The governing differential equation of air transfer is based on the conservation of mass principle, which dictates that the temporal discretisation of the dry air is equal to the spatial discretisation of the dry air flux. This can be expressed as:

$$\frac{\partial [(\theta_a + H_a \theta_w) \rho_{da}]}{\partial t} + \nabla [(v_a + H_a v_w) \rho_{da}] = 0 \quad (3.68)$$

where,

$H_a$  : is the Henry's volumetric coefficient of solubility.

$\rho_{da}$  : is the density of dry air [M][L]<sup>-3</sup>.

Substituting equations (3.5) and (3.6) for  $\theta_w$  and  $\theta_a$ , and rewriting equation (3.68) in terms of degree of saturation and porosity, the equation for air flow can be written as:

$$\frac{\partial[(nS_a + H_a nS_w)\rho_{da}]}{\partial t} + \nabla[(v_a + H_a v_w)\rho_{da}] = 0 \quad (3.69)$$

The various parameters involved in equation (3.69) for describing the air flow are discussed below.

Pollock (1986) adopted an approach to determine the air density. He considered the air transfer in unsaturated soils to be a mixture of dry air transfer and water vapour transfer. This mixture obeys all the laws of ideal gases which can be applied for both dry air and water vapour (Geraminagad and Saxena, 1986). The application of the ideal gas law to dry air leads to:

$$u_{da} = \rho_{da} R_{da} T \quad (3.70)$$

where,

$u_{da}$  : is the pore dry air pressure  $[M][L]^{-1}[T]^{-2}$ .

$R_{da}$  : is the specific gas constant of dry air  $[L]^2[T]^{-2}[K]^{-1}$ .

Applying Dalton's law of partial pressures to the pore-air mixture yields:

$$u_a = u_{da} + u_v \quad (3.71)$$

To determine the dry air density, substituting equations (3.28) for  $u_v$  and (3.70) for  $u_{da}$  into (3.71) and rearranging yields:

$$u_a = (\rho_{da} R_{da} T) + (\rho_v R_v T)$$

$$\rho_{da} = \frac{u_a}{R_{da} T} - \frac{R_v}{R_{da}} \rho_v \quad (3.72)$$

The time derivative of dry air density can then be written as:

$$\frac{\partial \rho_{da}}{\partial t} = \left[ \frac{1}{R_{da} T} \frac{\partial u_a}{\partial t} - \frac{u_a}{R_{da} T^2} \frac{\partial T}{\partial t} \right] - \frac{R_v}{R_{da}} \frac{\partial \rho_v}{\partial t} \quad (3.73)$$

By substituting equations (3.9) for the velocity of water  $v_w$  and (3.22) for the velocity of air  $v_a$  into (3.69) and rearranging the terms, the equation for dry air can be written as:

$$\frac{\partial [n(S_a + H_a S_w) \rho_{da}]}{\partial t} + \nabla \left[ \left( (-K_a \nabla u_a) + H_a \left( -K_w \left[ \nabla \left( \frac{u_w}{\gamma_w} \right) + \nabla z \right] \right) \right) \right] \rho_{da} = 0 \quad (3.74)$$

Equation (3.74) comprises various terms, Therefore, simplifying each term is necessary in order to make the governing equation of dry air flow written in terms of the three primary variables  $u_w$ ,  $u_a$  and  $T$ . The terms can be simplified as follows:

1. Applying product rule of differentiation to the first term of equation (3.74) yields:

$$\frac{\partial [(nS_a + H_a nS_w) \rho_{da}]}{\partial t} = n \rho_{da} \frac{\partial (S_a + H_a S_w)}{\partial t} + n (S_a + H_a S_w) \frac{\partial \rho_{da}}{\partial t} + \rho_{da} (S_a + H_a S_w) \frac{\partial n}{\partial t}$$

The first term on the right hand side of the above equation can be written as:

$$n \rho_{da} \frac{\partial (S_a + H_a S_w)}{\partial t} = n \rho_{da} \frac{\partial S_a}{\partial t} + n H_a \rho_{da} \frac{\partial S_w}{\partial t}$$

Substituting equation (3.7) for the degree of saturation of air  $S_a$  into this equation will result:

$$n \rho_{da} \frac{\partial (S_a + H_a S_w)}{\partial t} = n \rho_{da} \frac{\partial (1 - S_w)}{\partial t} + n H_a \rho_{da} \frac{\partial S_w}{\partial t} = -n \rho_{da} (H_a - 1) \frac{\partial S_w}{\partial t}$$

As a result, the first term of the equation (3.74) can be rewritten as:

$$n\rho_{da}(H_a - 1)\frac{\partial S_w}{\partial t} + n(S_a + H_a S_w)\frac{\partial \rho_{da}}{\partial t} + \rho_{da}(S_a + H_a S_w)\frac{\partial n}{\partial t}$$

2. The second term of equation (3.74) can be rewritten as:

$$\begin{aligned} & \nabla \left[ \left( (-K_a \nabla u_a) + H_a \left( -K_w \left[ \nabla \left( \frac{u_w}{\gamma_w} \right) + \nabla z \right] \right) \right) \rho_{da} \right] \\ &= \nabla \left[ \left( (-K_a \nabla u_a) + H_a \left( -K_w \left[ \frac{\nabla u_w + \nabla z \gamma_w}{\gamma_w} \right] \right) \right) \rho_{da} \right] \\ &= -\nabla(K_a \rho_{da} \nabla u_a) - \nabla \left[ \frac{H_a \rho_{da}}{\gamma_w} \nabla [K_w (\nabla u_w + \nabla(z\gamma_w))] \right] \end{aligned}$$

By substituting the simplified terms into equation (3.74), it can be written as:

$$\begin{aligned} & n\rho_{da}(H_a - 1)\frac{\partial S_w}{\partial t} + n(S_a + H_a S_w)\frac{\partial \rho_{da}}{\partial t} + \rho_{da}(S_a + H_a S_w)\frac{\partial n}{\partial t} \\ &= \nabla(K_a \rho_{da} \nabla u_a) + \nabla \left[ \frac{H_a \rho_{da}}{\gamma_w} \nabla [K_w (\nabla u_w + \nabla(z\gamma_w))] \right] \end{aligned} \quad (3.75)$$

By substituting equation (3.21) into the first term of (3.75) and rearranging,

$$n\rho_{da}(H_a - 1)\frac{\partial S_w}{\partial t} = n\rho_{da}(H_a - 1) \left[ \left[ \frac{\partial S_w}{\partial s} \frac{\partial u_a}{\partial t} - \frac{\partial S_w}{\partial s} \frac{\partial u_w}{\partial t} \right] + \frac{\partial S_w}{\partial T} \frac{\partial T}{\partial t} \right]$$

The first term of the above equation can be written in a simple form in terms of the three unknowns as:

$$n\rho_{da}(H_a - 1)\frac{\partial S_w}{\partial t} = C_{aw1} \frac{\partial u_w}{\partial t} + C_{aT1} \frac{\partial T}{\partial t} + C_{aa1} \frac{\partial u_a}{\partial t} \quad (3.76)$$

where,

$$C_{aw1} = -n\rho_{da}(H_a - 1)\frac{\partial S_w}{\partial s} \quad (3.77)$$

$$C_{aT1} = n\rho_{da}(H_a - 1)\frac{\partial S_w}{\partial T} \quad (3.78)$$

$$C_{aa1} = n\rho_{da}(H_a - 1)\frac{\partial S_w}{\partial s} \quad (3.79)$$

By substituting equation (3.35) into equation (3.73), the time derivative of the dry air density can be written as:

$$\frac{\partial \rho_{da}}{\partial t} = \left[ \frac{1}{R_{da}T} \frac{\partial u_a}{\partial t} - \frac{u_a}{R_{da}T^2} \frac{\partial T}{\partial t} \right] - \frac{R_v}{R_{da}} \left[ K_{fw} \frac{\partial u_w}{\partial t} + K_{ft} \frac{\partial T}{\partial t} + K_{fa} \frac{\partial u_a}{\partial t} \right]$$

Rewriting the right hand side terms in a simple form in terms of the three unknowns yields:

$$\frac{\partial \rho_{da}}{\partial t} = C_{daw} \frac{\partial u_w}{\partial t} + C_{daT} \frac{\partial T}{\partial t} + C_{daa} \frac{\partial u_a}{\partial t} \quad (3.80)$$

where,

$$C_{daw} = -\frac{R_v}{R_{da}} K_{fw} \quad (3.81)$$

$$C_{daT} = -\frac{\rho_a}{T} - \frac{R_v}{R_{da}} K_{fT} \quad (3.82)$$

$$C_{daa} = \frac{1}{R_{da}T} - \frac{R_v}{R_{da}} K_{fa} \quad (3.83)$$

By substituting equation (3.80) into the second term of equation (3.75), the second term of equation (3.75) can then be written as:

$$n(S_a + H_a S_w) \frac{\partial \rho_{da}}{\partial t} = n(S_a + H_a S_w) \left[ C_{daw} \frac{\partial u_w}{\partial t} + C_{daT} \frac{\partial T}{\partial t} + C_{daa} \frac{\partial u_a}{\partial t} \right]$$

Rewriting in a simple form in terms of the three unknowns:



$$n(S_a + H_a S_w) \frac{\partial \rho_{da}}{\partial t} = C_{aw2} \frac{\partial u_w}{\partial t} + C_{aT2} \frac{\partial T}{\partial t} + C_{aa2} \frac{\partial u_a}{\partial t} \quad (3.84)$$

where,

$$C_{aw2} = n(S_a + H_a S_w) C_{daw} \quad (3.85)$$

$$C_{aT2} = n(S_a + H_a S_w) C_{daT} \quad (3.86)$$

$$C_{aa2} = n(S_a + H_a S_w) C_{daa} \quad (3.87)$$

Finally, substituting equations (3.76) and (3.84) into equation (3.75) leads to the governing differential equation for the air transfer in unsaturated soils:

$$\begin{aligned} & \left[ C_{aw1} \frac{\partial u_w}{\partial t} + C_{aT1} \frac{\partial T}{\partial t} + C_{aa1} \frac{\partial u_a}{\partial t} \right] + \left[ C_{aw2} \frac{\partial u_w}{\partial t} + C_{aT2} \frac{\partial T}{\partial t} + C_{aa2} \frac{\partial u_a}{\partial t} \right] \\ & = \nabla(K_{aa} \nabla u_a) + \nabla[K_{aw} \nabla u_w] + J_a \\ & C_{aw} \frac{\partial u_w}{\partial t} + C_{aT} \frac{\partial T}{\partial t} + C_{aa} \frac{\partial u_a}{\partial t} = \nabla[K_{aw} \nabla u_w] + \nabla(K_{aa} \nabla u_a) + J_a \end{aligned} \quad (3.88)$$

where,

$$C_{aw} = C_{aw1} + C_{aw2} \quad (3.89)$$

$$C_{aT} = C_{aT1} + C_{aT2} \quad (3.90)$$

$$C_{aa} = C_{aa1} + C_{aa2} \quad (3.91)$$

$$K_{aw} = \frac{H_a \rho_{da}}{\gamma_w} K_w \quad (3.92)$$

$$K_{aa} = K_a \rho_{da} \nabla u_w \quad (3.93)$$

$$J_a = H_a \rho_{da} \nabla(K_w \nabla z) \quad (3.94)$$

### 3.5 The governing equation of heat transfer

There has been a continuous increase in temperature of earth due to climate change which is resulting in thermal expansion of oceans and seas. The change in temperature could have an effect on solute transport as the fluid viscosity and density will change which will affect on the solute migration in the aquifer. The effect of temperature change on saltwater intrusion is very important but it has not been studied in the present work and has been proposed as one of the subjects for future research. The mathematical formulation has been added here because temperature is included as one of the degrees of freedoms in the current model. The governing equation of heat transfer is derived based on the effects of three components: conduction, liquid convection and latent heat of vaporisation. The radiation effects are assumed to be negligible and hence are not included in the governing equation for heat transfer. The governing differential equation for heat transfer is derived based on the principle of conservation of energy. The conservation of energy for heat flow states that the temporal change in heat content  $\Omega$  must be equal to the special change in heat flux  $Q$  and can be written mathematically as:

$$\frac{\partial \Omega}{\partial t} + \nabla Q = 0 \quad (3.95)$$

The heat content of unsaturated soils  $\Omega$  is considered to be the sum of two components; soil heat storage capacity and the contribution resulting from the latent heat of vaporisation. Therefore, the latent heat energy can be written as:

$$\Omega = H_c (T - T_r) + nLS_a \rho_v \quad (3.96)$$

where,

$T, T_r$  : are the given and the reference temperatures respectively.

$L$  : is the latent heat of vaporisation  $[L]^2[T]^{-2}$ .

$H_c$  : is the heat capacity of the soil at the reference temperature which is defined as:

$$H_c = (1 - n)C_{ps}\rho_s + n(C_{pw}S_w\rho_w + C_{pv}S_a\rho_v + C_{pda}S_a\rho_{da}) \quad (3.97)$$

where,

$\rho_s$  : is the density of solid particles  $[M][L]^{-3}$ .

$C_{ps}, C_{pw}, C_{pv}, C_{pda}$  : are the specific heat capacities of solid particles, liquid, vapour and dry air respectively  $[L]^2[T]^{-2}[K]^{-1}$ .

The heat flux per unit area  $Q$  can be defined as (Ramesh, 1996):

$$Q = -\chi_T \nabla T + (v_v \rho_w + v_a \rho_v) L + (C_{pw} v_w \rho_w + C_{pv} v_v \rho_w + C_{pv} v_a \rho_v + C_{pda} v_a \rho_{da}) (T - T_r) \quad (3.98)$$

Where  $\chi_T$  is the intrinsic thermal conductivity of soil  $[M][L][T]^{-3}[K]^{-1}$ .

The thermal conductivity of unsaturated soil has been found to be a function of degree of saturation and can be expressed as (Ewen and Thomas, 1987):

$$\chi_T = \chi_T(S_w) \quad (3.99)$$

The heat flux equation (3.98) includes the effects of three components (Ramesh, 1996):

- 1- Conduction.
- 2- Latent heat flow in soil water vapour arising from vapour flow and
- 3- The rate of heat flow due to convection of sensible heat in (i) the liquid phase, (ii) the vapour phase associated with flow induced by vapour pressure gradient, (iii) the vapour phase movement associated with the bulk flow of air and (iv) the air phase.

Substituting equations (3.96) for  $\Omega$ , (3.97) for  $H_c$  and (3.98) for  $Q$  into (3.95), ignoring the term corresponding to soil deformation, the governing equation for heat transfer can be written as:

$$\begin{aligned} & H_c \frac{\partial T}{\partial t} + (T - T_r) \frac{\partial H_c}{\partial t} + nL \rho_v \frac{\partial S_a}{\partial t} + nL S_a \frac{\partial \rho_v}{\partial t} \\ & - \nabla(\chi_T \nabla T) + \rho_w L \nabla(v_v) + L \nabla(\rho_v v_a) + C_{pw} \rho_w \nabla[v_w (T - T_r)] \\ & + C_{pv} \rho_w \nabla[v_v (T - T_r)] + C_{pv} \nabla[\rho_v v_a (T - T_r)] + C_{pda} \nabla[\rho_{da} v_a (T - T_r)] = 0 \end{aligned} \quad (3.100)$$

The various terms of the governing equation of heat transfer in equation (3.100) require simplification, so that it can be expressed in terms of the three primary variables;  $u_w$ ,  $u_a$  and  $T$ . The simplification of each term is as following (Ramesh, 1996):

1- The time derivative of heat capacity which is represented by the second term in equation (3.100) can be written as:

$$\begin{aligned} \frac{\partial H_c}{\partial t} = & (-C_{ps}\rho_s + C_{pw}S_w\rho_w + C_{pv}S_a\rho_v + C_{pda}S_a\rho_{da}) \frac{\partial n}{\partial t} + nC_{pw}\rho_w \frac{\partial S_w}{\partial t} \\ & + nC_{pv}\rho_v \frac{\partial S_a}{\partial t} + nC_{pv}S_a \frac{\partial \rho_v}{\partial t} + nC_{pda}\rho_{da} \frac{\partial S_a}{\partial t} + nC_{pda}S_a \frac{\partial \rho_{da}}{\partial t} \end{aligned} \quad (3.101)$$

Equation (3.101) can be reduced to

$$\frac{\partial H_c}{\partial t} = \rho_{cp1} \frac{\partial n}{\partial t} + n\rho_{cp2} \frac{\partial S_w}{\partial t} + nC_{pv}S_a \frac{\partial \rho_v}{\partial t} + nC_{pda}S_a \frac{\partial \rho_{da}}{\partial t} \quad (3.102)$$

where,

$$\rho_{cp1} = -C_{ps}\rho_s + C_{pw}S_w\rho_w + C_{pv}S_a\rho_v + C_{pda}S_a\rho_{da} \quad (3.103)$$

$$\rho_{cp2} = (C_{pw}S_w\rho_w - C_{pv}\rho_v - C_{pda}\rho_{da}) \quad (3.104)$$

Substituting the degree of saturation from equation (3.21), the vapour density derivatives from equation (3.35) and the dry air density from equation (3.80) into equation (3.102) yields:

$$\begin{aligned} \frac{\partial H_c}{\partial t} = & n\rho_{cp2} \left[ -\frac{\partial S_w}{\partial s} \frac{\partial u_w}{\partial t} + \frac{\partial S_w}{\partial T} \frac{\partial T}{\partial t} + \frac{\partial S_w}{\partial s} \frac{\partial u_a}{\partial t} \right] \\ & + nC_{pv}S_a \left[ K_{fw} \frac{\partial u_w}{\partial t} + K_{fT} \frac{\partial T}{\partial t} + K_{fa} \frac{\partial u_a}{\partial t} \right] + nC_{pda}S_a \left[ C_{daw} \frac{\partial u_w}{\partial t} + C_{daT} \frac{\partial T}{\partial t} + C_{daa} \frac{\partial u_a}{\partial t} \right] \end{aligned}$$

or,

$$\frac{\partial H_c}{\partial t} = C_{Tw1} \frac{\partial u_w}{\partial t} + C_{TT1} \frac{\partial T}{\partial t} + C_{Ta1} \frac{\partial u_a}{\partial t} \quad (3.105)$$

where,

$$C_{Tw1} = -n\rho_{cp2} \frac{\partial S_w}{\partial s} + nC_{pv}S_a K_{fw} + nC_{pda}S_a C_{daw} \quad (3.106)$$

$$C_{TT1} = n\rho_{cp2} \frac{\partial S_w}{\partial T} + nC_{pv}S_a K_{fT} + nC_{pda}S_a C_{daT} \quad (3.107)$$

$$C_{Ta1} = n\rho_{cp2} \frac{\partial S_w}{\partial s} + nC_{pv}S_a K_{fa} + nC_{pda}S_a C_{daa} \quad (3.108)$$

2- The time derivative of degree of saturation is represented by the third term in equation (3.100). Substituting equations (3.7) and (3.21) the third term can be written as:

$$Ln\rho_v \frac{\partial S_a}{\partial t} = Ln\rho_v \frac{\partial(1-S_w)}{\partial t}$$

$$Ln\rho_v \frac{\partial S_a}{\partial t} = C_{Tw2} \frac{\partial u_w}{\partial t} + C_{TT2} \frac{\partial T}{\partial t} + C_{Ta2} \frac{\partial u_a}{\partial t} \quad (3.109)$$

where,

$$C_{Tw2} = Ln\rho_v \frac{\partial S_w}{\partial s} \quad (3.110)$$

$$C_{TT2} = -Ln\rho_v \frac{\partial S_w}{\partial T} \quad (3.111)$$

$$C_{Ta2} = -Ln\rho_v \frac{\partial S_w}{\partial s} \quad (3.112)$$

3- Similarly, the time derivative of vapour density is represented by the forth term in equation (3.100). Substituting equations (3.35) the forth term can be written as:

$$LnS_a \frac{\partial \rho_v}{\partial t} = LnS_a \left( K_{fw} \frac{\partial u_w}{\partial t} + K_{fT} \frac{\partial T}{\partial t} + K_{fa} \frac{\partial u_a}{\partial t} \right)$$

$$LnS_a \frac{\partial \rho_v}{\partial t} = C_{Tw3} \frac{\partial u_w}{\partial t} + C_{TT3} \frac{\partial T}{\partial t} + C_{Ta3} \frac{\partial u_a}{\partial t} \quad (3.113)$$

where,

$$C_{Tw3} = LnS_a K_{fw} \quad (3.114)$$

$$C_{TT3} = LnS_a K_{fT} \quad (3.115)$$

$$C_{Ta3} = LnS_a K_{fa} \quad (3.116)$$

4- Substituting the gradients of vapour velocity from equation (3.46) into the sixth term in equation (3.100) yields:

$$L\rho_w \frac{\partial v_v}{\partial t} = L\rho_w \left( K_{vw} \frac{\partial u_w}{\partial t} + K_{vT} \frac{\partial T}{\partial t} + K_{va} \frac{\partial u_a}{\partial t} \right)$$

$$L\rho_w \frac{\partial v_v}{\partial t} = K_{Tw1} \frac{\partial u_w}{\partial t} + K_{TT1} \frac{\partial T}{\partial t} + K_{Ta1} \frac{\partial u_a}{\partial t} \quad (3.117)$$

where,

$$K_{Tw1} = L\rho_w K_{vw} \quad (3.118)$$

$$K_{TT1} = L\rho_w K_{vT} \quad (3.119)$$

$$K_{Ta1} = L\rho_w K_{va} \quad (3.120)$$

5- The seventh term of equation (3.100) can be extended as:

$$L\nabla(v_a \rho_v) = L(\rho_v \nabla v_a + v_a \nabla \rho_v)$$

Substituting equations (3.22) and (3.35) into this term, will result:

$$L\nabla(v_a \rho_v) = L \left( \rho_v [-K_a \nabla u_a] + v_a \left[ K_{fw} \frac{\partial u_w}{\partial t} + K_{fT} \frac{\partial T}{\partial t} + K_{fa} \frac{\partial u_a}{\partial t} \right] \right) \quad (3.121)$$

Finally by substituting equations (3.105), (3.109), (3.113), (3.117) and (3.121) into (3.100), the equation (3.100) can be written as:

$$\begin{aligned}
& H_c \frac{\partial T}{\partial t} + (T - T_r) \left[ C_{Tw1} \frac{\partial u_w}{\partial t} + C_{TT1} \frac{\partial T}{\partial t} + C_{Ta1} \frac{\partial u_a}{\partial t} \right] \\
& + \left[ C_{Tw2} \frac{\partial u_w}{\partial t} + C_{TT2} \frac{\partial T}{\partial t} + C_{Ta2} \frac{\partial u_a}{\partial t} \right] + \left[ C_{Tw3} \frac{\partial u_w}{\partial t} + C_{TT3} \frac{\partial T}{\partial t} + C_{Ta3} \frac{\partial u_a}{\partial t} \right] \\
& - \nabla(\chi_T \nabla T) + \left[ K_{Tw1} \frac{\partial u_w}{\partial t} + K_{TT1} \frac{\partial T}{\partial t} + K_{Ta1} \frac{\partial u_a}{\partial t} \right] + L \nabla(\rho_v v_a) \\
& + C_{pw} \rho_w \nabla[v_w(T - T_r)] + C_{pv} \rho_w \nabla[v_v(T - T_r)] \\
& + C_{pv} \nabla[\rho_v v_a(T - T_r)] + C_{pda} \nabla[\rho_{da} v_a(T - T_r)]
\end{aligned} \tag{3.122}$$

More simplification for the last five terms of equation (3.122) can be done as:

$$\begin{aligned}
& L \nabla(\rho_v v_a) + \nabla \left[ C_{pw} \rho_w v_w + C_{pv} \rho_w v_v + C_{pv} \rho_v v_a + C_{pda} \rho_{da} v_a \right] (T - T_r) \\
& = L \nabla(\rho_v v_a) + (T - T_r) C_{pw} \rho_w \nabla v_w + (T - T_r) C_{pv} \rho_w \nabla v_v \\
& + (T - T_r) C_{pv} \{ v_a \nabla \rho_v + \rho_v \nabla v_a \} + (T - T_r) C_{pda} \{ v_a \nabla \rho_{da} + \rho_{da} \nabla v_a \}
\end{aligned} \tag{3.123}$$

By substituting the equations for the velocities of water, air and vapour (3.9), (3.22), (3.46) and equations for the gradients for the densities of vapour and dry air (3.35), (3.80) into equation (3.123) the equation will be (Ramesh, 1996):

$$\begin{aligned}
& \nabla(K_{Tw2} \nabla u_w) + \nabla(K_{TT2} \nabla T) + \nabla(K_{Ta2} \nabla u_a) + V_{Tw} \nabla u_w \\
& + V_{TT} \nabla T + V_{Ta} \nabla u_a + (T - T_r) C_{pw} \rho_w \nabla(\nabla z)
\end{aligned} \tag{3.124}$$

where,

$$K_{Tw2} = (T - T_r) \rho_w \left( \frac{C_{pw} K_w \rho_w}{\gamma_w} + C_{pv} K_{vw} \right) \tag{3.125}$$

$$K_{TT2} = (T - T_r) \rho_w C_{pv} K_{vT} \tag{3.126}$$

$$K_{Ta2} = (T - T_r) (\rho_w C_{pv} K_{va} + \rho_v C_{pv} K_a + \rho_{da} C_{pda} K_a) + L \rho_v K_a \tag{3.127}$$

$$V_{Tw} = (T - T_r) (C_{pv} v_a K_{fw} + C_{pda} v_a C_{daw}) + L v_a K_{fw} \tag{3.128}$$

$$\begin{aligned}
& V_{TT} = (C_{pw} v_w \rho_w + C_{pv} v_v \rho_w + C_{pv} v_a \rho_v + C_{pda} v_a \rho_{da}) \nabla T \\
& + (T - T_r) v_a (C_{pv} K_{fT} + C_{pda} C_{daT}) + L v_a K_{fT}
\end{aligned} \tag{3.129}$$

$$V_{Ta} = (T - T_r) v_a (C_{pv} K_{fa} + C_{pda} C_{daa}) + L v_a K_{fa} \tag{3.130}$$

Substituting equation (3.124) into (3.122) yields the governing equation for heat transfer in terms of the three primary variables; pore water pressure  $u_w$ , pore air pressure  $u_a$  and absolute temperature  $T$  as following:

$$C_{Tw} \frac{\partial u_w}{\partial t} + C_{TT} \frac{\partial T}{\partial t} + C_{Ta} \frac{\partial u_a}{\partial t} = \nabla(K_{Tw} \nabla u_w) + \nabla(K_{TT} \nabla T) + \nabla(K_{Ta} \nabla u_a) + V_{Tw} \nabla u_w + V_{TT} \nabla T + V_{Ta} \nabla u_a + J_T \quad (3.131)$$

where,

$$C_{Tw} = C_{Tw}(T - T_r) + C_{Tw2} + C_{Tw3} \quad (3.132)$$

$$C_{TT} = H_c + C_{TT1}(T - T_r) + C_{TT2} + C_{TT3} \quad (3.133)$$

$$C_{Ta} = C_{Ta1}(T - T_r) + C_{Ta2} + C_{Ta3} \quad (3.134)$$

$$K_{Tw} = K_{Tw1} + K_{Tw2} \quad (3.135)$$

$$K_{TT} = \chi_T + K_{TT1} + K_{TT2} \quad (3.136)$$

$$K_{Ta} = K_{Ta1} + K_{Ta2} \quad (3.137)$$

$$J_T = (T - T_r)C_{Pw} \rho_w \nabla(K_w \nabla z) \quad (3.138)$$

### 3.6 The governing equation for solute transport

This section is focusing on the phenomena that effect solute transport in soils. Several studies have evaluated various aspects of solute transport processes in saturated and unsaturated soils. Many analytical and numerical solutions have been developed for predicting the flow of solutes in groundwater. The majority of the work that has been done for unsaturated flow assumed constant or uniform water content. However, there has been relatively little work done for solute transport in a transient water and air flow field (Sander and Braddock, 2005). To study solute transport mechanisms consider a unit volume of soil (Figure 3.1). This volume is called a control volume and the boundaries of the element are called control surfaces (Istok, 1989).



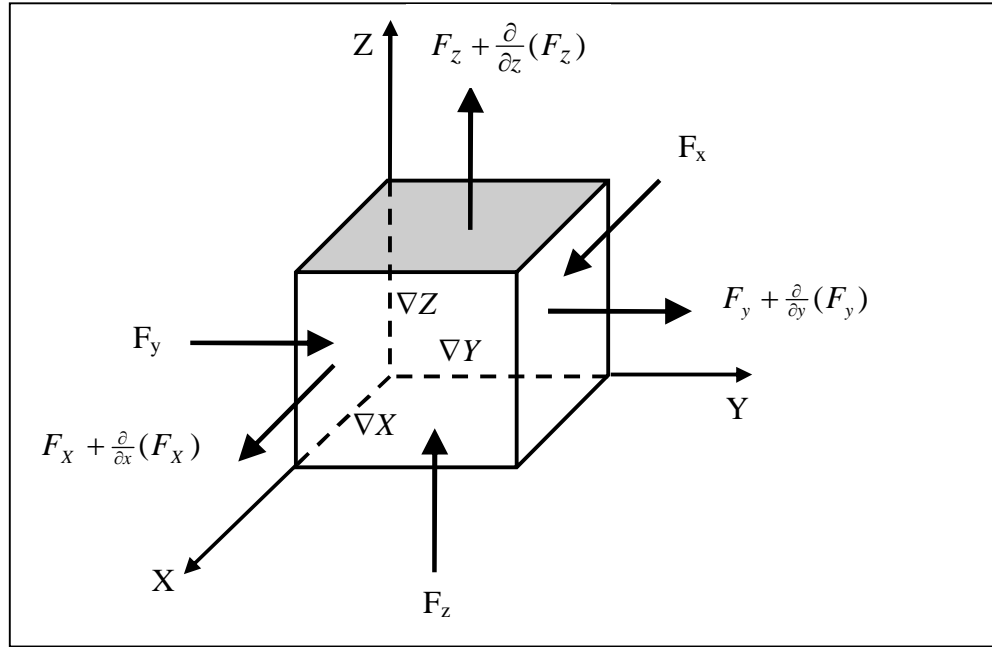


**Figure 3.1** Control volume of solute transport through porous media

The law of conservation of mass for solute transport requires that the rate of change of solute mass within the control volume is equal to the net rate at which solute is entered to the control volume through the control surface plus the net rate at which solute is produced within the control volume by various chemical and physical processes.

### 3.6.1 Net rate of solute inflow the control volume

The net rate of solute inflow the control volume is the difference between inflow and outflow and can be written as:

$$\text{Net rate of solute inflow} = F_x - (F_x + \frac{\partial}{\partial x}(F_x)) + F_y - (F_y + \frac{\partial}{\partial y}(F_y)) + F_z - (F_z + \frac{\partial}{\partial z}(F_z))$$

$$\text{Net rate of solute inflow} = -\frac{\partial}{\partial x}(F_x) - \frac{\partial}{\partial y}(F_y) - \frac{\partial}{\partial z}(F_z) \quad (3.139)$$

In porous media, solute transport occurs mainly by various processes including advection, diffusion, dispersion, adsorption, radioactive decay and biological degradation. These processes will be described in details (Istok, 1989).

### 3.6.1.1 Advection

The process by which solutes are transported by the bulk motion of the flowing groundwater is called advection. The rate of solute transport that occurs by advection is given by the product of the solute concentration  $c$  and the components of apparent groundwater velocity  $v_x, v_y$ . In terms of the two components of the solute transport in the  $x$  and  $y$  directions, the rate of solute transported by advection can be written as:

$$F_{x,advection} = v_{w_x} c \quad (3.140)$$

$$F_{y,advection} = v_{w_y} c \quad (3.141)$$

### 3.6.1.2 Diffusion

The process by which solutes are transported by the random thermal motion of solute molecules is called diffusion. The rate of solute transport that occurs by diffusion is given by Fick's Law. In terms of the two components of the solute transport in the  $x$  and  $y$  directions, the rate of solute transported by diffusion can be written as:

$$F_{x,diffusion} = -D_m \frac{\partial c}{\partial x} \quad (3.142)$$

$$F_{y,diffusion} = -D_m \frac{\partial c}{\partial y} \quad (3.143)$$

Where  $D_m$  is the molecular diffusion coefficient in the porous medium  $[L]^2[T]^{-1}$ .

The molecular diffusion coefficient for a solute in porous media is much smaller than the molecular diffusion coefficient for the same solute in aqueous solution. An empirical relationship for the molecular diffusion coefficient  $D_m$  can be written as (Istok, 1989):

$$D_m = \omega(\theta) D_{m0} \quad (3.144)$$

where,

$D_{mo}$  : is the molecular diffusion coefficient in aqueous solution  $[L]^2[T]^{-1}$

$\theta$  : is the volumetric water content

$\omega$  : is an empirical correction factor (ranging from 0.01 for very dry soils to 0.5 for saturated soils).

Values of the molecular diffusion coefficient are in the range of  $1.E^{-8}$  to  $1.E^{-10}$   $[L]^2[T]^{-1}$  at  $25^\circ$  C. Molecular diffusion coefficients are strongly temperature dependent, but are only weakly dependant on the concentration of other dissolved species. The small size of molecular diffusion coefficient means that the rate of solute transport by diffusion is usually very small relative to the rate of solute transport by advection and dispersion and may be negligible (Istok, 1989).

### 3.6.1.3 Mechanical Dispersion

Mechanical dispersion (or hydraulic dispersion) is a mixing or spreading process caused by small-scale fluctuation in groundwater velocity along the tortuous flow paths within individual pores. On a much larger scale mechanical dispersion can also be caused by the presence of heterogeneities within the aquifer. The rate of solute transport by mechanical dispersion is given by a generalized form of Fick's Law of diffusion. In terms of the two components of solute transport in x and y directions, the rate of solute transport by mechanical dispersion can be written as:

$$F_{x,dispersion} = -D_{w_{xx}} \frac{\partial}{\partial x} (\theta_w c) - D_{w_{xy}} \frac{\partial}{\partial y} (\theta_w c) \quad (3.145)$$

$$F_{y,dispersion} = -D_{w_{yx}} \frac{\partial}{\partial x} (\theta_w c) - D_{w_{yy}} \frac{\partial}{\partial y} (\theta_w c) \quad (3.146)$$

where  $D_{w_{xx}}$ ,  $D_{w_{xy}}$ ,  $D_{w_{yx}}$ ,  $D_{w_{yy}}$  are the coefficients of dispersivity tensor  $[L][T]^{-1}$ .

For water phase the coefficients of mechanical dispersion can be computed from the following expressions (Bear, 1987):

$$D_{w_{xx}} = \alpha_{L_w} \frac{\bar{v}_{w_x}^2}{|v|} + \alpha_{T_w} \frac{\bar{v}_{w_y}^2}{|v|} + D_{m_w} \quad (3.147)$$

$$D_{w_{yy}} = \alpha_{T_w} \frac{\bar{v}_{w_x}^2}{|v|} + \alpha_{L_w} \frac{\bar{v}_{w_y}^2}{|v|} + D_{m_w} \quad (3.148)$$

$$D_{w_{xy}} = D_{w_{yx}} = (\alpha_{L_w} - \alpha_{T_w}) \frac{\bar{v}_{w_x} \bar{v}_{w_y}}{|v|} + D_{m_w} \quad (3.149)$$

where,

$\alpha_{T_w}$  : is the transverse dispersivity for water phase [L].

$\alpha_{L_w}$  : is the longitudinal dispersivity for water phase [L].

$D_{m_w}$  : is the coefficient of water molecular diffusion [L]<sup>2</sup>[T]<sup>-1</sup>

$\bar{v}_{w_x}$  : is the component of the pore water velocity in x direction  $\bar{v}_{w_x} = \frac{v_x}{\theta_w}$

$\bar{v}_{w_y}$  : is the component of the pore water velocity in y direction  $\bar{v}_{w_y} = \frac{v_y}{\theta_w}$

$|v|$  : is the magnitude of the water velocity ( $|v| = \sqrt{\bar{v}_{w_x}^2 + \bar{v}_{w_y}^2}$ )

By substituting from equations (3.140), (3.141), (3.145) and (3.146) for the values of advection, dispersion and diffusion into equation (3.139) the net ret of solute inflow can be written as:

$$\begin{aligned} \text{The net ret of solute inflow} = & \frac{\partial}{\partial x} \left[ D_{w_{xx}} \frac{\partial}{\partial x} (\theta_w c) + D_{w_{xy}} \frac{\partial}{\partial y} (\theta_w c) \right] + \\ & \frac{\partial}{\partial y} \left[ D_{w_{yx}} \frac{\partial}{\partial x} (\theta_w c) + D_{w_{yy}} \frac{\partial}{\partial y} (\theta_w c) \right] \\ & - \left[ \frac{\partial}{\partial x} (v_{w_x} C) + \frac{\partial}{\partial y} (v_{w_y} C) \right] \end{aligned} \quad (3.150)$$

### 3.6.2 Net rate of solute production within the control volume

Several processes can act as sources or sinks for solute transport within the control volume including sorption/desorption, chemical reaction or biological degradation. For the case of transport involving a sorption/desorption reaction (Istok, 1989):



The net rate of reaction  $r$  between dissolved species  $A$  and sorbed species  $\bar{A}$ , can be written as:

$$r = \theta \frac{\partial C}{\partial t} = -\rho_b \frac{\partial \bar{C}}{\partial t} \quad (3.152)$$

where,

$\theta$  : is the volumetric water content of the porous medium.

$\rho_b$  : is the bulk density of the porous medium.

$C$  : is the concentration of the dissolved species  $A$  (mass of solute / volume of groundwater).

$\bar{C}$  : is the concentration of sorbed species  $\bar{A}$  (mass of solute / volume of dry porous media).

Equation (3.152) can be written as:

$$r = -k_f C + k_r \bar{C} \quad (3.153)$$

where,

$k_f$  : is the constant for the forward reaction ( $A \rightarrow \bar{A}$ ) and

$k_r$  : is the constant for reverse reaction ( $A \leftarrow \bar{A}$ ).

If the net rate of reaction is assumed to be zero (e.g., the reaction is in equilibrium), equation (3.153) can be solved directly for the concentration of the sorbed species  $\bar{A}$  and written as:

$$\bar{C} = \frac{k_f}{k_r} C = K_d C \quad (3.154)$$

Where  $K_d$  is the equilibrium distribution coefficient  $[L]^3[M]^{-1}$ .

The net rate of solute production due to a sorption/desorption reaction between a solute and the porous medium within the control volume can be obtained by combining equations (3.152) and (3.154), and be written as:

$$\left(\frac{\partial(\theta C)}{\partial t}\right)_{sorption} = -\rho_b K_d \frac{\partial C}{\partial t} \quad (3.155)$$

If the solute also undergoes radioactive decay or biological degradation, the net rate of solute production by this mechanism can be written as:

$$\left(\frac{\partial(\theta C)}{\partial t}\right)_{decay} = -\lambda(\theta C + \rho_b K_d C) \quad (3.156)$$

where,

$\lambda$  : is the decay constant for the solute.

The net rate of solute production due to a sorption/desorption reaction, radioactive decay or biological degradation between a solute and the porous medium within the control volume can be obtained by combining equations (3.155) and (3.156) and be written as:

$$\text{The net rate of solute production} = -\rho_b K_d \frac{\partial C}{\partial t} - \lambda(\theta C + \rho_b K_d C) \quad (3.157)$$

### 3.6.3 Governing equation of solute transport in saturated soil

By substituting equations (3.150) and (3.157) for the values the net rate of solute inflow and the net rate of solute production the governing equation of solute transport in saturated soil can be written as:

$$\begin{aligned} \frac{\partial(\theta_w c_w)}{\partial t} = & \frac{\partial}{\partial x} \left[ D_{w,xx} \frac{\partial}{\partial x} (\theta_w c) + D_{w,xy} \frac{\partial}{\partial y} (\theta_w c) \right] + \frac{\partial}{\partial y} \left[ D_{w,yx} \frac{\partial}{\partial x} (\theta_w c) + D_{w,yy} \frac{\partial}{\partial y} (\theta_w c) \right] \\ & - \left[ \frac{\partial}{\partial x} (v_{w,x} c) + \frac{\partial}{\partial y} (v_{w,y} c) \right] - \frac{\partial}{\partial t} (\rho_b K_d c) - \lambda (\theta c + \rho_b K_d c) \end{aligned} \quad (3.158)$$

Equation (3.158) can be written using simpler notations as:

$$\frac{\partial(\theta_w c_w)}{\partial t} + \frac{\partial}{\partial t} (\rho_b K_d c_w) + \nabla(v_w c_w) - \nabla(\theta_w D_w \nabla c_w) + \lambda(\theta c_w + \rho_b K_d c_w) = 0 \quad (3.159)$$

Equation (3.159) can be modified to include a retardation factor  $R$  as (AL-Najjar, 2006):

$$\frac{\partial(R\theta_w c_w)}{\partial t} + \nabla(v_w c_w) - \nabla(\theta_w D_w \nabla c_w) + \lambda_w \theta_w c_w R = 0 \quad (4.160)$$

where,

$$R = 1 + \frac{\rho_b K_d}{\theta_w} \quad (3.161)$$

Equation (3.160) can be written using simpler notations as (Javadi et al., 2008):

$$\frac{\partial(\theta c)}{\partial t} + \nabla(v c) - \nabla(D \nabla c) + \lambda c = 0 \quad (3.162)$$

where,

$$\theta = R\theta_w$$

$$v = v_w$$

$$D = D_w \theta_w$$

$$\lambda = \lambda_w \theta_w R$$

$$c = c_w$$

### 3.6.4 Governing equation of solute transport in unsaturated soil

Modelling the solute transport in the water and air phases requires a description of the mass transfer processes between the two phases. The concentration in each phase is proportional to the concentration in the other phase and they are related by Henry's Law:

$$H = \frac{c_a}{c_w} \quad (3.163)$$

where,  $H$ : is Henry's constant  $[T]^2[L]^{-1}[M]^{-1}$ .

For modelling the fluid flow and solute transport in unsaturated soils it is considered in this work that non-uniform velocity of water  $v_w$ , velocity of air  $v_a$ , volumetric water content  $\theta_w$  and volumetric air content  $\theta_a$ , will change with time according to the changes in the pore water pressure  $u_w$ , pore air pressure  $u_a$ , water degree of saturation  $S_w$  and air degree of saturation  $S_a$  (AL-Najjar, 2006).

The rate of solute transport by advection will include the effect of the air phase, so equation (3.140) and (3.141) can be written as:

$$F_{x,advection} = ((v_{w_x} + H v_{a_x})c) \quad (3.164)$$

$$F_{y,advection} = ((v_{w_y} + H v_{a_y})c) \quad (3.165)$$

Also, the rate of solute transport by mechanical dispersion will include the effect of the air phase, so equation (3.145) and (3.146) can be written as:



$$F_{x,dispersion} = \left( -D_{w_{xx}} \frac{\partial}{\partial x} (\theta_w c) - D_{w_{xy}} \frac{\partial}{\partial y} (\theta_w c) \right) + \left( -D_{a_{xx}} \frac{\partial}{\partial x} (\theta_a c) - D_{a_{xy}} \frac{\partial}{\partial y} (\theta_a c) \right) \quad (3.166)$$

$$F_{y,dispersion} = \left( -D_{w_{yx}} \frac{\partial}{\partial x} (\theta_w c) - D_{w_{yy}} \frac{\partial}{\partial y} (\theta_w c) \right) + \left( -D_{a_{yx}} \frac{\partial}{\partial x} (\theta_a c) - D_{a_{yy}} \frac{\partial}{\partial y} (\theta_a c) \right) \quad (3.167)$$

where  $D_{a_{xx}}$ ,  $D_{a_{xy}}$ ,  $D_{a_{yx}}$ ,  $D_{a_{yy}}$  are the coefficients of dispersivity tensor [L][T]<sup>-1</sup> for air phase, the coefficients of mechanical dispersion can be computed from the following expressions:

$$D_{a_{xx}} = \alpha_{L_a} \frac{\bar{v}_{a_x}^2}{|v|} + \alpha_{T_a} \frac{\bar{v}_{a_y}^2}{|v|} + D_{m_a} \quad (3.168)$$

$$D_{a_{yy}} = \alpha_{T_a} \frac{\bar{v}_{a_x}^2}{|v|} + \alpha_{L_a} \frac{\bar{v}_{a_y}^2}{|v|} + D_{m_a} \quad (3.169)$$

$$D_{a_{xy}} = D_{a_{yx}} = (\alpha_{L_a} - \alpha_{T_a}) \frac{\bar{v}_{a_x} \bar{v}_{a_y}}{|v|} + D_{m_a} \quad (3.170)$$

$\alpha_{T_a}$  : is the transverse dispersivity for air phase [L].

$\alpha_{L_a}$  : is the longitudinal dispersivity for air phase [L].

$\bar{v}_{a_x}$  : is the component of the pore air velocity in x direction  $\bar{v}_{a_x} = \frac{v_x}{\theta_a}$

$\bar{v}_{a_y}$  : is the component of the pore air velocity in y direction  $\bar{v}_{a_y} = \frac{v_y}{\theta_a}$

$|v|$  : is the magnitude of the air velocity ( $|v| = \sqrt{\bar{v}_{a_x}^2 + \bar{v}_{a_y}^2}$ )

$D_{m_a}$  : is the coefficient of air molecular diffusion [L]<sup>2</sup>[T]<sup>-1</sup>.

The governing equation of solute transport for unsaturated soil can be written similar to equation (3.158) as:

$$\begin{aligned}
\frac{\partial((\theta_w + H\theta_a)c_w)}{\partial t} = & - \left[ \left( \frac{\partial}{\partial x}(v_{w_x}c) + \frac{\partial}{\partial y}(v_{w_y}c) \right) + \left( \frac{\partial}{\partial x}(v_{a_x}c) + \frac{\partial}{\partial y}(v_{a_y}c) \right) \right] \\
& + \left\{ \frac{\partial}{\partial x} \left( D_{w_{xx}} \frac{\partial}{\partial x}(\theta_w c) + D_{w_{xy}} \frac{\partial}{\partial y}(\theta_w c) \right) + \frac{\partial}{\partial y} \left( D_{w_{yy}} \frac{\partial}{\partial y}(\theta_w c) + D_{w_{yx}} \frac{\partial}{\partial x}(\theta_w c) \right) \right\} \\
& + H \left\{ \frac{\partial}{\partial x} \left( D_{a_{xx}} \frac{\partial}{\partial x}(\theta_a c) + D_{a_{xy}} \frac{\partial}{\partial y}(\theta_a c) \right) + \frac{\partial}{\partial y} \left( D_{a_{yy}} \frac{\partial}{\partial y}(\theta_a c) + D_{a_{yx}} \frac{\partial}{\partial x}(\theta_a c) \right) \right\} \\
& - \frac{\partial}{\partial t}(\rho_b K_d C) - (\lambda_w \theta_w + H\lambda_a \theta_a)(1 + \rho_b K_d / \theta_w)c = 0
\end{aligned} \tag{3.171}$$

where  $\lambda_a$  is the chemical reaction rate for air [T]<sup>-1</sup>.

Equation (3.171) can be written using simpler notations similar to equation (3.159) as following:

$$\begin{aligned}
\frac{\partial((\theta_w + H\theta_a)c_w)}{\partial t} + \frac{\partial}{\partial t}(\rho_b K_d C) + \nabla(v_w c) + \nabla(v_a c) - \nabla(\theta_w D_w \nabla c) - \nabla(\theta_a D_a \nabla c) \\
+ (\lambda_w \theta_w + H\lambda_a \theta_a)(1 + \rho_b K_d / \theta_w)c = 0
\end{aligned} \tag{3.172}$$

Equation (3.172) can be modified to include a retardation factor  $R$  as:

$$\begin{aligned}
\frac{\partial((R\theta_w + H\theta_a)c_w)}{\partial t} + \nabla(v_w c) + \nabla(v_a c) - \nabla(\theta_w D_w \nabla c) - \nabla(\theta_a D_a \nabla c) \\
+ (\lambda_w \theta_w + H\lambda_a \theta_a)Rc = 0
\end{aligned} \tag{3.173}$$

Equation (3.173) can be written using simpler notations as (Javadi et al., 2008):

$$\frac{\partial((R\theta_w + H\theta_a)c)}{\partial t} + \nabla(vc) - \nabla(D\nabla c) + \lambda c = 0 \tag{3.174}$$

or

$$\frac{\partial(\theta c)}{\partial t} + \nabla(vc) - \nabla(D\nabla c) + \lambda c = 0 \tag{3.175}$$

where,

$$v = (v_{w_x} + v_{w_y}) + H(v_{a_x} + v_{a_y})$$

$$D = \theta_w \left( (D_{w_{xx}} + D_{w_{yy}}) + (D_{w_{yy}} + D_{w_{xx}}) \right) + H\theta_a \left( (D_{a_{xx}} + D_{w_{xy}}) + (D_{a_{yy}} + D_{a_{yx}}) \right)$$

$$\lambda = (\lambda_w \theta_w + H\lambda_a \theta_a) R$$

$$\theta = (R\theta_w + H\theta_a)$$

### 3.7 The governing differential equations

Equations (3.60), (3.88), (3.131) and (3.175) are considered as the governing differential equations for the coupled flow and transport in unsaturated soils and are listed below:

#### Moisture transfer:

$$C_{ww} \frac{\partial u_w}{\partial t} + C_{wT} \frac{\partial T}{\partial t} + C_{wa} \frac{\partial u_a}{\partial t} = \nabla(K_{ww} \nabla u_w) + \nabla(K_{wT} \nabla T) + \nabla(K_{wa} \nabla u_a) + J_w \quad (3.176)$$

#### Air transfer:

$$C_{aw} \frac{\partial u_w}{\partial t} + C_{aT} \frac{\partial T}{\partial t} + C_{aa} \frac{\partial u_a}{\partial t} = \nabla(K_{aw} \nabla u_w) + \nabla(K_{aa} \nabla u_a) + J_a \quad (3.177)$$

#### Heat transfer:

$$C_{Tw} \frac{\partial u_w}{\partial t} + C_{TT} \frac{\partial T}{\partial t} + C_{Ta} \frac{\partial u_a}{\partial t} = \nabla(K_{Tw} \nabla u_w) + \nabla(K_{TT} \nabla T) + \nabla(K_{Ta} \nabla u_a) \\ + V_{Tw} \nabla u_w + V_{TT} \nabla T + V_{Ta} \nabla u_a + J_T \quad (3.178)$$

#### Solute transport:

$$\frac{\partial(\theta c)}{\partial t} + \nabla(vc) - \nabla(D\nabla c) + \lambda c = 0 \quad (3.179)$$

The above four equations define the complete formulation of coupled flow and solute transport in unsaturated soil. The transient flow equations are solved in terms of three variables; pore water pressure  $u_w$ , pore air pressure  $u_a$  and absolute temperature  $T$  at different times. The transient solute transport equation is then solved for the value of solute concentration  $c$  at different times. This procedure is valid when changes in groundwater density due to changing solute concentration can be assumed to be small (Istok, 1998).

## **Numerical solution of governing equations of coupled fluid flow and solute transport**

### ***4.1 Introduction***

The governing differential equations of fluid flow and solute transport have been defined in chapter 3. The coupled fluid flow and solute transport in unsaturated soil is modeled using two sets of equations. The first set of equations describes water, air and heat flow. The second set describes solute transport. The numerical approach to achieve a solution to the governing differential equations will be described in this chapter. The nonlinear governing differential equations are solved using a finite element method in the space domain and a finite difference scheme in the time domain. The solution is divided into two parts. In the first part the flow equations for water, air and heat transfer will be solved simultaneously for the three primary variables; pore water pressure ( $u_w$ ), pore air pressure ( $u_a$ ) and absolute temperature ( $T$ ). In the second part solute transport equation will be solved for solute concentration ( $c$ ). This chapter presents an overview of the different mathematical models that can be used to solve coupled fluid flow and solute transport problem focusing on finite element and finite difference methods which are used in this work and then the numerical solution of the governing differential equations of the coupled fluid flow and solute transport is presented.

### ***4.2 Solution methods for differential equations***

Solution of differential equations governing a physical phenomenon means finding the unknowns in the governing equations with the associated boundary and initial conditions. There are a number of methods that can be used to solve such problems. The wide spectrum of these methods can be classified as analytical and numerical methods. Figure 4.1 shows a summary of solution methods for differential equations. These methods are described in the following sections with focus on the methods which are used in this study.

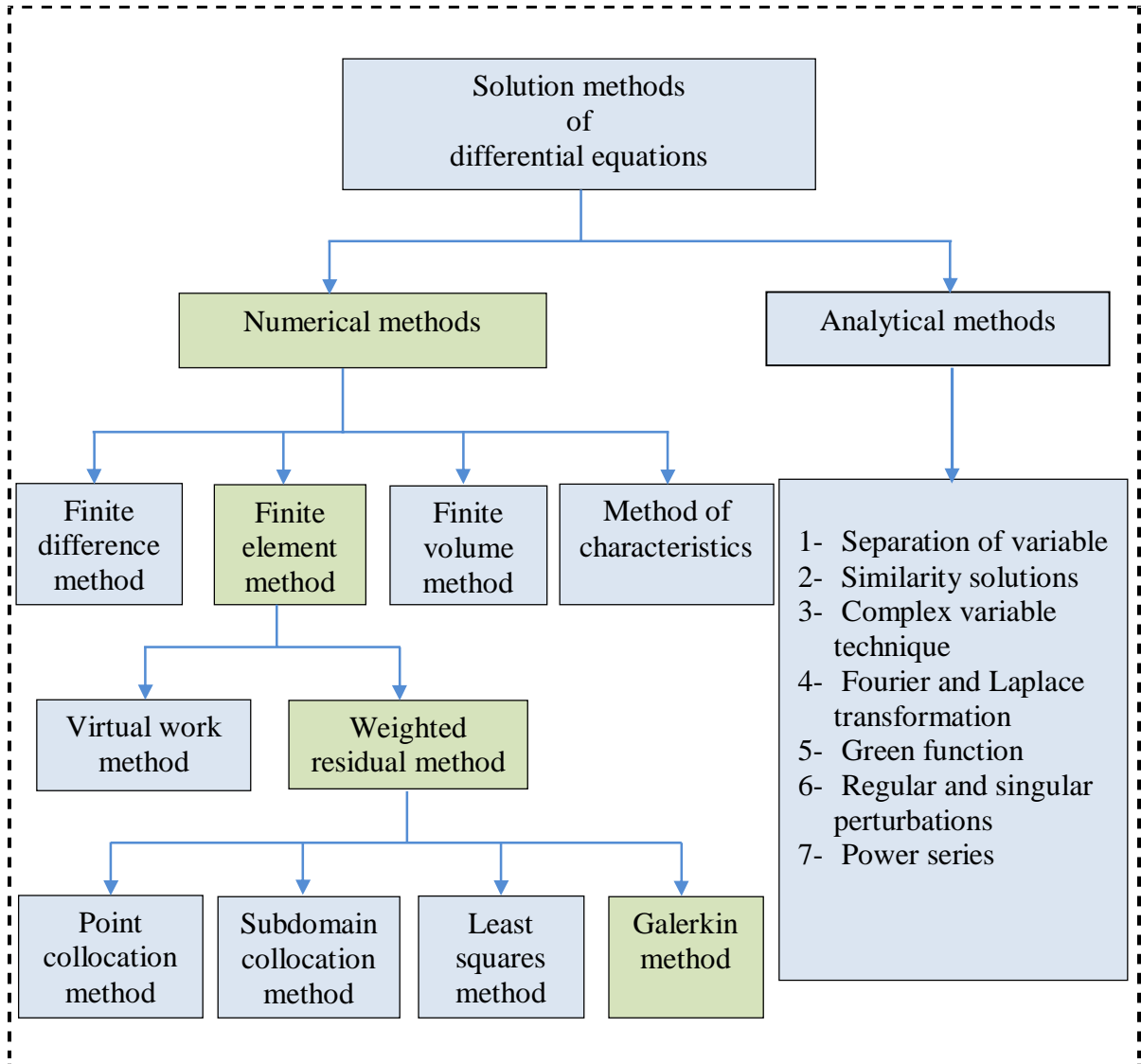


**Figure 4.1** Summary of the solution methods for differential equations

### 4.2.1 Analytical methods

Analytical methods can be used to obtain exact solutions for a number of problems. They are particularly used for linear problems and regions of simple or regular geometry. For nonlinear problems with regions of irregular geometry, very few analytical solutions exist and these are usually approximate solutions. The accuracy of the analytical methods can be

very good and exact in some cases but it requires several assumptions to simplify the problem which may be not valid for complicated problems. Many physical phenomena such as, coupled fluid flow and solute transport in porous media are governed by complex nonlinear partial differential equations. Solving such complex problems of nonlinear partial differential equations is generally intractable analytically. For such problems, the use of numerical methods to obtain approximate solutions is advantageous and preferable.

## ***4.2.2 Numerical methods***

A number of numerical methods can be used to solve complex nonlinear partial differential equations (Figure 4.1). The finite difference and finite element methods are the most popular methods that have been applied in the field of coupled fluid flow and solute transport in porous media.

### ***4.2.2.1 Finite difference method***

Finite difference method (FDM) is popular in simulation of large systems. The reason for this popularity is that the finite difference method is conceptually straightforward and the fundamental concepts are simply understood. The finite difference method is most suitable for problems with simple or regular geometry. It can be used in simple problems (e.g., isotropic and homogenous aquifer with regular boundary). The accuracy of finite difference method for such simple problems is quite good but this method becomes complicated and inefficient when the problem is nonlinear with irregular domain (i.e., anisotropic and heterogeneous aquifer with irregular boundary), (Istok, 1989).

### ***4.2.2.2 Finite element method***

The finite element method (FEM) has become a powerful numerical tool for the solution of a wide range of engineering problems. The finite element method was first used to solve groundwater flow and solute transport problems in the early 1970's (Istok, 1989). Since then, the method has gained wide acceptance in the field of fluid flow and solute transport

modeling. The finite element method is a technique which can produce near optimal approximate solutions to the partial differential equations of a certain problem. The implementation ultimately employs subdivision of the problem domain into a number of elements with small regions called finite elements. Many shapes are available for elements. The fundamental idea of the finite element method is to produce a set of algebraic equations, written on each finite element which are then collected together using a procedure called assembly to form the global matrix statement. The approximate values of the dependent variables are then determined via solution of this matrix statement using any linear algebra technique (Baker and Pepper, 1991).

The finite element method has a number of advantages that made it very popular (Daryl, 2002). The advantages of this method include the ability to handle;

1. irregular and curved geometric boundaries,
2. variable spacing of the nodes,
3. variable size of the elements,
4. unlimited numbers and kinds of boundary conditions,
5. anisotropic and heterogeneous materials,
6. nonlinear behavior and
7. dynamic effects.

The finite element method is useful in virtually every field of engineering analysis (Klaus, 1996). In this method, a complex region defining a continuum is discretized into simple geometric shapes called finite elements. The material properties and governing relationships are considered over these elements and expressed in terms of unknown values at element nodes. An assembly process, results in a set of equations. Solution of these equations gives the approximate behaviour of the continuum (Chandrupatla and Belegundu, 1991).

Certain steps in formulating a finite element model of solute transport problems are embodied in the developed finite element model. The steps of finite element analysis can be summarized as follows (Cheung et al., 1996):

1. Discretization of the problem domain into a number of sub-regions known as finite elements.
2. Selection of node and element interpolation functions.
3. Evaluation of individual element properties.
4. Formation of elements stiffness matrices.
5. Assembly of element matrices to form the global matrix.
6. Definition of the physical constraints (boundary and initial conditions).
7. Formulation of the global unknown vector.
8. Solution of system of equations for the unknown nodal variables.
9. Finally, computation of further parameters such as, hydrostatic head, fluid density, velocity, dispersion coefficients and other physically meaningful quantities from the computed nodal variables and element properties .

### ***4.3 Numerical solution of the governing equations***

The numerical solution of governing differential equations of coupled fluid flow and solute transport will be described in this section. The current work employs a two dimensional eight noded isoparametric element. The spatial discretization of the differential equations using the finite element method will be described in details. The solution method of temporal integration using the finite difference method is then employed to obtain the transient solution of the spatially discretised equations for both fluid flow and solute transport. The flow equations for water, air and heat transfer will be solved simultaneously to determine pore water pressure ( $u_w$ ), pore air pressure ( $u_a$ ) and absolute temperature ( $T$ ), and then solute transport equation will be solved for solute concentration  $c$ . The coupling mechanism of fluid flow and solute transport is presented in the final part of this chapter.



### 4.3.1 Spatial discretization of the moisture transfer governing equation

The governing differential equation for moisture transfer was derived in chapter 3, in terms of three primary unknowns;  $u_w$ ,  $u_a$  and  $T$ . Equation (3.60) may be rearranged and rewritten as:

$$\nabla[K_{ww}\nabla u_w] + \nabla[K_{wT}\nabla T] + \nabla[K_{wa}\nabla u_a] + J_w - C_{ww}\frac{\partial u_w}{\partial t} - C_{wT}\frac{\partial T}{\partial t} - C_{wa}\frac{\partial u_a}{\partial t} = 0 \quad (4.1)$$

The primary unknowns can be approximated using the shape function approach for eight node isoparametric element as:

$$u_w = \hat{u}_w = \sum_1^8 N_s u_{ws} \quad (4.2)$$

$$T = \hat{T} = \sum_1^8 N_s T_s \quad (4.3)$$

$$u_a = \hat{u}_a = \sum_1^8 N_s u_{as} \quad (4.4)$$

where,

$N_s$  : is the shape function.

$u_{ws}$  : is the nodal pore water pressure.

$T_s$  : is the nodal temperature.

$u_{as}$  : is the nodal pore air pressure.

The derivatives of the shape functions for equations (4.2) (4.3) and (4.4) can be expressed as:

$$\nabla \hat{u}_w = \sum_{s=1}^8 (\nabla N_s) u_{ws} \quad (4.5)$$

$$\nabla \hat{T} = \sum_{s=1}^8 (\nabla N_s) \cdot T_s \quad (4.6)$$

$$\nabla \hat{u}_a = \sum_{s=1}^8 (\nabla N_s) \cdot u_{as} \quad (4.7)$$

By replacing the primary unknowns in equation (4.1) with their shape functions approximations from equation (4.2), (4.3) and (4.4), equation (4.1) can be written as:

$$\nabla [K_{ww} \nabla \hat{u}_w] + \nabla [K_{wT} \nabla \hat{T}] + \nabla [K_{wa} \nabla \hat{u}_a] + J_w - C_{ww} \frac{\partial \hat{u}_w}{\partial t} - C_{wT} \frac{\partial \hat{T}}{\partial t} - C_{wa} \frac{\partial \hat{u}_a}{\partial t} = R_{\Omega_w} \quad (4.8)$$

where,

$R_{\Omega_w}$  : is the residual error introduced by the approximation functions.

Employing the Galerkin weighted residual approach to minimize the residual error, equation (4.8) can be written as (Ramesh, 1996):

$$\int_{\Omega^e} N_r \left[ \nabla [K_{ww} \nabla \hat{u}_w] + \nabla [K_{wT} \nabla \hat{T}] + \nabla [K_{wa} \nabla \hat{u}_a] + J_w - C_{ww} \frac{\partial \hat{u}_w}{\partial t} - C_{wT} \frac{\partial \hat{T}}{\partial t} - C_{wa} \frac{\partial \hat{u}_a}{\partial t} \right] d\Omega^e = 0 \quad (4.9)$$

where,

$\Omega^e$  : is the element domain.

$N_r$  : is the shape function.

Employing integration by parts to the first term of equation (4.9) yields:

$$\int_{\Omega^e} N_r \nabla [K_{ww} \nabla \hat{u}_w] d\Omega^e = \int_{\Omega^e} \nabla [N_r K_{ww} \nabla \hat{u}_w] d\Omega^e - \int_{\Omega^e} [K_{ww} \nabla \hat{u}_w \nabla N_r] d\Omega^e \quad (4.10)$$

Similarly, the second and third terms of the equation (4.9) can be written as:

$$\int_{\Omega^e} N_r \nabla [K_{wT} \nabla \hat{T}] d\Omega^e = \int_{\Omega^e} \nabla [N_r K_{wT} \nabla \hat{T}] d\Omega^e - \int_{\Omega^e} [K_{wT} \nabla \hat{T} \nabla N_r] d\Omega^e \quad (4.11)$$

$$\int_{\Omega^e} N_r \nabla [K_{wa} \nabla \hat{u}_a] d\Omega^e = \int_{\Omega^e} \nabla [N_r K_{wa} \nabla \hat{u}_a] d\Omega^e - \int_{\Omega^e} [K_{wa} \nabla \hat{u}_a \nabla N_r] d\Omega^e \quad (4.12)$$

The fourth term of the equation (4.9) has been defined in chapter 3 as:

$$J_w = \rho_w \nabla (K_w \nabla z)$$

Introducing this substitution and employing integration by parts, the fourth term can be written as:

$$\begin{aligned} \int_{\Omega^e} [N_r [J_w]] d\Omega^e &= \int_{\Omega^e} [N_r \nabla (\rho_w K_w \nabla z)] d\Omega^e \\ &= \int_{\Omega^e} [\nabla (N_r \rho_w K_w \nabla z)] d\Omega^e - \int_{\Omega^e} [(\rho_w K_w \nabla z) \nabla N_r] d\Omega^e \end{aligned} \quad (4.13)$$

Substituting equations (4.10), (4.11), (4.12) and (4.13) into equation (4.9), will result:

$$\begin{aligned} &\int_{\Omega^e} \left\{ \nabla [N_r K_{ww} \nabla \hat{u}_w] - [K_{ww} \nabla \hat{u}_w \nabla N_r] \right\} + \left\{ \nabla [N_r K_{wT} \nabla \hat{T}] - [K_{wT} \nabla \hat{T} \nabla N_r] \right\} \\ &+ \left\{ \nabla [N_r K_{wa} \nabla \hat{u}_a] - [K_{wa} \nabla \hat{u}_a \nabla N_r] \right\} + \left\{ \nabla (N_r \rho_w K_w \nabla z) - [(\rho_w K_w \nabla z) \nabla N_r] \right\} \\ &- N_r \left\{ C_{ww} \frac{\partial \hat{u}_w}{\partial t} + C_{wT} \frac{\partial \hat{T}}{\partial t} + C_{wa} \frac{\partial \hat{u}_a}{\partial t} \right\} d\Omega^e = 0 \end{aligned} \quad (4.14)$$

Equation (4.14) can be rearranged and rewritten as:

$$\begin{aligned}
 & \int_{\Omega^e} \left\{ \nabla [N_r K_{ww} \nabla \hat{u}_w] d\Omega^e + \nabla [N_r K_{wT} \nabla \hat{T}] d\Omega^e + \nabla [N_r K_{wa} \nabla \hat{u}_a] d\Omega^e + [\nabla (N_r \rho_w K_w \nabla z)] d\Omega^e \right\} \\
 & + \left\{ -[K_{ww} \nabla \hat{u}_w \nabla N_r] d\Omega^e - [K_{wT} \nabla \hat{T} \nabla N_r] d\Omega^e - [K_{wa} \nabla \hat{u}_a \nabla N_r] d\Omega^e - [(\rho_w K_w \nabla z) \nabla N_r] d\Omega^e \right\} \\
 & - N_r \left\{ C_{ww} \frac{\partial \hat{u}_w}{\partial t} + C_{wT} \frac{\partial \hat{T}}{\partial t} + C_{wa} \frac{\partial \hat{u}_a}{\partial t} \right\} d\Omega^e = 0
 \end{aligned} \tag{4.15}$$

Employing the Gauss-Green divergence theorem into the first term of equation (4.15) yields (Ramesh, 1996):

$$\begin{aligned}
 & \int_{\Omega^e} N_r \nabla \left\{ K_{ww} \nabla \hat{u}_w + K_{wT} \nabla \hat{T} + K_{wa} \nabla \hat{u}_a + \rho_w K_w \nabla z \right\} d\Omega^e \\
 & = \int_{\Gamma^e} N_r \left\{ K_{ww} \nabla \hat{u}_w + K_{wT} \nabla \hat{T} + K_{wa} \nabla \hat{u}_a + \rho_w K_w \nabla z \right\} n \cdot d\Gamma^e
 \end{aligned} \tag{4.16}$$

where,

$\Gamma^e$  : is the element boundary surface.

Substituting equation (4.16) into equation (4.15) yields:

$$\begin{aligned}
 & \int_{\Omega^e} \left\{ -[K_{ww} \nabla \hat{u}_w \nabla N_r] d\Omega^e - [K_{wT} \nabla \hat{T} \nabla N_r] d\Omega^e - [K_{wa} \nabla \hat{u}_a \nabla N_r] d\Omega^e - [(\rho_w K_w \nabla z) \nabla N_r] d\Omega^e \right\} \\
 & - N_r \left\{ C_{ww} \frac{\partial \hat{u}_w}{\partial t} + C_{wT} \frac{\partial \hat{T}}{\partial t} + C_{wa} \frac{\partial \hat{u}_a}{\partial t} \right\} d\Omega^e \\
 & + \int_{\Gamma^e} N_r \left\{ K_{ww} \nabla \hat{u}_w + K_{wT} \nabla \hat{T} + K_{wa} \nabla \hat{u}_a + \rho_w K_w \nabla z \right\} n \cdot d\Gamma^e = 0
 \end{aligned} \tag{4.17}$$

The surface integral in equation (4.17) is equal to the sum of liquid and vapor fluxes normal to the boundary surface. Substituting equations (3.9), (3.22) and (3.46) for water, air and vapour velocities into the last term of equation (4.17) yields:

$$\begin{aligned}
 & \int_{\Gamma^e} N_r \left\{ K_{ww} \nabla \hat{u}_w + K_{wT} \nabla \hat{T} + K_{wa} \nabla \hat{u}_a + \rho_w K_w \nabla z \right\} n \cdot d\Gamma^e \\
 &= \int_{\Gamma^e} N_r \left\{ \rho_w \left( -K_w \left[ \nabla \left( \frac{\hat{u}_w}{\gamma_w} \right) + \nabla z \right] \right) + \left( \rho_w \left( -K_{vw} \nabla \hat{u}_w + K_{va} \nabla \hat{u}_a + K_{vT} \nabla \hat{T} \right) + \rho_w \left( -K_a \nabla \hat{u}_a \right) \right) \right\} n \cdot d\Gamma^e \\
 &= \int_{\Gamma^e} -N_r \left\{ \rho_w \hat{v}_{wn} + \rho_w \hat{v}_{vd} + \rho_w \hat{v}_{va} \right\} d\Gamma^e
 \end{aligned} \tag{4.18}$$

where,

$\hat{v}_{wn}$  : is the approximation of water velocity normal to the boundary surface.

$\hat{v}_{vd}$  : is the approximation of diffusive vapour velocity normal to the boundary surface.

$\hat{v}_{va}$  : is the approximation of pressure vapour velocity normal to the boundary surface.

By introducing the derivatives of the shape functions from equations (4.5), (4.6) and (4.7) into equation (4.17) and substitute from equation (4.18), the final form of equation (4.17) can be written as:

$$\begin{aligned}
 & \int_{\Omega^e} [K_{ww} ((\nabla N_s) u_{ws})] \nabla N_r d\Omega^e + [K_{wT} ((\nabla N_s) T_s) \nabla N_r] d\Omega^e + [K_{wa} ((\nabla N_s) u_{as}) \nabla N_r] d\Omega^e \\
 & + [(\rho_w K_w \nabla z) \nabla N_r] d\Omega^e + N_r \left\{ C_{ww} \frac{\partial (N_s u_{ws})}{\partial t} + C_{wT} \frac{\partial (N_s T_s)}{\partial t} + C_{wa} \frac{\partial (N_s u_{as})}{\partial t} \right\} d\Omega^e \\
 & - \int_{\Gamma^e} N_r \left\{ \rho_w \hat{v}_{wn} + \rho_w \hat{v}_{vd} + \rho_w \hat{v}_{va} \right\} d\Gamma^e = 0
 \end{aligned}$$

$$\begin{aligned}
 & \int_{\Omega^e} [K_{ww} \nabla N^T \nabla N] d\Omega^e u_{ws} + \int_{\Omega^e} [K_{wT} \nabla N^T \nabla N] d\Omega^e T_s + \int_{\Omega^e} [K_{wa} \nabla N^T \nabla N] d\Omega^e u_{as} \\
 & + \int_{\Omega^e} [K_w \rho_w \nabla N^T \nabla z] d\Omega^e + \int_{\Omega^e} [C_{ww} N^T N] d\Omega^e \frac{\partial u_{ws}}{\partial t} + \int_{\Omega^e} [C_{wT} N^T N] d\Omega^e \frac{\partial T_s}{\partial t} \\
 & + \int_{\Omega^e} [C_{wa} N^T N] d\Omega^e \frac{\partial u_{as}}{\partial t} - \int_{\Gamma^e} N^T \left\{ \rho_w \hat{v}_{wn} + \rho_w \hat{v}_{vd} + \rho_w \hat{v}_{va} \right\} d\Gamma^e = 0
 \end{aligned} \tag{4.19}$$

where,

$N$  : is the shape function matrix.

The spatial discretization of the governing differential equation for water flow can then be written as:

$$C_{ww} \frac{\partial u_{ws}}{\partial t} + C_{wT} \frac{\partial T_s}{\partial t} + C_{wa} \frac{\partial u_{as}}{\partial t} + K_{ww} u_{ws} + K_{wT} T_s + K_{wa} u_{wa} = f_w \quad (4.20)$$

where,

$$C_{ww} = \sum_{e=1}^m \int_{\Omega^e} [N^T C_{ww} N] d\Omega^e \quad (4.21)$$

$$C_{wT} = \sum_{e=1}^m \int_{\Omega^e} [N^T C_{wT} N] d\Omega^e \quad (4.22)$$

$$C_{wa} = \sum_{e=1}^m \int_{\Omega^e} [N^T C_{wa} N] d\Omega^e \quad (4.23)$$

$$K_{ww} = \sum_{e=1}^m \int_{\Omega^e} [\nabla N^T K_{ww} \nabla N] d\Omega^e \quad (4.24)$$

$$K_{wT} = \sum_{e=1}^m \int_{\Omega^e} [\nabla N^T K_{wT} \nabla N] d\Omega^e \quad (4.25)$$

$$K_{wa} = \sum_{e=1}^m \int_{\Omega^e} [\nabla N^T K_{wa} \nabla N] d\Omega^e \quad (4.26)$$

$$f_w = \sum_{e=1}^m \int_{\Omega^e} [\nabla N^T (K_w \rho_w \nabla z)] d\Omega^e - \sum_{e=1}^m \int_{\Gamma^e} N^T \{ \rho_w \hat{v}_{wm} + \rho_w \hat{v}_{vd} + \rho_w \hat{v}_{va} \} \cdot d\Gamma^e \quad (4.27)$$

### 4.3.2 Spatial discretization of the air transfer governing equation

The governing differential equation for air transfer was also derived in chapter 3, in terms of three primary unknowns;  $u_w$ ,  $u_a$  and  $T$ . Equation (3.88) may be rearranged and rewritten as:

$$\nabla(K_{aw}\nabla u_w) + \nabla(K_{aa}\nabla u_a) + J_a - C_{aw}\frac{\partial u_w}{\partial t} - C_{aT}\frac{\partial T}{\partial t} - C_{aa}\frac{\partial u_a}{\partial t} = 0 \quad (4.28)$$

By replacing the primary unknowns in equation (4.28) with their shape functions approximations from equation (4.2), (4.3) and (4.4), equation (4.28) can be written as:

$$\nabla(K_{aw}\nabla \hat{u}_w) + \nabla(K_{aa}\nabla \hat{u}_a) + J_a - C_{aw}\frac{\partial \hat{u}_w}{\partial t} - C_{aT}\frac{\partial \hat{T}}{\partial t} - C_{aa}\frac{\partial \hat{u}_a}{\partial t} = R_{\Omega a} \quad (4.29)$$

where,

$R_{\Omega a}$  : is the residual error introduced by the approximation functions.

Employing Galerkin weighted residual approach to minimize the residual error, equation (4.29) may be written as (Ramesh, 1996):

$$\int_{\Omega^e} N_r \left[ \nabla(K_{aw}\nabla \hat{u}_w) + \nabla(K_{aa}\nabla \hat{u}_a) + J_a - C_{aw}\frac{\partial \hat{u}_w}{\partial t} - C_{aT}\frac{\partial \hat{T}}{\partial t} - C_{aa}\frac{\partial \hat{u}_a}{\partial t} \right] d\Omega^e = 0 \quad (4.30)$$

Employing integration by parts to the first term of equation (4.30) yields:

$$\int_{\Omega^e} N_r \nabla [K_{aw}\nabla \hat{u}_w] d\Omega^e = \int_{\Omega^e} \nabla [N_r K_{aw}\nabla \hat{u}_w] d\Omega^e - \int_{\Omega^e} [K_{aw}\nabla \hat{u}_w \nabla N_r] d\Omega^e \quad (4.31)$$

Similarly, the second term of the equation (4.30) can be written as:

$$\int_{\Omega^e} N_r \nabla [K_{aa} \nabla \hat{u}_a] d\Omega^e = \int_{\Omega^e} \nabla [N_r K_{aa} \nabla \hat{u}_a] d\Omega^e - \int_{\Omega^e} [K_{aa} \nabla \hat{u}_a \nabla N_r] d\Omega^e \quad (4.32)$$

The third term of the equation (4.30) has been defined in chapter 3 as:

$$J_a = H_a \rho_{da} \nabla (K_w \nabla z)$$

Introducing this substitution and employing integration by parts, the third term can be written as:

$$\begin{aligned} \int_{\Omega^e} [N_r [J_a]] d\Omega^e &= \int_{\Omega^e} [N_r \rho_{da} H_a \nabla (K_w \nabla z)] d\Omega^e \\ &= \int_{\Omega^e} [\nabla (N_r \rho_{da} H_a K_w \nabla z)] d\Omega^e - \int_{\Omega^e} [K_w \rho_{da} H_a \nabla z \nabla N_r] d\Omega^e \end{aligned} \quad (4.33)$$

Substituting equations (4.31), (4.32) and (4.33) into equation (4.30) leads to:

$$\begin{aligned} &\int_{\Omega^e} [\nabla [N_r K_{aw} \nabla \hat{u}_w] - [K_{aw} \nabla \hat{u}_w \nabla N_r] + \nabla [N_r K_{aa} \nabla \hat{u}_a] - [K_{aa} \nabla \hat{u}_a \nabla N_r] \\ &+ [\nabla (N_r \rho_{da} H_a K_w \nabla z)] - [K_w \rho_{da} H_a \nabla z \nabla N_r] - N_r \left\{ C_{aw} \frac{\partial \hat{u}_w}{\partial t} - C_{aT} \frac{\partial \hat{T}}{\partial t} - C_{aa} \frac{\partial \hat{u}_a}{\partial t} \right\} d\Omega^e = 0 \end{aligned} \quad (4.34)$$

Equation (4.34) can be rearranged and rewritten as:

$$\begin{aligned} &\int_{\Omega^e} [\nabla [N_r K_{aw} \nabla \hat{u}_w] + \nabla [N_r K_{aa} \nabla \hat{u}_a] + \nabla (N_r \rho_{da} H_a K_w \nabla z)] \\ &+ \{- [K_{aw} \nabla \hat{u}_w \nabla N_r] - [K_{aa} \nabla \hat{u}_a \nabla N_r] - [K_w \rho_{da} H_a \nabla z \nabla N_r]\} \\ &- N_r \left\{ C_{aw} \frac{\partial \hat{u}_w}{\partial t} - C_{aT} \frac{\partial \hat{T}}{\partial t} - C_{aa} \frac{\partial \hat{u}_a}{\partial t} \right\} d\Omega^e = 0 \end{aligned} \quad (4.35)$$

Employing Gauss-Green divergence theorem to the first term of equation (4.35) yields :



$$\begin{aligned}
 & \int_{\Omega^e} N_r \nabla \{ [K_{aw} \nabla \hat{u}_w] + [K_{aa} \nabla \hat{u}_a] + [(\rho_{da} H_a K_w \nabla z)] \} d\Omega^e \\
 & = \int_{\Gamma^e} N_r \{ [K_{aw} \nabla \hat{u}_w] + [K_{aa} \nabla \hat{u}_a] + [(\rho_{da} H_a K_w \nabla z)] \} n d\Gamma^e
 \end{aligned} \tag{4.36}$$

Substitution of equation (4.36) into (4.35) results:

$$\begin{aligned}
 & \int_{\Omega^e} \{ -[K_{aw} \nabla \hat{u}_w \nabla N_r] - [K_{aa} \nabla \hat{u}_a \nabla N_r] - [K_w \rho_{da} H_a \nabla z \nabla N_r] \} \\
 & - N_r \left\{ C_{aw} \frac{\partial \hat{u}_w}{\partial t} - C_{aT} \frac{\partial \hat{T}}{\partial t} - C_{aa} \frac{\partial \hat{u}_a}{\partial t} \right\} d\Omega^e \\
 & + \int_{\Gamma^e} N_r \{ [K_{aw} \nabla \hat{u}_w] + [K_{aa} \nabla \hat{u}_a] + [(\rho_{da} H_a K_w \nabla z)] \} n d\Gamma^e = 0
 \end{aligned} \tag{4.37}$$

The surface integral in equation (4.37) is equal to the sum of free and dissolved air fluxes normal to the boundary surface and can be written as (Ramesh, 1996):

$$\begin{aligned}
 & \int_{\Gamma^e} N_r \{ [K_{aw} \nabla \hat{u}_w] + [K_{aa} \nabla \hat{u}_a] + [(\rho_{da} H_a K_w \nabla z)] \} n d\Gamma^e \\
 & = \int_{\Gamma^e} N_r \{ (\hat{v}_a + H_a \hat{v}_w) \rho_{da} \} n d\Gamma^e \\
 & = \int_{\Gamma^e} N_r \{ (\rho_{da} H_a \hat{v}_w) + (\rho_{da} \hat{v}_a) \} n d\Gamma^e
 \end{aligned} \tag{4.38}$$

Substitution for the water and air velocities defined in chapter 3 in equations (3.9) and (3.22) into equation (4.38) leads to:

$$\begin{aligned}
 & \int_{\Gamma^e} N_r \left\{ \rho_{da} H_a \left[ -K_w \left[ \nabla \left( \frac{u_w}{\gamma_w} \right) + \nabla z \right] \right] + (\rho_{da} [-K_a \nabla u_a]) \right\} n d\Gamma^e \\
 & = \int_{\Gamma^e} -N_r \{ \rho_{da} \hat{v}_{fn} + \rho_{da} \hat{v}_{an} \} d\Gamma^e
 \end{aligned} \tag{4.39}$$

where,

$\hat{v}_{fn}$  : is the approximation of velocity of free dry air.

$\hat{v}_{an}$  : is the approximation of velocity of dissolved dry air.

By introducing the derivatives of the shape functions from equations (4.5), (4.6) and (4.7) into equation (4.37) and substituting from equation (4.39), the final form of equation (4.37) can be written as:

$$\begin{aligned} & \int_{\Omega^e} [K_{aw} \nabla N^T \nabla N] d\Omega^e u_{ws} + \int_{\Omega^e} [K_{aa} \nabla N^T \nabla N] d\Omega^e u_{as} + \int_{\Omega^e} [K_w \rho_{da} H_a \nabla N^T \nabla z] d\Omega^e \\ & + \int_{\Omega^e} [C_{aw} N^T N] d\Omega^e \frac{\partial u_{ws}}{\partial t} + \int_{\Omega^e} [C_{aT} N^T N] d\Omega^e \frac{\partial T_s}{\partial t} \\ & + \int_{\Omega^e} [C_{aa} N^T N] d\Omega^e \frac{\partial u_{as}}{\partial t} - \int_{\Gamma^e} N^T \rho_{da} \{ \hat{v}_{fn} + \hat{v}_{an} \} d\Gamma^e = 0 \end{aligned} \quad (4.40)$$

The spatial discretization of governing differential equation for air flow can be written as:

$$C_{aw} \frac{\partial u_{ws}}{\partial t} + C_{aT} \frac{\partial T_s}{\partial t} + C_{aa} \frac{\partial u_{as}}{\partial t} + K_{aw} u_{ws} + K_{aa} u_{as} = f_a \quad (4.41)$$

where,

$$C_{aw} = \sum_{e=1}^m \int_{\Omega^e} [N^T C_{aw} N] d\Omega^e \quad (4.42)$$

$$C_{aT} = \sum_{e=1}^m \int_{\Omega^e} [N^T C_{aT} N] d\Omega^e \quad (4.43)$$

$$C_{aa} = \sum_{e=1}^m \int_{\Omega^e} [N^T C_{aa} N] d\Omega^e \quad (4.44)$$

$$K_{aw} = \sum_{e=1}^m \int_{\Omega^e} [\nabla N^T K_{aw} \nabla N] d\Omega^e \quad (4.45)$$

$$K_{aa} = \sum_{e=1}^m \int_{\Omega^e} [\nabla N^T K_{aa} \nabla N] d\Omega^e \quad (4.46)$$

$$f_a = \sum_{e=1}^m \int_{\Omega^e} [\nabla N^T (K_w \rho_{da} H_a \nabla z)] d\Omega^e - \sum_{e=1}^m \int_{\Gamma^e} N^T \rho_{da} \{ \hat{v}_{fn} + \hat{v}_{an} \} d\Gamma^e \quad (4.47)$$

### 4.3.3 Spatial discretization of the heat transfer governing equation

The governing differential equation for heat transfer was also derived in chapter 3, in terms of three primary unknowns;  $u_w$ ,  $u_a$  and  $T$ . Equation (3.131) may be rearranged and rewritten as:

$$\begin{aligned} & \nabla(K_{Tw} \nabla u_w) + \nabla(K_{TT} \nabla T) + \nabla(K_{Ta} \nabla u_a) \\ & + V_{Tw} \nabla u_w + V_{TT} \nabla T + V_{Ta} \nabla u_a + J_T - C_{Tw} \frac{\partial u_w}{\partial t} - C_{TT} \frac{\partial T}{\partial t} - C_{Ta} \frac{\partial u_a}{\partial t} = 0 \end{aligned} \quad (4.48)$$

By replacing the primary unknowns in equation (4.48) with their shape functions approximations from equation (4.2), (4.3) and (4.4), equation (4.48) can be written as:

$$\begin{aligned} & \nabla(K_{Tw} \nabla \hat{u}_w) + \nabla(K_{TT} \nabla \hat{T}) + \nabla(K_{Ta} \nabla \hat{u}_a) \\ & + V_{Tw} \nabla \hat{u}_w + V_{TT} \nabla \hat{T} + V_{Ta} \nabla \hat{u}_a + J_T - C_{Tw} \frac{\partial \hat{u}_w}{\partial t} - C_{TT} \frac{\partial \hat{T}}{\partial t} - C_{Ta} \frac{\partial \hat{u}_a}{\partial t} = R_{\Omega T} \end{aligned} \quad (4.49)$$

where,

$R_{\Omega T}$  : is the residual error introduced by the approximation functions.

Employing Galerkin weighted residual approach to minimize the residual error, equation (4.49) may be written as (Ramesh, 1996):

$$\begin{aligned} & \int_{\Omega^e} N_r \left[ \nabla(K_{Tw} \nabla \hat{u}_w) + \nabla(K_{TT} \nabla \hat{T}) + \nabla(K_{Ta} \nabla \hat{u}_a) \right. \\ & \left. + V_{Tw} \nabla \hat{u}_w + V_{TT} \nabla \hat{T} + V_{Ta} \nabla \hat{u}_a + J_T - C_{Tw} \frac{\partial \hat{u}_w}{\partial t} - C_{TT} \frac{\partial \hat{T}}{\partial t} - C_{Ta} \frac{\partial \hat{u}_a}{\partial t} \right] d\Omega^e = 0 \end{aligned} \quad (4.50)$$

Employing integration by parts to the first term of equation (4.50) yields:

$$\int_{\Omega^e} N_r [\nabla(K_{Tw} \nabla \hat{u}_w)] d\Omega^e = \int_{\Omega^e} [N_r K_{Tw} \nabla \hat{u}_w] d\Omega^e - \int_{\Omega^e} [K_{Tw} \nabla \hat{u}_w \nabla N_r] d\Omega^e \quad (4.51)$$

Similarly, the second and the third terms of the equation (4.50) can be written as:

$$\int_{\Omega^e} N_r \nabla [K_{TT} \nabla \hat{T}] d\Omega^e = \int_{\Omega^e} \nabla [N_r K_{TT} \nabla \hat{T}] d\Omega^e - \int_{\Omega^e} [K_{TT} \nabla \hat{T} \nabla N_r] d\Omega^e \quad (4.52)$$

$$\int_{\Omega^e} N_r \nabla [K_{Ta} \nabla \hat{u}_a] d\Omega^e = \int_{\Omega^e} \nabla [N_r K_{Ta} \nabla \hat{u}_a] d\Omega^e - \int_{\Omega^e} [K_{Ta} \nabla \hat{u}_a \nabla N_r] d\Omega^e \quad (4.53)$$

The seventh term of the equation (4.50) has been determined in chapter 3 as:

$$J_T = (T - T_r) C_{Pw} \rho_w \nabla (K_w \nabla z)$$

Introducing this substitution and employing integration by parts, the seventh term can be written as:

$$\begin{aligned} \int_{\Omega^e} [N_r [J_T]] d\Omega^e &= \int_{\Omega^e} [N_r (T - T_r) C_{Pw} \rho_w \nabla (K_w \nabla z)] d\Omega^e \\ &= \int_{\Omega^e} [\nabla (N_r (T - T_r) C_{Pw} \rho_w \nabla K_w \nabla z)] d\Omega^e - \int_{\Omega^e} [(T - T_r) C_{Pw} \rho_w K_w \nabla z \nabla N_r] d\Omega^e \end{aligned} \quad (4.54)$$

Substituting equations (4.51), (4.52), (4.53) and (4.54) into equation (4.50) leads to:

$$\begin{aligned} &\left[ \int_{\Omega^e} \nabla [N_r K_{Tw} \nabla \hat{u}_w] d\Omega^e - \int_{\Omega^e} [K_{Tw} \nabla \hat{u}_w \nabla N_r] d\Omega^e \right] + \left[ \int_{\Omega^e} \nabla [N_r K_{TT} \nabla \hat{T}] d\Omega^e - \int_{\Omega^e} [K_{TT} \nabla \hat{T} \nabla N_r] d\Omega^e \right] + \\ &\left[ \int_{\Omega^e} \nabla [N_r K_{Ta} \nabla \hat{u}_a] d\Omega^e - \int_{\Omega^e} [K_{Ta} \nabla \hat{u}_a \nabla N_r] d\Omega^e \right] + \left[ \int_{\Omega^e} N_r V_{Tw} \nabla \hat{u}_w d\Omega^e \right] + \left[ \int_{\Omega^e} N_r V_{TT} \nabla \hat{T} d\Omega^e \right] \\ &+ \left[ \int_{\Omega^e} N_r V_{Ta} \nabla \hat{u}_a d\Omega^e \right] \\ &+ \left[ \int_{\Omega^e} [\nabla (N_r (T - T_r) C_{Pw} \rho_w \nabla K_w \nabla z)] d\Omega^e - \int_{\Omega^e} [(T - T_r) C_{Pw} \rho_w K_w \nabla z \nabla N_r] d\Omega^e \right] \\ &- \int_{\Omega^e} N_r \left[ C_{Tw} \frac{\partial \hat{u}_w}{\partial t} + C_{TT} \frac{\partial \hat{T}}{\partial t} + C_{Ta} \frac{\partial \hat{u}_a}{\partial t} \right] d\Omega^e = 0 \end{aligned} \quad (4.55)$$

Equation (4.55) can be rearranged as:

$$\begin{aligned}
 & \left\{ \int_{\Omega^e} \nabla [N_r K_{Tw} \nabla \hat{u}_w] d\Omega^e + \int_{\Omega^e} \nabla [N_r K_{TT} \nabla \hat{T}] d\Omega^e + \int_{\Omega^e} \nabla [N_r K_{Ta} \nabla \hat{u}_a] d\Omega^e + \int_{\Omega^e} [\nabla (N_r (T - T_r) C_{Pw} \rho_w \nabla K_w \nabla z)] d\Omega^e \right\} \\
 & + \left\{ \int_{\Omega^e} N_r V_{Tw} \nabla \hat{u}_w d\Omega^e + \int_{\Omega^e} N_r V_{TT} \nabla \hat{T} d\Omega^e + \int_{\Omega^e} N_r V_{Ta} \nabla \hat{u}_a d\Omega^e \right\} \\
 & + \left\{ - \int_{\Omega^e} [K_{Tw} \nabla \hat{u}_w \nabla N_r] d\Omega^e - \int_{\Omega^e} [K_{TT} \nabla \hat{T} \nabla N_r] d\Omega^e - \int_{\Omega^e} [K_{Ta} \nabla \hat{u}_a \nabla N_r] d\Omega^e - \int_{\Omega^e} [(T - T_r) C_{Pw} \rho_w K_w \nabla z \nabla N_r] d\Omega^e \right\} \\
 & + \left\{ - \int_{\Omega^e} N_r \left[ C_{Tw} \frac{\partial \hat{u}_w}{\partial t} + C_{TT} \frac{\partial \hat{T}}{\partial t} + C_{Ta} \frac{\partial \hat{u}_a}{\partial t} \right] d\Omega^e \right\} = 0
 \end{aligned} \tag{4.56}$$

Applying Gauss-Green divergence theorem for the first term of equation (4.56) yields:

$$\begin{aligned}
 & \int_{\Omega^e} \nabla N_r \left\{ [K_{Tw} \nabla \hat{u}_w] + [K_{TT} \nabla \hat{T}] + [K_{Ta} \nabla \hat{u}_a] + [K_{Ta} \nabla \hat{u}_a] + [(T - T_r) C_{Pw} \rho_w \nabla K_w \nabla z] \right\} d\Omega^e \\
 & = \int_{\Gamma^e} N_r \left\{ [K_{Tw} \nabla \hat{u}_w] + [K_{TT} \nabla \hat{T}] + [K_{Ta} \nabla \hat{u}_a] + [K_{Ta} \nabla \hat{u}_a] + [(T - T_r) C_{Pw} \rho_w \nabla K_w \nabla z] \right\} n d\Gamma^e
 \end{aligned} \tag{4.57}$$

Substituting (4.57) into equation (4.56) results:

$$\begin{aligned}
 & \left\{ \int_{\Omega^e} [K_{Tw} \nabla \hat{u}_w \nabla N_r] d\Omega^e + \int_{\Omega^e} [K_{TT} \nabla \hat{T} \nabla N_r] d\Omega^e + \int_{\Omega^e} [K_{Ta} \nabla \hat{u}_a \nabla N_r] d\Omega^e \right\} \\
 & + \left\{ \int_{\Omega^e} [(T - T_r) C_{Pw} \rho_w K_w \nabla z \nabla N_r] d\Omega^e \right\} \\
 & + \left\{ \int_{\Omega^e} N_r \left[ C_{Tw} \frac{\partial \hat{u}_w}{\partial t} + C_{TT} \frac{\partial \hat{T}}{\partial t} + C_{Ta} \frac{\partial \hat{u}_a}{\partial t} \right] d\Omega^e \right\} \\
 & - \left\{ \int_{\Omega^e} N_r V_{Tw} \nabla \hat{u}_w d\Omega^e + \int_{\Omega^e} N_r V_{TT} \nabla \hat{T} d\Omega^e + \int_{\Omega^e} N_r V_{Ta} \nabla \hat{u}_a d\Omega^e \right\} \\
 & - \int_{\Gamma^e} N_r \left\{ [K_{Tw} \nabla \hat{u}_w] + [K_{TT} \nabla \hat{T}] + [K_{Ta} \nabla \hat{u}_a] + [K_{Ta} \nabla \hat{u}_a] + [(T - T_r) C_{Pw} \rho_w \nabla K_w \nabla z] \right\} n d\Gamma^e = 0
 \end{aligned} \tag{4.58}$$

The surface integral in equation (4.58) is equal to the sum of free and dissolved heat fluxes normal to the boundary surface. Substituting equations (3.9), (3.22) and (3.46) for water, air and vapour velocities into the last term of equation (4.58) yields:

$$\begin{aligned}
 & \int_{\Gamma^e} N_r \left\{ [K_{Tw} \nabla \hat{u}_w] + [K_{TT} \nabla \hat{T}] + [K_{Ta} \nabla \hat{u}_a] + [K_{Ta} \nabla \hat{u}_a] + [(T - T_r) C_{pw} \rho_w \nabla K_w \nabla z] \right\} n d\Gamma^e \\
 & = \int_{\Omega^e} N_r \left[ \nabla(-\lambda_T \nabla \hat{T}) \right] + \left[ \rho_w L \nabla (K_{va} \nabla \hat{u}_a + K_{vw} \nabla \hat{u}_w + K_{vT} \nabla \hat{T}) \right] + \left[ L \nabla (\rho_v K_a \nabla \hat{u}_a) \right] \\
 & + \left[ (T - T_r) C_{pw} \rho_w K_w \nabla \hat{u}_w + (T - T_r) C_{pw} \rho_w K_w \nabla z \right] \\
 & + \left[ (T - T_r) C_{pv} \rho_w (K_{va} \nabla \hat{u}_a + K_{vw} \nabla \hat{u}_w + K_{vT} \nabla \hat{T}) \right] \\
 & + \left[ (T - T_r) C_{pv} \rho_v K_a \nabla \hat{u}_a + (T - T_r) C_{pda} \rho_{da} K_a \nabla \hat{u}_a \right] n d\Gamma^e \\
 & = \int_{\Gamma^e} N_r (F_{h1} + F_{h2} + F_{h3} + F_{h4} + F_{h5} + F_{h6}) d\Gamma^e
 \end{aligned} \tag{4.59}$$

where,

$F_{h1} = (-\lambda_T \nabla \hat{T})$  : is the approximation of heat flux normal to the boundary surface due to conduction.

$F_{h2} = \rho_w L \nabla (K_{va} \nabla \hat{u}_a + K_{vw} \nabla \hat{u}_w + K_{vT} \nabla \hat{T}) + L \nabla (\rho_v K_a \nabla \hat{u}_a)$  : is the approximation of heat flux normal to the boundary surface due to latent heat transfer by vapour movement.

$F_{h3} = (T - T_r) (C_{pw} \rho_w K_w \nabla \hat{u}_w + C_{pw} \rho_w K_w \nabla z)$  : is the approximation of heat flux normal to the boundary surface due to heat transfer by liquid movement.

$F_{h4} = (T - T_r) C_{pv} \rho_w (K_{va} \nabla \hat{u}_a + K_{vw} \nabla \hat{u}_w + K_{vT} \nabla \hat{T})$  : is the approximation of heat flux normal to the boundary surface due to heat transfer by vapour movement resulting from vapour pressure gradient.

$F_{h5} = (T - T_r) C_{pv} \rho_v K_a \nabla \hat{u}_a$  : is the approximation of heat flux normal to the boundary surface due to heat transfer by vapour movement resulting from bulk flow of air, and

$F_{h6} = (T - T_r) C_{pda} \rho_{da} K_a \nabla \hat{u}_a$  : is the approximation of heat flux normal to the boundary surface due to heat transfer by dry air movement resulting from an air pressure gradient.

By introducing the derivatives of the shape function equations from equation (4.5), (4.6) and (4.7) into equation (4.58) and substituting from equation (4.59), the final form of equation (4.58) can be written as:

$$\begin{aligned}
 & \left\{ \int_{\Omega^e} [K_{Tw} \nabla N^T \nabla N] d\Omega^e u_{ws} + \int_{\Omega^e} [K_{TT} \nabla N^T \nabla N] d\Omega^e T_s + \int_{\Omega^e} [K_{Ta} \nabla N^T \nabla N] d\Omega^e u_{as} \right. \\
 & \left. + \int_{\Omega^e} [(T - T_r) C_{Pw} \rho_w K_w \nabla N^T \nabla z] d\Omega^e \right\} \\
 & - \left\{ \int_{\Omega^e} [N^T V_{Tw} \nabla N] d\Omega^e u_{ws} + \int_{\Omega^e} [N^T V_{TT} \nabla N] d\Omega^e T_s + \int_{\Omega^e} [N^T V_{Ta} \nabla N] d\Omega^e u_{as} \right\} \\
 & + \left\{ \int_{\Omega^e} [N^T C_{Tw} N] d\Omega^e \frac{\partial u_{ws}}{\partial t} + \int_{\Omega^e} [N^T C_{TT} N] d\Omega^e \frac{\partial T_s}{\partial t} + \int_{\Omega^e} [N^T C_{Ta} N] d\Omega^e \frac{\partial u_{as}}{\partial t} \right\} \\
 & - \int_{\Gamma^e} N^T (F_{h1} + F_{h2} + F_{h3} + F_{h4} + F_{h5} + F_{h6}) d\Gamma^e = 0
 \end{aligned} \tag{4.60}$$

The spatial discretization of the governing differential equation for heat flow can be written as:

$$C_{Tw} \frac{\partial u_{ws}}{\partial t} + C_{TT} \frac{\partial T_s}{\partial t} + C_{Ta} \frac{\partial u_{as}}{\partial t} + K_{Tw} u_{ws} + K_{TT} T_s + K_{Ta} u_{as} = f_T \tag{4.61}$$

where,

$$C_{Tw} = \sum_{e=1}^m \int_{\Omega^e} [N^T C_{Tw} N] d\Omega^e \tag{4.62}$$

$$C_{TT} = \sum_{e=1}^m \int_{\Omega^e} [N^T C_{TT} N] d\Omega^e \tag{4.63}$$

$$C_{Ta} = \sum_{e=1}^m \int_{\Omega^e} [N^T C_{Ta} N] d\Omega^e \tag{4.64}$$

$$K_{Tw} = \sum_{e=1}^m \int_{\Omega^e} [\nabla N^T K_{Tw} \nabla N + N^T V_{Tw} \nabla N] d\Omega^e \tag{4.65}$$

$$K_{TT} = \sum_{e=1}^m \int_{\Omega^e} [\nabla N^T K_{TT} \nabla N + N^T V_{TT} \nabla N] d\Omega^e \tag{4.66}$$

$$K_{Ta} = \sum_{e=1}^m \int_{\Omega^e} [\nabla N^T K_{Ta} \nabla N + N^T V_{Ta} \nabla N] d\Omega^e \tag{4.67}$$

$$f_T = \sum_{e=1}^m \int_{\Omega^e} [(T - T_r) C_{Pw} \rho_w K_w \nabla N^T \nabla z] d\Omega^e - \sum_{e=1}^m \int_{\Gamma^e} N^T (F_{h1} + F_{h2} + F_{h3} + F_{h4} + F_{h5} + F_{h6}) d\Gamma^e \tag{4.68}$$

### 4.3.4 Spatial discretization of the solute transport governing equation

In this work the numerical solution for solute transport governing differential equation have been stated for saturated and unsaturated soils as following:

#### 4.3.4.1 Solute transport in saturated soils

The governing differential equation for solute transport in saturated soils was derived in chapter 3 in equation (3.162) as:

$$\frac{\partial(\theta c)}{\partial t} + \nabla(vc) - \nabla(D\nabla c) + \lambda c = 0 \quad (4.69)$$

The primary unknowns can be approximated using the shape function approach for eight node isoparametric element as:

$$\theta c = \hat{\theta} \hat{c} = \sum_1^8 N_s \theta c_s \quad (4.70)$$

$$c = \hat{c} = \sum_1^8 N_s c_s \quad (4.71)$$

where,  $c_s$  : is the nodal solute concentration.

By replacing the primary unknowns in equation (4.69) with their shape function approximations from equations (4.70) and (4.71), equation (4.69) can be written as:

$$\frac{\partial(\theta \hat{c})}{\partial t} + \nabla(v \hat{c}) - \nabla(D \nabla \hat{c}) + \lambda \hat{c} = R_{\Omega c} \quad (4.72)$$

where,



$R_{\Omega_c}$  : is the residual errors introduced by the approximation function.

Employing the Galerkin weighted residual approach to minimize the residual error represented by equation (4.72) and integrating the equation over the spatial domain  $\Omega^e$  yields (AL-Najjar, 2006):

$$\int_{\Omega^e} N_r \left[ \frac{\partial(\theta\hat{c})}{\partial t} + \nabla(v\hat{c}) - \nabla(D\hat{c}) + \lambda\hat{c} \right] d\Omega^e = 0 \quad (4.73)$$

In equation (4.73) it is convenient to integrate all the spatial derivatives by parts as following:

The first term can be written as:

$$\int_{\Omega^e} N_r \frac{\partial(\theta\hat{c})}{\partial t} d\Omega = \sum_1^8 \frac{\theta c}{\Delta t} \int_{\Omega^e} NN d\Omega^e \quad (4.74)$$

The advection which is represented by the second term can be written as:

$$\int_{\Omega^e} \nabla(v\hat{c}) N_r d\Omega^e = -v_{wx} \sum_1^8 c \int_{\Omega^e} N \frac{\partial N}{\partial x} d\Omega^e - v_{wy} \sum_1^8 c \int_{\Omega^e} N \frac{\partial N}{\partial y} d\Omega^e \quad (4.75)$$

The dispersion-diffusion term which is represented by the third term can be written as:

$$\begin{aligned} \int_{\Omega^e} \nabla(D\nabla\hat{c}) N_r d\Omega^e &= D_{wxx} \theta_w \sum_1^8 c \int_{\Omega^e} \frac{\partial N}{\partial x} \frac{\partial N}{\partial x} d\Omega^e + D_{wxy} \theta_w \sum_1^8 c \int_{\Omega^e} \frac{\partial N}{\partial x} \frac{\partial N}{\partial y} d\Omega^e \\ &+ D_{wyy} \theta_w \sum_1^8 c \int_{\Omega^e} \frac{\partial N}{\partial y} \frac{\partial N}{\partial y} d\Omega^e + D_{wyx} \theta_w \sum_1^8 c \int_{\Omega^e} \frac{\partial N}{\partial y} \frac{\partial N}{\partial x} d\Omega^e \end{aligned} \quad (4.76)$$

Combining equations (4.75) and (4.76) yields:

$$\int_{\Omega^e} N_r \left[ \nabla \left\{ (v_{wx} + v_{wy}) \hat{c} \right\} - \nabla \left\{ (D_{wxx} + D_{wxy}) + (D_{wyy} + D_{wyx}) \theta_w \nabla \hat{c} \right\} \right] d\Omega^e = 0 \quad (4.77)$$

Discretization of equation (4.77) yields (Javadi et al, 2008):

$$N_r \left( v_{wx} \hat{c} - (D_{wxx} + D_{wxy}) \theta_w \nabla \hat{c} \right) \Big|_{\Omega^e} - \int_{\Omega^e} \left( v_{wx} \hat{c} - (D_{wxx} + D_{wxy}) \theta_w \nabla \hat{c} \right) \frac{\partial N_r}{\partial x} d\Omega^e = 0 \quad (4.78)$$

$$N_r \left( v_{wy} \hat{c} - (D_{wyy} + D_{wyx}) \theta_w \nabla \hat{c} \right) \Big|_{\Omega^e} - \int_{\Omega^e} \left( v_{wy} \hat{c} - (D_{wyy} + D_{wyx}) \theta_w \nabla \hat{c} \right) \frac{\partial N_r}{\partial y} d\Omega^e = 0 \quad (4.79)$$

Substituting equations (4.78) and (4.79) into (4.77), equation (4.77) can be rewritten as:

$$\begin{aligned} & N_r \left( v_{wx} \hat{c} - (D_{wxx} + D_{wxy}) \theta_w \nabla \hat{c} \right) \Big|_{\Omega^e} + N_r \left( v_{wy} \hat{c} - (D_{wyy} + D_{wyx}) \theta_w \nabla \hat{c} \right) \Big|_{\Omega^e} - \\ & \int_{\Omega^e} \left( v_{wy} \hat{c} - (D_{wyy} + D_{wyx}) \theta_w \nabla \hat{c} \right) \frac{\partial N_r}{\partial y} d\Omega^e - \int_{\Omega^e} \left( v_{wx} \hat{c} - (D_{wxx} + D_{wxy}) \theta_w \nabla \hat{c} \right) \frac{\partial N_r}{\partial x} d\Omega^e = 0 \end{aligned} \quad (4.80)$$

The fourth term in equation (4.73) can be written as:

$$\int_{\Omega^e} N_r \lambda \hat{c} d\Omega = \sum_1^8 \lambda \hat{c} \int_{\Omega^e} NN d\Omega^e \quad (4.81)$$

Substituting the four terms from equations (4.74), (4.80) and (4.81) into (4.73), equation (4.73) can be written as:

$$\begin{aligned} & \sum_1^8 \frac{\theta c}{\Delta t} \int_{\Omega^e} NN d\Omega^e + N_r \left( v_{wx} \hat{c} - (D_{wxx} + D_{wxy}) \theta_w \nabla \hat{c} \right) \Big|_{\Omega^e} + N_r \left( v_{wy} \hat{c} - (D_{wyy} + D_{wyx}) \theta_w \nabla \hat{c} \right) \Big|_{\Omega^e} - \\ & \int_{\Omega^e} \left( v_{wy} \hat{c} - (D_{wyy} + D_{wyx}) \theta_w \nabla \hat{c} \right) \frac{\partial N_r}{\partial y} d\Omega^e - \int_{\Omega^e} \left( v_{wx} \hat{c} - (D_{wxx} + D_{wxy}) \theta_w \nabla \hat{c} \right) \frac{\partial N_r}{\partial x} d\Omega^e \\ & + \sum_1^8 \lambda \hat{c} \int_{\Omega^e} NN d\Omega^e = 0 \end{aligned} \quad (4.82)$$

The integral in equation (4.82) can be evaluated for each element using the following equation (AL-Najjar, 2006):

$$\sum_1^8 \left[ \int_{\Omega^e} \frac{\theta c}{\Delta t} A_{ij} + N_r (vc - D \frac{\partial c}{\partial x} \frac{\partial c}{\partial y}) \Big|_{\Omega^e} - \int_{\Omega^e} (vc B_{ij} - Dc E_{ij} + \lambda c A_{ij}) \right] = 0 \quad (4.83)$$

where, the elemental integrals in equation (4.83) are given by:

$$A_{ij} = \int N N d\Omega^e \quad (4.84)$$

$$B_{ij} = \int N \frac{\partial N}{\partial x} N \frac{\partial N}{\partial y} d\Omega^e \quad (4.85)$$

$$E_{ij} = \int \frac{\partial N}{\partial x} \frac{\partial N}{\partial y} \frac{\partial N}{\partial x} \frac{\partial N}{\partial y} d\Omega^e \quad (4.86)$$

The discretized global finite element equation for a single component of solute transport can be written as (Javadi et al, 2008):

$$M \frac{dc}{dt} + Hc = F^c \quad (4.87)$$

where,

$$M = \sum_1^n \int_{\Omega^e} \frac{\theta c}{\Delta t} A_{ij} \quad (4.88)$$

$$H = \sum_1^n \int_{\Omega^e} vc B_{ij} + Dc E_{ij} + \lambda c A_{ij} \quad (4.89)$$

$$F^c = \sum_1^n N_r (vc - D \frac{\partial c}{\partial x} \frac{\partial c}{\partial y}) \Big|_{\Omega^e} \quad (4.90)$$

#### 4.3.4.2 Solute transport in unsaturated soils

The governing differential equation of solute transport in unsaturated soil was also defined in chapter 3 in equation (3.175) as:

$$\frac{\partial(\theta c)}{\partial t} + \nabla(vc) - \nabla(D\nabla c) + \lambda c = 0 \quad (4.91)$$

By replacing the primary unknowns in equation (4.91) with their shape function approximations from equations (4.70) and (4.71), equation (4.91) can be written as:

$$\frac{\partial(\theta \hat{c})}{\partial t} + \nabla(v\hat{c}) - \nabla(D\nabla \hat{c}) + \lambda \hat{c} = R_{\Omega c} \quad (4.92)$$

Employing the Galerkin weighted residual approach to minimize the residual error represented by equation (4.92) and integrating the equation over the spatial domain  $\Omega^e$  yields (AL-Najjar, 2006):

$$\int_{\Omega^e} N_r \left[ \frac{\partial(\theta \hat{c})}{\partial t} + \nabla(v\hat{c}) - \nabla(D\nabla \hat{c}) + \lambda \hat{c} \right] d\Omega^e = 0 \quad (4.93)$$

In equation (4.93) it is convenient to integrate all the spatial derivatives by parts as following:

The first term can be written as:

$$\int_{\Omega^e} N_r \frac{\partial(\theta \hat{c})}{\partial t} d\Omega = \sum_1^8 \frac{\theta c}{\Delta t} \int_{\Omega^e} N N d\Omega^e \quad (4.94)$$

The advection which is represented by the second term can be written as:

$$\int_{\Omega^e} \nabla(v\hat{c})N_r d\Omega^e = -(v_{wx} + Hv_{ax}) \sum_1^8 c \int_{\Omega^e} N \frac{\partial N}{\partial x} d\Omega^e - (v_{wy} + Hv_{ay}) \sum_1^8 c \int_{\Omega^e} N \frac{\partial N}{\partial y} d\Omega^e \quad (4.95)$$

The dispersion-diffusion term which is represented by the third term can be written as:

$$\begin{aligned} \int_{\Omega^e} \nabla(D\nabla\hat{c})N_r d\Omega^e &= (D_{wxx}\theta_w + HD_{axx}\theta_a) \sum_1^8 c \int_{\Omega^e} \frac{\partial N}{\partial x} \frac{\partial N}{\partial x} d\Omega^e \\ &+ (D_{wxy}\theta_w + HD_{axy}\theta_a) \sum_1^8 c \int_{\Omega^e} \frac{\partial N}{\partial x} \frac{\partial N}{\partial y} d\Omega^e \\ &+ (D_{wyy}\theta_w + HD_{ayy}\theta_a) \sum_1^8 c \int_{\Omega^e} \frac{\partial N}{\partial y} \frac{\partial N}{\partial y} d\Omega^e \\ &+ (D_{wyx}\theta_w + HD_{ayx}\theta_a) \sum_1^8 c \int_{\Omega^e} \frac{\partial N}{\partial y} \frac{\partial N}{\partial x} d\Omega^e \end{aligned} \quad (4.96)$$

By combining equations (4.95) and (4.96) as:

$$\begin{aligned} \int_{\Omega^e} N_r \left[ \nabla \left\{ (v_{wx} + v_{wy}) + H(v_{ax} + v_{ay}) \right\} \hat{c} - \nabla \left\{ \theta_w (D_{wxx} + D_{wxy}) + (D_{wyy} + D_{wyx}) \right. \right. \\ \left. \left. + H\theta_a (D_{axx} + D_{axy}) + (D_{ayy} + D_{ayx}) \right\} \nabla \hat{c} \right] d\Omega^e = 0 \end{aligned} \quad (4.97)$$

Discretization of equation (4.97) yields (Javadi et al, 2008):

$$\begin{aligned} N_r \left( (v_{wx} + Hv_{ax}) \hat{c} - \left\{ (D_{wxx} + D_{wxy}) \theta_w + (D_{axx} + D_{axy}) H\theta_a \right\} \nabla \hat{c} \right) \Big|_{\Omega^e} - \\ \int_{\Omega^e} \left( (v_{wx} + Hv_{ax}) \hat{c} - \left\{ (D_{wxx} + D_{wxy}) \theta_w + (D_{axx} + D_{axy}) H\theta_a \right\} \nabla \hat{c} \right) \frac{\partial N_r}{\partial x} d\Omega^e = 0 \end{aligned} \quad (4.98)$$

$$\begin{aligned} N_r \left( (v_{wy} + Hv_{ay}) \hat{c} - \left\{ (D_{wyy} + D_{wyx}) \theta_w + (D_{ayy} + D_{ayx}) H\theta_a \right\} \nabla \hat{c} \right) \Big|_{\Omega^e} - \\ \int_{\Omega^e} \left( (v_{wy} + Hv_{ay}) \hat{c} - \left\{ (D_{wyy} + D_{wyx}) \theta_w + (D_{ayy} + D_{ayx}) H\theta_a \right\} \nabla \hat{c} \right) \frac{\partial N_r}{\partial y} d\Omega^e = 0 \end{aligned} \quad (4.99)$$

Substituting from equations (4.98) and (4.99) into equation (4.97), equation (4.97) can be written as:

$$\begin{aligned}
 & N_r \left( (v_{wx} + H v_{ax}) \hat{c} - \left( \{ (D_{wxx} + D_{wxy}) \} \theta_w \{ (D_{axx} + D_{axy}) \} H \theta_a \right) \nabla \hat{c} \right) \Big|_{\Omega^e} + \\
 & N_r \left( (v_{wy} + H v_{ay}) \hat{c} - \left( \{ (D_{wyy} + D_{wyx}) \} \theta_w + \{ (D_{ayy} + D_{ayx}) \} H \theta_a \right) \nabla \hat{c} \right) \Big|_{\Omega^e} - \\
 & \int_{\Omega^e} \left( (v_{wx} + H v_{ax}) \hat{c} - \left( \{ (D_{wxx} + D_{wxy}) \} \theta_w \{ (D_{axx} + D_{axy}) \} H \theta_a \right) \nabla \hat{c} \right) \frac{\partial N_r}{\partial x} d\Omega^e - \\
 & \int_{\Omega^e} \left( (v_{wy} + H v_{ay}) \hat{c} - \left( \{ (D_{wyy} + D_{wyx}) \} \theta_w + \{ (D_{ayy} + D_{ayx}) \} H \theta_a \right) \nabla \hat{c} \right) \frac{\partial N_r}{\partial y} d\Omega^e = 0
 \end{aligned} \tag{4.100}$$

The fourth term of equation (4.93) can be written as:

$$\int_{\Omega^e} N_r \lambda \hat{c} d\Omega = \sum_1^8 \lambda \hat{c} \int_{\Omega^e} N N d\Omega^e \tag{4.101}$$

Substituting the four terms from equations (4.94), (4.100) and (4.101) into (4.93), equation (4.93) can be written as:

$$\begin{aligned}
 & \sum_1^8 \frac{\theta c}{\Delta t} \int_{\Omega^e} N N d\Omega^e + N_r \left( (v_{wx} + H v_{ax}) \hat{c} - \left( \{ (D_{wxx} + D_{wxy}) \} \theta_w \{ (D_{axx} + D_{axy}) \} H \theta_a \right) \nabla \hat{c} \right) \Big|_{\Omega^e} \\
 & + N_r \left( (v_{wy} + H v_{ay}) \hat{c} - \left( \{ (D_{wyy} + D_{wyx}) \} \theta_w + \{ (D_{ayy} + D_{ayx}) \} H \theta_a \right) \nabla \hat{c} \right) \Big|_{\Omega^e} - \\
 & \int_{\Omega^e} \left( (v_{wx} + H v_{ax}) \hat{c} - \left( \{ (D_{wxx} + D_{wxy}) \} \theta_w \{ (D_{axx} + D_{axy}) \} H \theta_a \right) \nabla \hat{c} \right) \frac{\partial N_r}{\partial x} d\Omega^e - \\
 & \int_{\Omega^e} \left( (v_{wy} + H v_{ay}) \hat{c} - \left( \{ (D_{wyy} + D_{wyx}) \} \theta_w + \{ (D_{ayy} + D_{ayx}) \} H \theta_a \right) \nabla \hat{c} \right) \frac{\partial N_r}{\partial y} d\Omega^e + \sum_1^8 \lambda \hat{c} \int_{\Omega^e} N N d\Omega^e = 0
 \end{aligned} \tag{4.102}$$

The integral in equation (4.102) can be evaluated for each element using the following equation (AL-Najjar, 2006):

$$\sum_1^8 \left[ \int_{\Omega^e} \frac{\theta c}{\Delta t} A_{ij} + N_r \left( v c - D \frac{\partial c}{\partial x} \frac{\partial c}{\partial y} \right) \Big|_{\Omega^e} - \int_{\Omega^e} \left( v c B_{ij} - D c E_{ij} + \lambda c A_{ij} \right) \right] = 0 \tag{4.103}$$

where, the elemental integrals in equation (4.103) are given by:

$$A_{ij} = \int NNd\Omega^e \quad (4.104)$$

$$B_{ij} = \int N \frac{\partial N}{\partial x} N \frac{\partial N}{\partial y} d\Omega^e \quad (4.105)$$

$$E_{ij} = \int \frac{\partial N}{\partial x} \frac{\partial N}{\partial y} \frac{\partial N}{\partial x} \frac{\partial N}{\partial y} d\Omega^e \quad (4.106)$$

The discretized global finite element equation for single component of solute transport takes the form (Javadi et al, 2008):

$$M \frac{dc}{dt} + Hc = F^c \quad (4.107)$$

where,

$$M = \sum_1^n \int_{\Omega^e} \frac{\theta c}{\Delta t} A_{ij} \quad (4.108)$$

$$H = \sum_1^n \int_{\Omega^e} vcB_{ij} + DcE_{ij} + \lambda cA_{ij} \quad (4.109)$$

$$F^c = \sum_1^n N_r (vc - D \frac{\partial c}{\partial x} \frac{\partial c}{\partial y}) \Big|_{\Omega^e} \quad (4.110)$$

### 4.3.5 Temporal discretization of the coupled fluid flow and heat transfer

The spatially discretized equations for coupled flow of water, air and heat are given by the equations (4.20), (4.41) and (4.61) respectively. These equations can be combined in a matrix form as:

$$\begin{bmatrix} K_{ww} & K_{wa} & K_{wT} \\ K_{aw} & K_{aa} & K_{aT} \\ K_{Tw} & K_{Ta} & K_{TT} \end{bmatrix} \begin{bmatrix} u_{ws} \\ u_{as} \\ T_s \end{bmatrix} + \begin{bmatrix} C_{ww} & C_{wa} & C_{wT} \\ C_{aw} & C_{aa} & C_{aT} \\ C_{Tw} & C_{Ta} & C_{TT} \end{bmatrix} \begin{bmatrix} \dot{u}_{ws} \\ \dot{u}_{as} \\ \dot{T}_s \end{bmatrix} = \begin{bmatrix} f_w \\ f_a \\ f_T \end{bmatrix} \quad (4.111)$$

where,

$$\dot{u}_{ws} = \frac{\partial u_{ws}}{\partial t} \quad (4.112)$$

$$\dot{T}_s = \frac{\partial T_s}{\partial t} \quad (4.113)$$

$$\dot{u}_{as} = \frac{\partial u_{as}}{\partial t} \quad (4.114)$$

Equation (4.111) can be rewritten in the following form (Istok, 1989):

$$K(\phi) + C \left[ \frac{\partial \phi}{\partial t} \right] = [F] \quad (4.115)$$

where,

$K$  : is the assemblage conductance matrix.

$C$  : is the assemblage capacitance matrix.

$F$  : is the vector of source or sink.

$\phi$  : is the vector of unknowns.



$$K = \begin{bmatrix} K_{ww} & K_{wa} & K_{wT} \\ K_{aw} & K_{aa} & K_{aT} \\ K_{Tw} & K_{Ta} & K_{TT} \end{bmatrix} ; C = \begin{bmatrix} C_{ww} & C_{wa} & C_{wT} \\ C_{aw} & C_{aa} & C_{aT} \\ C_{Tw} & C_{Ta} & C_{TT} \end{bmatrix} ; F = \begin{bmatrix} f_w \\ f_a \\ f_T \end{bmatrix} ; \phi = \begin{bmatrix} u_{ws} \\ u_{as} \\ T_s \end{bmatrix}$$

Equation (4.115) is a system of ordinary differential equations, whose solution provides values of unknowns at each node in the finite element mesh. This equation is highly non linear and can only be solved using the iteration procedure. The finite difference approach can be used to discretize the governing equations for fluid flow. Therefore, the time discretisation of equation (4.115) can be written as (Istok, 1989):

$$[C + \theta K \Delta t] \phi_{i+1} = [C - (1 - \theta) K \Delta t] \phi_i + [(1 - \theta) F_i + \theta F_{i+1}] \Delta t \quad (4.116)$$

where,

$i$  : is the iteration number.

$\theta$  : takes the value of 0, 1/2 or 1 for the forward, central, and backward difference schemes respectively. A value of  $\theta$  equal to 1 (for the backward difference scheme) has been used in the current work as it proved its efficiency in solving highly non-linear equations. Equation (4.116) can be rewritten as:

$$K_{eff} \phi_{i+1} = F_{eff} \quad (4.117)$$

where

$$K_{eff} = [C + \theta K \Delta t] \quad (4.118)$$

$$F_{eff} = [C - (1 - \theta) K \Delta t] \phi_i + [(1 - \theta) F_i + \theta F_{i+1}] \Delta t \quad (4.119)$$

The iteration procedure commences with assuming an initial value for  $\phi_i$  as an initial conditions. Therefore, the right hand side terms  $F_{eff}$  of equation (4.117) can be obtained at the beginning of the time step, the first assumption for  $\phi_{i+1}$  is assumed to be the result of

the previous time step  $\phi_i$ , therefore the value of  $\phi_{i+1}$  for the first iteration can be obtained by :

$$\phi_{i+1} = K_{eff}^{-1} F_{eff} \quad (4.120)$$

The iterative solution proceeds till the problem converges. It is assumed that convergence occurs when the following norm criterion is satisfied;

$$\left| \frac{\phi_{i+1}^{n+1} - \phi_i^{n+1}}{\phi_i^{n+1}} \right| \leq tolerance \quad (4.121)$$

where,  $n$  : is the time step level.

A solution of the fully coupled flow and heat transformation formulation can be achieved in equation (4.116) which will give pore water pressure  $u_w$ , pore air pressure  $u_a$  and temperature  $T$  at various points within the soil and at different times, taking into account the interaction between the flow of water, air and heat.

### 4.3.6 Temporal discretization of solute transport

The spatially discretized equation for solute transport in saturated and unsaturated soils is given by equations (4.87) and (4.107) respectively. As explained earlier in equations (4.115) and (4.116), the finite difference approach can be used to discretize the governing equations for solute transport. Therefore, equation (4.115) and (4.116) can be written for solute transport as (Istok, 1989):

$$H[\varphi] + M \left[ \frac{\partial \varphi}{\partial t} \right] = [F^c] \quad (4.122)$$

$$[M + \theta H \Delta t] \varphi_{i+1} = [M - (1 - \theta) H \Delta t] \varphi_i + [(1 - \theta) F^c_i + \theta F^c_{i+1}] \Delta t \quad (4.123)$$

where,

$\varphi$  : is the vector of unknowns.

$M$  ,  $H$  and  $F^c$  : are matrices defined by equations (4.88), (4.89) and (4.90) respectively.

Equation (4.123) can be rewritten as:

$$H_{eff} \varphi_{i+1} = F^c_{eff} \quad (4.124)$$

where

$$H_{eff} = [M + \theta H \Delta t] \quad (4.125)$$

$$F^c_{eff} = [M - (1 - \theta) H \Delta t] \varphi_i + [(1 - \theta) F^c_i + \theta F^c_{i+1}] \Delta t \quad (4.126)$$

Similarly, the iteration procedure commences with assuming an initial value for  $\varphi_i$  as an initial conditions, therefore, the right hand side terms  $F^c_{eff}$  of equation (4.124) can be obtained at the beginning of the time step. The first assumption for  $\varphi_{i+1}$  is assumed to be the result of the previous time step  $\varphi_i$ , therefore the value of  $\varphi_{i+1}$  for the first iteration can be obtained by:

$$\varphi_{i+1} = H_{eff}^{-1} F^c_{eff} \quad (4.127)$$

Similarly, the iterative solution proceeds till the problem converges. The convergence occurs when the norm criterion is satisfied in equation (4.121).

A solution of the solute transport equation can be achieved in equation (4.123) which will give the distribution of the solute concentrations  $c$  at various points within the unsaturated soil and at different times, taking into account the interaction between the flow of water, heat and various mechanisms of solute transport.

#### 4.4 Coupling of fluid flow and solute transport equations

The numerical solution of coupled fluid flow and solute transport in soil is based on solving the governing equations with appropriate boundary and initial conditions by an iterative solution scheme as described in the following steps:

- 1- The required data including, control parameters, geometric data and initial and boundary conditions for fluid flow, heat transfer and solute concentration are entered and checked.
- 2- The iterative routine starts at a given time step with an estimate of unknowns based on the values of the previous time step.
- 3- Solution of the fluid flow and heat transfer equations provides the nodal values of pore water pressure  $u_w$ , pore air pressure  $u_a$  and temperature  $T$  at each point in the grid at the next time step.
- 4- The nodal values of hydraulic head, fluid velocity, dispersion coefficient and fluid density are computed according to the updated values of pressure. Through Darcy's law and a constitutive equation relating fluid density to salt concentration, the fluid flow and solute transport equations are coupled and solved.

The hydraulic head  $h_w$  is calculated as (Fredlund and Rahardjo, 1993):

$$h_w = \frac{u_w}{\rho_w g} + z \quad (4.128)$$

The fluid velocity is calculated according to Darcy's law as (Darcy, 1856):

$$v_w = -K_w \left[ \nabla \left( \frac{u_w}{\gamma_w} \right) + \nabla z \right] \quad (4.129)$$

The constitutive equation relating the fluid density to concentration can be used to update the density as (Rastogi, 2004):

$$\rho = \rho_f (1 + \varepsilon C) \quad (4.130)$$

where,  $\varepsilon = \frac{\rho_s - \rho_f}{\rho_f}$  and  $\rho_f$ ,  $\rho_s$  are the freshwater and the seawater densities respectively  $[M][L]^{-3}$ .

- 5- Solution of solute transport equation provides the nodal values of concentration using the updated parameters obtained in step 4.
- 6- The procedure (step 3 to step 5) is repeated by evaluating the concentration-dependant parameters again with the updated values of concentration and solving the governing equations at the same time level.
- 7- The cycle is repeated until the convergence criterion is satisfied and then the results are recorded.
- 8- The results of the current time step are stored and used as initial values for the next time step.
- 9- The cycle is repeated at each time step until the last time step.

The developed finite element model is an extension to a model that was developed by AL-Najjar, (2006). The model has been extended to include density-dependent flow and an algorithm has been implemented to incorporate density-dependency of flow in the original model. The solute transport formulation has been extended to include new transport mechanisms. The model has been applied to study seawater intrusion and the effect of climate change and sea level rise on coastal aquifers. Also, a simulation-optimisation model has been developed by integrating the FE model and a genetic algorithm to optimize arrangements for SWI control. A flow chart of the numerical solution algorithm is shown in Figure 6.1.

The application of the proposed model requires sufficient and accurate data. The types of data required for the application of the proposed model are mainly based on the representation of the fluid flow and solute transport process. Thus, the data file used by both coupled flow and transport analyses contains the initial values of pore water pressure  $u_{ow}$ , pore air pressure  $u_{oa}$ , temperature  $T_o$  and solute concentration  $c_o$  at all nodes of the domain, longitudinal and transverse dispersivity values, molecular diffusion coefficient, density, porosity of the soil and the boundary conditions on boundaries of the domain for a particular site.

## **Validation and application of the simulation model**

### ***5.1 Introduction***

A finite element model for saturated/unsaturated fluid flow and solute transport (SUFT) has been developed. The developed model is transient, density-dependant and the dispersion is velocity dependant. The coupled fluid flow and solute transport model can handle a wide range of real-world problems including the simulation of groundwater flow and solute transport separately and coupled fluid flow and solute transport in addition to saltwater intrusion in coastal aquifers. This chapter presents the validation and application of the developed model. The model is validated against a number of problems from literature to examine its capabilities to handle solute transport problems through saturated/unsaturated porous media with density-dependant flow. Then, the model is applied to a number of real case studies for predicting saltwater intrusion in coastal aquifers in different locations of the world.

### ***5.2 Calibration, validation, and verification of the model***

Numerical models may be used to predict fluid flow or solute transport in soils. These models may also be used to evaluate different remediation alternatives. However, errors and uncertainties in a fluid flow and solute transport analysis make any model prediction no better than an approximation. Therefore, all model predictions should be expressed as a range of possible outcomes that reflect the assumptions involved and uncertainty in model input data and parameter values. Numerical model application can be considered to be two distinct processes. The first process is model development resulting in a software product, and the second process is application of that product for a specific purpose. The developed model should be calibrated and validated to ensure its accuracy before the application.

Calibration of a numerical model refers to the process in which model input parameters are adjusted, either manually or through formal mathematical procedures, until the model output matches the field-observed conditions satisfactorily. The model output variables can be hydraulic heads, flow rates, solute concentrations, or mass removal rates, depending on the objectives of the simulation. In practical model applications, model input parameters are never completely defined and are always associated with various uncertainties, no matter how many measurements have been made or how thoroughly site conditions have been characterised (Gunduz, 2004). Verification of a numerical model has been defined as the process in which the calibrated model is shown to be capable of reproducing a set of field observations independent of those used in model calibration. Validation of a numerical model is the process in which the calibrated model is shown, through a postaudit, to be capable of predicting future conditions with sufficient precision (Anderson and Woessner, 1992). Once the developed model is calibrated, verified and validated, it can be used for predictive simulations.

The fluid flow approaches to the governing equations suggest a natural way to define dimensionless groups that characterize the advection and diffusion. When numerically solving the solute transport equation, the appropriate dimensionless groups are Courant and Peclet numbers. These dimensionless groups have been found to be useful aids in characterizing the behavior of the numerical methods and for choosing appropriate discretizations. In order that accurate solutions are obtained, several guides on the discretization should be followed. Daus et al. (1985) used numerical experiments to demonstrate the behaviour of the finite element method in cases where the Peclet and Courant number criteria are not met. They showed that if the Peclet and Courant number criteria are not met there are no general rules for predicting the solution behaviour. Courant and Peclet numbers are described below:

### ***Courant Number***

Courant number is described mathematically as a function of the velocity of the fluid  $v$ , time step and spatial grid sizes  $\Delta x$  as:

$$C_r = \frac{v\Delta t}{\Delta x} \quad (5.1)$$

Courant number should be chosen ( $C_r \leq 1$ ) so that the equation satisfies the the Courant-Friedrichs-Lewy condition (CFL condition) (Courant et al., 1928). In mathematics, the Courant-Friedrichs-Lewy condition is a condition for certain algorithms for solving partial differential equations to be convergent. As a consequence, the time step must be less than a certain time in many explicit time-marching computer simulations, otherwise the simulation will produce wildly incorrect results.

### ***Peclet Number***

Peclet number is a relationship between the advective and diffusive components of solute transport and is expressed as the ratio of the product of the average interstitial velocity  $v$ , times the characteristic length, divided by the coefficient of molecular diffusion  $D_m$  :

$$P_e = \frac{v\Delta x}{D_m} \quad (5.2)$$

Small values indicate diffusion dominance whereas large values indicate advection. For purely advective problems Peclet number will equal to infinity as:

$$P_e = \frac{v\Delta x}{D} = \frac{\Delta x}{\alpha_L} = \infty \quad (5.3)$$

where,  $\alpha_L$  is the longitudinal dispersivity (m). Peclet number should be chosen ( $P_e \leq 2$ ).

The error measure shows that while the oscillations are smaller for larger Peclet numbers, the solution is not much more accurate (Binning, 1994).



### ***5.3 Numerical results***

Coupled fluid flow and solute transport models play an important role in many areas of engineering. The analysis of saltwater intrusion into coastal aquifers and salinization of groundwater is one of these areas. Therefore, a clear understanding of solute transport and the relevant transport processes is important for engineers. The numerical modeling can be used to further understanding of the seawater intrusion mechanism. Furthermore, numerical predictions could be used as an alternative means to assist coastal water resources planning in lieu of field data. In the following sections the developed finite element model (SUFT) is validated by application to a number of examples from the literature, including the simulation of groundwater flow alone, solute transport alone and coupled fluid flow and solute transport, and saltwater intrusion in coastal aquifers.

#### ***5.3.1 Example (1): Transient groundwater flow***

This example presents a transient flow in a confined aquifer in one dimension. A transient flow problem is one in which the unknown variable is time dependant. Transient problems are also called time dependant, nonequilibrium, or unsteady problems. This example represents a transient groundwater flow in a confined aquifer shown in Figure 5.1. The aquifer length is 100 m and the depth is 10 m. The domain has been divided into ten elements (10x10) m. The purpose is to simulate changes in head with time due to drop the water level in the reservoir from 16 m to 11 m. The boundary conditions are no flow along the top and bottom boundaries, 16 m head on the left boundary and 11 m head on the right boundary. The initial conditions are 16 m head everywhere in the aquifer. The boundary conditions are shown in Figure 5.1 (Wang and Anderson, 1982).

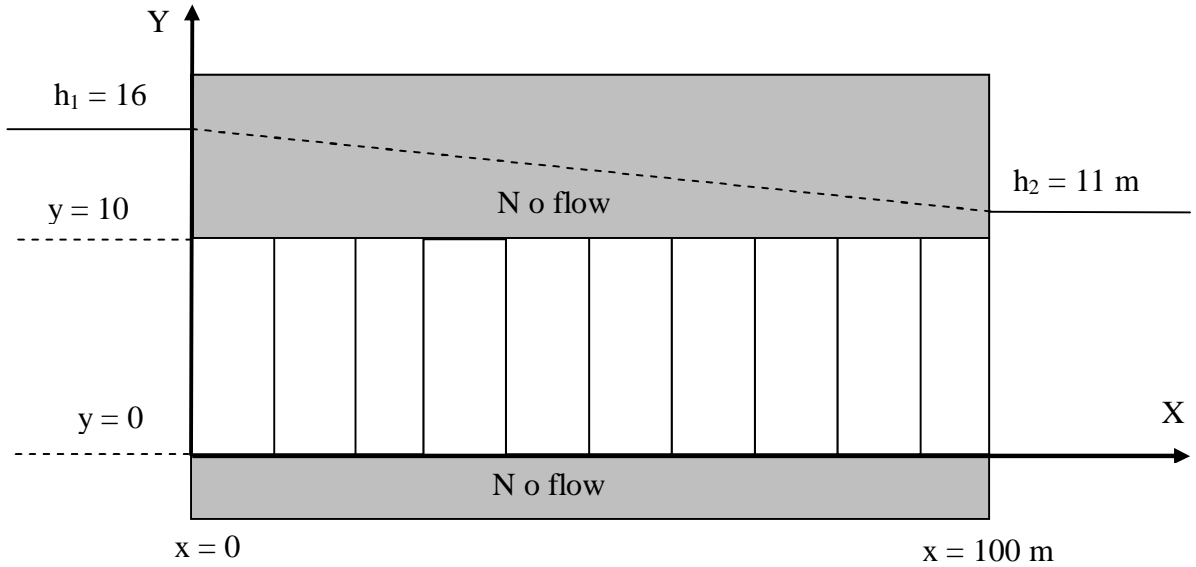


**Figure 5.1** Boundary and initial conditions of example (1)

The developed model (SUFT) has been used to calculate the distribution of head in the aquifer at each time step for total time of 500 min and  $\Delta t$  equal to 5 min. The results are shown in Figure 5.2.

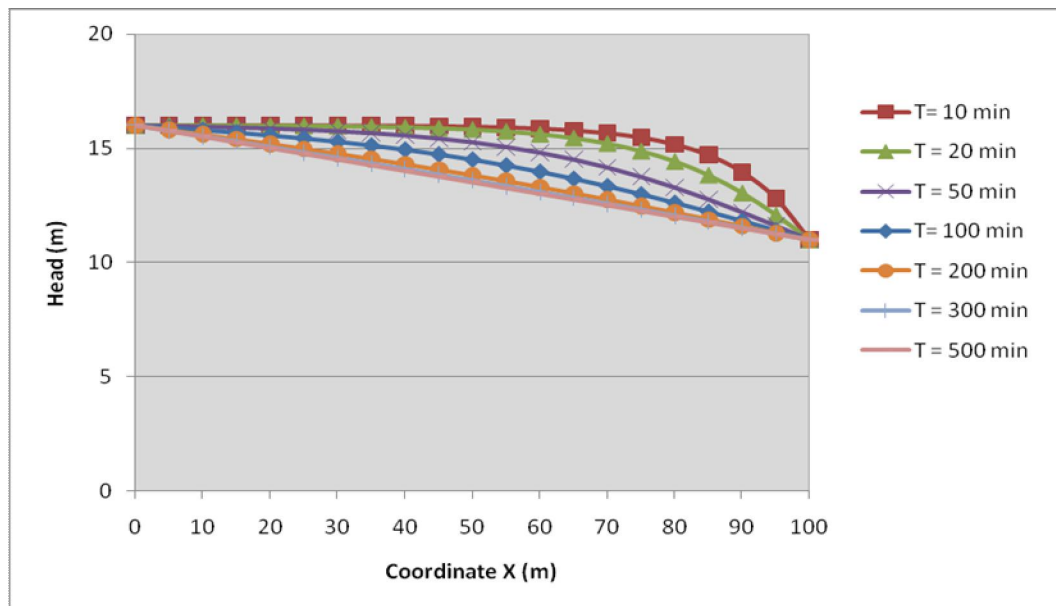


**Figure 5.2** Head distribution at different times in the reservoir

The results are compared with those reported by Wang and Anderson (1982), who presented a solution to this problem using the finite difference and finite element methods using rectangular elements. Figure 5.3 shows the results of the current model (SUFT) compared with the results of Wang and Anderson (1982). As shown the current results match with, a high accuracy, the published results for this problem.

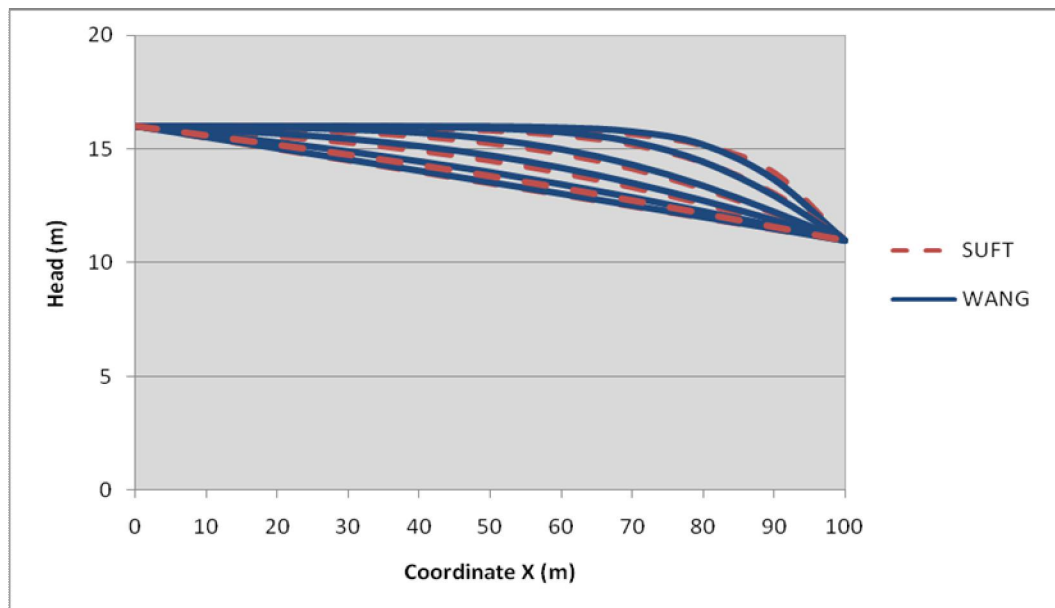


**Figure 5.3** Comparison between the current model and Wang and Anderson results for head distribution in the reservoir

### 5.3.2 Example (2): Transient solute transport

The current finite element model is applied to simulate transient solute transport in saturated soil in the confined aquifer presented in example (1). The boundary conditions are chosen to be  $c=10$  on the left boundary and  $c=0$  on the right boundary as shown in Figure 5.4. The initial conditions are  $c=0$  everywhere in the aquifer. The flow velocity is equal to 0.1m/day, the longitudinal and the transverse dispersion coefficients are 1 and 0.1 m respectively (Wang and Anderson, 1982). The purpose of this example is to simulate changes in solute concentration  $c$  through time in the aquifer.

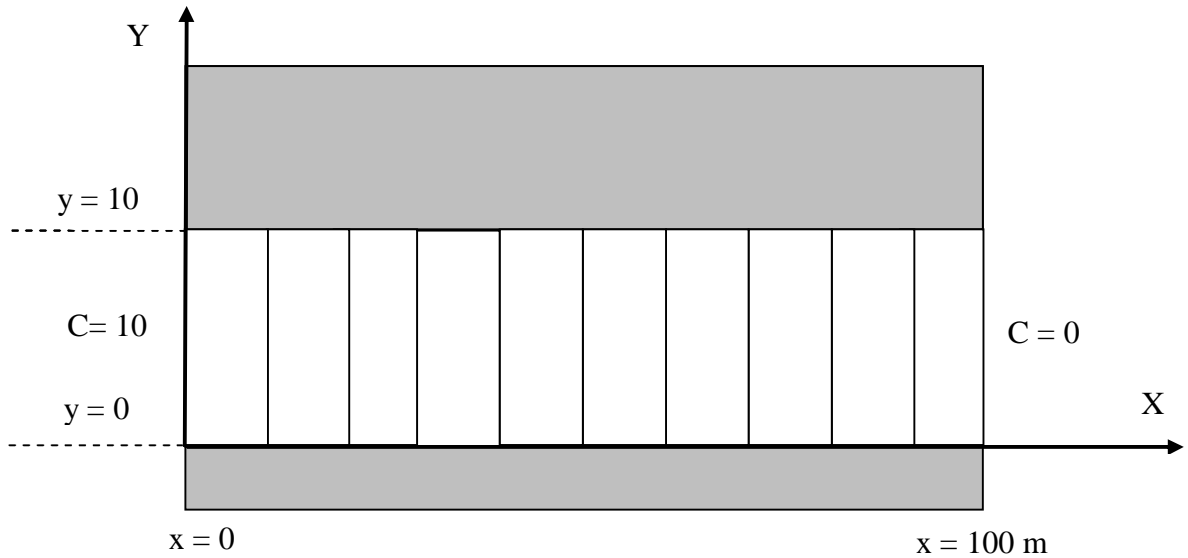


**Figure 5.4** Boundary and initial conditions of example (2)

The developed model has been used to calculate the distribution of solute concentration in the aquifer at each time step for total time of 500 min and  $\Delta t$  equal to 5 min. The results of the current code are shown in Figure 5.5.

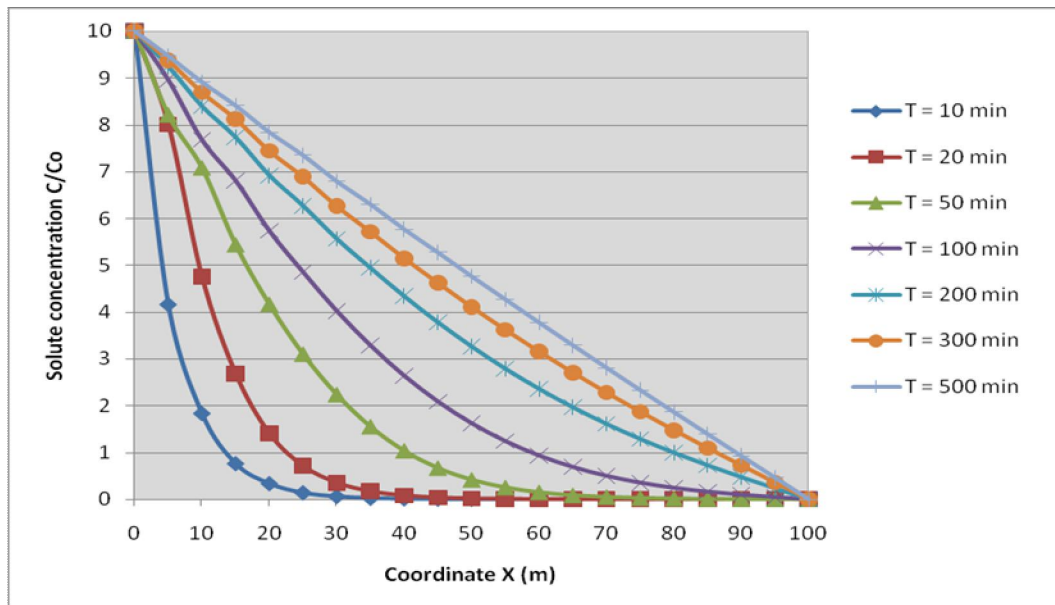


**Figure 5.5** Solute concentrations distribution at different times in the reservoir

Wang and Anderson (1982) presented a finite element model to solve advective-dispersive transport. A comparison of the current results with Wang and Anderson (1982) at time  $t=10, 50, 100, 200, 300,$  and  $500$  sec, is shown in Figure 5.6. The results show a good agreement with the other results and the difference is due to using different techniques and mesh size.

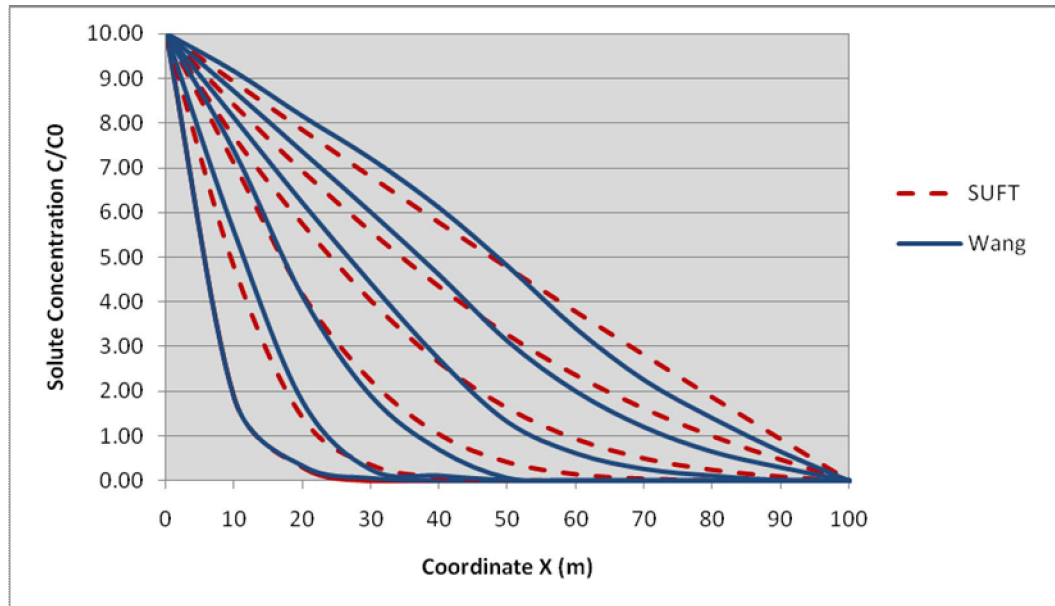


**Figure 5.6** Comparison between the current model and Wang and Anderson results for solute concentrations distribution in the reservoir

### 5.3.3 Example (3): Saltwater intrusion in confined aquifer (Henry's problem)

This example concerns couple groundwater flow and solute transport in a confined aquifer. In this example the developed model is applied to one of the most popular benchmark problems in seawater intrusion into a confined coastal aquifer, widely known as Henry's saltwater intrusion problem (Henry, 1964). This case involves seawater intrusion into a confined aquifer studied in vertical cross section perpendicular to the coast. Henry developed the first analytical solution including the effect of dispersion in confined coastal aquifer under steady-state conditions. He assumed a constant dispersive coefficient in the aquifer.

Henry's problem was studied by Pinder and Cooper (1970), Lee and Cheng (1974), Segol et al. (1975), Huyakorn et al. (1987), Frind (1982), Cheng et al. (1998) and Rastogi et al. (2004). The aquifer under consideration is uniform and isotropic and bounded above and below by impermeable strata. The aquifer is exposed to stationary seawater intrusion body on the right side and a constant freshwater flux on the left side. The aquifer boundary conditions allow convective mass transport out of the system over the top portion (20%). Figure 5.7 shows the aquifer and the boundary conditions.

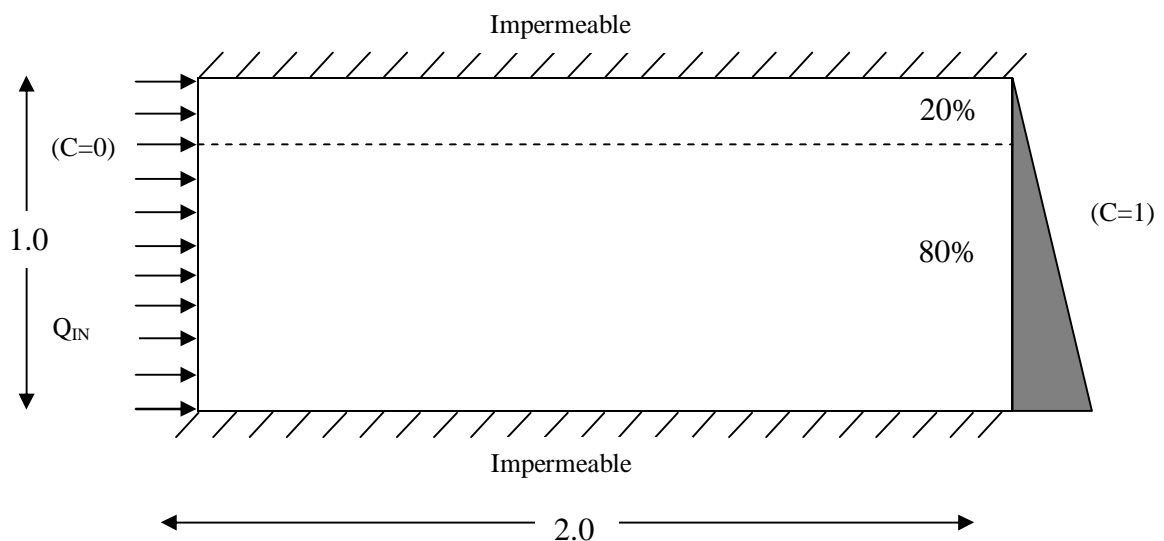


**Figure 5.7** Boundary conditions of Henry's problem

The objective of this example is to compare the results of the current model with the previous published results to test the capability of the current model to give acceptable results for the solution of Henry's problem (1964).

### **Boundary Conditions**

The boundary conditions of Henry's problem are defined in Figure 5.7. No flow occurs across the top and bottom boundaries. The freshwater source is set along the left vertical boundary and is implemented by employing source nodes along the left vertical boundary, which inject freshwater at a rate of  $Q_{in}$ , and concentration of  $c_{in}$ . Specified pressure is set at hydrostatic seawater pressure with ( $\rho_s=1025 \text{ kg/m}^3$ ) along the right vertical boundary through the use of specified pressure nodes. The soil parameters used in Henry's problem are shown in Table 5.1.

**Table 5.1** The parameters used in Henry's problem

$D_m$ : coefficient of water molecular diffusion ( $\text{m}^2/\text{sec}$ )	$6.6 \times 10^{-6}$
$\alpha_T$ : transverse dispersivity (m)	0.0
$\alpha_L$ : longitudinal dispersivity (m)	0.0
$n$ : porosity	0.35
$\mu$ : fluid viscosity	0.001
$Q_{in}$ : inland fresh water flux ( $\text{m}^3/\text{sec}$ )	$6.6 \times 10^{-5}$
$g$ : gravitational acceleration (m/sec)	9.81
$\rho_w$ : density of fresh water ( $\text{kg.m}^{-3}$ )	1000
$\rho_s$ : density of sea water ( $\text{kg.m}^{-3}$ )	1025
$K$ : hydraulic conductivity (m/sec)	$1 \times 10^{-2}$
$k$ : permeability ( $\text{m}^2$ )	$1 \times 10^{-9}$

### ***Initial Conditions***

Freshwater concentration and natural steady-state pressures are initially set everywhere in the aquifer. The natural initial pressure values are obtained through an extra initial simulation that calculates steady pressures for the conditions of freshwater concentration ( $c=0$ ) throughout, with the boundary conditions described above.

### ***Simulation setup***

Dimensions of the problem are selected to allow for simple comparison with the steady-state dimensionless solution of Henry (1964), and with a number of other published simulation models. The aquifer region is represented by quadrilateral isoparametric (eight-noded) elements, the mesh consisting of 661 nodes and 200 elements, each of size 0.1 m by 0.1 m. Mesh thickness is 1.0 m and mesh width is 2.0 m. A total simulation time of  $t=100.0$  min, is selected and the time step size is  $\Delta t = 60$  sec. To test and compare the model under consideration, the results are compared with four cases from the literature as following:

- 1- Steady-state constant dispersion,
- 2- Steady-state variable dispersion,
- 3- Transient constant dispersion, and
- 4- Transient variable dispersion.

The results of the current model together with results of other models are presented in the following sections. Seawater wedge is chosen to be represented by ( $c/c^* = 0.5$ ) isochlor, which is an approach adapted by many researchers.

#### ***5.3.3.1 Steady-state constant dispersion***

In the case of constant dispersion, Henry's solution assumes the dispersion is presented by a constant coefficient of diffusion, rather than by velocity-dependant dispersivity. In the literature, two values for molecular diffusion coefficient ( $D_m$ ) have been used;  $18.8571 \times 10^{-6}$  and  $6.6 \times 10^{-6}$  [ $m^2/sec$ ]. The total dispersion coefficient  $D$ , is equal to the product of porosity and molecular diffusivity,  $D = nD_m$  (Voss and Provost (2003)). To match the values of Henry's solution, values of  $D = 6.6 \times 10^{-6}$  and  $2.31 \times 10^{-6}$ , are used. The results of the current code compared with INTERA and SUTRA codes (Voss and Provost, 2003) for the higher



value of diffusion  $D_m = 18.8571 \times 10^{-6}$  and  $D = 6.6 \times 10^{-6}$  with both the longitudinal and transverse dispersivities set to zero are shown in Figure 5.8.

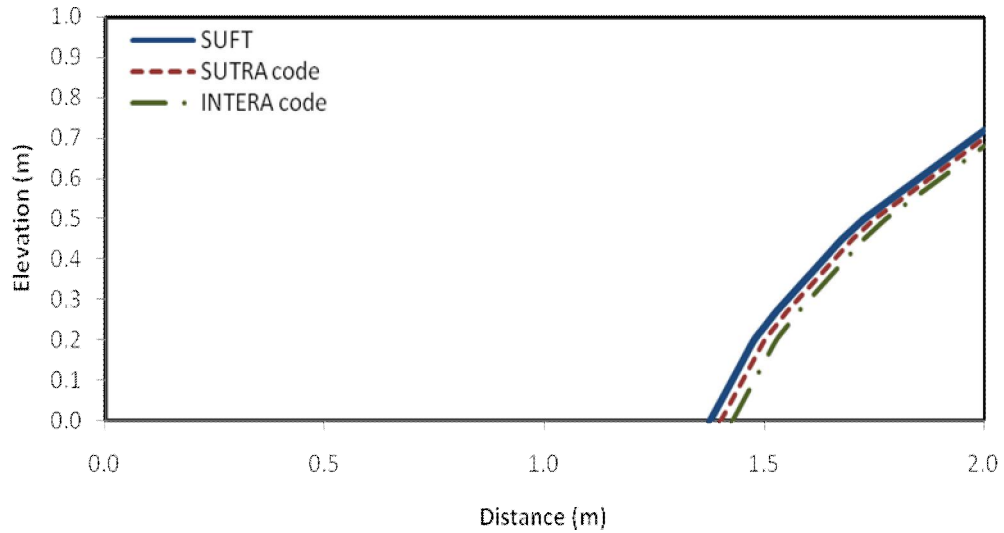


**Figure 5.8** 0.5 Isochlor for steady-state constant dispersion ( $D = 6.6 \times 10^{-6}$ )

For the lower value of diffusion  $D_m = 6.6 \times 10^{-6}$  and  $D = 2.31 \times 10^{-6}$ , the results are shown in Figure 5.9. The results are compared with Pinder and Cooper (1970) (method of characteristics), Segol et al. (1975) (finite element method), Frind (1982) (finite element method), and SUTRA (finite element-finite difference method), (Voss and Provost (2003).

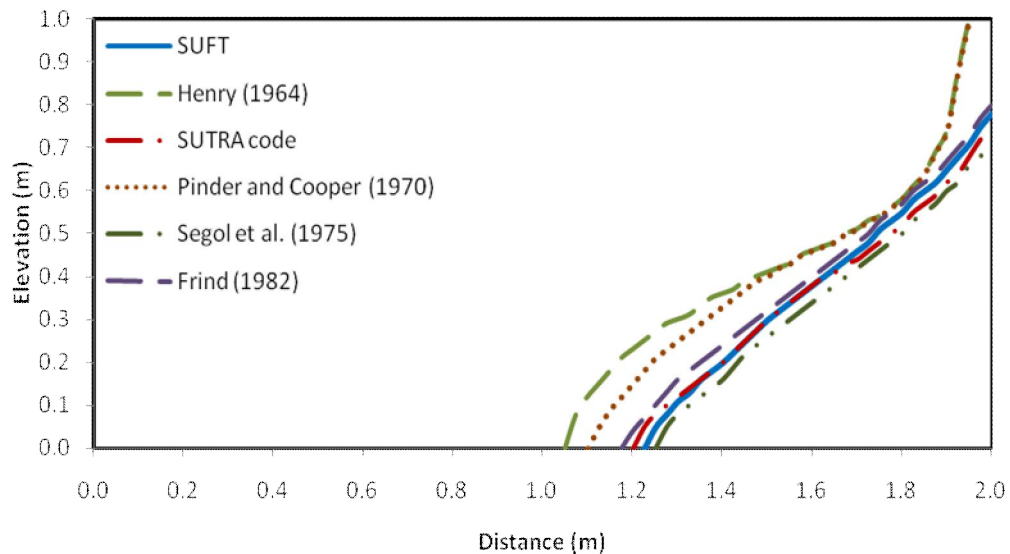


**Figure 5.9** 0.5 Isochlor for steady-state constant dispersion ( $D = 2.31 \times 10^{-6}$ )

From Figures 5.8 and 5.9, it can be seen that the results obtained using the current code match well with the results from INTERA, SUTRA and other codes.

### 5.3.3.2 Steady-state variable dispersion

In Henry's solution and those of some other researches it was assumed that dispersion is represented by a constant coefficient of diffusion, rather than being velocity-dependent. However, Rastogi et al. (2004) considered the dispersion coefficients to be velocity-dependent under steady state conditions and selected values for longitudinal and transverse dispersivities as 0.5 and 0.1 m respectively. The results of the current model are compared with some known solutions. Figure 5.10, shows the results of position of the 0.5 isochlor obtained by the present code compared with the results of Henry (1964), Pinder and Cooper (1970), Lee and Cheng (1974) and Rastogi et al. (2004). The present results match nicely with the existing solutions. The shape of the interface is S-type and similar to the known shapes (Rastogi et al., 2004).

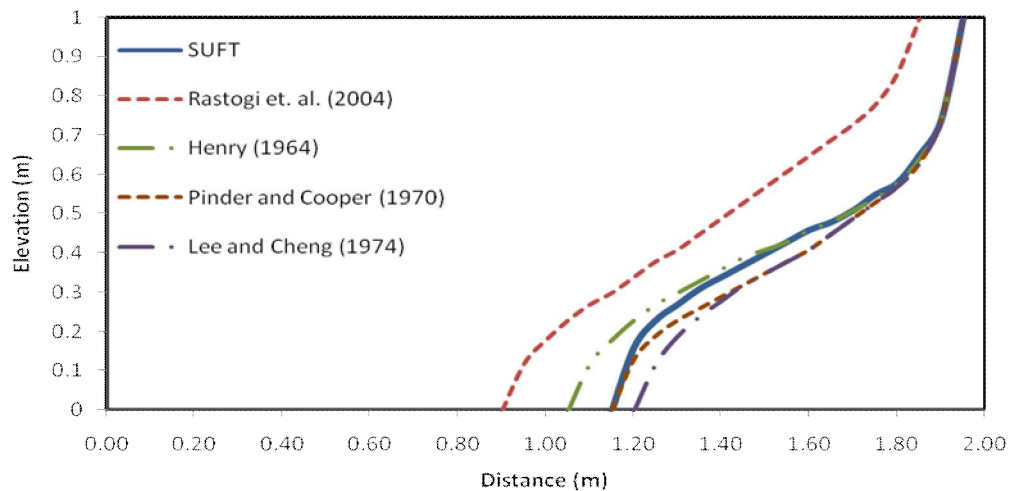


**Figure 5.10** 0.5 Isochlor for steady-state variable dispersion

### 5.3.3.3 Transient constant dispersion

In this case, the developed model results are compared with a two-dimensional finite volume unstructured mesh method (FVUM), which was developed by Liu et al. (2001) for analyzing the evolution of the saltwater intrusion into coastal aquifer systems. The model of Liu et al. (2001) considered transient groundwater flow and solute transport in a coastal aquifer and was validated by comparing the results for Henry's problem with those of Huyakorn et al. (1987) and Cheng et al. (1998). Dimensions of the problem are selected to allow comparison with the solution of Liu et al. (2001). The thickness is 100.0 m and width is 200.0 m. The domain consists of twenty by ten elements, each of size 10.0 m by 10.0 m, (NN=661, NE=200). A total simulation time of  $t=6000$  days, is used with time step size of  $\Delta t = 5$  days (Liu et al., 2001).

Two cases are selected for the validation; constant dispersion and variable dispersion. In the first case, a constant dispersion value is used based on the molecular diffusion coefficient set equal to  $6.6 \times 10^{-2}$  ( $\text{m}^2/\text{d}$ ), and both the longitudinal and transverse dispersivities were set to zero. Figure 5.11, shows the results in terms of position of 0.5 isochlor obtained by the present model compared with the results of Huyakorn et al. (1987), Cheng et al. (1998) and Liu et al. (2001).

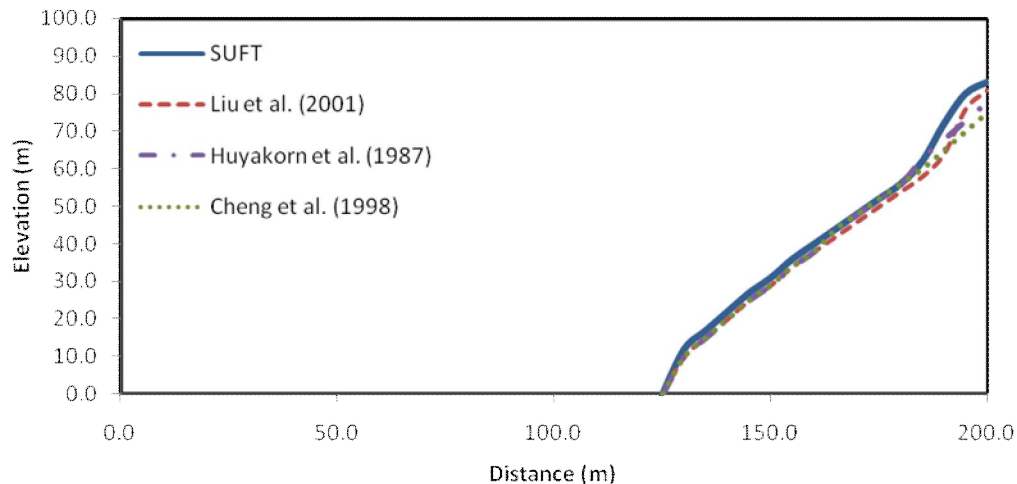


**Figure 5.11** 0.5 Isochlor for transient constant dispersion

### 5.3.3.4 Transient variable dispersion

For the variable dispersion case, the dispersion coefficient is considered velocity-dependant rather than constant. The diffusion coefficient is set to zero and both the longitudinal and transverse dispersivities are 3.5 m. Figure 5.12 shows the results of the current code compared with Liu et al. (2001). It can be observed from Figures 5.11 and 5.12 that the results are in good agreement with previously published solutions by Liu et al. (2001).

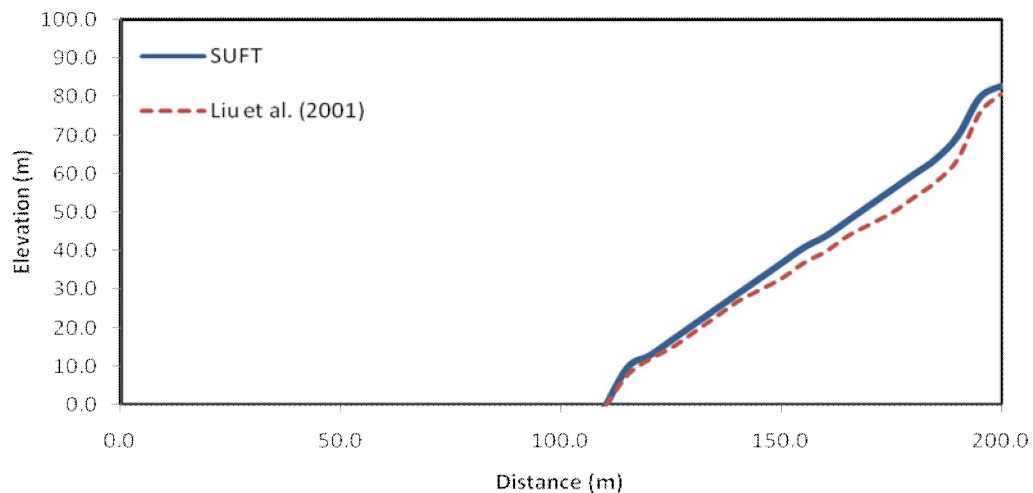


**Figure 5.12** 0.5 Isochlor for transient variable dispersion

### 5.3.3.5 Effect of variability in dispersion and density on SWI

To illustrate the effect of dispersion coefficient on the distribution of solute concentration and saltwater intrusion in coastal aquifers, the results of the finite element analyses were obtained for two cases of constant dispersion coefficient and variable dispersion coefficient and compared with those of Huyakorn et al. (1987), Cheng et al. (1998) and Liu et al. (2001) as shown above. In the case of variable dispersion, the dispersion coefficient is considered to be velocity-dependant rather than constant. Figure 5.13 shows a comparison between 0.5 isochlors due to constant dispersion and variable (velocity-dependant) dispersion coefficient. As shown in Figure 5.13 the intrusion of saltwater increases in land in the case of variable dispersion coefficient (velocity-dependant) (Liu et al., 2001).

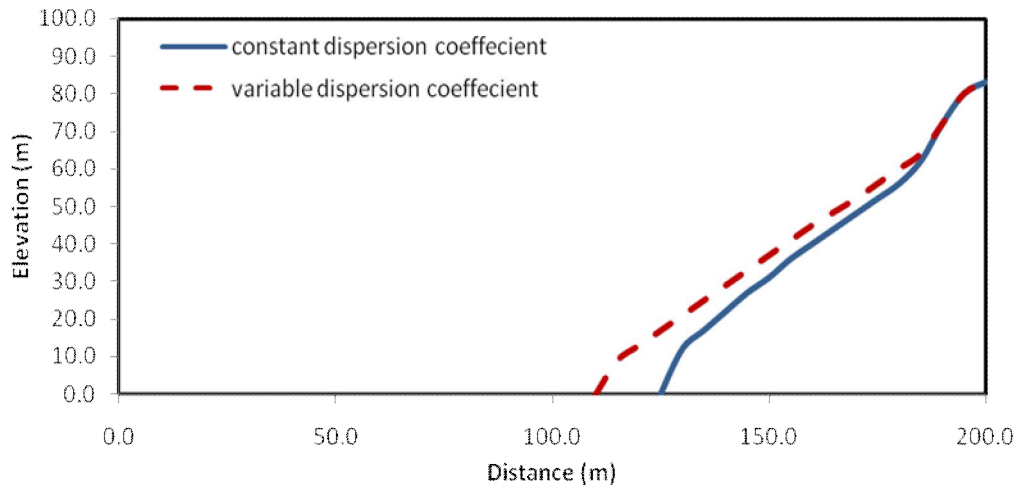


**Figure 5.13** 0.5 Isochlor for constant and variable dispersion coefficient

To illustrate the effect of fluid density on the distribution of solute concentration and saltwater intrusion in coastal aquifers, the results of the finite element analyses were obtained for two cases, constant density and variable density. Figure 5.14 shows a comparison between 0.5 isochlor due to constant density and variable density. The densities of fresh water  $\rho_f$  and seawater  $\rho_s$  are considered 1.0 and 1.025 Mg/m<sup>3</sup> respectively. Due to the difference between the two densities being very small as 0.025, the effect of variation in density is small. Figure 5.14 show that the increase in sweater density decreases the intrusion of saltwater.

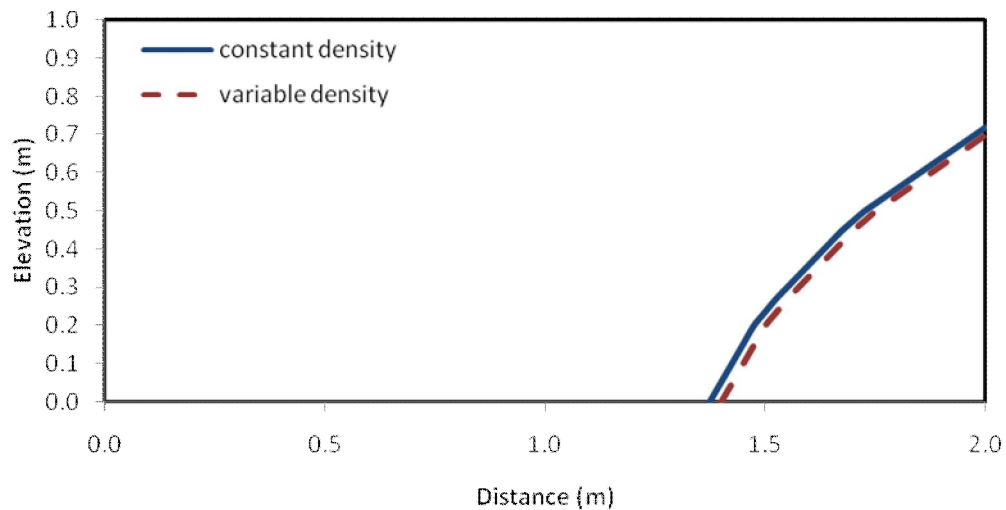


**Figure 5.14** 0.5 Isochlor for constant and variable density

## 5.4 Case studies

In the previous section, the developed model was verified against a number of examples to show its ability to simulate groundwater flow and solute transport separately and coupled fluid flow and solute transport in soil. This section presents the application of the model to four case studies to predict seawater intrusion into coastal aquifers in different locations of the world. The first case is a hypothetical case from the literature that was investigated by Kawatani (1980). The second is saltwater intrusion into Madras aquifer in India (Sherif et al., 1990). The third is saltwater intrusion in Biscayne aquifer at Coulter area near Miami, Florida, USA (Lee and Cheng, 1974) and finally saltwater intrusion in Gaza aquifer in Palestine (Qahman and Larabi, 2006).

### 5.4.1 Case (1): A hypothetical case study

In this case the developed model is applied to a hypothetical case from the literature. The problem was investigated by Kawatani (1980). He considered the case of an unconfined coastal aquifer with a channel carrying fresh water on the land side (Figure 5.15). The water infiltration from the channel creates a constant water table above the sea level which can help in controlling saltwater intrusion. Kawatani (1980) presented a finite element model to study saltwater intrusion and Sherif et al. (1990) presented a steady-state solution to this problem.

#### *Site description*

The region of the study is 500 x 20 m. The water table on the land side (fresh water level in the channel) is 0.35 cm above the sea level leading a hydraulic gradient of  $7 \times 10^{-4}$ . The hydraulic conductivities in x-direction  $K_x$  and y-direction  $K_y$  are 0.06 cm/min and 0.006 cm/min respectively. The effective porosity is 0.25 and dispersion coefficients in x-direction  $D_x$  and y-direction  $D_y$  are 5 and 0.5 cm<sup>2</sup>/min respectively. The longitudinal and transverse dispersivities  $\alpha_L$  and  $\alpha_T$  are 5 and 2.5 m. The density of fresh water  $\rho_f$  and seawater  $\rho_s$  are 1.0 and 1.025 t/m<sup>3</sup> respectively (Sherif et al., 1990).

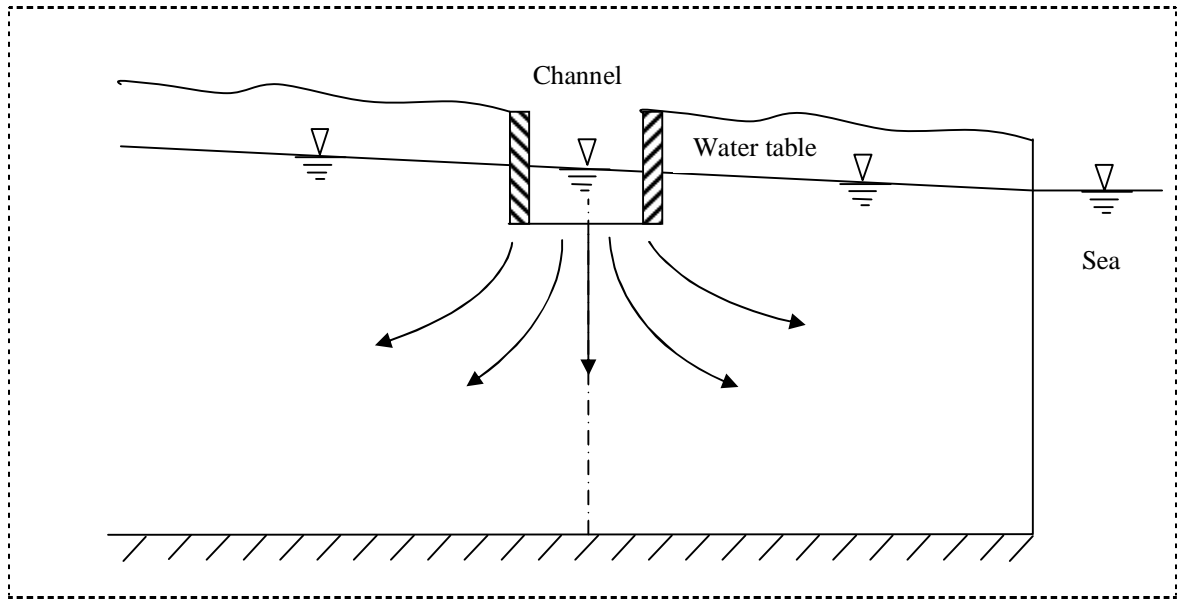


**Figure 5.15** Problem description of unconfined coastal aquifer with fresh water channel at land side

### ***Boundary conditions***

In this study, the same domain with the same hydraulic parameters and boundary conditions is considered to compare the results with those of Kawatani (1980) and Sherif et al. (1990). The aquifer under consideration is homogenous and isotropic and bounded above and below by impermeable strata. The aquifer is exposed to stationary seawater intrusion body on the right side and a constant freshwater head from the channel on the left side. The aquifer boundary conditions allow convective mass transport out of the system over the top portion (20%). Figure 5.16 shows the boundary conditions applied in this case. The domain was represented by quadrilateral isoparametric (eight-noded) elements, the mesh consisting of 400 elements and 1409 nodes. The time step of 5 days is used with total time of 250 days.

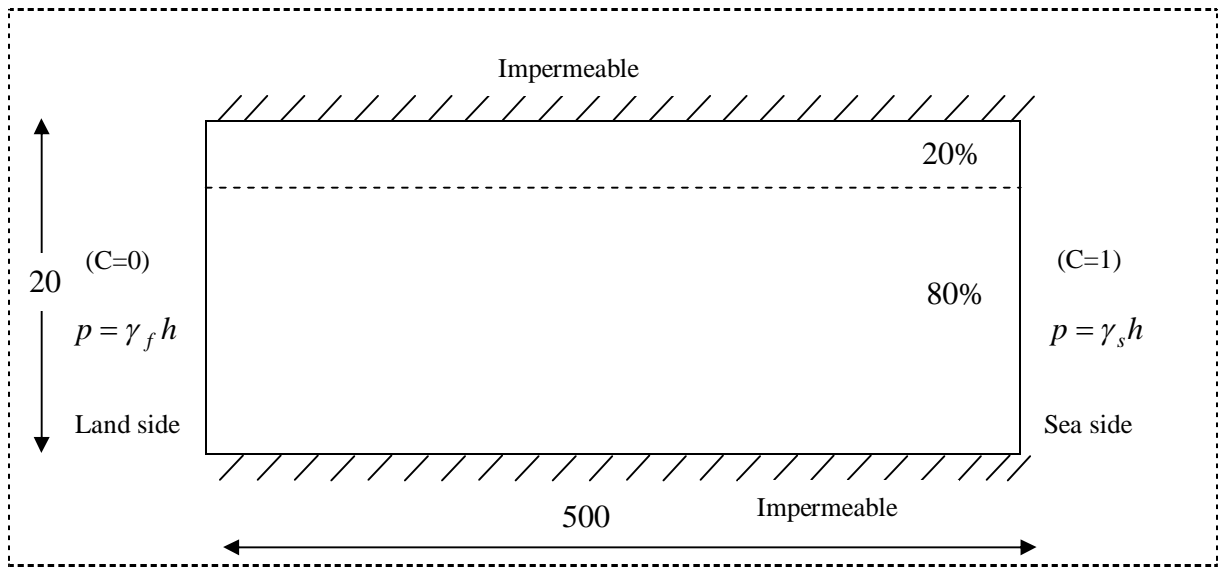


**Figure 5.16** Boundary conditions of the hypothetical case

### Results

Figure 5.17 shows 0.5, 0.25, 0.1, 0.05 and 0.005 isochlor contours obtained by the current model and those of Kawatani (1980) and Sherif et al. (1990). The agreement between the results is good. A possible explanation for the discrepancies between the results is the different numerical schemes and different grid systems used.

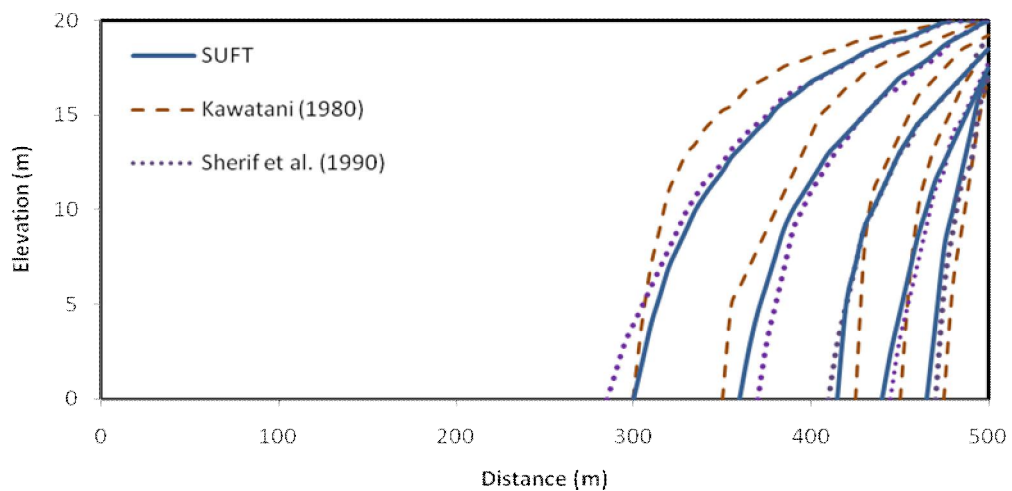


**Figure 5.17** 0.5, 0.25, 0.1, 0.05 and 0.005 Isochlor contours of the hypothetical case



### **5.4.2 Case (2): Madras aquifer, India**

This case presents a real problem of saltwater intrusion in Madras coastal aquifer in south India. Saltwater intrusion in Madras coastal aquifer has been studied by a number of researches such as; Rouve and Stroessinger (1980) and Sherif et al. (1990) who applied finite element models to predict the saltwater intrusion in this aquifer. The aquifer thickness at the sea boundary is 30 m. Because the thickness is small, the limit up to which the influence of hydrodynamic dispersion can be expected is about 3.0 km (Sherif et al. (1990).

#### **Site description**

The study region which was considered by Rouve and Stroessinger (1980) and Sherif et al. (1990) is 2600 x 30 m. a coefficient of permeability of  $3 \times 10^{-3}$  m/sec and porosity of 0.35 were considered. The longitudinal and transverse dispersivities  $\alpha_L$  and  $\alpha_T$  were taken as 66.6 and 6.6 m, respectively. The density of fresh water  $\rho_f$  and seawater  $\rho_s$  are 1.0 and 1.025 t/m<sup>3</sup>. Molecular diffusion was set equal to  $1 \times 10^{-6}$  m<sup>2</sup>/sec.

#### **Boundary conditions**

The same domain with the same hydraulic parameters and boundary conditions are considered to compare the results with Rouve and Stroessinger (1980) and Sherif et al. (1990). The aquifer is leaky and heterogeneous but for simplicity Rouve and Stroessinger assumed that the aquifer is confined and homogeneous. The piezometric heads at the seaside was set equal to 40 m and 41 m at the land side. Figure 5.18 shows the boundary conditions applied in this case. The domain was represented by quadrilateral isoparametric (eight-noded) element, the mesh consisting of 390 elements and 1437 nodes.

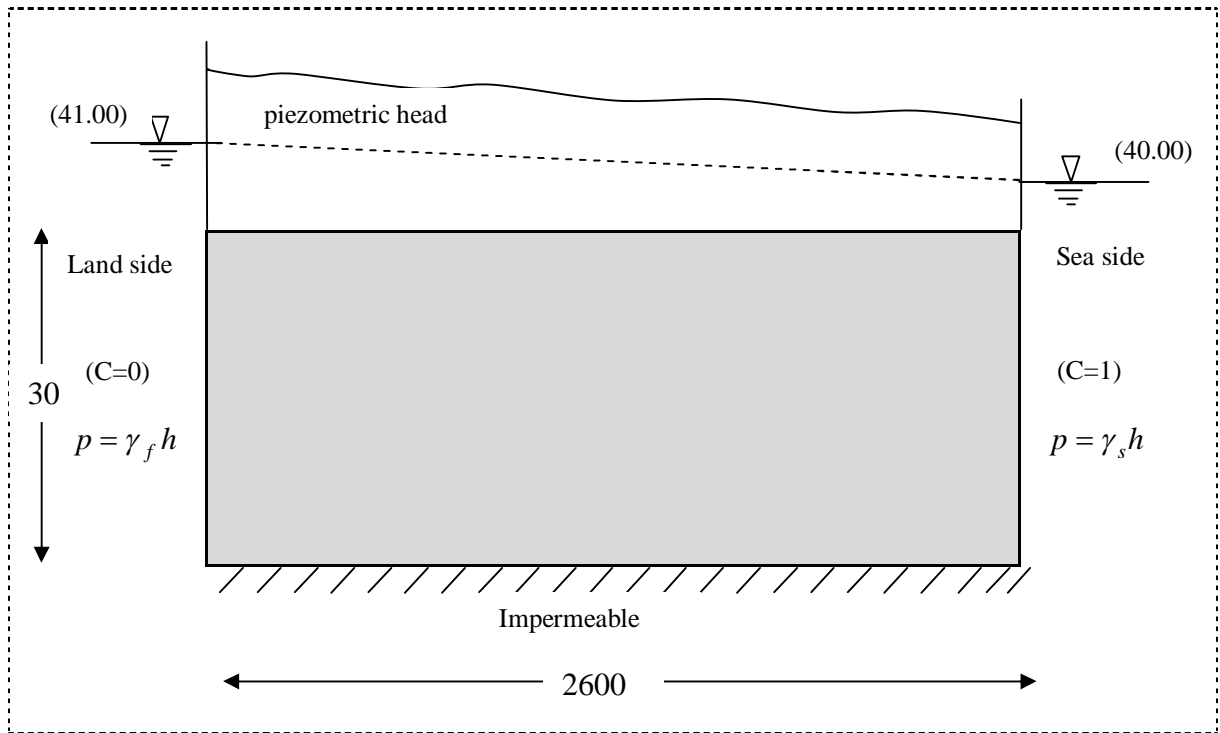


**Figure 5.18** Boundary conditions of Madras aquifer

### Results

The developed model is applied to the idealized representation of the Madras aquifer. No observations about salinity distribution in the Madras aquifer were available. The results are compared with those of Rouve and Stroessinger (1980) and Sherif et al. (1990). Figure 5.19 shows 35, 17.5, 10, 5 and 2.0 equi-concentration lines obtained by the current model and those of Rouve and Stroessinger (1980) and Sherif et al. (1990). The results of the current code match well with the other results. Rouve and Stroessinger (1980) and Sherif et al. (1990) used steady-state finite element analysis for the current case and considered velocity-independent dispersion whereas in the current study transient variable-density flow and velocity-dependant dispersion coefficients are considered which resulted in further salt advancement inland as shown in Figure 5.19.

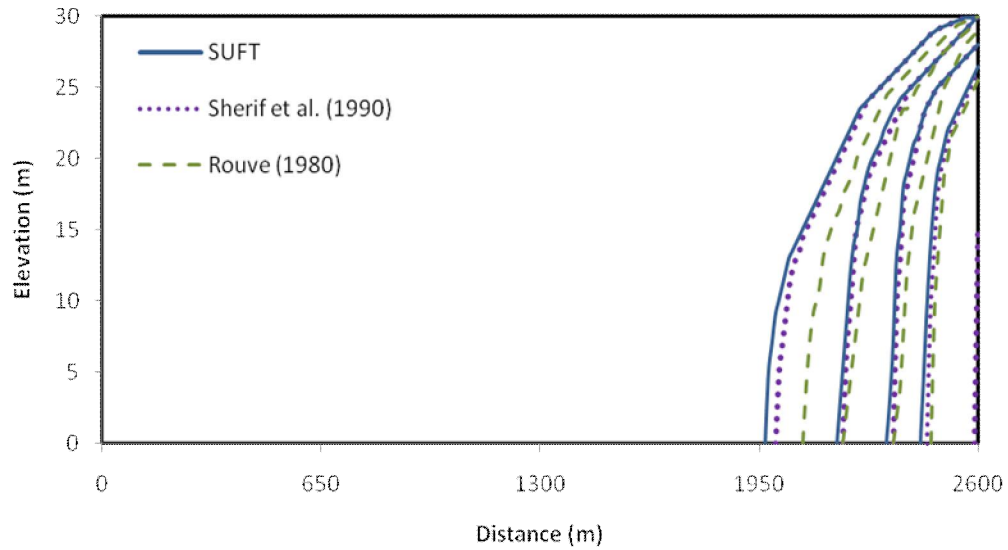


**Figure 5.19** 35, 17.5, 10, 5 and 2.0 equi-concentration lines in Madras aquifer

### 5.4.3 Case (3): Biscayne aquifer, Florida, USA

Lee and Cheng (1974) presented steady-state 2-D finite element model using triangular elements to study saltwater encroachment to Biscayne aquifer at Coulter area, Florida, USA, where a field investigation had been made by Kohout (1960a, b). The developed model is applied to simulate saltwater intrusion into Biscayne aquifer and the results are compared with those reported by Lee and Cheng (1974) and the observations of Kohout (1960a, b).

#### *Site description*

The geologic and hydraulic aspects of Biscayne aquifer have been investigated and reported by Kohout (1960a, b). The aquifer average depth is 100 ft below mean sea level. It is observed that the transition zone is quite thick and the toe of the saltwater is approximately 1600 ft from the shore, whereas the 0.5 isochlor (9500 ppm chloride) is located at the bottom of the aquifer about 1400 ft from the bay. The study region which is considered in this study is 300 x 30 m (Lee and Cheng (1974) and Kohout (1960a, b)). A coefficient of permeability of  $3 \times 10^{-10}$  m/sec and porosity of 0.39 are considered. The longitudinal and

transverse dispersivities  $\alpha_L$  and  $\alpha_T$  are taken as 5.0 and 0.5 m, respectively. The density of fresh water  $\rho_f$  and seawater  $\rho_s$  are 1.0 and 1.025 t/m<sup>3</sup>. The dispersion coefficients in x-direction  $D_x$  and y-direction  $D_y$  are velocity-dependant.

### **Boundary conditions**

The same hydraulic parameters and boundary conditions were considered to compare the results with Lee and Cheng (1974) and Kohout (1960a, b). The schematic sketch of the Biscayne aquifer at Coulter area and the corresponding boundary conditions applied in this case are shown in Figure 5.20. The domain is represented by quadrilateral isoparametric (eight-noded) element, the mesh consisting of 250 elements and 861 nodes.

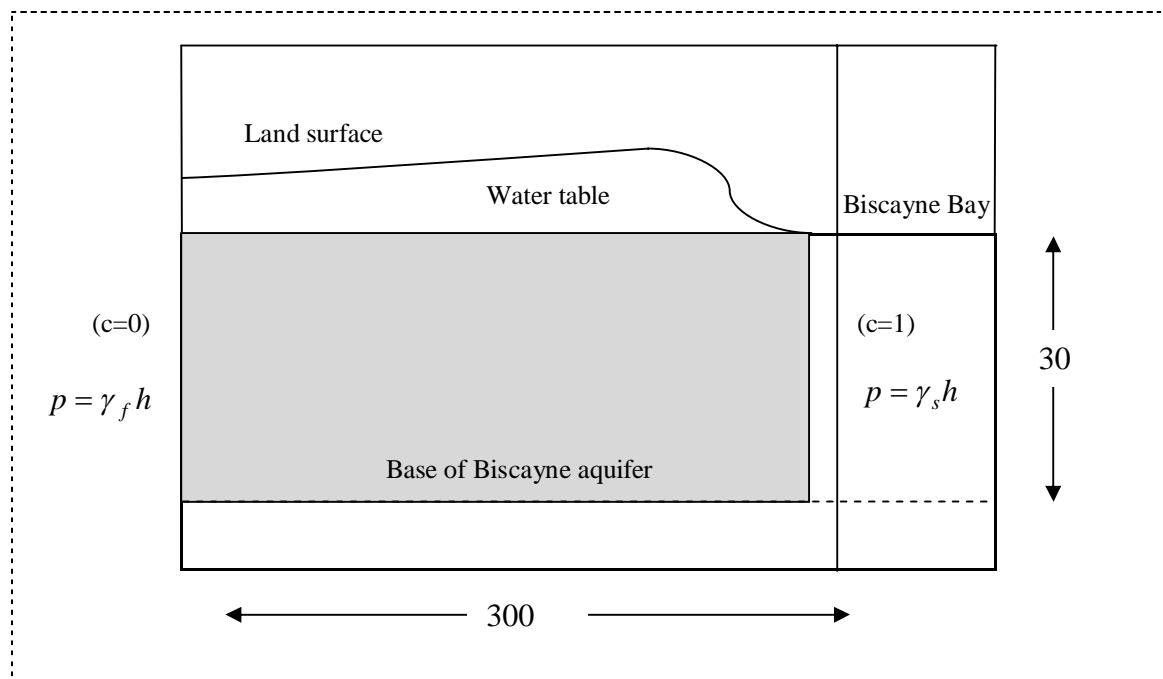


**Figure 5.20** Schematic sketch and boundary conditions of Biscayne aquifer, Florida

## Results

The flow in Biscayne aquifer is studied to test the applicability of the present model to simulate saltwater intrusion into coastal aquifers. The results were compared with those of Lee and Cheng (1974) and the observations of Kohout (1960a, b). Figure 5.21 shows 1, 0.75, 0.5 and 0.25 isochlor contours obtained by the current model and those of Lee and Cheng (1974), whose compared their results with the observations of Kohout (1960a, b). Good qualitative agreement exists between the current predictions and Lee and Cheng and Kohout's observations.

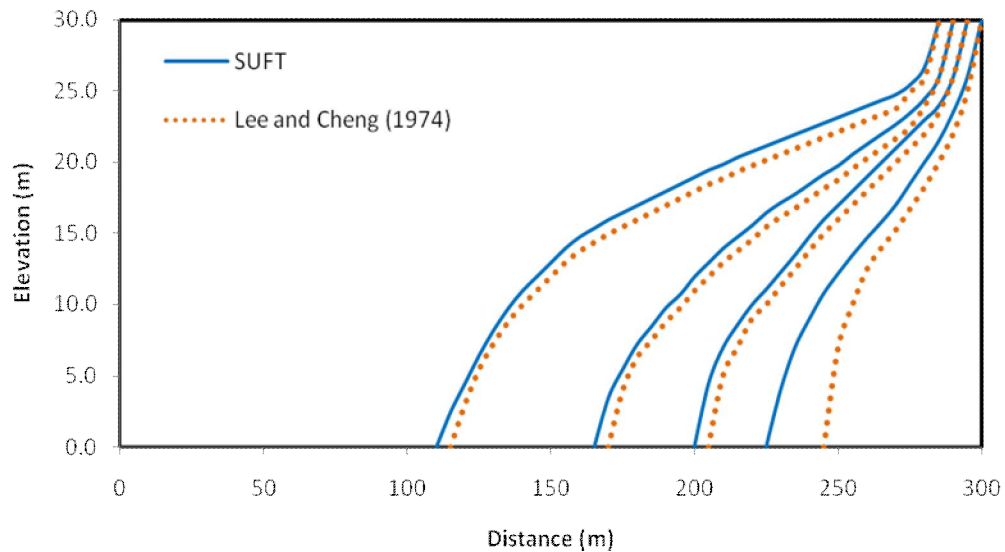


**Figure 5.21** 1, 0.75, 0.5 and 0.25 isochlor counters in Biscayne aquifer, Florida

#### 5.4.4 Case (4): Gaza Aquifer, Palestine

A real world problem is addressed in this case, the coastal aquifer of Gaza Strip which is intruded by saltwater. Gaza strip has a coastline of about 45 km and a total area of about 365 km<sup>2</sup>. Gaza strip is home to about 1.5 million Palestinians. The aquifer is the only source of fresh water in Gaza, and provides more than 95% of the water consumed in the Strip for agriculture, domestic and industrial uses. Water is obtained by pumping of more than 3000 wells, with a total estimated annual yield of about 140 million cubic meters (Qahman and Larabi, 2006). Gaza aquifer is a part of the shallow sandy coastal aquifer which stretches from Israel through Gaza into the Sinai Peninsula in Egypt as shown in Figure 5.22.

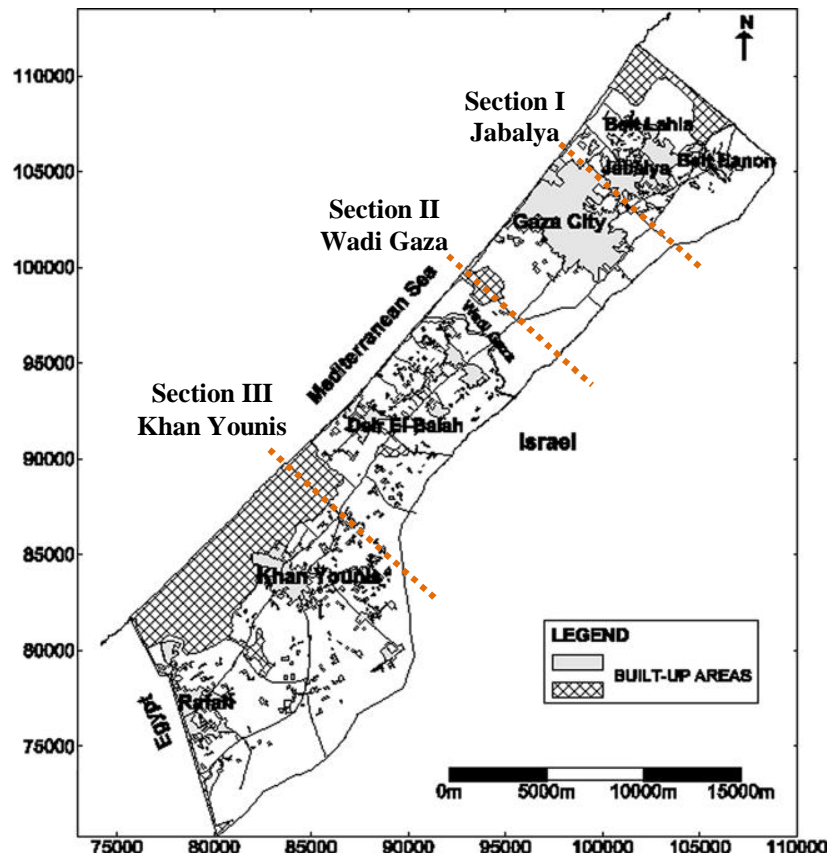


**Figure 5.22** Location map of Gaza strip  
(Source: EPD/IWACO-EUROCONSULT 1996)

A very critical and rapidly worsening component of humanitarian crisis in the Gaza strip is the water crisis. Over-abstraction of water from the aquifer over period of time (several decades) has caused severe depletion and saltwater intrusion from the Mediterranean Sea. The flow of water in the aquifer is naturally toward the sea, though in many places the flow has been reversed due to over-abstraction of groundwater which has led to the intrusion of seawater into the aquifer. Another major problem for the Gaza aquifer is pollution; contamination consists of fertilizers and pesticides and untreated sewage. The pollution, exacerbated by the conflict's impact on Gaza's waste-treatment facilities, has resulted in widespread contamination of the aquifer. Moreover, climate change predictions suggest an imminent catastrophe; as temperature rises, the droughts would exacerbate, and as the sea level rises, saltwater intrusion would speed up. Rising sea level poses another challenge to the Gaza population as it might lead to the submerging of much of Gaza's territory. Saltwater intrusion and pollution of the aquifer affect adversely both the human population of the Gaza Strip and its environment. High salinity has been directly linked to a skyrocketing rate of kidney diseases in Gaza. Saltwater intrusion poses a great threat to the municipal supply and industrial growth in the Strip (Qahman, 2004).

Seawater intrusion in Gaza aquifer has been studied by a number of researchers (e.g., Yakirevich et al. (1998); Qahman and Zhau (2001); Moe et al. (2001); Qahman and Larabi (2003a, b) and Qahman and Larabi (2006)). Yakirevich et al. (1998) used SUTRA code and Qahman and Larabi (2003b) used SEAWAT code to simulate saltwater intrusion in the Gaza aquifer. Numerical simulations showed that the rate of seawater intrusion during 1997-2003 was expected to be 20-45 m/year. The developed model considering coupled flow and solute transport with variable density effects on groundwater flow, is applied to simulate groundwater flow and saltwater intrusion in Gaza aquifer. Coupling flow and transport computations allows the effects of fluid density gradients associated with solute concentration gradients to be incorporated into groundwater flow simulations.

### ***Description of the study area***

Gaza Strip is a part of the Mediterranean coastal plain between Egypt and Israel. It forms a long and narrow rectangle shape of 45 km long and width of 5 to 10 km. Gaza Strip is a foreshore plain gradually sloping westward. The groundwater flow is mainly westward toward the Mediterranean Sea and the maximum thickness of the saturated zone is 120 m near the sea. Three vertical cross sections have been selected to study the intrusion of seawater in the aquifer at Jabalya, Wadi Gaza and Khan Yunis (Figure 5.22). The first section at Jabalya is located in the north of Gaza Strip with a length of 5000 m and average depth of 100 m. The second section at Wadi Gaza is located in the middle of Gaza Strip with a length of 2000 m and average depth of 100 m. The third section at Khan Yunis is located in the south of Gaza Strip with a length of 5000 m and average depth of 100 m with inclined top and bottom. The aquifer is considered confined, homogeneous and isotropic with respect to freshwater hydraulic conductivities, molecular diffusion, and longitudinal and transverse dispersivities. The aquifer system is subjected to seawater intrusion along the sea face boundary and a uniformly distributed lateral flow along the inland face, a constraint head of 1m is considered. The hydraulic conductivities  $K_x$  and  $K_y$  are 0.2 m/day and 0.1 m/day respectively. The effective porosity is 0.35 and the longitudinal and transverse dispersivities  $\alpha_L$  and  $\alpha_T$  are 50 and 0.1 m respectively. The density of fresh water  $\rho_f$  and seawater  $\rho_s$  are 1.0 and 1.025 t/m<sup>3</sup> respectively (Qahman, 2004).

### ***Boundary conditions***

The flow boundary conditions consist of impermeable boundaries along the top and the bottom of the aquifer. Constant head and concentration are specified to the model along the coast. Hydrostatic pressure is assumed along the vertical boundary of the sea side. The aquifer is charged with freshwater at constant flux from the inland side. The prescribed constant concentration (TDS) of 35 kg/m<sup>3</sup> is considered (Qahman, 2004).



### Results

The developed model is applied to simulate saltwater intrusion in the selected three vertical cross sections in order to predict the intrusion of seawater in different locations in the Gaza aquifer. The concentration distributions for the three cross sections are presented in Figures 5.23, 5.24 and 5.25.

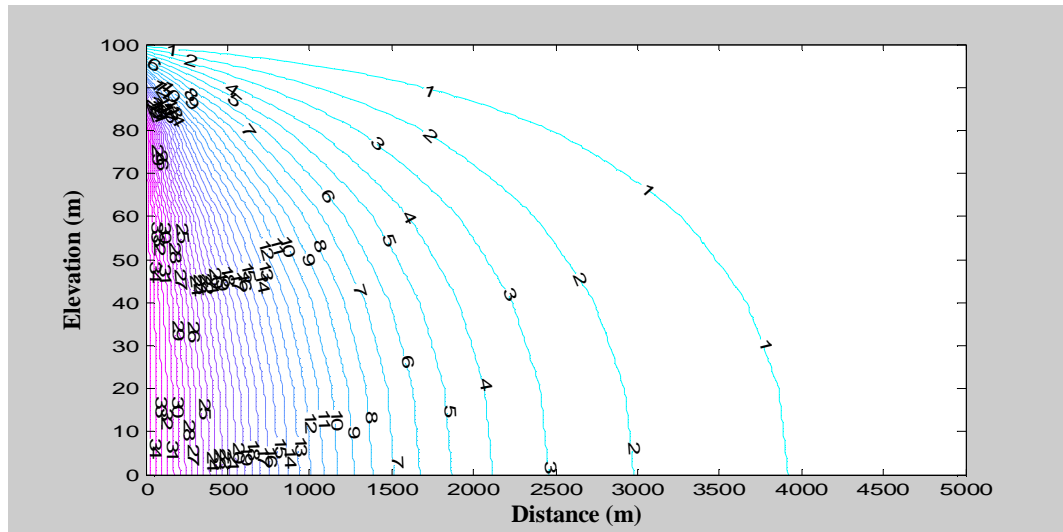


**Figure 5.23** Isolines of TDS concentration ( $\text{kg/m}^3$ ) calculated by (SUFT) along Jabalya

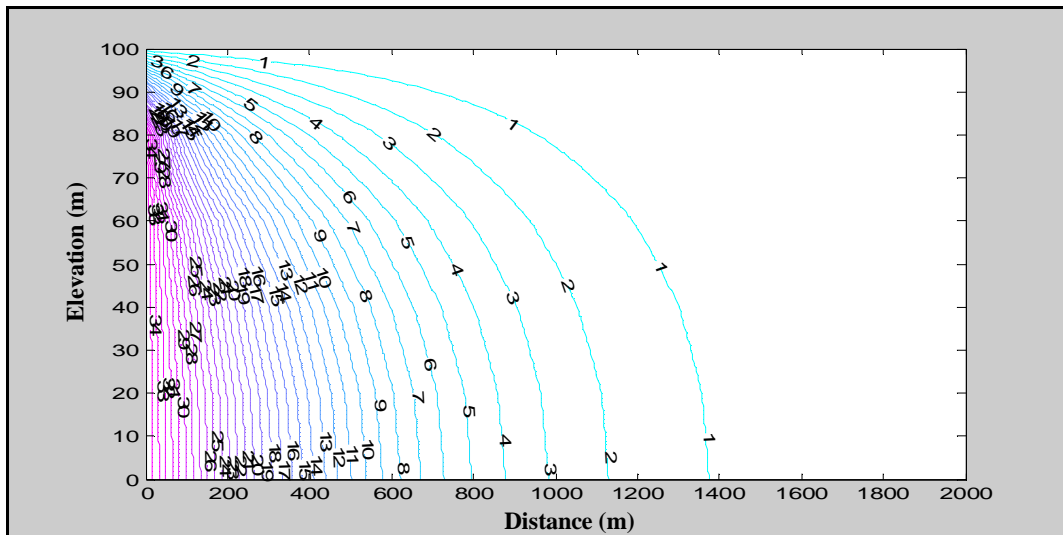


**Figure 5.24** Isolines of TDS concentration ( $\text{kg/m}^3$ ) calculated by (SUFT) along Wadi Gaza

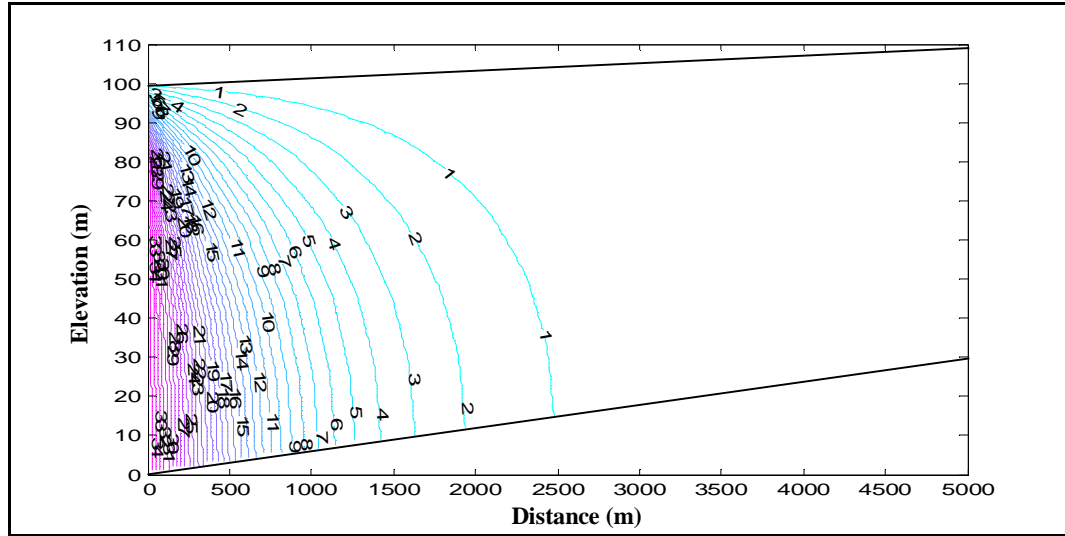


**Figure 5.25** Isolines of TDS concentration ( $\text{kg/m}^3$ ) calculated by (SUFT) along Khan Yunis

The results of the present model show that the aquifers is subject to a sever seawater intrusion problem and groundwater is unsuitable for human uses. At Khan Yunis, isoline 2 (2000 ppm) intruded inland to a distance of about 2.0 km measured along the bottom boundary (Figure 5.25). On the other hand, at Jabalia, the same isoline intruded inland to a distance of about 3.0 km (Figure 5.23). The intrusion reduction at Khan Yunis might be attributed to the upward slope toward inland side at this section. At Wadi Gaza, isoline 2 (2000 ppm) intruded inland to a distance of about 1.2 km, measured along the bottom boundary (Figure 5.24).

The results of the geophysical survey obtained by PWA/CAMP (2000), indicated that the extent of saltwater intrusion ranged between 1 km and 2 km at Khan Yunis cross section. Qahman and Larabi (2006) used SEWAT code to simulate saltwater intrusion in Gaza aquifer. The estimated extent of seawater wedge from seawater intrusion until year 2003 along Khan Yunis ranged between 1 and 2 km which is similar to the results obtained by the geophysical survey (see Figure 5.26). Also the results of the present model indicated that the intrusion of seawater at this section is about 2 km (Figure 5.25).

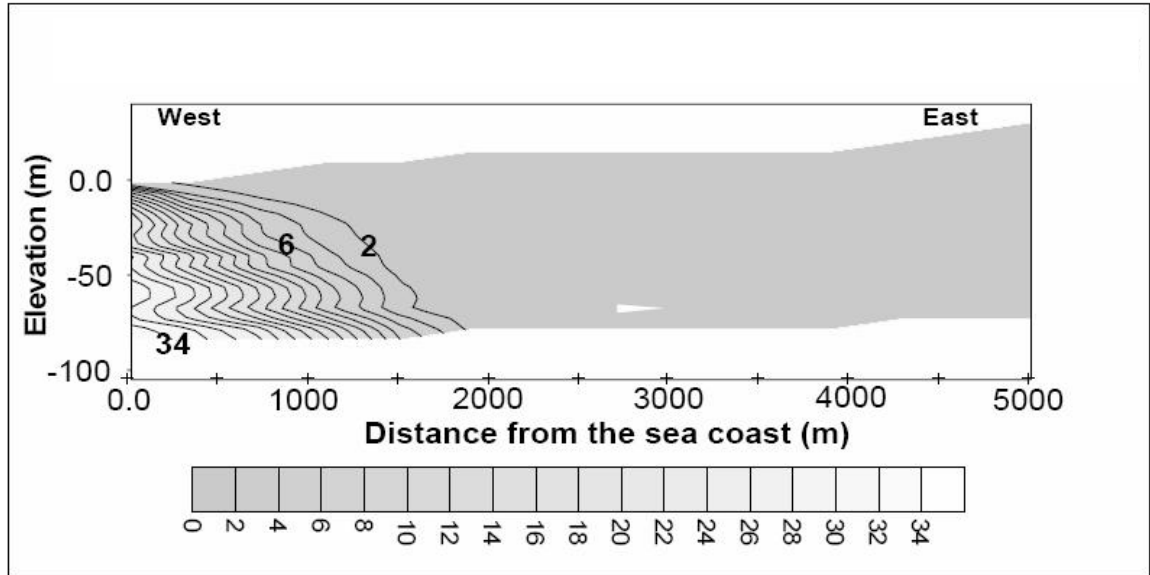


**Figure 5.26** Isolines of TDS concentration ( $\text{kg/m}^3$ ) calculated by SEAWAT along Khan Yunis (Qahman and Larabi, 2006)

Qahman and Larabi (2006) also used SEAWAT to simulate saltwater intrusion along Jabalia and the estimated extent of seawater wedge was about 3 km until year 2003 (Figure 5.27) which is similar to the results obtained by present model (Figure 5.23).

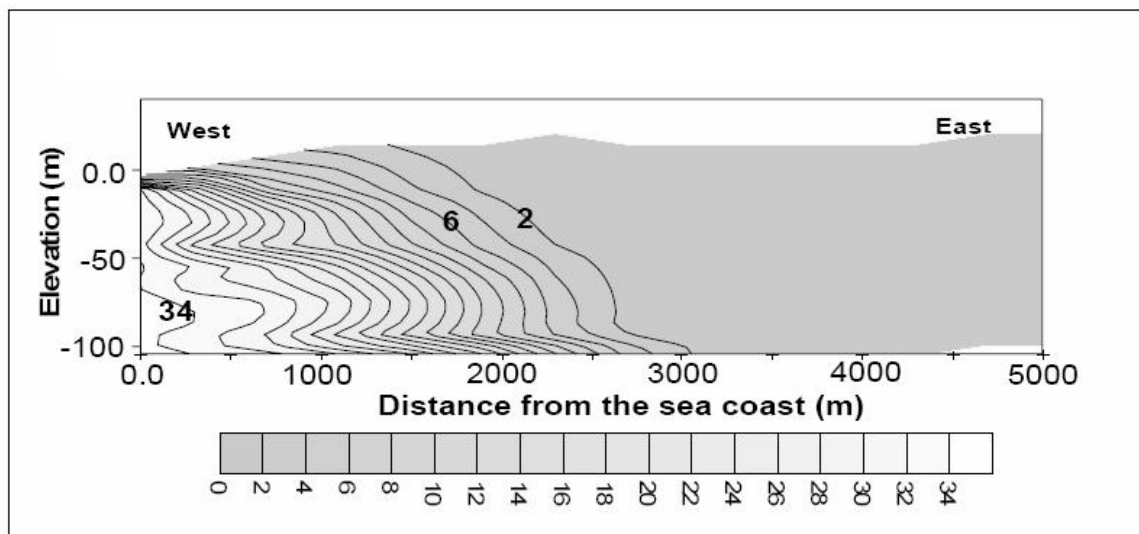


**Figure 5.27** Isolines of TDS concentration ( $\text{kg/m}^3$ ) calculated by SEAWAT along Jabalya (Qahman and Larabi, 2006)

The results of the developed model gave a good agreement with the results of previous models applied to Gaza aquifer (e.g. Qahman and Zhou (2001); Qahman and Larabi (2003a, b); Qahman and Larabi (2006) and results of the geophysical survey obtained by PWA/CAMP (2000)). The discrepancy in results of the current model and the work of Qahman and Larabi (2006) is due to the fact that they have considered the aquifer to be divided to three sub-aquifers overlaying each other and separated by impervious or semi-pervious clayey layers. For simplicity the aquifer has been considered homogenous in the current study. However, the results generally match those of Qahman and Larabi, with the difference being in the shape of the contour lines. Qahman and Larabi (2006) also used SEWAT code to simulate saltwater intrusion in the Gaza aquifer in horizontal plane using two different scenarios of pumping. The special distribution of TDS concentration predicted by SEWAT is shown in Figure 5.28. It is shown that the intrusion of seawater at Khan Younis is about 2 km, Jabalya about 3 km and Wadi Gaza about 1.2 km which is consistent with the results of the present model. The results of the present model in vertical view have been compared with SEWAT results in horizontal view. The comparison between the two models shows a good agreement in terms of concentration distribution in vertical sections obtained by the current model and horizontal section obtained by SEWAT.

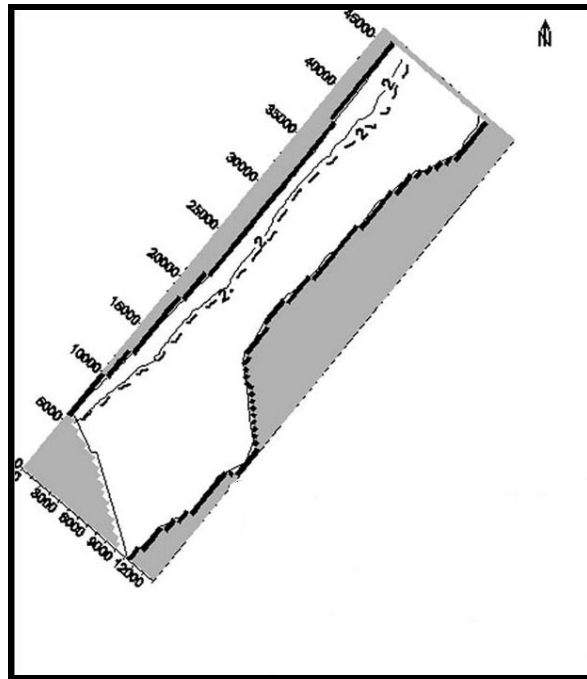


**Figure 5.28** Extant of TDS concentration calculated by SEAWAT  
(Qahman and Larabi, 2006)

Seawater intrusion in the Gaza aquifer was simulated using the developed model in vertical sections and concentration contours of salt distribution in the aquifer were presented and compared with the results of SEWAT which was used to simulate seawater intrusion in the Gaza aquifer in vertical and horizontal sections. The results of the model predictions and comparison were presented and discussed. A good agreement was observed between the results of the present model in vertical cross sections and the results of SEWAT in the horizontal cross section for the case of Gaza aquifer in terms of concentration distribution. The construction of 2D horizontal and vertical sections can be used to obtain a 3D picture of seawater intrusion in coastal aquifers.

### ***5.5 Summary***

In this work, a 2-D finite element model (SUFT) has been developed to study saltwater intrusion in coastal aquifers. The developed model can handle a wide range of real SWI problems. The developed model for simulating saltwater intrusion considers transient, density-dependent flow and velocity-dependant dispersion. The developed finite element model has been applied to a number of examples from the literature for validating the model capability to simulate groundwater flow, solute transport and coupled fluid flow and solute transport. The developed model has been validated against one of the most popular benchmark problems in seawater intrusion in coastal aquifers, widely known as Henry's saltwater intrusion problem. Many researchers validated their codes against Henry's problem as well known cases of saltwater intrusion in order to reveal the capability of such models to simulate saltwater intrusion in coastal aquifer. The current model has also been applied for four different cases of Henry's problem and gave good results for all of them compared with the published results from other researchers. After validation of the model it was applied to a number of real cases studies to predict seawater intrusion in coastal aquifers in different locations of the world. A hypothetical case from the literature, saltwater intrusion in Madras aquifer in India, saltwater intrusion in Biscayne aquifer in Florida and saltwater intrusion in the Gaza aquifer in Palestine have been simulated by the developed mode. The current model gave good results compared with other publications. The results show that the current model is capable of predicting with good accuracy saltwater intrusion in coastal aquifers.

## **Development and application of simulation-optimization model**

### ***6.1 Introduction***

Management of water resources in coastal areas is very important as these areas are heavily populated with increasing the demand for fresh water. Groundwater is considered the main sources of water in many coastal areas. The increase of water demands increases the withdrawal from aquifers which has resulted in lowering water tables and caused saltwater intrusion. Saltwater intrusion is one of the main causes of groundwater quality degradation and a major challenge in management of groundwater resources in coastal regions. Saltwater intrusion causes an increase in chloride concentration of groundwater which places limitations on its uses. Therefore, efficient control of seawater intrusion is very important to protect groundwater resources from depletion.

This chapter presents development and application of a simulation-optimization (S/O) model to control seawater intrusion in coastal aquifers using different management models. The model is based on the integration of a genetic algorithm optimization technique and a coupled transient density-dependent finite element model, which has been developed in this work for simulation of seawater intrusion. The simulation model is used to compute heads and salt concentrations in the aquifer and the optimization model is used to determine the optimal locations, depths, abstraction/recharge rates to minimize the total cost. The management scenarios considered include abstraction of brackish water, recharge of fresh water and combination of abstraction and recharge. The objectives of these management scenarios include minimizing the total costs for construction and operation, minimizing salt concentrations in the aquifer and determining the optimal depths, locations and abstraction/recharge rates for the wells. Also, a new methodology is presented to control seawater intrusion in coastal aquifers. In the proposed methodology ADR (abstraction, desalination and recharge), seawater intrusion is controlled by abstracting brackish water, desalinating it using reverse osmosis and partially recharging it to the aquifer.

Development of S/O approach for the control of saltwater intrusion in coastal aquifers is a major achievement of the present study. It marks the first time (based on the literature) that such coupling models are used for controlling saltwater intrusion in coastal aquifers. The developed S/O model is applied to a hypothetical case (Henry's problem) and number of real world case studies to control saltwater intrusion using three management models. The efficiencies of the three management models are examined and compared. The results show that all three models could be effective but using the ADR methodology results in the lowest cost and salt concentration in aquifers and maximum movement of freshwater/saline water interface towards the sea. The developed model is an effective tool to control seawater intrusion in coastal aquifers and can be applied in areas where there is a risk of seawater intrusion (Abd-Elhamid and Javadi, 2010).

## ***6.2 Optimization techniques***

The optimization problem can be solved through trial-and-error adjustment or through a formal optimization technique. Numerical simulation models can be used to examine a limited number of design options by trial-and-error. The trial-and-error method is simple and thus widely used, testing and checking hundreds to thousands of trial solutions is tedious and cannot guarantee that the optimal solution has been identified. In contrast, the optimization technique can be used to search for the optimal solution in a wide search space of design variables, and equally important, to prove whether a particular management scenario or remedial alternative is feasible in terms of meeting the management objective and satisfying all the constraints.

An optimization model is defined in terms of an objective function and a set of constraints. The objective function can be formulated as the net present value of the management cost or the total pumping rate and, if the one-time drilling and installation costs are negligible compared to the cumulative pumping and treatment costs. The total cost includes the capital cost of drilling and installation, operation cost associated with pumping or recharge and the treatment costs. Groundwater management problem includes two sets of variables; decision variables and state variables. Decision variables are the variables that used to define different alternative decisions, such as; pumping or injection rate of a well, well location

and well depth. Decision variables can be managed in the calculation process to identify the optimal management policy or strategy. State variables are the variables that describe the flow and transport conditions of an aquifer, such as; heads and salt concentrations, which are the dependant variables in flow and transport equations. In a coupled S/O model, simulation components update the state variables and optimization components determine optimal values of decision variables (Zheng and Bennett, 2002).

Coupling flow and solute transport models with optimization techniques to address important groundwater quality management problems has started early 1980s. The motivation for the development of S/O approach for the control of saltwater intrusion is the enormous cost of groundwater remediation. The S/O approach has been shown to be capable of reducing the remediation costs of contaminated land in several real-world applications (Zheng and Bennett, 2002). The S/O approach can be used efficiently in groundwater remediation system design and in other groundwater quality management problems including saltwater intrusion control. The S/O approach is interesting because it can both account for the complex behavior of a groundwater flow system and identify the best management strategy to achieve a given set of prescribed constraints.

Optimization models are widely used in groundwater planning and management. In recent years, a number of simulation models have been combined with optimization techniques to address groundwater management problems. The combined simulation and optimization model accounts for the complex behavior of the groundwater system and identifies the best management strategy under consideration of the management objectives and constraints. In the last two decades, genetic algorithms (GAs) have received increased attention from academic and industrial communities for dealing with a wide range of optimization problems. Mckinney and Lin (1994) applied a GA to groundwater resources management and pump-and-treat system design. Ritzel et al. (1994) solved a multi-objective groundwater contamination problem using GA. Johnson and Rogers (1995) used GA and neural network to select the optimal well locations and pumping rates in a remediation design problem. Zheng and Wang (2001) applied a GA to pump-and-treat system design optimization under field conditions.



### **6.3 Genetic algorithm (GA)**

GA is an optimization technique based on the process of biological evolution. GA was first introduced by Holland (1975) and followed by Goldberg (1989), Davis (1991), Michalewicz (1992), Mckinney and Lin (1995) and Haupt and Haupt (1998) among others. GAs are a family of combinatorial methods that search for solutions of complex problems using an analogy between optimization and natural selection. GA mimics biological evolution based on the Darwinist theory of survival of the fittest, where the strongest offspring in a generation are more likely to survive and reproduce. The GA method starts with randomly generating an initial set of solutions, called the initial population. Each member of this population represents a possible solution of the problem, encoded as a chromosome. A chromosome is a string of symbols, usually a binary bit string. The population of chromosomes evolves through a cycle that involves selection, crossover and mutation. Each cycle is referred to as a generation. After many generations, the population will contain chromosomes that represent near optimal solutions to the problem. GA was applied to a wide variety of problems in engineering including groundwater management, water resources and seawater intrusion. An overview to the application of GA in these fields is presented in the following sections (Zheng and Bennett, 2002).

#### **6.3.1 GA in groundwater management**

GA has been applied to a number of groundwater management problems. A number of researchers incorporated groundwater simulation models with GA to solve groundwater management problems such as; maximizing extraction from an aquifer, minimizing the cost of water supply, minimizing the cost of aquifer remediation and pump-and-treat. Among the researchers who applied GA to groundwater management problems are Mckinny and Lin (1994), Rogers and Dowla (1994), El Harrouni et al. 1996) and Aly and Peralta (1999). Recently, GA has been used to identify cost effective solutions for pump-and-treat groundwater remediation design. A number of researchers have applied GA to solve groundwater pollution remediation problems (e.g. Chan Hilton and Culver 2000; Smalley et al. 2000; Haiso and Chang 2002; Maskey et al, 2002; Gopalakrishnan et al. 2003; Espinoza at al. 2005; Horng et al. 2005 and Chan Hilton and Culver 2005).

### ***6.3.2 GA in water resources management***

In the field of water resources management GA has been applied to a variety of problems such as; calibration of rainfall-runoff models, pipe network systems and operation of reservoirs systems. A number of researches applied GA for calibration of rainfall-runoff models (e.g. Wang (1991); Franchini (1996) and Mulligan and Brown (1998)). A large number of applications in pipe network optimization using GA were presented by Goldgerg (1989), Murphy et al. (1993), Simpson et al. (1994), Halhal et al. (1997), Savic and Walters (1997) and Farmani et al. (2005a,b). GA has also been used to optimize the operation of reservoirs systems by Esat and Hall (1994), Oliveira and Loucks (1997) and Wardlaw and Sharif (1999).

### ***6.3.3 GA in seawater intrusion management***

Although there have been many applications of GA in the field of water resources and groundwater management, the applications of GA to control seawater intrusion has been limited. For the first time in this study GA is applied to study the control of seawater intrusion using ADR system. As the construction and operation costs of such system are very high, thus, the optimal management has the potential to reduce costs substantially. A number of models have been developed to analyze the control of saltwater intrusion in coastal aquifers, based on the two different approaches; sharp interface or diffusive interface (density-dependent). Development and application of optimization techniques to study saltwater intrusion considering a sharp interface between freshwater and seawater was presented by a number of researchers such as; Shamir et al. (1984) presented a multi-objective linear programming model to relate the location of the interface toe and the magnitude of pumping and recharge. Willis and Finney (1988) presented a planning and management model for control of seawater intrusion in the Yun Lin regional groundwater basin in Taiwan. The management model was formulated as a problem of optimal control and solved using MINOS optimization model. Essaid (1990) used the finite difference simulation model SHARP to simulate the aquifer system response within the control model. The objective function of the model was a function of freshwater and seawater heads and locations and magnitude of groundwater pumping or artificial recharge.

Finney et al. (1992) presented the development and application of a quasi three-dimensional optimal control model for groundwater management in the Jakarta coastal aquifer basin based on the sharp interface assumption. Hallaji and Yazicigil (1996) presented seven groundwater management models to determine the optimal planning and policies for a coastal aquifer in southern Turkey threatened by saltwater intrusion. They linked steady-state and transient finite element simulation models to linear and quadratic optimization models using response function to maximize withdrawals and minimize pumping cost with the prevention of saltwater intrusion. Emch and Yeh (1998) developed S/O model to manage water use within a coastal region. Two objectives are considered; cost-effective allocation of surface water and groundwater supplies, and minimization of saltwater intrusion. The flow model was simulated using a quasi-three-dimensional finite difference model based on sharp interface and was linked to an optimization model, MINOS. Tracy (1998) developed S/O model for the optimal management of Santa Barbara city's water resources during draught. The model linked the groundwater simulation model MODFLOW with a linear programming model to minimize the cost of water supply subject to water demand and hydraulic head constraints to control saltwater intrusion.

Cheng et al. (2000) presented an optimization model based on sharp interface approach to optimize pumping in saltwater-intruded coastal aquifers. A genetic algorithm (GA) was utilized for the search of the optimum solution. Benhachmi et al. (2001a) presented an optimization management technique with an economic objective to maximize the benefits from allocation of abstraction wells while minimizing the intrusion of saltwater into wells. A sharp interface approach was incorporated into a simple genetic algorithm to search for optimal solution. Benhachmi et al. (2001b) used a sharp-interface analytical approach to simulate groundwater flow on a horizontal plane. The model was incorporated into a simple genetic algorithm for optimal pumping rates and salinity control with an economic objective. Cheng et al. (2001) used a sharp interface model to simulate saltwater intrusion and a genetic algorithm for optimization. The objective was to maximize freshwater extraction without causing saltwater intrusion into the wells. Moreaux and Reynaud (2001) developed an analytical model based on sharp interface between freshwater and saltwater to determine the optimal use of a coastal aquifer under saline intrusion. Gau and Liu (2002)

presented a decision model based on the loss function concept to estimate the optimum yield from a groundwater basin and control saltwater intrusion in Yun-Lin area, Taiwan.

Zhou et al. (2003) used a quasi three-dimensional finite element model to simulate the spatial and temporal distribution of groundwater levels in an aquifer system. They developed a linear programming model to maximize the total groundwater pumping from the aquifer with the control of saltwater intrusion by restricting the water levels in the aquifer. Benhachmi et al. (2003) presented the same methodology used by Cheng et al. (2000), with considering the economic benefit from the pumped water and minimizing utility cost of lifting the water in the objective function. Park and Aral (2004) presented the same methodology used by Cheng et al. (2000), but they used an iterative sub-domain method, in which the GA searched for the optimal solution by perturbing the well locations and pumping rates simultaneously. The numerical results obtained from the proposed method were compared with the work of Cheng et al. (2000). The results of comparison yielded slightly higher pumping rates than what was reported in Cheng et al. (2000). Bhattacharjya and Datta (2005) developed S/O model for the optimal management of saltwater intrusion in coastal aquifers. 3-D density-dependant flow and transport models were approximated using a trained neural network to calculate salt concentration and linked to GA-based optimization model to maximize the withdrawal of water from a coastal aquifer, with controlling saltwater intrusion. Reichard and Johnson (2005) developed S/O model to control saltwater intrusion in the west coast basin of coastal Los Angeles using two management options, increased injection into barrier wells and delivery of surface water to replace current pumpage.

On the other hand, development and application of optimization techniques in association with saltwater intrusion considering density-dependant flow are relatively recent and very few. Das and Datta (1999a, 1999b) presented a multi-objective management model. The objectives were to maximize pumping from the freshwater zone and minimize pumping from the saline zone in order to control saltwater intrusion. The nonlinear finite-difference of the density-dependent miscible flow and salt transport model for seawater intrusion in coastal aquifers was embedded within constraints of the management model. Das and Datta (2000) developed a nonlinear optimization method for minimizing total sustainable yield

from specific location of the aquifer while satisfying salinity constraints. Gordu et al. (2001) developed a management model to maximize the total pumping rate from wells considering saltwater intrusion into the aquifer. They used SUTRA code for groundwater simulation and the general algebraic modelling system code to execute the optimization model.

Gordon et al. (2001) developed a model for optimal management of a regional aquifer under salinization. The source of salinization was from irrigation water percolating over some part of the aquifer, influx of saline water from faults in the aquifer bottom, and inflow from laterally adjacent saline water bodies. The objectives of management were to maximize the total amount of water pumped for use and to minimize the total amount of salt extracted with the water. The simulation model used a finite-element formulation for the flow and a streamline upwind Petrov-Galerkin formulation for the transport. The model computed the gradient of the state variables (heads and concentrations) with respect to the decision variables (pumping rates at wells). The gradients were then used in a Bundle-Trust non-smooth optimization procedure to achieve an improved solution. Rao and Rao (2004) presented S/O approach to control saltwater intrusion through a series of extraction wells. They used SEAWAT code to simulate saltwater intrusion and the simulated annealing algorithm for solving the optimization problem. Two objective functions were considered: first to maximize groundwater pumpage for beneficial purposes and second to minimize the pumping in extraction wells which were used to extract saline water and dispose to the sea.

Park et al. (2008) investigated effects of saltwater pumping to protect an over-exploiting freshwater pumping well. They used S/O numerical model taking into account various parameters to identify the minimum saltwater pumping rate required to protect the over-exploiting pumping well. Arvanitidou et al. (2010) applied a generic operational tool for the optimal management of coastal aquifers to a real unconfined coastal aquifer in the Greek island Kalymnos. They combined a numerical model that predicts the seawater intrusion due to flow perturbations and the optimization method of GA. The presented management scenarios were based on the hydrodynamic control of seawater intrusion due to the operation of a network of productive wells and the seasonal use of a recharge canal which is an alternative method for increasing aquifer sustainable productivity.

According to the literature, only few researchers have considered the transition zone between the freshwater and seawater by incorporating density-dependent miscible flow and solute transport in management of coastal aquifers. Also, the majority of the presented management models did not consider the economic value of those systems. This work presents the development and application of S/O model to control seawater intrusion in coastal aquifers using three management models; abstraction of brackish water, recharge of fresh water and combination of abstraction and recharge. The objectives of these management models include minimizing the total costs for construction and operation, minimizing salt concentrations in the aquifer and determining the optimal depths, locations and abstraction/recharge rates of the wells. A new methodology is presented to control seawater intrusion in coastal aquifers. In the proposed ADR methodology seawater intrusion is controlled by abstracting brackish water, desalinating it using reverse osmosis and recharging to the aquifer (Abd-Elhamid and Javadi, 2010).

#### ***6.4 Simulation-Optimization model***

Simulation models have been applied for management of groundwater resources seeking for optimal management strategy by trial-and-error. This has proved to be time consuming and laborious. In addition, the results obtained may not be optimal. The main reason for this is the inability of this approach to consider important physical and operational restrictions. To accommodate these restrictions, coupling of the simulation model with a management model is the generally adopted procedure. For groundwater systems, combined simulation and management models may adequately predict the behavior of the system and provide the best solution for problems such as planning of long term water supply or preventing seawater intrusion. A relatively small number of studies have concentrated on the control of saltwater intrusion. To the author knowledge, no attempt has been made in the literature to develop or use S/O model to study optimal control of seawater intrusion using a combination of abstraction and recharge wells.

The proposed ADR methodology has not been used before in the control of seawater intrusion. The only related work in the literature appears to be that of Mahesha (1996c) and Rastogi et al. (2004) who used a simulation model to study the effect of abstraction and/or recharge on seawater intrusion by trial-and-error. Therefore the focus of this study is on development and application of S/O model to effectively determine the optimal solution for control of seawater intrusion. In this work the reduction in cost is achieved by determining the optimal depths, locations and abstraction/recharge rates while also minimizing salt concentration in the aquifer. The main objective of this study is to determine a cost-effective method to control the intrusion of seawater in coastal aquifers. The three main factors contributing to the construction and operation costs are considered as the decision variables:

- 1- The depth of abstraction and/or recharge wells: Reduction in depth of abstraction/recharge wells leads to reduction in construction cost.
- 2- The location of well (distance from the seashore): Location of abstraction/recharge wells can have a significant effect on reduction of the required abstraction/recharge rates to maintain the freshwater/seawater interface in optimal position, reduction of concentration of salt in the aquifer and reduction of operational cost.
- 3- Abstraction/recharge rates: Reduction of abstraction/recharge rates leads to reduction in the operational cost.

Considering the three main factors mentioned above, the objectives of optimization are; minimization of depths for the wells, determination of optimum locations for the wells, and minimization of the abstraction/recharge rates subject to a number of constraints. Appropriate weights for the objectives can be obtained by involving decision makers. In this work minimization of the overall cost of construction and operation is considered as the main objective. The sum of salt concentration in the region is calculated and is maintained below a specified value or minimized. The proposed S/O model consists of two main components. The first is a simulation model to compute hydraulic heads and salt concentrations in the aquifer. The second component is a GA-based evolutionary optimization model that uses the results of the simulation model to compute and minimize the objective function. The simulation model, the optimization technique and the integration of simulation and optimization models are described below.

### **6.4.1 Simulation model**

Modelling of fluid flow and solute transport for a site involves development of a mathematical model of the site system being studied and to use this model to predict the value of hydraulic heads and salt concentrations at points of interest at different times. Numerical simulation of seawater intrusion, assuming that mixing occurs at the transition zone between seawater and freshwater, involves the solution of the partial differential equations representing the conservation of mass for the variable-density fluid (flow equations) and for the dissolved solute (transport equation). The governing equation and numerical solution were presented in chapters 3 and 4. The output of the simulation model is the pore water pressures and salt concentrations at every point within the domain. The predicted values of pore water pressure are used to calculate pressure head and total head, through Bernoulli's equation.

The flow and transport equations are coupled through Darcy's law and a constitutive equation relating fluid density to salt concentration. This coupling between the flow and transport equations makes the problem of seawater intrusion highly nonlinear. To simulate the flow and transport processes, the flow and transport equations are discretized in space and time using the finite element and finite difference techniques. The numerical solution of coupled fluid flow and solute transport is based on solving the governing equations with the boundary and initial conditions by the iterative solution scheme was described in chapter 4. The flow equations are solved to compute pore water at all nodes. The pressure head, fluid velocity and fluid density are then calculated. The calculated velocities are used to define the dispersion coefficient for the solute transport equation. The solute transport equation is then solved for concentrations at every node in the domain and this process is repeated for every time step. A flow chart of the numerical solution algorithm is shown in Figure 6.1.



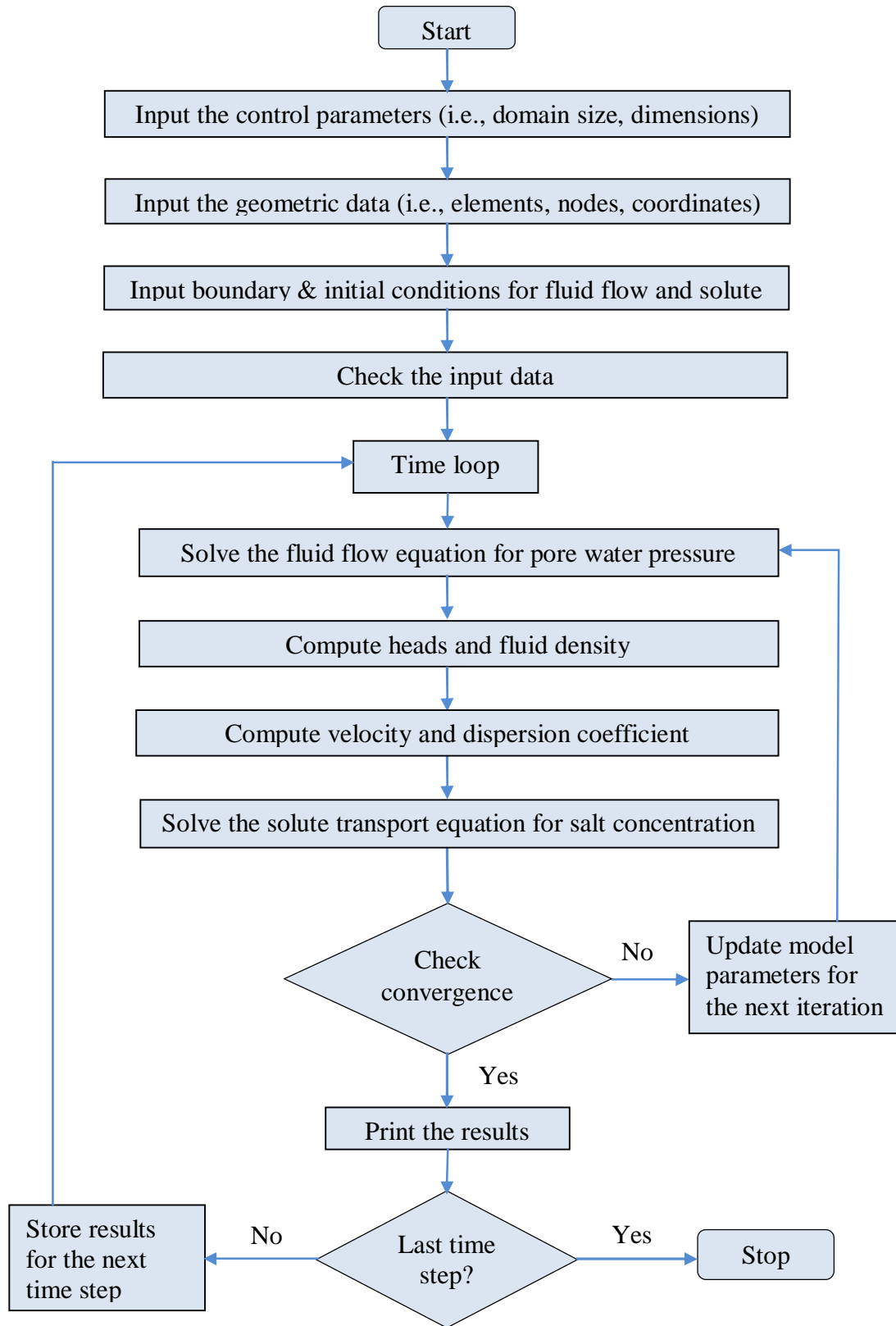


**Figure 6.1** Flow chart of the solution algorithm

### **6.4.2 Genetic Algorithm Optimization model**

Genetic algorithms (GAs) have received much attention regarding their potential as global optimization techniques for problems with large and complex search spaces. GAs have many advantages over the traditional optimization methods. In particular, they do not require function derivatives and work on function evaluations alone. They have a better possibility of locating the global optimum as they search a population of points rather than a single point and they can allow for consideration of design spaces consisting of a mix of continuous and discrete variables. GAs operate on a population of trial solutions that are initially generated at random. The genetic algorithm seeks to maximize the fitness of the population by selecting the fittest individuals, based on Darwin's theory of survival of the fittest, and using their genetic information in mating and mutation operations to create a new population of solutions. Many variations of the GA have been developed, but the algorithm implemented here can be summarized as being a simple binary encoded GA with roulette wheel selection, uniform crossover and an elitist replacement strategy.

Saltwater intrusion control problem is formulated as an optimization problem of finding the optimum management options in terms of depths, locations and abstraction/recharge rates for abstraction/recharge wells to reduce the construction and operation costs and minimize salt concentrations in the aquifer. Different sets of values for the design parameters are generated and evolved using the principles of genetic algorithm and the behavior of each of the generated management systems (corresponding to a set of design parameters) is analyzed using the finite element model to evaluate its fitness in competition with other generated systems. During successive generations the genetic algorithm operators gradually improve the fitness of the solution and direct the search towards the optimal or near optimal solution. GAs have some control parameters such as population size  $n$ , and probabilities for applying genetic operators, e.g., crossover probability  $P_c$ , usually 0.7 to 1, and mutation probability  $P_m$ , usually 0.01 to 0.1 (Qahman and Larabi 2006).

In this work, a simple genetic algorithm code written in FORTRAN is used. The selection scheme used is tournament selection with a shuffling technique for choosing random pairs

for mating. The routine includes binary coding for the individuals, jump mutation, creep mutation, and the option for single-point or uniform crossover. The steps followed for finding the optimal solution can be summarized as:

- 1- An initial population of decision variables is generated randomly in the form of binary strings. The binary strings are then decoded to real values representing the design parameters of the system.
- 2- The values of the design variables are used by the FE model to compute the hydraulic heads and salt concentrations for different points within the domain.
- 3- The calculated values of heads and concentrations are used by the GA process to evaluate the objective function (fitness) values for all members of the population.
- 4- The processes of selection, crossover and mutation are performed as in a simple genetic algorithm procedure and a new population of individuals (new generation) is created.
- 5- The new generation replaces the current generation and the entire process (steps 2-4) is repeated until convergence is achieved or the maximum number of generations is exceeded.

A flowchart for the genetic algorithm used is shown in Figure 6.2.

### ***6.4.3 Integration of the simulation and optimization models***

The simulation-optimization model developed in this work is based on the integration of a GA with a coupled transient density-dependent FE simulation model for flow and solute transport. In the developed simulation-optimization framework, the simulation model is repeatedly called by the GA to calculate the response of the system to each set of design variables generated by the GA. The simulation model is used to compute pressure heads and salt concentrations for every node in the domain. These values for pressure heads and salt concentrations are returned to the GA routine and used to evaluate the objective function value and determine the fitness of the solution in competition with other generated solutions. Figure 6.3 shows the schematic steps of the simulation-optimization model.

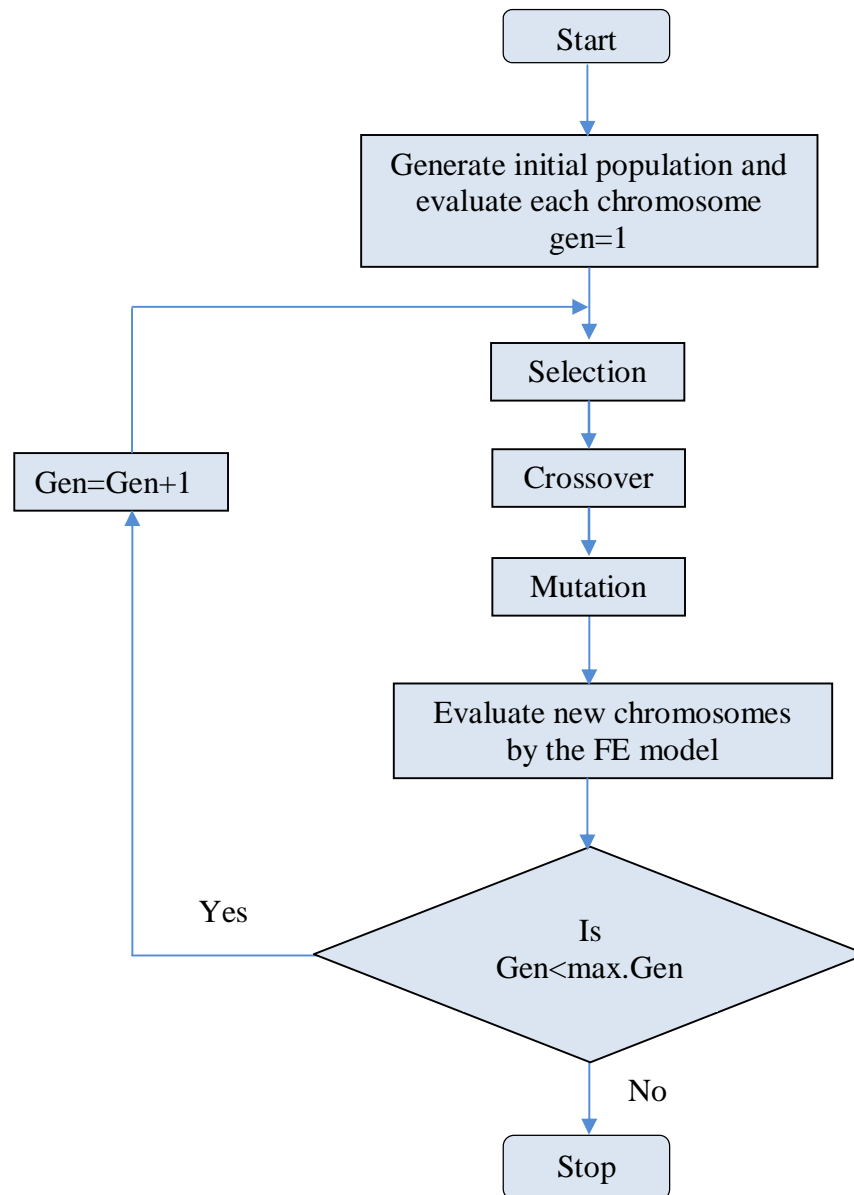


**Figure 6.2** Flowchart for the genetic algorithm

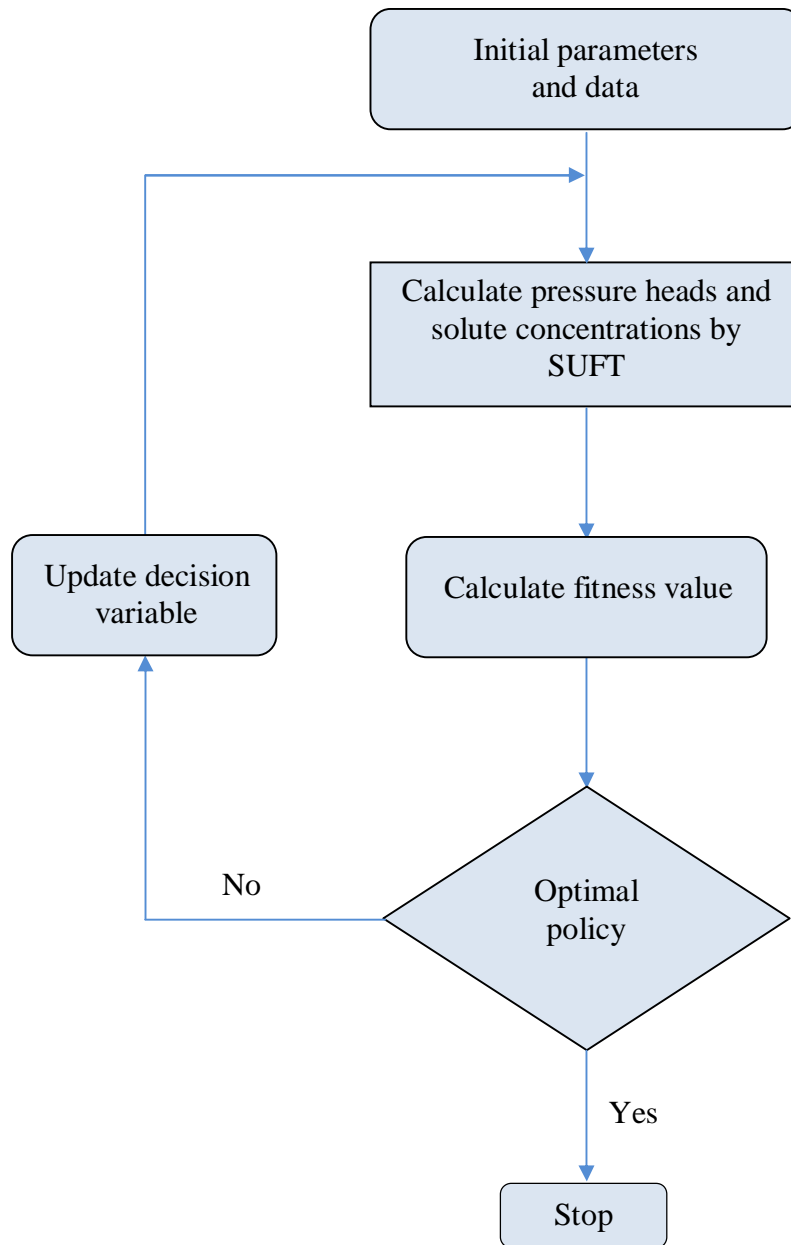


**Figure 6.3** Flow chart of the schematic steps of the simulation-optimization model

### 6.5 Formulation of the management models

An appropriate management strategy can provide an efficient and cost-effective approach to control seawater intrusion in coastal aquifers. A GA-based optimization approach is used in this work to incorporate a seawater intrusion simulation model within an optimization-based management model to evolve an optimal management strategy. Three management models are developed in this work to control seawater intrusion in coastal aquifers; abstraction of brackish water, recharge of fresh water and combination between abstraction and recharge. The main objective of the simulation-optimization models is to minimize the construction and operation costs by identifying the optimal depths, locations and abstraction/recharge rates for abstraction and/or recharge wells to control the intrusion of seawater. Figure 6.4 shows the design variables considered in the simulation-optimization model.

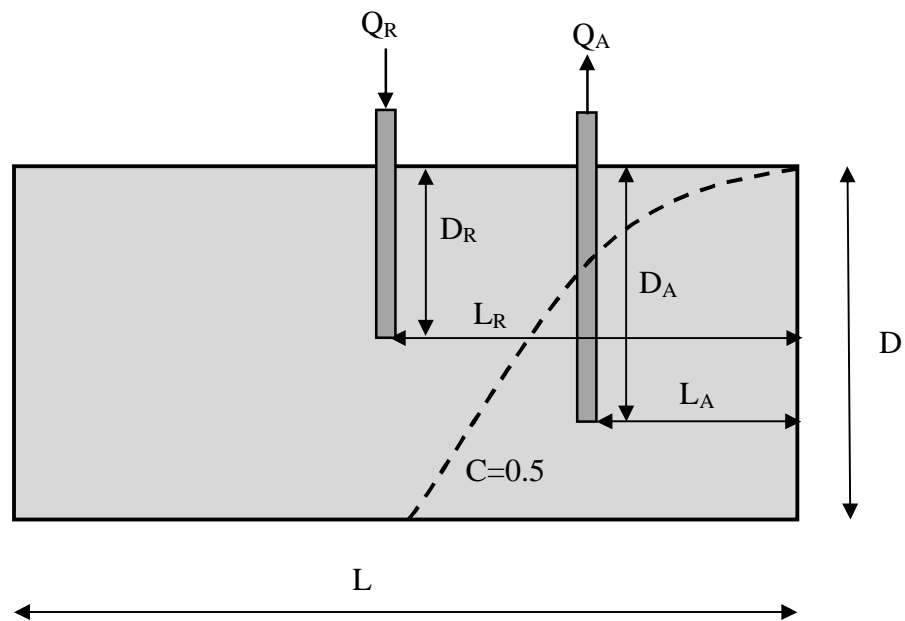


**Figure 6.4** Schematic sketch for potential locations and depths for the abstraction and recharge wells

### 6.5.1 Management model 1: (Abstraction wells)

Management of coastal aquifers often requires consideration of multiple objectives. One management option could be to abstract brackish water from the saline zone to decrease the volume of saline water and retard the position of the freshwater-seawater interface. However, abstraction of brackish water from a coastal aquifer, in some cases, may increase the intrusion of seawater. Therefore, the management objective should also minimize the total amount of salt in the aquifer. The objective of model 1 is to minimize the total construction and operation costs of abstraction wells and to minimize the total amount of salt in the aquifer. This can be achieved by determining the optimum depth, location and the abstraction rate of abstraction well to reduce the total cost. The decision variables are therefore location, depth and abstraction rate and the state variables are; pressure heads and salt concentrations at every node in the domain that are computed by the simulation model. The objective functions of model 1 can be represented mathematically as follows:

$$\text{Min } f_1 = \sum_{i=1}^N c_i \quad (6.1)$$

$$\text{Min } f_2 = \sum_{i=1}^N Q_{A_i} (C_A + C_T) \quad (6.2)$$

$$\text{Min } f_3 = \sum_{i=1}^N D_{A_i} (C_{DW}) \quad (6.3)$$

where

$f$  : is the objective function in terms of the total cost

$N$  : is the total number of nodes in the domain

$D_A$  : is depth of abstraction well (m)

$Q_A$  : is the abstraction rate (m<sup>3</sup>/sec)

$c$  : is total amount of solute mass in the aquifer (mg/l)

$C_A$  : is the cost of abstraction (\$/m<sup>3</sup>)

$C_T$  : is the cost of treatment (\$/m<sup>3</sup>)

$C_{DW}$  : is the cost of installation/drilling of well (\$/m)

To deal with multiple objective functions the weighted sum of each objective function can be used to form a single scalar objective function (Park and Aral, 2004). This brings the difficulty of adjusting the weight of each objective, which can be considered to be a management decision. However, it is recognized that a single scalar objective function generated is not capable of representing the vector tendency of each objective. Nonetheless, in this work the single scalar objective function approach is used for simplicity. This approach was used by many researchers such as Gordon (2001) Park and Aral (2004) and Qahman and Larabi (2006). The final objective functions of model 1 can be represented as:

$$\text{Min } f = P_1 \sum_{i=1}^N c_i + P_2 \sum_{i=1}^N Q_{A_i} (C_A + C_T) + P_3 \sum_{i=1}^N D_{A_i} (C_{DW}) \quad (6.4)$$

where  $P_1$ ,  $P_2$  and  $P_3$  are the weighting parameters, which are chosen based on the literature.

The management objective must be achieved within a set of constraints, which can be derived from technical, economic, legal or political considerations. The constraints in this model include; well depth, well location and abstraction rate and can be expressed as:

$$Q_{A_{\min}} < Q_{A_i} < Q_{A_{\max}} \quad (6.5)$$

$$L_{A_{\min}} < L_{A_i} < L_{A_{\max}} \quad (6.6)$$

$$D_{A_{\min}} < D_{A_i} < D_{A_{\max}} \quad (6.7)$$

Equations 6.5-6.7 represent side constraints, where  $Q_{A_{\min}}$ ,  $Q_{A_{\max}}$  are the minimum and maximum values of abstraction rate,  $L_{A_{\min}}$ ,  $L_{A_{\max}}$  are the minimum and maximum distances from the abstraction well to the sea shore and  $D_{A_{\min}}$  and  $D_{A_{\max}}$  are the minimum and maximum depths of the abstraction well. In this management model the costs of installation/drilling of well, abstraction and treatment (i.e. desalination) are introduced based on the literature. According to the literature these costs are considered as; cost of



installation/drilling of well per unit depth: \$1000, cost of abstraction per cubic meter: \$0.42 and cost of treatment (i.e. desalination) per cubic meter: \$0.6 (Qahman and Larabi, 2006).

### 6.5.2 Management model 2: (Recharge wells)

The second management model is designed to search for the optimal arrangement for recharge of fresh water into the aquifer to control seawater intrusion. The management model involves recharge of freshwater to increase the volume of freshwater in the aquifer to retard the position of the freshwater/seawater interface. However, recharge of fresh water may increase the total cost required to prevent seawater intrusion due to the large amount of water required for recharge and the availability and cost of fresh water in coastal areas. Therefore, this management model is used to minimize the cost of water required to be recharged. The objective of model 2 is to minimize the total construction and operation costs of recharge wells and to minimize the total amount of salt in the aquifer. Location, depth and recharge rate are considered as the decision variables to be optimized to reduce the total cost. A single scalar objective function is used by combining of a number of objectives, following a procedure similar to the one adopted in the management model 1.

The objective function of model 2 can be represented as:

$$\text{Min } f = P_1 \sum_{i=1}^N c_i + P_4 \sum_{i=1}^N Q_{R_i} (C_{PW} + C_R) + P_5 \sum_{i=1}^N D_{R_i} (C_{DW}) \quad (6.8)$$

Where

$f$  : is the management objective function in terms of the total cost

$P_4$  and  $P_5$ : are the weighting parameters

$Q_R$  : is the recharge rate ( $\text{m}^3/\text{sec}$ )

$D_R$  : is the depth of recharge well (m)

$C_R$  : is the cost of recharge ( $\$/\text{m}^3$ )

$C_{PW}$  : is the price of water ( $\$/\text{m}^3$ )

The constraints of model 2 can be expressed as:

$$Q_{R_{\min}} < Q_{R_i} < Q_{R_{\max}} \quad (6.9)$$

$$L_{R_{\min}} < L_{R_i} < L_{R_{\max}} \quad (6.10)$$

$$D_{R_{\min}} < D_{R_i} < D_{R_{\max}} \quad (6.11)$$

Equation (6.9) constrains the recharge rate of an recharge well between specified minimum and maximum values  $Q_{R_{\min}}$ ,  $Q_{R_{\max}}$ . Equation (6.10) is a constraint on the distance of recharge well from the seashore between specified minimum and maximum values  $L_{R_{\min}}$ ,  $L_{R_{\max}}$ . Equation (6.11) is a constraint on the depth of recharge well between specified minimum and maximum values  $D_{R_{\min}}$  and  $D_{R_{\max}}$ . In management model 2 the costs of installation/drilling of well, recharge and price of water including transportation is introduced based on the available data from the literature. These costs are assumed to be as follows; cost of installation/drilling of well per unit depth: \$1000, cost of recharge per cubic meter: \$0.48 and price of water per cubic meter: \$1.5 (Qahman and Larabi, 2006).

### 6.5.3 Management model 3: (Abstraction and Recharge wells)

Management model 3 is developed in order to combine management models 1 and 2 to prevent/control seawater intrusion. The objective of management model 3 is to minimize the total construction and operation costs of abstraction and recharge wells and to minimize the total amount of salt in the aquifer. Locations, depths and abstraction/recharge rates of the abstraction and recharge wells are considered as decision variables.

The objective function of model 3 can be represented as:

$$\begin{aligned} \text{Min } f = & P_1 \sum_{i=1}^N c_i + P_2 \sum_{i=1}^N Q_{A_i} (C_A + C_T) + P_3 \sum_{i=1}^N D_{A_i} (C_{DW}) \\ & + P_4 \sum_{i=1}^N Q_{R_i} (C_R) + P_5 \sum_{i=1}^N D_{R_i} (C_{DW}) \end{aligned} \quad (6.12)$$

The same constraints as in equations (6.5, 6.6, 6.7, 6.9, 6.10, and 6.11) are used in management model 3.

The design of optimal ADR system aims to determine the optimal locations, depths and abstraction/recharge rates of the abstraction and/or recharge wells, to minimize the total cost of construction and operation of abstraction and recharge wells and treatment of abstracted water, and to minimize the total amount of salt in the aquifer. Management model 3 is used to apply the new methodology ADR to control seawater intrusion in order to get the optimal design parameters. The results of applying the three management models are presented and discussed in the following section. Also, a comparison is presented between the three models in terms of total cost, total amount of water abstracted or recharged and total salt concentration in the aquifer.

## ***6.6 Application of the simulation-optimization model***

This section presents the application of the developed simulation-optimization model to control seawater intrusion in coastal aquifers. The objective of the management model is to minimize the total cost of construction and operation to control saltwater intrusion in coastal aquifers. The three management models are applied to a hypothetical coastal aquifer (Henry's problem) and a real world case study, Biscayne aquifer, Florida, USA.

### ***6.6.1 A hypothetical case study (Henry's problem)***

This example presents the application of the developed simulation-optimization model to control seawater intrusion in a hypothetical confined coastal aquifer. This problem is known as Henry's problem (Henry, 1964). The geometry and initial and boundary conditions are shown schematically in Figure 5.7 (chapter 5). The dimensions of the aquifer are considered to be 200 m (length) and 100 m (depth). The finite element mesh consists of 661 nodes and 200 elements, each of size 10.0 m by 10.0 m. The simulation parameters for the problem are given in Table 5.1 (chapter 5). The results of the finite element simulation (without optimization) are shown in Figure 6.5 which shows 0.5 isochlor in the aquifer.

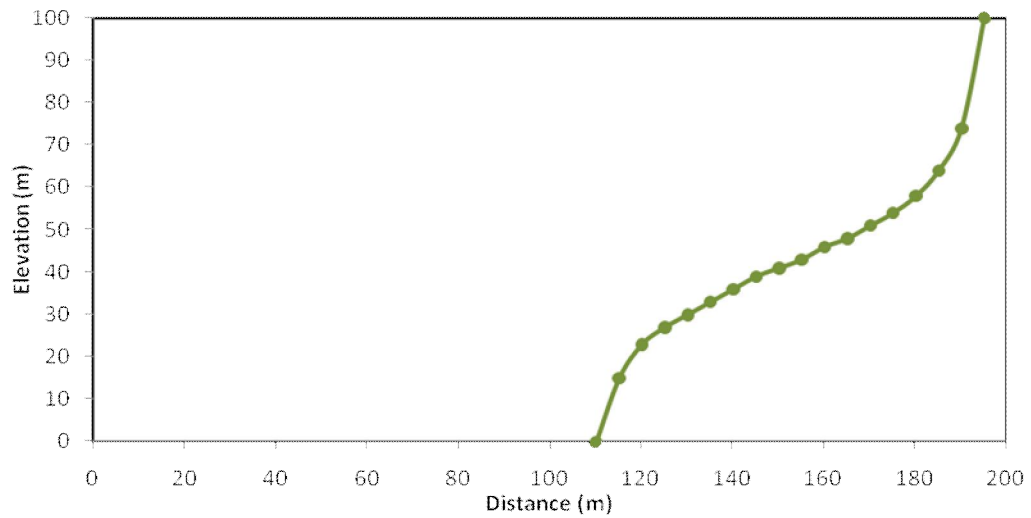


**Figure 6.5** 0.5 isochlor for the hypothetical case study

Potential locations and depths for the abstraction and recharge wells are shown in Figure 6.6.

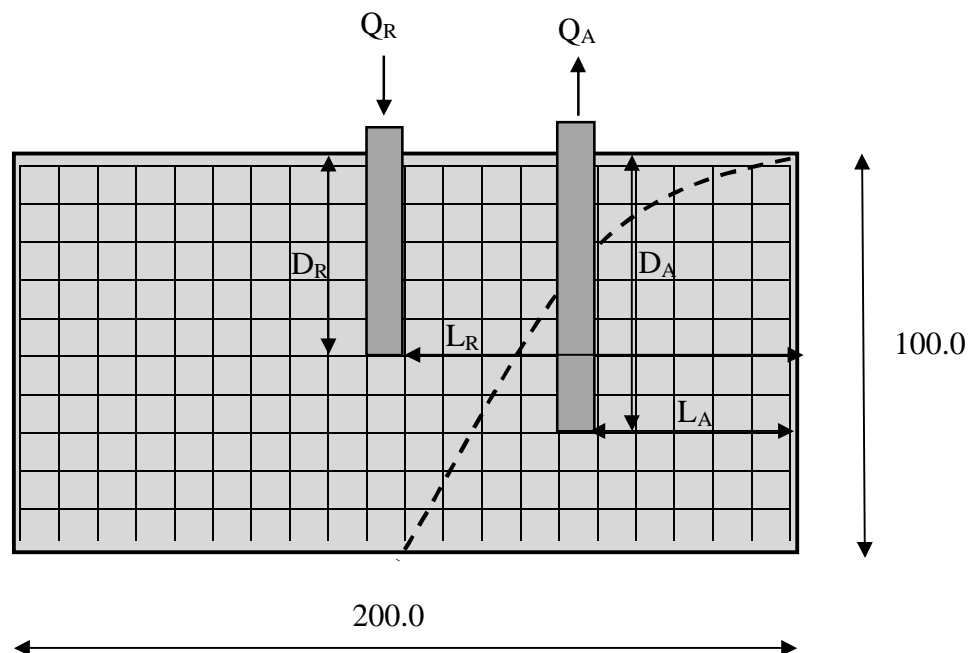


**Figure 6.6** Schematic sketch for potential locations and depths for the abstraction and recharge wells of the hypothetical case study

In the developed S/O framework, initially a population of sets of design variables (locations, depths and abstraction and/or recharge rates for the wells) is generated randomly by the GA. The FE model is then called to evaluate the response of the system to each set of design variables in the population in the form of heads and salt concentrations throughout the domain. The computed values for pressure heads and salt concentrations are returned to the GA routine and used to evaluate the objective function value and determine the fitness of each solution in competition with other generated solutions. The population then undergoes the genetic operations of selection, cross over and mutation to create a new population. The parameters used by GA are: population size = 10, maximum generations = 100, the values of crossover and mutation probabilities are 0.7 and 0.03 respectively. The upper and lower limits for the side constraints are listed in Table 6.1.

**Table 6.1** Summary of the upper and lower constraints for the hypothetical case study

Parameter	value
$Q_{\min}$ (m <sup>3</sup> /s)	0.0
$Q_{\max}$ (m <sup>3</sup> /s)	0.1
$L_{\min}$ (m)	0.0
$L_{\max}$ (m)	200.0
$D_{\min}$ (m)	0.0
$D_{\max}$ (m)	100.0

The application of the proposed simulation-optimization model to the current case has been done in two steps. In the first step, the simulation model is applied with the initial and boundary conditions to compute heads and salt concentrations at every node in the domain. In the second step, the simulation-optimization model is applied to determine the decision variables; well depths, locations and abstraction/recharge rates subject to constraints which have been defined for the three management models presented above. The objective function for the three models is to minimize the total cost associated with well locations, depths and abstraction/recharge rates. The results obtained from the simulation-optimization model for the three management models are presented in Table 6.3 and discussed in the following section.

### 6.6.1.1 Application of management model 1

In management model 1 the objective is to minimize the total construction and operation costs of using abstraction wells to control seawater intrusion. The construction costs include installation and drilling costs, while operation costs include abstraction and treatment (i.e. desalination) costs. The values of the costs used in this case are listed in Table 6.2 (Qahman and Larabi, 2006).

**Table 6.2** Summary of the values of costs

Parameter	Value
$C_A$ (\$/m <sup>3</sup> )	0.42
$C_T$ (\$/m <sup>3</sup> )	0.6
$C_{DW}$ (\$/m)	1000.0
$C_R$ (\$/m <sup>3</sup> )	0.48
$C_{PW}$ (\$/m <sup>3</sup> )	1.5

The optimization problem for management model 1, as defined in equation (6.4) and subject to the constraints defined by equations (6.5), (6.6) and (6.7), is solved using the genetic algorithm to obtain the optimum depth, location, abstraction rate to minimize the cost of construction and operation of the system and the salt concentrations in the aquifer. The results in terms of the optimal depth, location and abstraction rate for the well, together with the corresponding total cost are summarized in Table 6.3. Using management model 1 the value of the total cost is determined as \$2.62 million per year. The optimal depth is 90 m, the optimal location is 50 m from the seashore and the optimal abstraction rate is 0.083 (m<sup>3</sup>/sec) while the total concentration in the aquifer is reduced from 167 to 149 (mg/l). The final optimized concentration distribution for this model is shown in Figure 6.7 in the form of 0.5 isochlor. Figure 6.7 shows how the distribution of salt and the interface between saline water and fresh water are affected by the current scenario of control.

### ***6.6.1.2 Application of management model 2***

In the second management model the objective is to determine the optimal well location, depth and recharge rate to minimize the total construction and operation costs of using recharge wells to control seawater intrusion. The optimization problem for management model 2, as defined in equation (6.8) subject to the constraints defined in equations (6.9), (6.10) and (6.11) is solved using the GA to obtain the optimum depth, location, recharge rate and minimum cost of constructing and operating the system. The optimized well depth, location and recharge rate in addition to the optimal total cost are listed in Table 6.3. Using management model 2 the total cost is \$5.72 million per year. The optimal depth is 60 m, the optimal location is 90 m from the seashore and the optimal recharge rate is 0.095 (m<sup>3</sup>/sec) while the total concentration has reduced from 167 to 151 (mg/l). The final optimized concentration distribution for this model is shown in Figure 6.7.

### ***6.6.1.3 Application of management model 3***

The third management model is based on combination of management models 1 and 2. This model seeks to minimize the total construction and operation costs of using both abstraction and recharge wells to control seawater intrusion. The optimization problem for management model 3, as defined in equation (6.12) and the constraints used in management models 1 and 2 is solved to obtain the optimum depths, locations, abstraction/recharge rates for both abstraction and recharge wells to minimize the cost of construction and operation of the system. The results in terms of the optimal depths, locations and abstraction and recharge rates in addition to the corresponding total cost are listed in Table 6.3. Using management model 3 the value of the minimized objective function is \$1.32 million per year. The optimal depths for abstraction and recharge wells are 90 and 80 m respectively; the optimal locations for abstraction and recharge wells are 50 and 110 m from the seashore and the optimal rates for abstraction and recharge wells are 0.048 and 0.018 (m<sup>3</sup>/sec) respectively. The total concentration in the aquifer has reduced from 167 to 142 (mg/l). The final optimized concentration distribution for this model is shown in Figure 6.7.

**Table 6.3** Summary of the results obtained from the simulation-optimization models for the hypothetical case study

Model	Norm. L	Norm. D	Q (m <sup>3</sup> /s)	Norm. C	Q (Mm <sup>3</sup> /year)	F (cost \$/year)
No management model	No abstraction or recharge wells have been used			167		
Abstraction well A	50	90	0.083	149	2.6	2.62E+6
Recharge well R	90	60	0.095	151	3.0	5.72E+6
Abstraction and Recharge well A	50	90	0.048	142	1.5	1.32E+6
R	110	80	0.018	142	0.5	

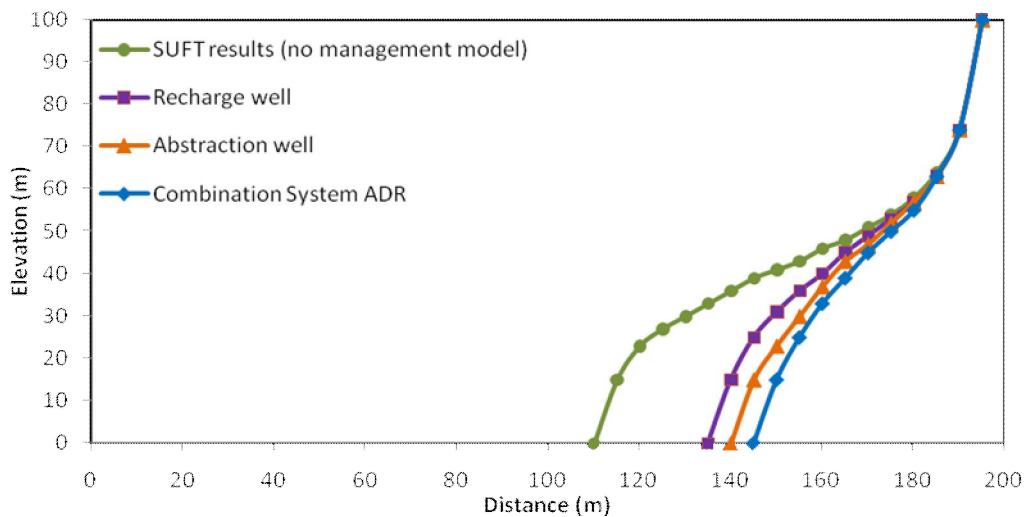


**Figure 6.7** 0.5 isochlor distribution from simulation-optimization models for the hypothetical case



### 6.6.1.4 Discussion

This case presented the application of simulation-optimization model to control seawater intrusion in a hypothetical coastal aquifer. Three management models with different objective functions were considered. The results of the simulation-optimization model for the three management scenarios were presented and compared. The results show that the developed model is capable of determining the optimal depths, locations and abstraction or recharge rates for the wells and minimizing the total cost of construction and operation. Comparison between total costs, salt concentrations in the aquifer and abstraction/recharge rates for the three management models are presented in Figures 6.8, 6.9 and 6.10. From these figures it can be concluded that:

- 1- Using recharge wells alone, requires a higher cost of \$5.72 million per year mainly due to the price of water and its transportation. Using abstraction wells alone requires a lower cost of \$2.62 million per year. However, using a combination of abstraction, treatment (i.e. desalination) and recharge results in the lowest cost of \$1.32 million per year which represents 50% of the abstraction costs and 25% of the recharge costs.
- 2- Using the management model 2 involving recharge wells only, requires recharge of 3 ( $\text{Mm}^3/\text{year}$ ) of fresh water. Using abstraction wells (management model 1) requires abstraction of 2.6 ( $\text{Mm}^3/\text{year}$ ) of saline water. However, using model 3 requires abstraction of 1.5 ( $\text{Mm}^3/\text{year}$ ) of saline water and recharge of 0.5 ( $\text{Mm}^3/\text{year}$ ) of fresh water which is less than the total amount of water abstracted or recharged in management models 1 or 2.
- 3- Using the management model 2 (recharge wells only), reduced the total salt concentration in the aquifer from 167 to 151(mg/l) and using abstraction wells (management model 1) reduced the salt concentration to 149 (mg/l). However, using model 3 reduced salt concentration to 142 (mg/l) which is less than the amount of salt concentration achieved using management models 1 and 2.
- 4- The third model gave the lowest cost partly because the cost associated with the supply of water used for recharge does not apply in this case as the required water is provided primarily from the desalination plant. In addition the excess treated water can be directly used for other purposes. Management model 3 appears to be very

efficient and more practical, as it requires substantially lower cost and leads to further advancement of the freshwater-seawater interface towards the sea and lower concentration of salt in the aquifer.

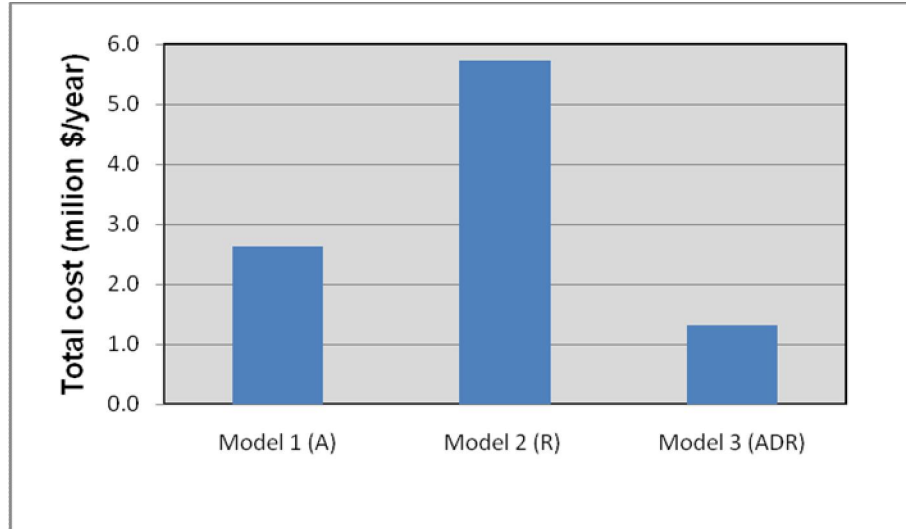


**Figure 6.8** Comparison between total costs of model 1, 2 and 3 for the hypothetical case study

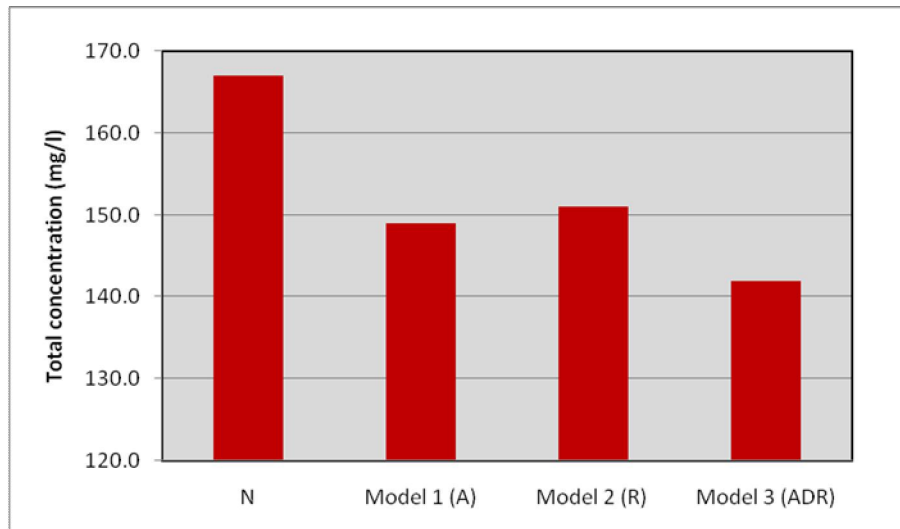


**Figure 6.9** Comparison between total salt concentrations remaining in the aquifer of model 1, 2 and 3 for the hypothetical case study

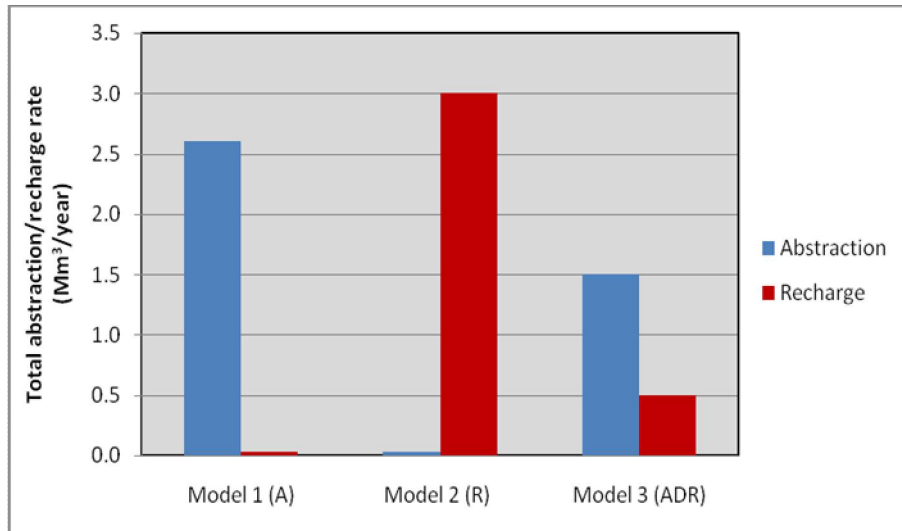


**Figure 6.10** Comparison between total abstraction/recharge rates of model 1, 2 and 3 for the hypothetical case study

### 6.6.2 Real world case study (*Biscayne aquifer, Florida, USA*)

In this case the developed simulation-optimization model is applied to a real case study to control saltwater intrusion in a coastal aquifer. The real world problem is selected from the coastal area of Biscayne aquifer at Coulter area, Florida, USA. The aquifer average depth is 30.0 m below mean sea level and the length is 300.0 m. The domain is discretized using two dimensional grid ( $\Delta X = \Delta Y = 6$  m). The mesh consists of 250 elements and 861 nodes. Coefficient of permeability of  $3 \times 10^{-10}$  m/sec and porosity of 0.39 were considered. The longitudinal and transverse dispersivities  $\alpha_L$  and  $\alpha_T$  were taken as 5.0 and 0.5 m, respectively. The density of fresh water  $\rho_f$  and seawater  $\rho_s$  are 1.0 and 1.025 t/m<sup>3</sup> respectively. The schematic sketch of the Biscayne aquifer and the corresponding boundary conditions applied in this case are shown in Figure 5.20 (chapter 5). The Biscayne aquifer is simulated using the developed finite element code and the results of simulation, without optimization are shown in Figure 6.11 in the form of 0.25, 0.5, 0.75 and 1.0 isochlor contours.

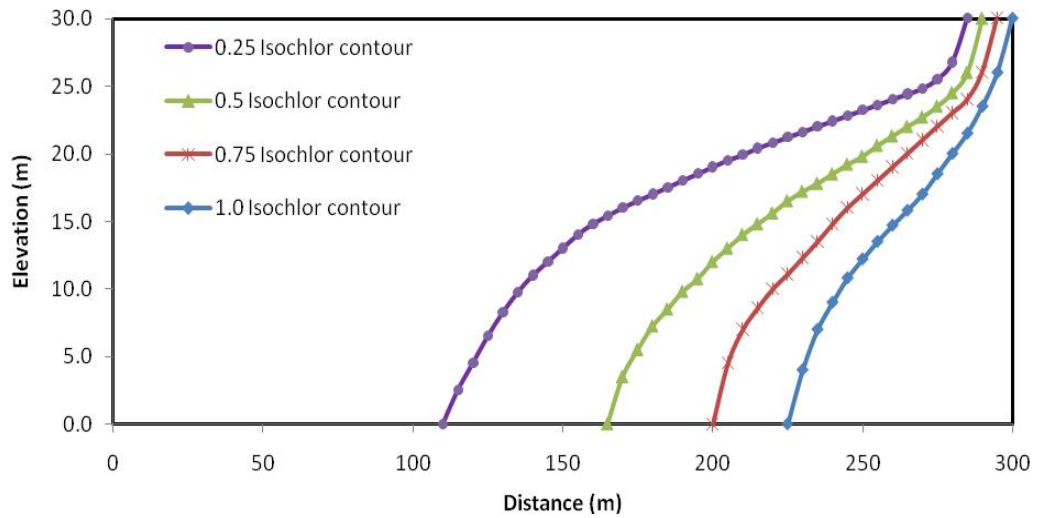


**Figure 6.11** Isochlor counters in Biscayne aquifer, Florida

Potential locations and depths for the abstraction and recharge wells are shown in Figure 6.12.

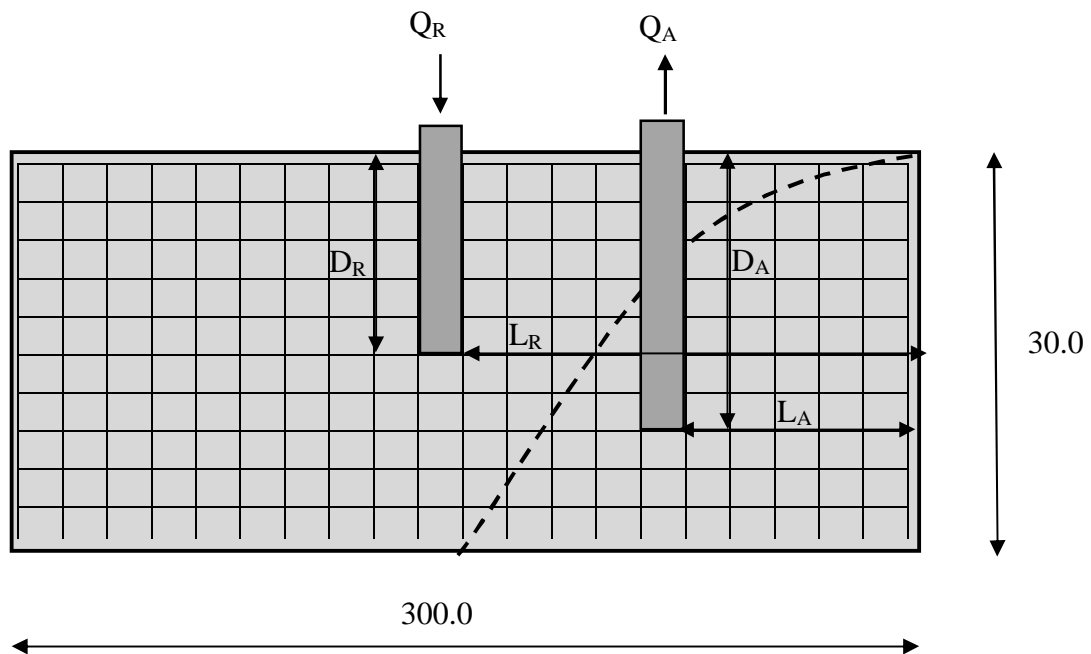


**Figure 6.12** Schematic sketch for potential locations and depths for the abstraction and recharge wells of Biscayne aquifer, Florida

The GA is applied using the following parameters: population size = 10, maximum generations =100, the values of crossover and mutation probabilities are 0.7 and 0.03 respectively. The values of the costs used in this example according to the literature are presented in Table 6.2. The upper and lower limits for depths, locations and abstraction/recharge rates are listed in Table 6.4.

**Table 6.4** Summary of the upper and lower of constraints for Biscayne aquifer, Florida

Parameter	Value
$Q_{\min}$ (m <sup>3</sup> /s)	0.0
$Q_{\max}$ (m <sup>3</sup> /s)	0.01
$L_{\min}$ (m)	0.0
$L_{\max}$ (m)	300.0
$D_{\min}$ (m)	0.0
$D_{\max}$ (m)	30.0

The simulation model is applied with the initial and boundary conditions to compute pressure head and salt concentration at every node in the interred domain. The results of the finite element simulation (with no optimization) are shown Figure 6.11 in the form of isochlor contours in the aquifer. The simulation-optimization model is then applied to minimize the costs and obtain the optimal depths, locations and abstraction/recharge rates for the wells. The final optimized concentrations distribution for this example is summarized in Figure 6.13. The results obtained from the simulation-optimization model for the three management models are presented in Table 6.5 and discussed in the following sections.

### ***6.6.2.1 Application of management model 1***

Management model 1 is applied to minimize the total construction and operation costs of using abstraction wells. The optimization problem for management model 1 aims to determine the optimum depth, location, abstraction rate to minimize the cost of constructing and operating the system. The optimized well depth, location and abstraction rate in addition to the optimal cost are listed in Table 6.5. Using management model 1, the value of total cost is determined as \$0.25 million per year. The optimal depth is 24 m, the optimal location is 66 m from the sea shore and the optimal abstraction rate is 0.008 (m<sup>3</sup>/sec) while the total concentration in the aquifer has reduced from 305 to 248 (mg/l).

### ***6.6.2.2 Application of management model 2***

The objective of the second management model is to determine the optimal well location, depth and recharge rate to minimize the total construction and operation costs of using recharge wells to control saltwater intrusion. The optimized well depth, location and recharge rate and the optimal total cost are presented in Table 6.5. Using management model 2 the total cost is \$0.5 million per year. The optimal depth is 24 m, the optimal location is 156 m from the sea shore and the optimal abstraction rate is 0.009 (m<sup>3</sup>/sec) while the total concentration in the aquifer has reduced from 305 to 255 (mg/l).

### ***6.6.2.3 Application of management model 3***

The management model 3 which combines models 1 and 2 aims to minimize the total construction and operation costs of using both abstraction and recharge wells to control saltwater intrusion. The optimized well depths, locations and abstraction and recharge rates and the optimal total cost are listed in Table 6.5. Using management model 3 the total cost is \$0.13 million per year. The optimal depths for abstraction and recharge wells are 24 and 18 m, respectively. The optimal locations for abstraction and recharge wells are 72 and 186 m respectively from the sea shore and the optimal rates for abstraction and recharge wells are 0.005 and 0.002 (m<sup>3</sup>/sec), respectively while the total concentration in the aquifer has reduced from 305 to 227 (mg/l).

**Table 6.5** Summary of the results obtained from the simulation-optimization models for Biscayne aquifer, Florida

Model	Norm. L	Norm. D	Q (m <sup>3</sup> /s)	Norm. C	Q (Mm <sup>3</sup> /year)	F (cost \$/year)
No management model	No abstraction or recharge wells have been used			305		
Abstraction well A	66	24	0.008	248	0.252	0.25 E+6
Recharge well R	156	24	0.009	255	0.283	0.5 E+6
Abstraction and Recharge well A	72	24	0.005	227	0.158	0.13 E+6
R	186	18	0.002	227	0.063	

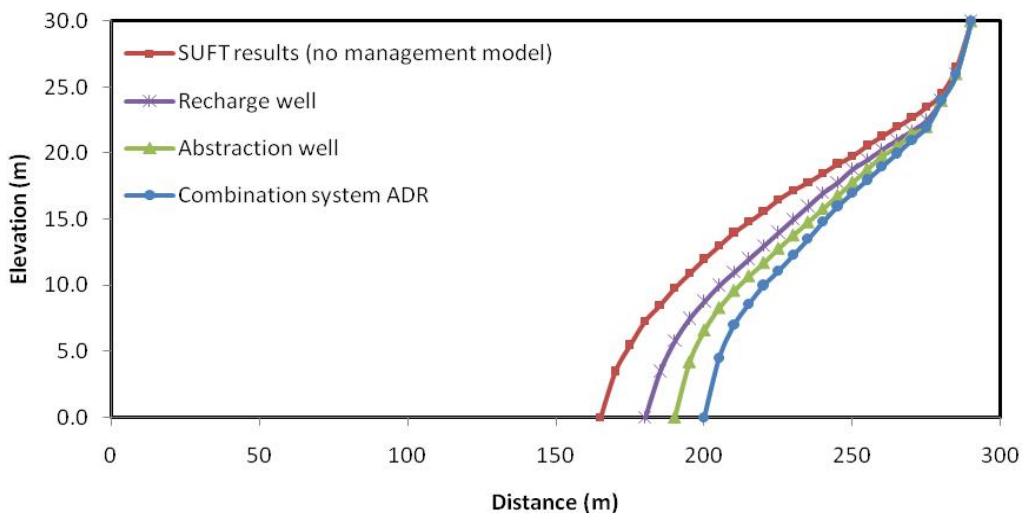


**Figure 6.13** 0.5 isochlor distribution from simulation-optimization models for Biscayne aquifer, Florida

### 6.6.2.4 Discussion

In this case the application of the simulation-optimization model to control saltwater intrusion to a real world case study using the three management models is presented. The results are presented in Table 6.5. Comparisons between total costs, total salt concentrations in the aquifer and total abstraction/recharge rates are presented in Figures 6.14, 6.15 and 6.16.

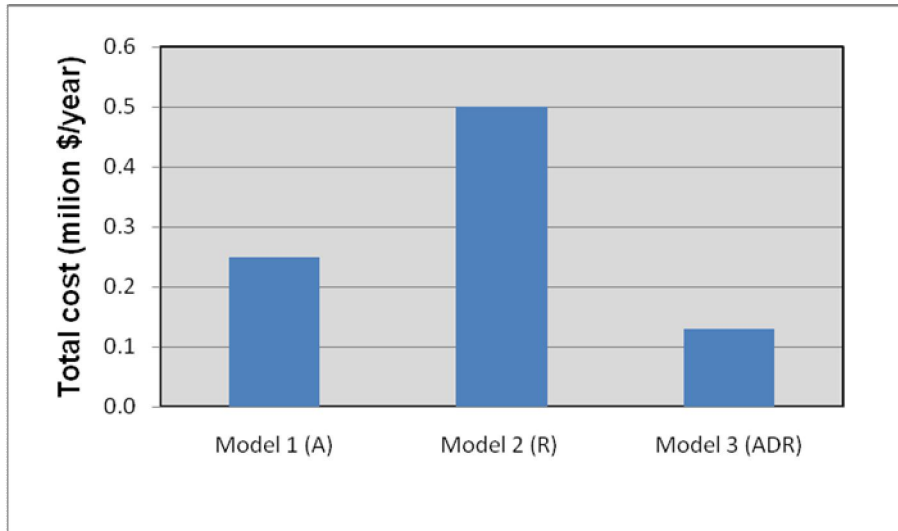


**Figure 6.14** Comparison between total costs of model 1, 2 and 3 of Biscayne aquifer, Florida

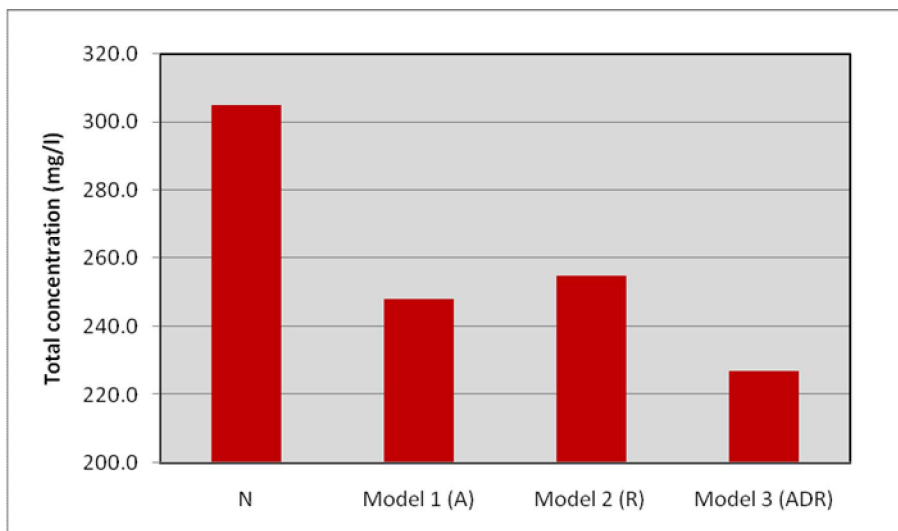


**Figure 6.15** Comparison between total salt concentrations remaining in the aquifer of model 1, 2 and 3 for Biscayne aquifer, Florida



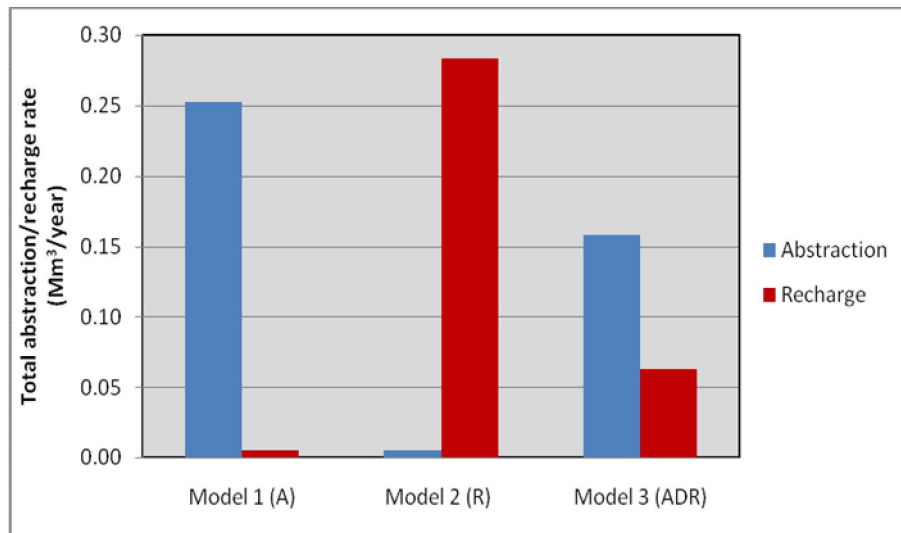


**Figure 6.16** Comparison between total abstraction/recharge rates of model 1, 2 and 3 for Biscayne aquifer, Florida

From the above comparison charts it can be noticed that using the proposed system ADR in model 3 reduced salt concentration from 305 to 227 (mg/l) which is less than the amount of salt concentration reduced by model 1 (248 mg/l) or 2 (255mg/l) furthermore, using ADR requires abstraction of 0.158 (Mm<sup>3</sup>/year) of saline water and recharge of 0.063 (Mm<sup>3</sup>/year) of fresh water which is less than the amount of water abstracted using model 1 (0.252 Mm<sup>3</sup>/year) or recharged using model (0.283 Mm<sup>3</sup>/year). It is also gives the lowest cost (\$0.13 million per year) compared with the cost for recharge (\$0.5 million per year) and abstraction (\$0.25 million per year) which represents 50% of the abstraction costs and 25% of the recharge costs.

## 6.7 Summary

A simulation-optimization model was developed to study the control of seawater intrusion in coastal aquifers using three management models; abstraction of brackish water, recharge of fresh water and combination of abstraction and recharge. The developed model was applied to evaluate the three management scenarios to control seawater intrusion in coastal aquifers and to determine the optimal locations, depths and rates of abstraction and/or recharge wells in addition to minimizing the construction and operation costs. The

efficiencies of the proposed management scenarios have been examined and compared. The results show that all three scenarios could be effective in controlling seawater intrusion but using model 3; i.e., ADR methodology, resulted in the lowest cost and salt concentration in aquifers and maximum movement of freshwater/saline water interface towards the sea. The results also show that for the case studies considered in this work, the amount of abstracted and treated water is three times the amount required for recharge; therefore the remaining treated water can be used directly for different proposes. The developed model is an effective tool to control seawater intrusion in coastal aquifers and can be applied in areas where there is a risk of seawater intrusion. The application of ADR methodology through the third model appears to be more efficient and more practical, since it is a cost-effective method to control seawater intrusion. Therefore, it can be used for sustainable development of water resources in coastal areas where it provides a new source of water that comes from treated water.

## **Effect of climate change and sea level rise on saltwater intrusion**

### ***7.1 Introduction***

Climate change is increasing at an alarming rate due to human activities and natural processes. Scientists worry that human societies and natural ecosystems might not adapt to rapid climate change. Majority of climatologists believe that human activities are responsible for most of the climate change by increasing the emission of greenhouse gases that increase the temperature of the earth. A small number of scientists state that natural processes could have caused global warming. Those processes include increase in the energy emitted by the sun. But the vast majority of climatologists believe that increases in the sun's energy have contributed only slightly to recent warming. Continued climate change might, over centuries, melt large amounts of ice from glaciers, caps and sheet. As a result, the sea levels would rise throughout the world. Many coastal areas would experience flooding, erosion, loss of wetlands, and entry of seawater into fresh groundwater aquifers. High sea levels would submerge some coastal cities, small island nations, and other inhabited regions.

Climate change, sea level rise and saltwater intrusion present the future challenge of water resources management in coastal areas. Scientists expect that the climate change will continue over the current century in spite of the international efforts to reduce greenhouse gases emission. This change is expected to exacerbate already existing environmental problems in many countries. In particular, coastal areas all over the world are expected to suffer from impacts of sea level rise (SLR), as well as other impacts, in addition to already existing problems of coastal erosion, subsidence, pollution, land use pressure and deterioration of ecosystems. Global mean sea-level rise has been estimated between 1.0-2.0 mm/yr during the last century (IPCC, 1996). Future sea-level rise due to atmospheric climate change is expected to occur at a rate greatly exceeding that of the recent past. By 2100 it is expected that the rise in sea levels would be between 20 cm to 88 cm (IPCC, 2001).

The most important direct effects of sea level rise on coastal regions are; coastal erosion, shoreline inundation and saltwater intrusion into coastal aquifers. The problem is quite serious and presents the present and future challenges for all interested in this subject including; hydrologists, environmental engineers and civil/geotechnical engineers. The solution of this problem is not easy and requires many organizations all over the world to work together to face the incoming disaster. This chapter reviews the causes of climate change and their effects on coastal areas. Also, the effects of sea level rise on saltwater intrusion and methods of controlling erosion, inundation and saltwater intrusion are discussed. The final section of the chapter presents the application of the developed model (SUFT) to study the effects of likely climate change and sea level rise on saltwater intrusion in coastal aquifers.

## ***7.2 Climate change***

Climate change is a result of natural and/or man-made activities. The average temperature of the globe has changed over the past century due to the increase in concentrations of greenhouse gases mainly carbon dioxide (CO<sub>2</sub>), nitrous oxide (N<sub>2</sub>O) and methane (CH<sub>4</sub>). The main human activities that contribute to global warming are the burning of fossil fuels such as coal, oil, and natural gas. Most of the burning occurs in automobiles, in factories, and electric power plants that provide energy for houses and office buildings. The burning of fossil fuels creates greenhouse gases that slow the escape of heat to space. Greenhouse gases allow solar radiation to pass through the atmosphere to the earth surface, but they intercept and store the infrared radiation emitted from the earth surface. This leads to warming of the atmosphere. This phenomenon is known as global warming which is considered the main cause of climate change. The increase in concentration of greenhouse gases is associated with a corresponding increase in the average global temperature which is expected to be higher by the end of the current century. Measurements showed that the average temperature of the earth has risen by 0.5-0.7° C, during the last century. A significant increase in the concentration of greenhouse gases is expected in the current century. Studies indicated an increase of average global temperature of the earth by 1.4-5.8° C by the end of this century.

Figure 7.1 shows different scenarios for estimating the future change in global temperature of earth from 1900 to 2100 (IPCC, 2001).

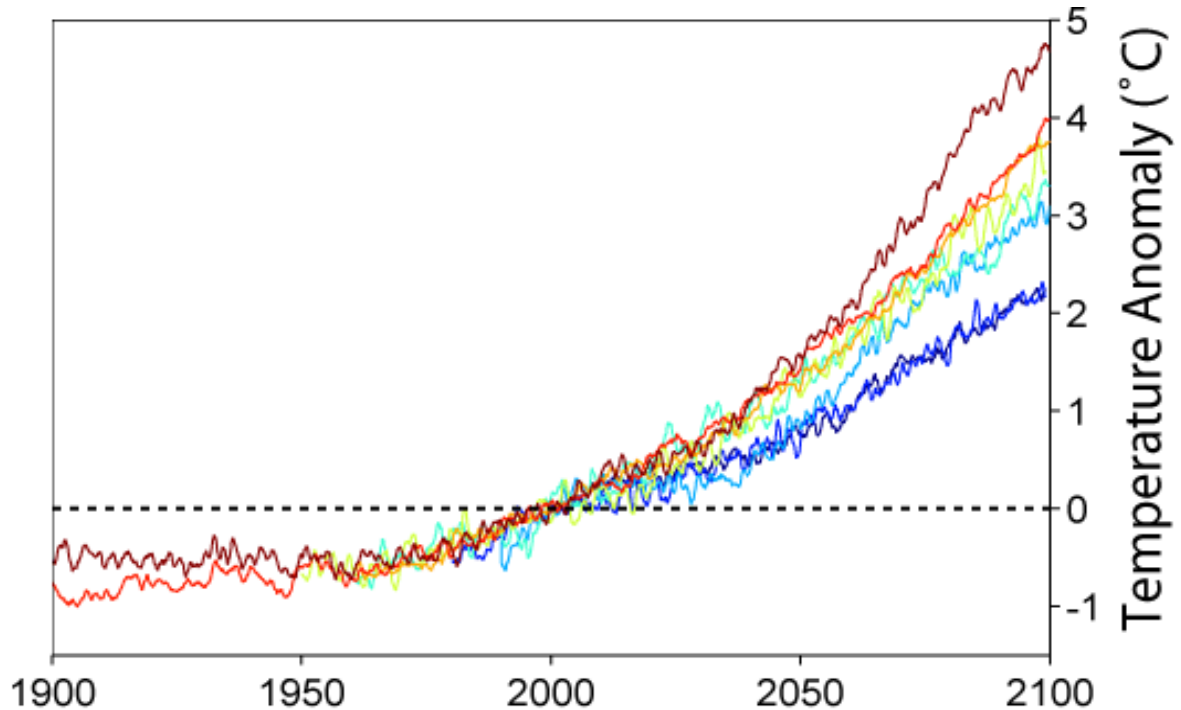


**Figure 7.1** Scenarios for estimating average global temperature of earth (IPCC, 2001)

Continued global warming could have many damaging effects. It might harm plants and animals that live in the sea. It could also force animals and plants on land to move to new habitats. Weather patterns could change, causing flooding, drought, and an increase in damaging storms. Global warming could melt enough polar ice to raise the sea level. In certain parts of the world, human disease could spread and crop yields could decline. Global warming and climate change have a serious consequence on hydrologic cycle components as it changes the quantity and quality of the components in space, time and frequently domain (Sherif et al, 1999). Therefore, the increase of greenhouse gases emission should be controlled to protect the earth and its inhabitants from these serious changes.

### ***7.3 Sea level rise***

Residents of coastal areas are becoming increasingly concerned about the effects of climate change as well as sea level rise because of possible higher rates of erosion, inundation and saltwater intrusion. Climate change also has a great effect on coastal aquifers which are subject to saltwater intrusion because it leads to the increase of mean sea level which has a direct effect on saltwater intrusion. The increase in global temperature will warm the land surface, oceans and seas. This warming will decrease the atmospheric pressure which will in turn lead to the increase of water level in the oceans and seas. The rise in seas and oceans water levels is for a number of reasons including:

- 1- Thermal expansion of oceans and seas,
- 2- Melting of glaciers and ice caps and
- 3- Greenland and Antarctic ice sheets melting.

Climate change has already caused changes in the sea levels during the last decades. Computer models help climatologists to analyze past climate changes and predict future changes. Scientists use climate models to describe how various factors affect the temperature of Earth's surface. Such models help climatologists to estimate the future changes in temperature and sea levels. The global mean sea-level has risen by 10-20 cm over the past century as estimated by Intergovernmental Panel of Climate Change (IPCC 1996). Future sea-level rise is expected to occur at a rate greatly exceeding that of the recent past; the predicted increase in the sea level rise is in the range of 20-88 cm within the next 100 years (IPCC 2001). A number of studies have been carried out to estimate the future sea level changes based on past sea level changes due to thermal expansion, glaciers and ice caps and Greenland and Antarctic ice sheets melting. Figure 7.2 shows the estimated global average sea level rise between 1990 and 2100 (IPCC, 2001).

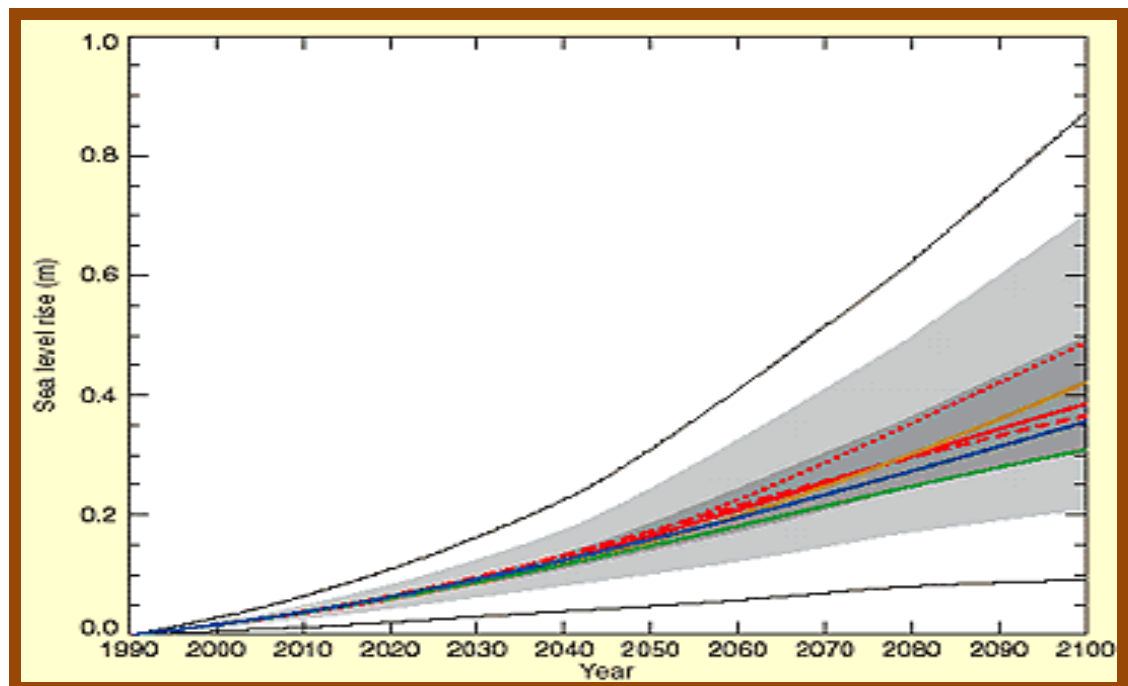


**Figure 7.2** Scenarios for estimating global average sea level rise (IPCC, 2001).

### ***7.3.1 Effects of sea level rise on coastal areas***

Continued climate change and sea level rise could have many effects on the coastal areas on the long term including (Canning, 2001):

- 1- increase of coastal erosion,
- 2- coastal inundation of unprotected low lying areas,
- 3- subsidence of shore cities which lie in low land,
- 4- change in the tidal prism,
- 5- seawater intrusion,
- 6- coastal water table rise which has led to;
  - agricultural soil saturation,
  - long duration of flooding,
  - impendence of on-site sewage disposal and
  - corrosion of underground pipes and tanks.

The coastal erosion may lead to partial or full submergence of some coastal cities which lie in low land. Sea level rise also threatens the groundwater storage in coastal aquifers because the sea level rise imposes an additional pressure head at the seaside which helps to move saltwater into the aquifer. The rise in sea levels will shift the mixing zone further inland. The extraction wells that are located in fresh groundwater may then be located in saline water as shown in Figure 7.3 and consequently, the abstraction rates of these wells may be reduced or the wells may be abandoned. This is considered one of the most serious impacts of sea level rise on coastal regions. In addition, crops will suffer from salt damage due to the increased salinity of the soil, which could have serious economic effects.

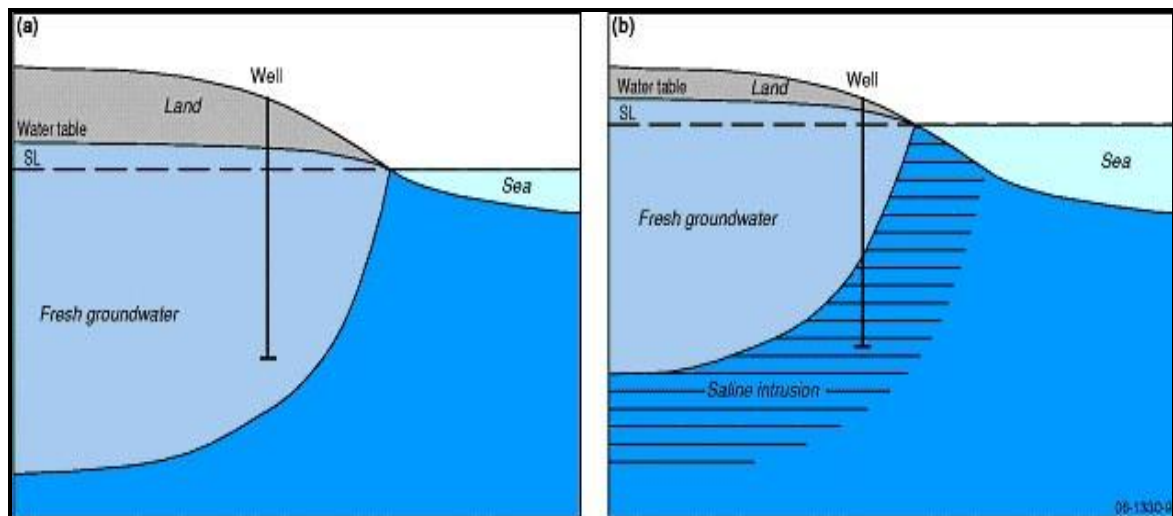


**Figure 7.3** Effect of sea level rise on abstraction wells

The effects of climate change and sea level rise on saltwater intrusion in the long term should be considered and controlled because few centimeters rise in sea levels could have a great effect on saltwater intrusion and help to shift the transition zone more inland. Some investigations have been done to study the likely effect of climate change and sea level rise on saltwater intrusion in different locations of the world. For example, in the Nile Delta aquifer in Egypt investigations have shown that saltwater intrusion is very vulnerable to climate change and sea level rise. It is expected that some shore cities will be submerged and the saltwater will intrude kilometers inside the Delta by the end of the current century due to the increase in the Mediterranean Sea level. Also saltwater intrusion has serious



effects on coastal cities as it leads to the contamination and depletion of groundwater. For example, in Gaza strip the main source of water is groundwater and the population growth rate is excessively high. The shortage of water has resulted in over-pumping from the aquifer which has led to dramatic increase in the intrusion of saltwater. With the continuous population growth and over-pumping it is expected that during the next decade the aquifer will be completely polluted by saline water and inhabitants should find a new source of water. Therefore, the control of saltwater intrusion has become essential in these areas in order to protect the groundwater resources. The next section discusses the effects of sea level rise on erosion, inundation and saltwater intrusion.

### ***7.3.1.1 Erosion and inundation***

Climate change and sea level rise may result in extensive shore erosion and shoreline inundation. Sand transport on beaches is controlled by wave action which can move sand in both onshore and offshore directions. Waves break the beach profile and cut the beach face back, depositing the sand offshore. Thus, the erosion of beaches during an essentially static sea level is caused by waves carrying sand offshore. With a significant rise in sea levels there will be an acceleration of beach erosion because:

- 1- The higher water level allows waves to act further up on the beach which results in more erosion;
- 2- At higher sea levels, waves can get closer to the shore before breaking and cause increased erosion;
- 3- Deeper water also decreases wave refraction and thus increases the capacity of alongshore transport;
- 4- Higher sea levels could change the source or sediments by decreasing river transport to the sea as the river mouth is flooded.

A rise of sea levels will cause coastal inundation, an effect that is difficult to separate from the effect of shore erosion where erosion is occurring. At the water line, typical beach profile have a slope that can vary from 1:5 to 1:100, so a 1 cm sea level rise can move the shoreline from 5 to 100 cm inland in addition to landward movement of the profile owing to erosion. Deeper coastal water caused by sea level rise will increase the tidal range along

the coast, which will increase the effects on inundation. Also, submergence of low level cities will increase with the increase in sea levels in different locations of the world.

### ***7.3.1.2 Saltwater intrusion***

Saltwater intrusion is a major problem in coastal regions as it increases the salinity of groundwater and water may become unsuitable for human use. Salinization of groundwater is considered a special category of pollution that threatens groundwater resources, because mixing a small quantity of saltwater in the groundwater makes freshwater unsuitable and can result in abandonment of freshwater supply. High population growth rate in the coastal regions where about two third of the world population live has increased water demand; this has lead to excessive abstraction from the aquifers which has resulted in the migration of saltwater towards the aquifers. Over-pumping results in decrease of water table or piezometric head and hence more intrusion will occur. Furthermore, the rise in sea levels accelerates the saltwater intrusion into the aquifers because it imposes an additional pressure head on the sea side of the aquifer.

The relationship between sea level rise and saltwater intrusion can be approximately estimated according to the Ghyben-Herzberg relationship, which states that the depth of interface below mean sea level equals to 40 times the height of the potentiometric surface above the mean sea level. Therefore, a one meter increase in sea level rise could cause a 40 m reduction of freshwater thickness as shown in Figure 7.4. With the impact of sea level rise combined with over-pumping the problem becomes very serious and requires practical measures to protect the available water resources from pollution.

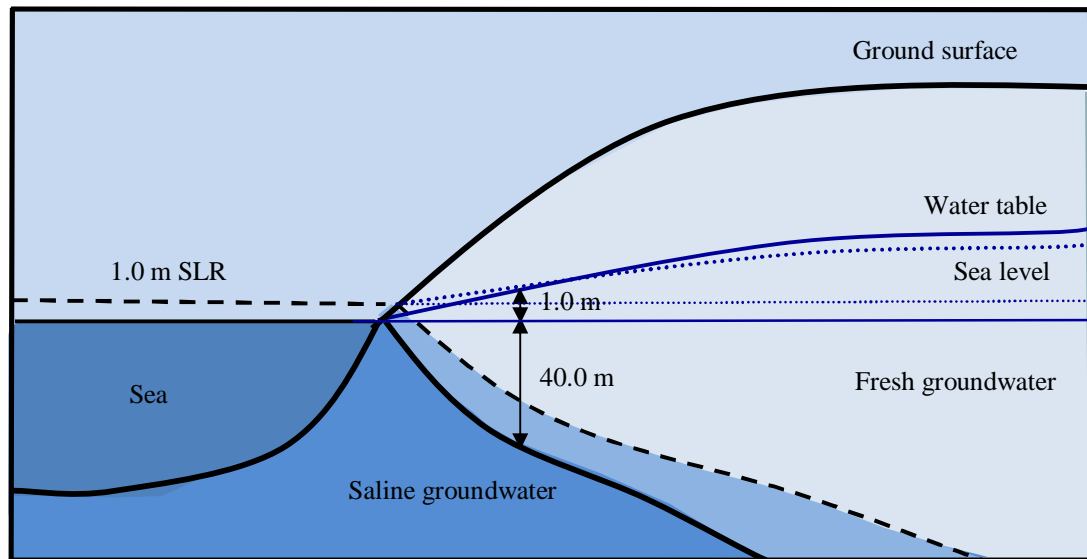


**Figure 7.4** The relationship between sea level rise and saltwater intrusion

### ***7.3.2 Methods of controlling the effects of sea level rise on coastal areas***

This section presents specific methods of controlling coastal erosion, shoreline inundation and saltwater intrusion, which is caused by sea level rise.

#### ***7.3.2.1 Control of erosion and inundation***

To prevent shoreline erosion and inundation one must be keep waves from attacking the shore by intersecting them seaward of the surf zone or by armoring that portion of the shore profile where erosion occurs. Erosion can be prevented by reducing the ability of waves to transport sand or by increasing the supply of sand available for transport by waves so that the sand is not removed from the beach to satisfy the sand transport capacity. In coastal regions, inundation caused by the rise in sea level and the increase in tide range can be prevented by constructing a water-tight continuous structure such as dike or retaining structure. Increased wave attack owing to higher water levels or water attack at higher elevations because of the raised sea levels will require many coastal structures to be stabilized to suite the new levels of water. Higher sea levels will diminish the functionality

of certain structures such as breakwaters that become more easily overtopped by waves. Such structures would have to be raised to maintain their effectiveness.

Sorenson et al. (2001) presented an overview of coastal engineering methods to control shore erosion and inundation due to sea level rise. A number of methods can be employed to control the effects of coastal erosion and shoreline inundation. These methods can be classified as hard, soft and miscellaneous. Hard structures include; offshore breakwaters, perched beach, groins, revetments, dikes, floodwalls, seawalls, bulkheads and dams. Soft structures include; artificial beach nourishment, dune building and marsh building. Miscellaneous responses include; elevation of structure and strengthening of the existing structure. These control methods should consider economical, political and environmental impacts on shore areas.

### ***7.3.2.2 Control of saltwater intrusion***

Over-pumping causes fall in groundwater levels below the mean sea levels in some areas. Also, sea level rise accelerates the intrusion of saline water. Several control methods can be used to prevent or retard saltwater intrusion into coastal aquifers such as; reduction of abstraction from the aquifers, moving wells further inland, use of subsurface barriers to prevent the inflow of seawater into the aquifers, increase the recharge to the aquifers either by surface spread or injection wells to increase the volume of fresh water that retard the intrusion of saltwater, abstraction of saline water to reduce the volume of saltwater or use a combination of these methods. The selection of the appropriate method to control saltwater intrusion should consider technical, economical and environmental aspects and sustainable development of water resources in coastal areas (Abd-Elhamid and Javadi, 2010). Different methods of controlling saltwater intrusion including a new methodology ADR presented in this research were discussed in details in chapter 2.

### ***7.4 Simulation of saltwater intrusion considering sea level rise***

The majority of the models developed to simulate and control saltwater intrusion do not consider the effects of climate change and sea level rise in the simulation process. Only, few researchers have considered the effects of climate change and sea level rise on saltwater intrusion. EL Raey (1999) carried out an assessment of vulnerability and expected socioeconomic losses in the Nile Delta coasts due to the impact of sea level rise of 50 cm by 2100, in particular in Alexandria, Port Said, Egypt. Sherif and Singh (1999) investigated the effects of likely climate change on seawater intrusion in the Nile Delta aquifer, Egypt, and Madras aquifer, India. The study found that seawater intrusion is vulnerable to climate change and sea level rise. Canning (2001) presented the certainties and uncertainties of climate variability for Washington's marine water, and suggested some areas of management concern and research need. He has also presented a review to the historical sea level rise due to climate change in Puget Sound. Oude-Essink and Schaars (2002) developed a model to simulate groundwater flow, heat and salinity distribution, and seepage and salt load flux to the surface water system. The model was used to assess the effects of future development such as climate change, sea level rise, land subsidence as well as human activities on qualitative and quantitative aspects of the groundwater system. Tiruneh and Motz (2004) investigated the effect of sea level rise on the freshwater-saltwater interface, using SEWAT. They coupled the impact of pumping with the rise in sea levels and recharge based on selected climate change scenarios.

Also some models were developed to study the effects of sea level variations due to tides on saltwater intrusion. Chen and Hsu (2004) developed a two-dimensional time-independent finite difference model to simulate the tidal effects on the intrusion of seawater in confined and unconfined aquifers. Mulrennan and Woodroffe (1998) examined the pattern and process of saltwater intrusion into the coastal plains of the lower Mary River, northern Territory, Australia, due to the effect of tides. Lazar et al. (2004) measured and characterized the fresh water-saline water interface fluctuations by sea tides, by measurements of electrical conductivity taken across the interface.

Sonnenborg et al. (2010) presented an integrated and distributed hydrological model for a coastal catchment on the island of Zealand, Denmark. They applied different scenarios for different mean sea level rise in the range from 0.5-1.0 m. The rising seawater level resulted in inflow of saltwater to the lake especially during late summer and autumn where the lake water level is relatively low and storm events results in high sea levels. The study showed that adaptation measures are needed already at a sea level rise of approximately 0.5 m if not saltwater inflow should destroy the lake as a fresh water resource. Payne (2010) developed a three dimensional finite element model for variable-density flow and solute-transport to simulate different rates of sea-level rise and variation in onshore freshwater recharge in the Hilton Head Island, South Carolina, USA. The results for this case showed that the greatest effect on the existing saltwater plume occurred from reducing recharge and suggested recharge may be a more important consideration in saltwater intrusion management than estimated rates of sea level rise.

### ***7.5 Application of SUFT to investigate the effect of sea level rise***

In this work, the effect of sea level rise on saltwater intrusion is simulated using a density-dependant finite element model. The development, validation and application of the transient variable-density finite element model for the simulation of fluid flow and solute transport in saturated/unsaturated soils was presented in chapters 3, 4 and 5. This part presents the prediction of the intrusion of saline water in coastal aquifers due to likely climate change and sea level rise. For the purpose of numerical modelling, a future rate of sea level rise from 2000 to 2100 is considered based of the average measured rate of rise (1 cm/year) which represents a moderate expectation (IPCC, 2001). To investigate the effect of sea level rise on saltwater intrusion the developed model is applied to a hypothetical case study (Henry's problem) and two real world cases studies in Biscayne aquifer, Florida, USA and Gaza aquifer, Palestine.

#### ***7.5.1 Case (1): A hypothetical cases study***

This case presents a hypothetical confined coastal aquifer which is developed based on the well-known Henry's problem (Henry, 1964). The aquifer is homogeneous and an isotropic.

The aquifer is subjected to seawater intrusion along the sea face boundary and a uniformly distributed lateral flow along the inland face. The geometry and initial and boundary conditions and simulation parameters were presented in chapter 5. The dimensions of the aquifer are 200 m (length), 100 m (depth). The domain is discretized using two dimensional grid ( $\Delta X = \Delta Y = 10\text{m}$ ). The total number of elements is 200 elements and the total number of nodes is 661 nodes. The flow boundary conditions include impermeable boundaries along the top and the bottom of the domain. Hydrostatic pressure is assumed along the vertical boundaries of the sea side and land side. At the inland side the concentration is zero (freshwater condition), while at the coastal side the relative concentration of seawater is imposed for a height 80 m from the aquifer bottom. Initial conditions are zero heads and zero concentrations throughout the domain. The results of simulation using the SUFT code, without consideration of sea level rise (SLR) are shown Figure 7.5 which shows 0.5 isochlor in the aquifer.

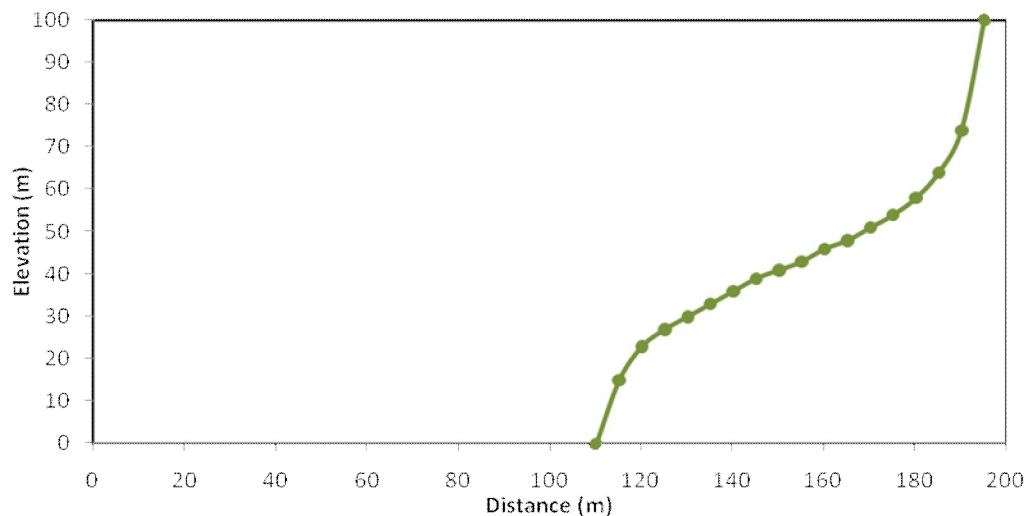


**Figure 7.5** 0.5 isochlor for the hypothetical case study (no SLR)

The change in seawater levels are incorporated into the simulation model by specifying an annual increase of 1 cm/year in the mean sea level. This rate implies a total increase of 100 cm by 2100. These simulations were carried out to assess the effects of the changing saltwater boundary condition on water flow and the position of the fresh water/saltwater interface in response to sea level rise. The saltwater intrusion in the aquifer is simulated under different seawater levels; no sea level rise (static condition) and sea level rise after

25, 50, 75 and 100 years. The application of the simulation model to the current case has been done on two steps. In the first step, the simulation model is applied with the initial and boundary conditions to compute heads and salt concentrations at every node in the interred domain with no change in seawater level. The distribution of salt concentrations without changes in sea level is shown in Figure 7.5 which shows the 0.5 isochlor contour before changing the water level on the sea side. In the second step, the simulation model is applied to simulate the effect of sea level rise on water levels and the position and movement of the fresh water/saltwater interface. The new position of fresh water/saltwater interface is determined by a change in sea level by 1 cm/year from 2000 to 2100.

The results obtained from the simulation for the two steps are presented in Figures 7.5 and 7.6. In case 1 (no SLR), the 0.5 isochlor contour moved inland by 90 m measured at the bottom boundary from the sea side as shown in Figure 7.5. In case 2 (SLR changing by 1 cm/year), the change in sea level affected the position of fresh water/saltwater interface and moved the transition zone more inland as shown in Figure 7.6. The 0.5 isochlor contour moved inland by 92 m after 25 years, 94 m after 50 year, 96 m after 75 year and 98 m after 100 year. The results indicate that the change of sea level has a significant effect on the position of fresh water/saline water interface as shown in Figure 7.6.

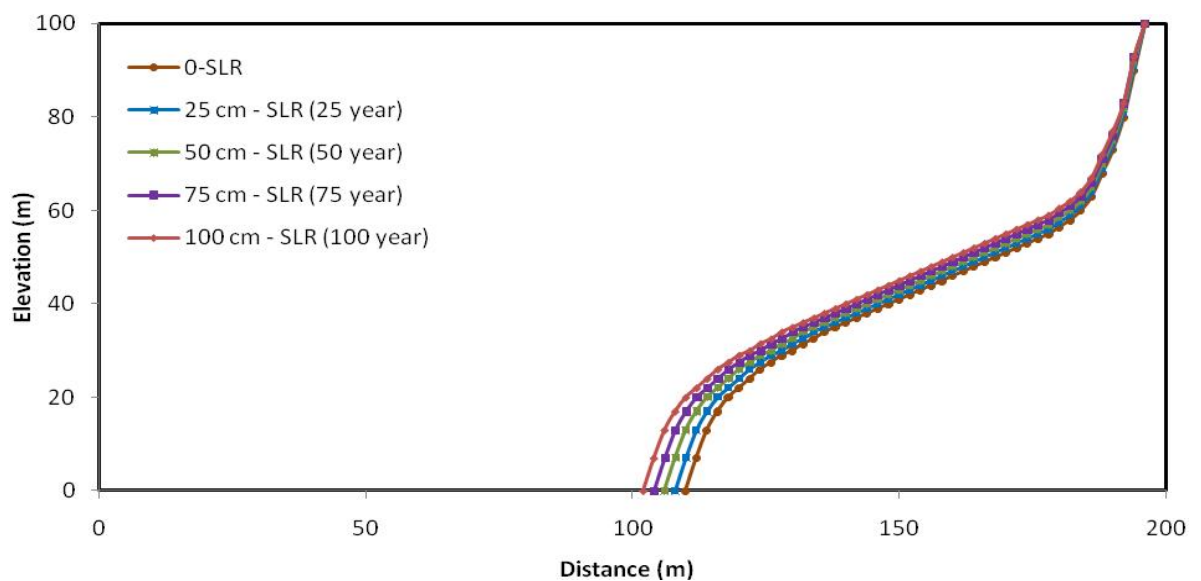


**Figure 7.6** 0.5 isochlor for the hypothetical case study (with SLR)



### 7.5.2 Case (2): Biscayne aquifer, Florida, USA

In this case the developed simulation model is applied to a real case study to simulate saltwater intrusion in a coastal aquifer considering sea level rise. Also, the effect of lowering water table due to over-pumping is considered. The real world problem is selected from the coastal area of Biscayne aquifer at Coulter area, Florida, USA. The aquifer has an average depth of 30.0 m below mean sea level and width of 300.0 m. The domain is discretized using two dimensional grid ( $\Delta X = \Delta Y = 6$  m). The mesh consists of 250 elements and 861 nodes. The schematic sketch of the Biscayne aquifer at Coulter area and the corresponding boundary conditions were presented in chapter 5. The aquifer is simulated using the developed finite element model and the results of simulation, without changes in sea level are shown in Figure 7.7 in the form of 0.25, 0.5, 0.75 and 1.0 isochlor contours.

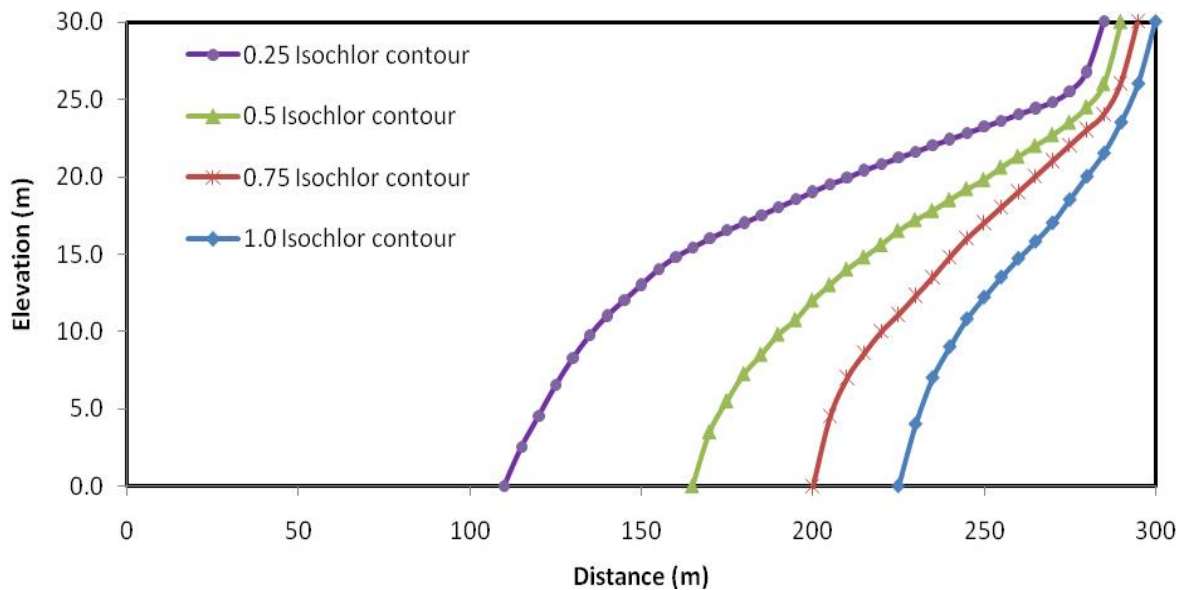


**Figure 7.7** Isochlor contours in Biscayne aquifer, Florida (no SLR)

The change in seawater levels are incorporated into the simulation model by specifying an annual increase of 1 cm/year in the mean sea level as a model boundary condition to assess the effects of SLR on water flow and the position of the fresh water/saltwater interface. The saltwater intrusion in the aquifer is simulated under different seawater levels; no sea level rise (static condition) and sea level rise after 50 and 100 year. The distribution of salt concentrations without changes in sea level is shown in Figure 7.7.

The model is then applied to simulate the effect of sea level rise on the position and movement of the fresh water/saltwater interface. The new position of fresh water/saltwater interface is determined by changes in sea level by 50 and 100 cm after 50 and 100 years respectively. The results of the new positions of the contours after 50 and 100 years are shown in Figure 7.8.

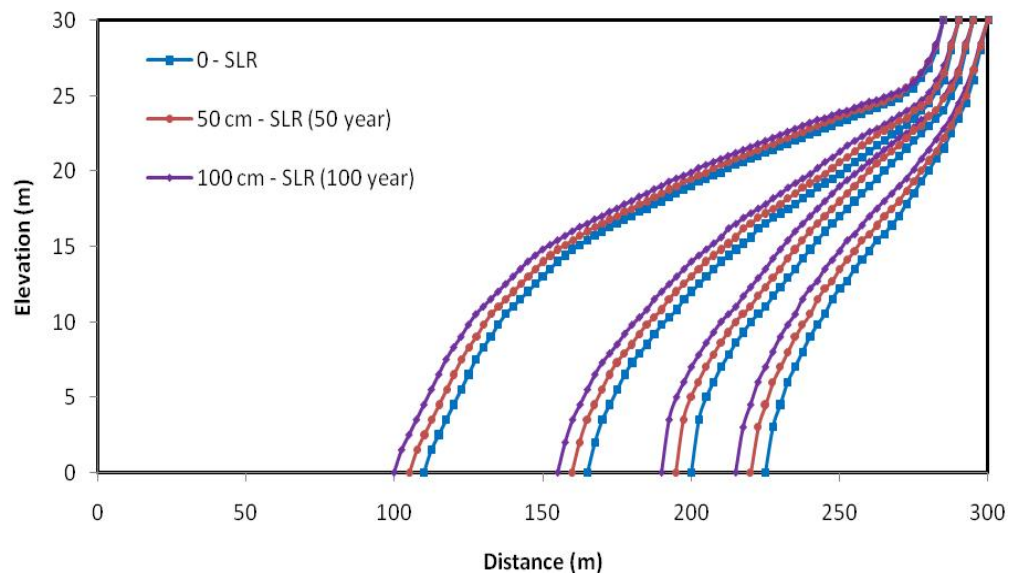


**Figure 7.8** Isochlor contours in Biscayne aquifer, Florida (with SLR, 50, 100 year)

To investigate the combined effect of sea level rise and lowering of water table due to over-pumping on the position of fresh water/saltwater interface, three scenarios are considered. In these scenarios, the shore line is maintained at its current location and the effect of submergence of low lands by seawater is not considered.

**Scenario 1;** The water level in the sea is raised by 100 cm, the groundwater table is kept unchanged and all the other parameters are kept to their original values.

**Scenario 2;** The piezometric head on the land side is lowered by 30 cm to investigate the effect of additional pumping from the aquifer, the water level in the sea is kept unchanged and all the other parameters are kept to their original values.

**Scenario 3;** The water level in the sea is raised by 100 cm, the piezometric head on the land side is lowered by 30 cm and all the other parameters are kept to their original values.

The results of the three scenarios are shown in Figure 7.9 in the form of 0.5 isochlores for the different scenarios after 100 years.

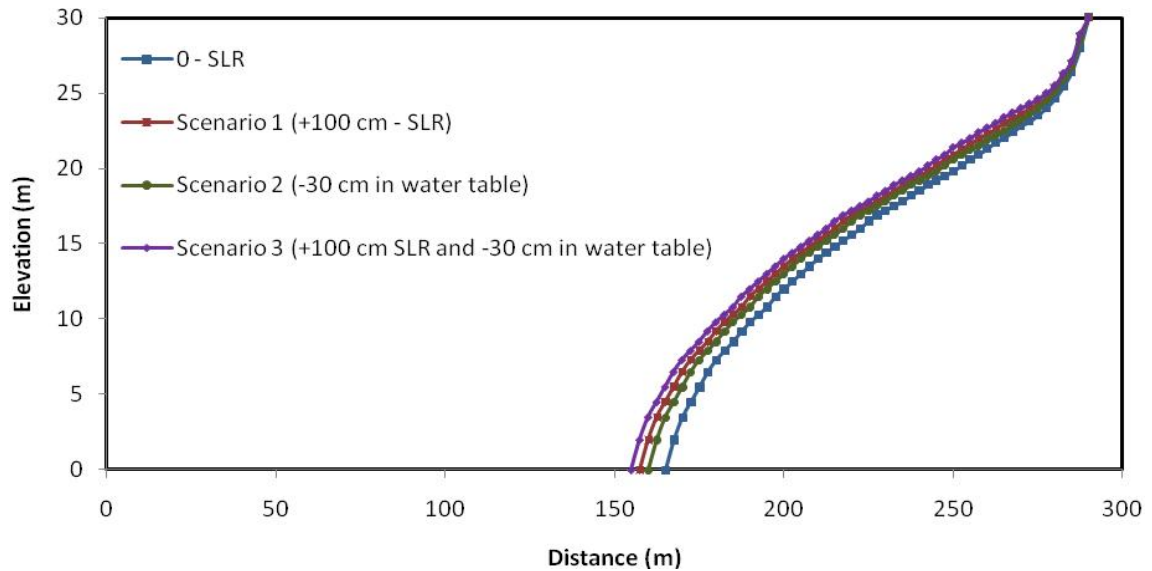


**Figure 7.9** 0.5 Isochlor contours in Biscayne aquifer, Florida using three scenarios

In the case where no sea level rise was considered, the 0.5 isochlor contour moved inland by 135 m measured at the bottom boundary from the sea side as shown in Figure 7.7. In scenario 1 (+100 cm SLR), the 0.5 isochlor contour moved inland by 142 m measured at the bottom boundary from the sea side as shown in Figure 7.9. In this case the sea level rise affected the position of fresh water/saltwater interface. In scenario 2 (-30 cm in water table), the 0.5 isochlor contour moved inland by 139 m. It is shown that lowering the water table or piezometric head on the land side due to additional pumping from the aquifer also affected the position of fresh water/saltwater interface. However, the 0.5 isochlor contour in scenario 3 moved inland by 145 m due to the combination of both sea level rise and lowering water table.

### 7.5.3 Case (3): Gaza Aquifer, Palestine

Another real world problem is addressed in this case, the coastal aquifer of Gaza Strip. The developed model is applied to simulate saltwater intrusion in Gaza aquifer considering the effect of sea level rise and lowering water table due to over-pumping. Three cross sections at Jabalya, Wadi Gaza and Khan Yunis are simulated (Chapter 5) to assess the current situation of seawater intrusion in the aquifer and the results are compared with the results obtained by Qahman and Larabi (2006). The cross section at Jabalya is located in the north of Gaza Strip with a length of 5000 m and average depth of 100 m. The domain is discretized using two dimensional grid ( $\Delta X=50$  and  $\Delta Y=20$  m). The mesh consists of 500 elements and 606 nodes. The boundary conditions applied in this case and model parameters were presented in chapter 5. Gaza aquifer is simulated using the developed finite element model and the results of simulation, without changes in sea level are shown in Figure 7.10. This case was also simulated by Qahman and Larabi (2006) who used the SEWAT code to simulate saltwater intrusion. The extent of seawater wedge along Jabalia is about 3 km presented by isoline 2 (2000 ppm) which intruded inland to a distance of 3.0 km measured along the bottom boundary (see Figure 7.10).

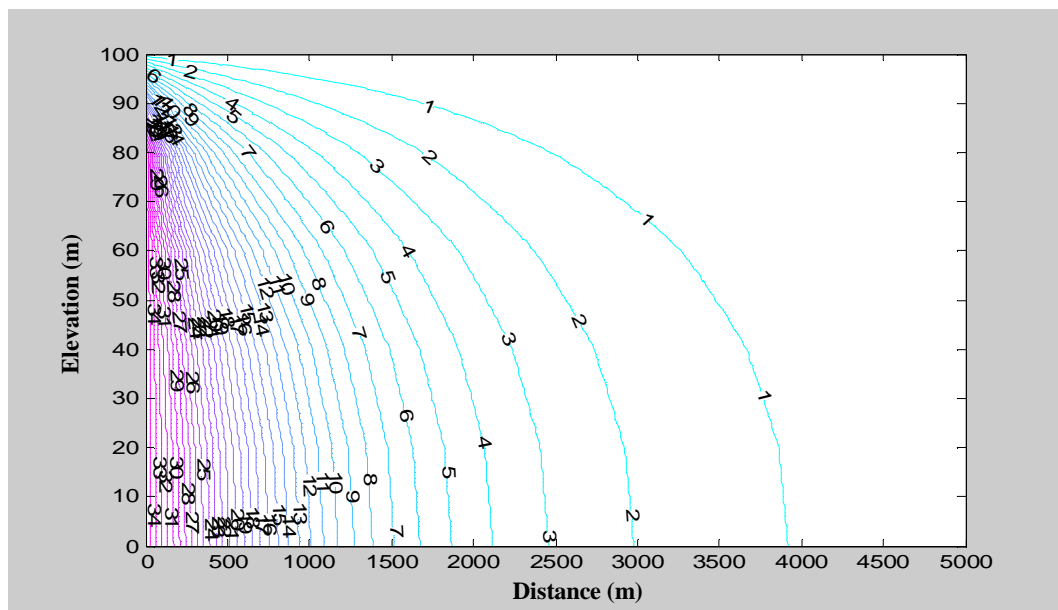


**Figure 7.10** Isolines of TDS concentration ( $\text{kg/m}^3$ ) along Jabalya (no SLR)

In this case the effects of sea level rise and lowering water table due to over-pumping on the position of fresh water/saltwater interface are investigated considering three scenarios. In these scenarios, the shore line is maintained at its current location and the effect of submergence of low lands by seawater is not considered. In the first scenario, the water level in the sea is raised by 100 cm, the free water table is kept unchanged and all other parameters are kept to their original values. In the second scenario, the piezometric head on the land side is lowered by 0.5 m to investigate the effect of additional pumping from the aquifer, the water level in the sea is kept unchanged and all other parameters are kept to their basic values. In the third scenario, the water level in the sea is raised by 100 cm, the piezometric head on the land side is lowered by 0.5 m and all other parameters are kept to their basic values. The results of the three scenarios are shown in Figures 7.11, 7.12 and 7.13.

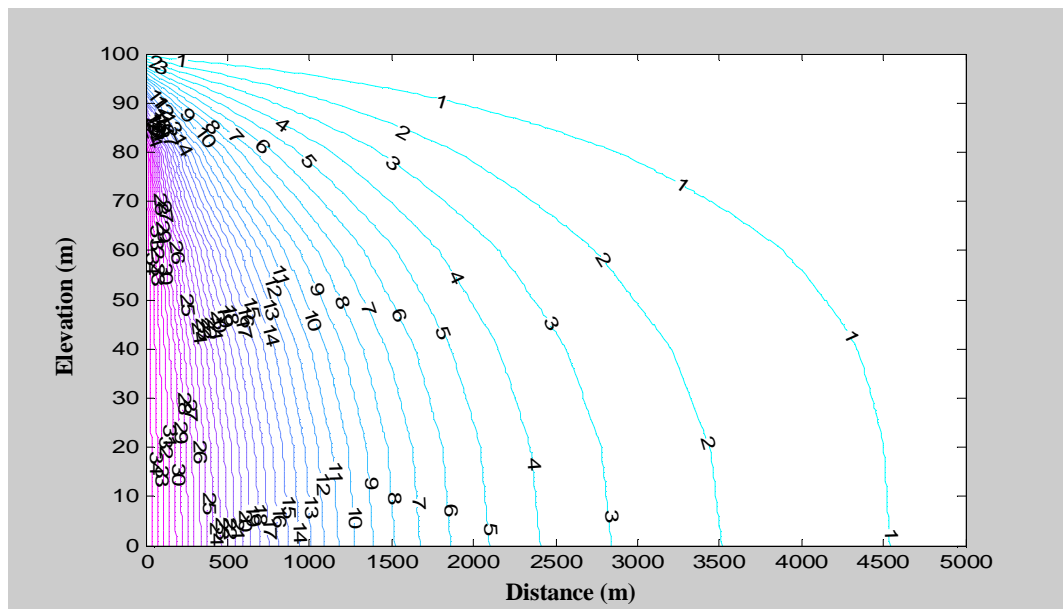


**Figure 7.11** Isolines of TDS concentration ( $\text{kg}/\text{m}^3$ ) along Jabalya (Scenario 1)

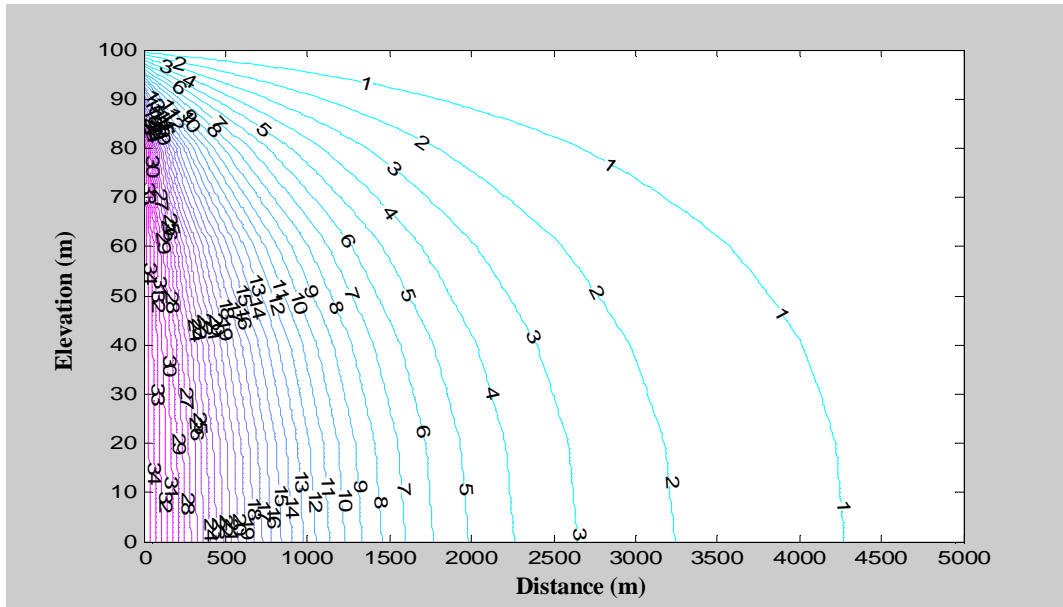


Figure 7.12 Isolines of TDS concentration ( $\text{kg/m}^3$ ) along Jabalya (Scenario 2)

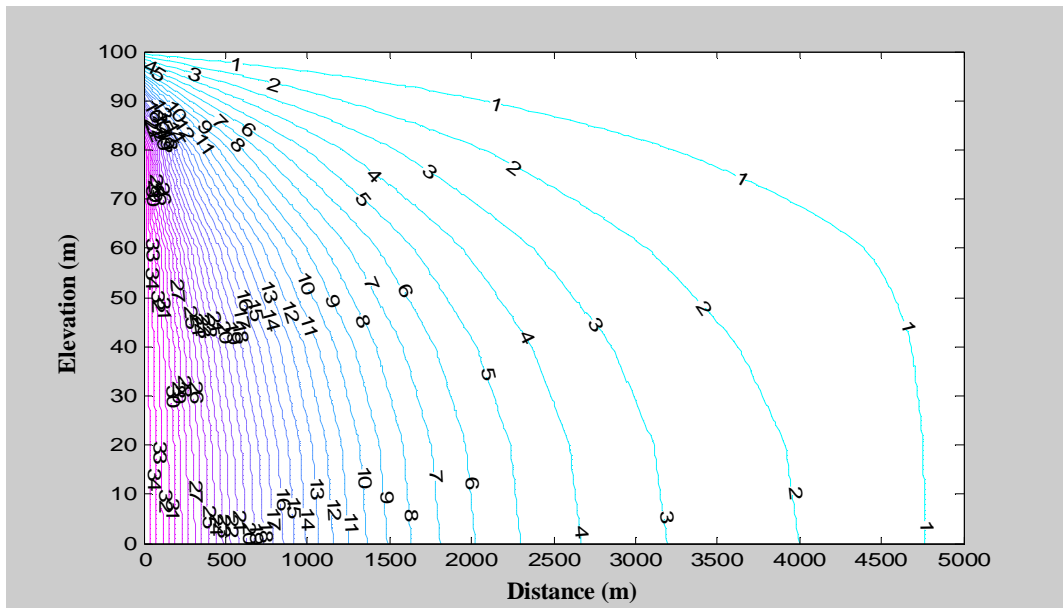


Figure 7.13 Isolines of TDS concentration ( $\text{kg/m}^3$ ) along Jabalya (Scenario 3)

In the first scenario (+1 m SLR), isoline 2 intruded inland to a distance of about 3.5 km measured at the bottom boundary from the sea side. In the second scenario (-0.5 m lower in water table), isoline 2 intruded inland to a distance of about 3.25 km. However, isoline 2 in the third scenario intruded inland to a distance of about 4.0 km, due to the combination of both sea level rise and lowering water table. The Gaza aquifer is nearly contaminated by saline water and urgent actions are needed to prevent such intrusion because groundwater is the only source of water for about 1.5 million Palestinian living in Gaza strip.

## **7.6 Summary**

The rate of climate change is increasing rapidly due to human activities. Human societies and natural ecosystems may not be able to adapt to rapid climate change. The increase in the global temperature will warm the land surface, oceans and seas and melt the ice caps, which will in turn lead to the increase in water levels in the oceans and seas. The rise in water levels could have damaging effects on residents of coastal areas because of higher rates of erosion, inundation and saltwater intrusion. The rise in water levels may lead to partial or full submergence of some coastal cities which lie in low lands. Sea level rise also threatens groundwater storage in coastal aquifers as it imposes an additional pressure head at the seaside which accelerates saltwater intrusion. The study of the effects of climate change and sea level rise on coastal areas has become an important subject. In this study the effect of climate change and sea level rise on coastal aquifers is studied using the developed numerical model. The results of the model indicate that the sea level rise has a significant effect on the position of fresh water/saltwater interface. Furthermore, lowering of water table or piezometric head due to additional pumping from the aquifer also affects the position of fresh water/saltwater interface. The combination of both sea level rise and lowering water table has a greater effect on the position on fresh water/saltwater interface.

## Conclusions and recommendations

### 8.1 Conclusions

Seawater intrusion represents a great risk to groundwater resources in coastal areas as it raises the salinity to levels exceeding acceptable drinking water standards. Salinization of groundwater is considered one of the main pollutants in coastal aquifers. Moreover, climate-change predictions suggest that as temperatures rise, the droughts would exacerbate, and as the sea level rises, saltwater intrusion would speed up. Rising sea level poses another challenge to the coastal areas as it could lead to the submergence of much of coastal cities in different parts of the world. Although some research has been done to investigate saltwater intrusion however, only a limited amount of work has concentrated on the control of saltwater intrusion to protect groundwater resources in coastal areas which represent the most densely populated areas in the world, where 70% of the world's population live.

This work presented a new methodology (ADR) to control saltwater intrusion into coastal aquifers. Two main approaches were used in this study; the first approach was the development of a coupled transient finite element model of fluid flow and solute transport in porous media to simulate saltwater intrusion and the second was the development of a simulation-optimization model to control saltwater intrusion in coastal aquifers using different management scenarios. The development of the numerical model for predicting solute transport through saturated/unsaturated soils is a major theme considered in this work. The presented simulation-optimization model to control saltwater intrusion is another main theme considered in this work. The application of the proposed methodology ADR to control saltwater intrusion is a major achievement of this work. Also the application of the developed model to simulate the effect of sea level rise due to climate change is another achievement.



The achieved objectives in this work include:

- A coupled fluid flow and solute transport model was developed to solve the governing equation of solute transport together with three balance equations for water and air flow with heat transfer which provide values of solute concentration, pore water pressure, pore air pressure and temperature at different points within the flow region at different times.
- The numerical model was validated by application to several standard examples from literature followed by application to a number of case studies involving seawater intrusion in coastal aquifers.
- The numerical results illustrated the performance of the presented model to handle a wide range of real problems including the simulation of fluid flow alone, solute transport alone and coupled fluid flow and solute transport.
- The results showed that the developed numerical model is capable of predicting, with a good accuracy, the movement and extension of saltwater in coastal aquifers.
- The developed model for simulating saltwater intrusion considers transient, density-dependent flow in saturated/unsaturated porous media. Dispersion is considered to be velocity-dependant. Also, different mechanisms which affect solute transport in porous media including, advection, diffusion, dispersion, adsorption, chemical reactions and biological degradation are considered.
- A simulation-optimization model was developed for the control of saltwater intrusion in coastal aquifers using three management scenarios including; abstraction of brackish water, recharge of fresh water and combination of abstraction and recharge. The objectives of these management scenarios include minimizing the total costs for construction and operation, minimising salt concentrations in the aquifer and determining the optimal depths, locations and abstraction/recharge rates for the wells.
- A new methodology (ADR) to control seawater intrusion in coastal aquifers by abstracting brackish water, desalinating it using small scale RO and recharging to the aquifer was presented. The results showed that this methodology is an efficient and cost-effective method to control seawater intrusion in coastal aquifers.
- The developed model was applied to study the effects of the likely climate change and sea level rise and/or over-pumping on saltwater intrusion in coastal aquifers.

## ***8.2 Recommendations for future work***

This study has touched a serious real world problem which has become of considerable concern in many countries with coastal areas. It presented a first step in developing a simulation-optimization model to control saltwater intrusion in coastal aquifers. This work presents a new methodology ADR to control saltwater intrusion in coastal aquifers through the application of a simulation-optimization model. As has been discussed there are several benefits for using ADR methodology to control saltwater intrusion however this work is regarded as a first step in developing simulation-optimization models and more work can be done in the future. A list of possible topics for future work is as follows:

- ❖ Extend the current model to combine horizontal simulation with vertical simulation to obtain a 3D picture of seawater intrusion and determine the distance between wells and the number of wells required to control SWI using ADR.
- ❖ Extend the current model from 2D to 3D, which would give more realistic simulation for practical applications of most of saltwater intrusion problems.
- ❖ More work needs to be carried out on the experimental study of saltwater intrusion in coastal aquifers and comparison with numerical results.
- ❖ The effect of temperature on the intrusion of saltwater and the flow in vadoze zone also needs further investigation.
- ❖ Integrating the developed model with a decision support system for sustainable development of water resources management in coastal areas is another possibility for future work.

## References

- Abarca, E., Carrera, J., Voss, C. I. and Sanchez-Vila, X. (2002). "Effect of aquifer bottom morphology on seawater intrusion", *Proceeding of the 17<sup>th</sup> Salt Water Intrusion Meeting, Delft, the Netherlands*.
- Abd-Elhamid, H. F. and Javadi, A. A. (2008a). "Mathematical models to control saltwater intrusion in coastal aquifer", *Proceeding of GeoCongress, New Orleans, Louisiana, USA*.
- Abd-Elhamid, H. F. and Javadi, A. A. (2008b). "An investigation into control of saltwater intrusion considering the effects of climate change and sea level rise", *Proceeding of 20<sup>th</sup> SWIM, June 23-27, 2008, Naples, Florida, USA*.
- Abd-Elhamid, H. F. and Javadi, A. A. (2010). "A Simulation-Optimization Model to Study the Control of Seawater Intrusion in Coastal Aquifers Using ADR Methodology", *Proceeding of 21<sup>st</sup> SWIM, June 21-26, 2010, Azores, Portugal*.
- Abderahman, W. A. (2001). "Energy and water in arid developing countries: Saudi Arabia a case-study", *International journal of water resources development*, 17(2): 247-255.
- Afonso, M. D., Jaber, J. O. and Mohsen, M. S. (2004). "Brackish groundwater treatment by reverse osmosis in Jordan", *Elsevier, Desalination*, 164: 157-171.
- Aharmouch, A. and Larabi, A. (2001). "Numerical modelling of saltwater interface upconing in coastal aquifers", *Proceeding of the 1<sup>st</sup> international conference and workshop on saltwater intrusion and coastal aquifers, monitoring, modelling, and management (Morocco)*.
- Ahuja, L. R. and Lehman, O. R. (1983). "The extent and nature of rainfall-soil interaction in the release of soluble chemicals to runoff", *Journal of Environmental Quality*, 12: 34-40.

- Al-azzan, Y., Safar, M. and Mesri, A. (2003). "Reverse osmosis brine staging treatment of subsurface water", *Elsevier, Desalination*, 155: 141-151.
- Alf, G., Angela, H., Martin, L., Berthold, R. and Andre, S. (2002). "Numerical and hydrochemical modelling of saltwater intrusion into a pleistocene aquifer-case study Grobbeuthen, Brandenburg", *Proceeding of the 17<sup>th</sup> Salt Water Intrusion Meeting, Delft, the Netherlands*.
- Al-Hadidi, M. S. (1999). "Brackish water management and use in Jordan", *Elsevier science, Desalination and Environment*, 126: 41-44.
- Al-Najjar, M. M. (2006). "Finite element modelling of contaminant transport in unsaturated soils", *PhD thesis, School of Engineering, Mathematics and Computer Sciences, University of Exeter, UK*.
- Allen, D. M., Mastuo, G., Suchy, M. and Abbey, D. G. (2001). "A multidisciplinary approach to studying the nature and occurrence of saline groundwater in the gulf islands, British Columbia, Canada", *Proceeding of the 1<sup>st</sup> international conference and workshop on saltwater intrusion and coastal aquifers, monitoring, modelling, and management (Morocco)*.
- Alonso, E. E., Battle, F., Gens, A. and Lioret, A. (1988). "Consolidation analysis of partially saturated soil. Application to earthdam construction", *Numerical methods in Geomechanics. Innsbruck*, 1303-1308.
- Aly, A. H. and Peralta, R. C. (1999). "Optimal design of aquifer cleanup systems under uncertainty using a neural network and a genetic algorithm", *Water Resources Research*, 35(8): 2523-2532.
- Amaziane, B., Cheng, A. H.-D., Naji, A. and Ouazar, D. (2004). "Stochastic optimal pumping under no-intrusion constraints in coastal aquifers", *Proceeding of the 18<sup>th</sup> Salt Water Intrusion Meeting, Cartagena (Spain)*.

- Anderson, M. P and Woessner, W. W. (1992). "The role of the postaudit in model validation", *Advances in Water Resources*, 15(3): 167-174.
- Aral, M. M. (1990). "Groundwater Modelling in Multilayer Aquifers: Unsteady Flow", *Lewis Publishers, Inc, Boca Raton, Florida, USA*.
- Arvanitidou, S. K., Koutitas, C. G. and Katsifarakis, K. L. (2010). "Using a computational optimization tool for the management of an aquifer at Kalymnos island in Greece", *Proceeding of 21<sup>st</sup> SWIM, Azores, Portugal*.
- Bachmat, Y. (1967). "On the similitude of dispersion phenomena in homogeneous and isotropic porous media", *Water Resources Research*, 3(4): 1079-1083.
- Bajjali, W. (2005). "Model the effect of four artificial recharge dams on the quality of groundwater using geostatistical methods in GIS environment, Oman", *Journal of Spatial Hydrology*, 5(2): 1-15.
- Baker, A. J. and Pepper, D. W. (1991). "Finite Elements 1.2.3", *McGraw-Hill Companies, Inc., New York, USA*.
- Bakheet, M. (2006). "Prospects of Water Desalination in the Gaza Strip", *MSc. Thesis, Department of Civil Engineering, Colorado State University*.
- Bakkar, M., Schaars, F. and Borden, D. (2004). "Modelling coastal aquifers with the sea water intrusion (SWI) package for the MODFLOW", *Proceeding of the 18<sup>th</sup> Salt Water Intrusion Meeting, Cartagena (Spain)*.
- Barreto, J., Nuno, M. A. and Haie, N. (2001). "Modelling of rural usage of groundwater subject to saltwater intrusion", *Proceeding of the 1<sup>st</sup> international conference and workshop on saltwater intrusion and coastal aquifers, monitoring, modelling, and management (Morocco)*.
- Barrocu G., Cau, P., Muscas, L., Soddu, S. and Uras, G. (2004). "Predicting groundwater salinity changes in the coastal aquifer of Arborea (central-western

- Sardinia)", *Proceeding of the 18<sup>th</sup> Salt Water Intrusion Meeting, Cartagena (Spain)*.
- Barry, D. A., Parlange, Y. and Sivaplan, M. (1993). "A class of exact solutions for Richards' equation", *Journal of Hydrology*, 142: 29-46.
- Barsi, M. H. (2001). "Two new methods for optimal design of subsurface barrier to control seawater intrusion", *PhD thesis, department of Civil and Geological Engineering, University of Manitoba, Winnipeg, Manitoba, Canada*.
- Bear, J. (1961). "On the tensor form of dispersion in porous media", *Journal of Geophysical Research*, 66(4): 1185-1197.
- Bear, J. (1979). "Hydraulics of groundwater", *McGraw-Hill, New York, USA*.
- Bear, J. and Verruijt, A. (1987). "Modelling of groundwater flow and pollution", *Reidel publishing company, Dordrecht, The Netherland*.
- Bear, J., Tasang, C. F. and Marsily, G. D. (1993). "Flow and contaminant Transport in Fractured Rock", *Academic Press, Inc., San Diego, California, USA*.
- Bear, J., Cheng, A. H., Sorek, S., Quazar, D. and Herrera, I. (1999). "Seawater intrusion in coastal aquifers, concepts, methods and practices", *Kluwer Academic publisher, Dordrecht, The Netherlands. ISBN 0-7923-5573-3*.
- Bear, J., Zhou, Q. and Bensabat, J. (2001). "Three dimensional simulation of seawater intrusion in heterogeneous aquifers, with application to the coastal aquifer of Israel", *Proceeding of the 1<sup>st</sup> international conference and workshop on saltwater intrusion and coastal aquifers, monitoring, modelling, and management (Morocco)*.
- Benhachmi, M. K., Ouazar, D., Naji, A., Cheng, A. H.-D. and El Harrouni, K. (2001a). "Optimal management of saltwater-intruded coastal aquifer by simple genetic algorithm", *Proceeding of the 1<sup>st</sup> international conference and workshop on*

*saltwater intrusion and coastal aquifers, monitoring, modelling, and management (Morocco).*

Benhachmi, M. K., Ouazar, D., Naji, A., Cheng, A. H.-D. and El Harrouni, K. (2001b). "Chance constrained optimal management in saltwater-intruded coastal aquifers using genetic algorithm", *Proceeding of the 1<sup>st</sup> international conference and workshop on saltwater intrusion and coastal aquifers, monitoring, modelling, and management (Morocco).*

Benhachmi, M. K., Ouazar, D., Naji, A., Cheng, A. H.-D and Harrouni, K. E. (2003). "Pumping Optimization in Saltwater Intruded Aquifers by Simple Genetic Algorithm- Deterministic Model", *Proceeding of Coastal Aquifers Intrusion Technology: Mediterranean Countries International Conference (TIAC'03), 1:291-293, Alicante, Spain.*

Benson, D. A., Huntly, D. and Johnson, P. C. (1993). "Modelling vapour extraction and general transport in the presence of NAPL mixtures and nonideal conditions", *Groundwater*, 31(3): 437-445.

Benson, D. A., Carey, A. E. and Wheatcraft, S. W. (1998). "Numerical adjective flux in highly variable velocity field exemplified by saltwater intrusion", *Journal of Contaminant Hydrology*, 34: 207-233.

Bhattacharjya, R. K. and Datta, B. (2004). "An ANN-GA approach for solving saltwater intrusion management problem in coastal aquifers", *Proceeding of the 18<sup>th</sup> Salt Water Intrusion Meeting, Cartagena (Spain).*

Bhattacharjya, R., K. and Datta, B. (2005). "Optimal management of coastal aquifers using linked simulation optimization approach", *Water Resources Management*, 19: 295-320.

Binning, P. J. (1994). "Modelling unsaturated zone flow and contaminant transport in the air and water phases", *Ph.D. Dissertation, Princeton University, New Jersey, USA.*

- Bixio, A., Putti, M., Tosi, L., Carbognin, L. and Gambolati, G. (1998). "Finite element modelling of saltwater in the Venice aquifer system", *Transactions on Ecology and the Environment*, 17: 1743-3541.
- Bocanegra, E. M. and Massone, H. E. (2004). "Exploitation of coastal aquifers in Latin America and the Caribbean. Problems and solutions", *Proceeding of the 18<sup>th</sup> Salt Water Intrusion Meeting, Cartagena (Spain)*.
- Bower, J. W., Motez, L. H. and Durden, D. W. (1999). "Analytical solution for the critical conditions of saltwater upconing in a leaky artesian aquifer", *Elsevier, Journal of hydrology*, 221: 43-54.
- Brunke, H. P. and Schelkes, K. (2001). "A sharp-interface-based approach to salt water intrusion problems- model development and applications", *Proceeding of the 1<sup>st</sup> international conference and workshop on saltwater intrusion and coastal aquifers, monitoring, modelling, and management (Morocco)*.
- Canning, D. J. (2001). "Climate variability, climate change, and sea-level rise in Puget Sound: possibilities for the future", *Report, Washington Department of Ecology and JISAO/SMA Climate Impact Group, University of Washington*.
- Canot, E., Dieuleveult, C. and Erhel, J. (2006). "A parallel software for a saltwater intrusion problem", *Technical Report by John von Newman Institute for Computing NIC*.
- Cau, P., Lecca, G., Muscas, L., Barrocu, G. and Uras, G. (2002). "Seawater intrusion in the plain of Oristano (Sardinia, Italy)", *Proceeding of the 17<sup>th</sup> Salt Water Intrusion Meeting, Delft, the Netherlands*.
- Celia, M. A., Bouloutas, E. T. and Zarba, R. L. (1990). "A general mass-conservative numerical solution for the unsaturated flow equation", *Water Resources Research*, 26(7): 1483-1496.



- Chan Hilton, A. B. and Culver, T. B. (2000). "Constraint handling for genetic algorithms in optimal remediation design", *Journal of Water Resources Planning and Management*, 126(3): 128-137.
- Chan Hilton, A. B. and Culver, T. B. (2005). "Groundwater remediation design under uncertainty using genetic algorithms", *Journal of Water Resources Planning and Management*, 131(1): 25-34.
- Chandrupatla, T. R. and Belegundu, A. D. (1991). "Introduction to Finite Element in Engineering. Prentice-Hall International Editions Companies", *Inc., New Jersey, USA*.
- Chen, B. F. and Hsu, S. M. (2004). "Numerical study of tidal effects on seawater intrusion in confined and unconfined aquifers by time-independent finite-difference method", *ASCE Journal of Waterway, Port, Coastal, and Ocean Engineering*, 130(4):191–206.
- Cheng, J., Strobl, R. O., Yeh, G., Lin, H. and Choi, W. (1998). "Modelling of 2D density-dependant flow and transport in the subsurface", *Journal of Hydrologic Engineering*, 3(4): 248-257.
- Cheng, A. H.-D, Halhal, D., Naji, A. and Ouazar, D. (2000). "Pumping optimization in saltwater-intruded coastal aquifers", *Water Resources Research*, 36(8):2155-2165.
- Cheng, A., H.-D., Dalhal, D., Naji, A. and Ouazar, D. (2001). "Pumping optimization in saltwater-intruded coastal aquifer", *Proceeding of the 1<sup>st</sup> international conference and workshop on saltwater intrusion and coastal aquifers, monitoring, modelling, and management (Morocco)*.
- Cheung, Y. K., Lo, S. H. and Leung, A. Y. T. (1996). "Finite Element Implementation", *Blackwell Since Ltd, Cambridge, USA*.

- Christensen, F. D., Engesgaard, P. and Kipp, K. L. (2001). "A reactive transport investigation of a seawater intrusion experiment in a shallow aquifer, Shanshage, Denmark", *Proceeding of the 1<sup>st</sup> international conference and workshop on saltwater intrusion and coastal aquifers, monitoring, modelling, and management (Morocco)*.
- Connell, L. D. and Bell, P. R. F. (1993). "Modelling moisture movement in revegetating waste heaps 1. Development of a finite element model for liquid and vapour transport", *Water Resources Research*, 29(5): 1435-1444.
- Cooper, H. H. (1959). "A hypothesis concerning the dynamic balance of fresh water and saltwater in a coastal aquifer", *Journal of Geophysical Research*, Vol. 64.
- Courant, R., Fredrichs, K. O and Levy, H. (1928). "Uber die partiellen differenzengleichungen der mathematischen physik", *Mathematische Annalen*, 100(1): 32-47.
- Couvillion, R. J. and Hartley, J. G. (1985). "Analysis of drying front movement in a moist soil without the use of a moving boundary approach", *International Conference of Numerical Methods for Transient and Coupled Problems, Venice, Italy*.
- Crowe, A. S., Shikaze, S. G. and Patacek, C. J. (2004). "Numerical modelling of groundwater flow and contaminant transport to point pelee marsh, Ontario Canada", *Hydrological Processes Journal*, 18: 239-314.
- Culver, T. B., Shoemaker, C. A. and Lion, L. W. (1991). "Impact of vapour sorption on the subsurface transport of volatile organic compounds: A numerical model and analysis", *Water Resources Research*, 27(9): 2259-2270.
- Dakshanamurthy, V. and Fredlund, D. G. (1981). "A mathematical model for predicting moisture flow in an unsaturated soil under hydraulic and temperature gradients", *Water Resources Journal*, 17(3): 714-722.

- Darcy, H. (1856). "les fontains publiques de la ville de Dijon", *V. Dalmont, Paris*: 590-594.
- Daryl, L. L. (2002). "Finite Element Method. Third edition", *Wadsworth Group. Brooks Cole, USA*.
- Das, A. and Datta, B. (1999a). "Development of multiojective management models for coastal aquifers", *Journal of Water Resources planning and Management*, 125:76-87.
- Das, A. and Datta B. (1999b). "Development models for sustainable use of coastal aquifers", *Irrigation and Drainage Engineering*, 125: 112-121.
- Das, A. and Datta, B. (2000). "Optimization based solution of density dependent seawater intrusion in coastal aquifers", *Journal of Hydrologic Engineering*, 5(1):82-89.
- Daus, A. D., Frind, E. O. Sudicky, E. A. (1985). "Comparative error analysis in finite element formulations of the advection-dispersion equation", *Advances in Water Resources*, 8: 86-95.
- Davis, L. (1991). "Handbook of genetic algorithm", *Van Nostrand Reinhold, New Yourk, USA*.
- Day, P. R. (1956). "Dispersion of a moving salt-water boundary advancing through a saturated sand", *Transactions, American Geophysical Union*, 37: 595-601.
- Demirel, Z. (2004). "The history and evaluation of saltwater intrusion into a coastal aquifer in Mersin, Turkey", *Elsevier, Journal of Environmental Management*, 70: 275-282.
- Dick, E. (1983). "Accurate Petrov-Galerkin methods for transient convective diffusion problems", *International Journal for Numerical Methods in Engineering*, 19: 1425-1433.

- Doulgeris, C. and Zissis, T. (2005). " Simulation of seawater intrusion in three-dimensional confined aquifers", *Geophysics Research*, 7: 02780.
- Edet, A. E. and Okereke, C. S. (2001). "A regional study of saltwater intrusion in south eastern Nigeria based on the analysis of geoelectrical and hydrochemical data", *Environmental Hydrology*, 40: 1278-1289.
- Edlefsen, N. E. and Anderson, A. B. C. (1943). "Thermodynamics of soil Moisture", *Hilgardia*, 15(2): 31-298.
- Ekwurzel, B., Moran, J. E., Hudson, G. B., Bissani, M., Blake, R., Krimissa, M., Mosleh, N., Marah, H., Safsaf, N., Hsissou, Y. and Bouchaou, M. (2001). "An isotopic investigation of salinity and water sources in the Souss-Massa Basin, Morocco", *Proceeding of the 1<sup>st</sup> international conference and workshop on saltwater intrusion and coastal aquifers, monitoring, modelling, and management (Morocco)*.
- El Fleet, M. and Baird, J. (2001). "The development and application of groundwater models to simulate the behaviour of groundwater resources in the Tripoli aquifer, Libya)", *Proceeding of the 1<sup>st</sup> international conference and workshop on saltwater intrusion and coastal aquifers, monitoring, modelling, and management (Morocco)*.
- El Harrouni, K., Ouazar, D., Walters, G. A. and Cheng, A. H.-D. (1998). "Groundwater optimization and parameter estimation by genetic algorithm and dual reciprocity boundary element method", *Eng. Anal. Boundary. Manage.*, 124: 129-139.
- EL Moujabber, M., Bou, S. B., Darwish, T. and Atallah, T. (2006). "Comparison of different indicators for groundwater contamination by seawater intrusion on the Lebanese coast", *Water Resources Management*, 20: 161-180.
- El Raey, M., Dewidar, Kh. and El Hattab, M. (1999). "Adaptation to the impact of sea level rise in Egypt", *Climate Research*, 12: 117-128.

- El Sheikh, R., Ahmed, M. and Hamdan, S. (2003). "Strategy of water desalination in the Gaza strip", *Elsevier, Desalination*, 156: 39-42.
- Emch, P. G. and Yeh, W. W-G. (1998). "Management model for conjunctive use of coastal surface water and groundwater", *Journal of Water Resources Planning and Management*, 124(3): 129-139.
- Esat, V. and Hall, M. J. (1994). "Water resources system optimization using genetic algorithm", *Hydroinformatics 94, International conference on Hydroinformatics, Rotterdam, The Netherland*, 225-231.
- Espinoza, F. P., Minsker, B. M. and Goldberg, D. E. (2005). "Adaptive hybrid genetic algorithm for ground water remediation design", *Journal of Water Resources planning and Management*, 131(1): 14-24.
- Essaid, H. I. (1990). "A multi-layered sharp interface model of coupled freshwater and saltwater in coastal systems: model development and application", *Water Resources Research*, 27(7): 1431-1454.
- Essink, H. P. and Schaars, F. (2002). "Impact of climate changes on the groundwater system of the water board of the Rijnland, the Netherlands", *Proceeding of the 17<sup>th</sup> Salt Water Intrusion Meeting, Delft, the Netherlands*.
- Ewen, J. and Thomas, H. R. (1987). "The thermal problem a new method and its use on unsaturated sand", *Geotechnique*, 37:91-105.
- Ewen, J. and Thomas, H. R. (1989). "Heating unsaturated medium sand", *Geotechnique*, 39(3): 455-470.
- Farmani, R., Walters, G. A. and Savic, D. A. (2005a). "Trade-off between total cost and reliability for Anytown water distribution network", *Journal of Water Resources planning and Management*, 131(3): 161-171.

- Farmani, R., Savic, D. A. and Walters, G. A. (2005b). "Evolutionary Multi-Objective Optimization in Water Distribution Network Design", *Journal of Engineering Optimization*, 37(2): 167-185.
- Fick, A. (1855) .Ann. Der.Phys. Liepzieg.94:59-86
- Finney, B., Samsuhadi, A. and Willis, R. (1992). "Quasi-3-dimensional optimization of Jakarta Basin", *Journal of Water Resources planning and Management*, 118:18-31.
- Fitterman, D. V. and Deszcz-Pan, M. (2001). "Saltwater intrusion in Everglades National Park, Florida measured by airborne electromagnetic surveys", *Proceeding of the 1<sup>st</sup> international conference and workshop on saltwater intrusion and coastal aquifers, monitoring, modelling, and management (Morocco)*.
- Fitzgerald, R., Riordan, P. and Harley, B. (2001). "An integrated set of codes to support a variety of coastal aquifer modelling approaches", *First international conference on saltwater intrusion and coastal aquifers monitoring, modeling, and management. Essaouira, Morocco*.
- Franchini, M. (1996). "Use of a genetic algorithm combined with a local search method for the automatic calibration of conceptual rainfall-runoff models", *Journal of Hydrological Sciences*, 41(1): 21-40.
- Fredlund, D. G. (1981). "Seepage in saturated soils. Panel discussion: Ground water and seepage problems", *Proceeding of the 10<sup>th</sup> Int. Conf. Soil Mech. Fdn. Engng. Stockholm*, 629-641.
- Fredlund, D. G. and Rahardjo, H. (1993). "Soil Mechanics for Unsaturated soils", *New York: Wiley*
- Frind, E. O. and Verge, M. J. (1978). "Three dimensional modelling of groundwater flow systems", *Water Resources Research*, 14(5): 844-856.

- Frind, E. O. (1982). "Simulation of long-term transient density-dependent transport in groundwater", *Water Resources Research*, 5(2): 73-88.
- Gao, H., Vesovic, V., Butler A. and Wheeler, H. (2001). "Chemically reactive multi-component transport simulation in soil and groundwater: 2. Model demonstration", *Environmental Geology*, 41: 280-284.
- Gau, H. S. and Liu, C. W. (2002). "Estimation of the optimum yield in Yun-Lin area of Taiwan using loss function analysis", *Elsevier, Journal of Hydrology*, 263: 177-187.
- Gawin, D., Baggio, P. and Schrefler, B. A. (2005). "Coupled heat, water and gas flow in deformable porous media", *International Journal for Numerical Methods in Fluids*, 20: 969-987.
- Gaye, C. B. (2001). "Isotope technique for monitoring groundwater salinization", *Proceeding of the 1<sup>st</sup> international conference and workshop on saltwater intrusion and coastal aquifers, monitoring, modelling, and management (Morocco)*.
- Gee, G. W., Kincaid, C. T. Lenhard, R. J. and Simmons, C. S. (1991). "Recent studies of flow and transport in the vadose zone", *Reviews of Geophysics, Supplement*, 227-239.
- Georgpoulou, E., Kotronarou, A., Koussis, A., Restrepo, P. J., Gomez-Gotor, A., Jimenez, J. and Rodriguez, J. (2001). "A methodology to investigate brackish groundwater desalination coupled with aquifer recharge by treated wastewater as an alternative strategy for water supply in Mediterranean areas", *Elsevier, Desalination*, 136: 307-315.
- Geraminegad, M. and Saxena, S. (1986). "A coupled thermoelastic model for saturated-unsaturated porous media", *Geotechnique*, 36(4): 539-550.

- Ghafouri, H. R. and Parsa, J. (1998). "Finite element modelling of seawater intrusion into well-mixed estuaries", *Transactions on Ecology and the Environment*, 17: 1743-3541.
- Ghyben, B. W. (1889). "Nota in verband met de voorgenomen put boring Nabij Amsterdam", *Tydschrift Van Het Koninklyk Institute Van Ingenieurs, the Hahue, the Netherlands*, pp. 21.
- Gingerich, S. B. and Voss, C. I. (2002). "Three-dimensional variable-density flow simulation of coastal aquifer in southern Oahu, Hawaii, USA", *Proceeding of the 17<sup>th</sup> Salt Water Intrusion Meeting, Delft, the Netherlands*.
- Goldberg, D. E. (1989). "Genetic Algorithms in Search, Optimization and Machine Learning", *Addison-Wesley-Longman, Reading, Mass.*
- Gopalakrishnan, G., Minsker, B. S. and Goldberg, D. E. (2003). "Optimal sampling in a noisy genetic algorithm for risk based remediation design", *Hydroinformatics*, 5(1): 11-25.
- Gordon, E., Shamir, U. and Bensabat, J. (2001). "Optimal extraction of water from regional aquifer under salinization", *Journal of Water Resources planning and Management*, 127(2):71-77.
- Gordu, F., Yurtal, R. and Motz, L. H. (2001). "Optimization of groundwater use in the Goksu Delta at Silifke, Turkey", *Proceeding of the 1<sup>st</sup> international conference and workshop on saltwater intrusion and coastal aquifers, monitoring, modelling, and management (Morocco)*.
- Gotovac, H. Andricevic, R. and Vranjes, M. (2001). "Effects of aquifer heterogeneity on the intrusion of sea water", *Proceeding of the 1<sup>st</sup> international conference and workshop on saltwater intrusion and coastal aquifers, monitoring, modelling, and management (Morocco)*.



- Gottardi, G. and Venutlelli, M. (2001). "UPF: two-dimensional finite-element groundwater flow model for saturated-unsaturated soils", *Computers & Geosciences*, 27: 179-189.
- Green, D. W., Dabiri, H., Weinaug, C. F. and Prill, R. (1970). "Numerical modelling of unsaturated groundwater flow and comparison of the model to a field experiment", *Water Resources Research*, 6(3): 862-874.
- Gunduz, O. (2004). "Coupled flow and contaminant transport modelling in large watersheds". *Ph.D. Dissertation, Georgia Institute and Technology, Atlanta, Georgia, USA*.
- Gurdu, F., Motz, L. H. and Yurtal, R. (2001). "Simulation of seawater intrusion in the Goksu Delta at Silifke, Turkey", *Proceeding of the 1<sup>st</sup> international conference and workshop on saltwater intrusion and coastal aquifers, monitoring, modelling, and management (Morocco)*.
- Halhal, D., Walters, G. A., Ouazar, D. and Savic, D. A. (1997). "Water network rehabilitation with structured messy genetic algorithm", *Water Resources Planning and Management*, 123: 137-146.
- Hallaji, K. and Yazicigil, H. (1996). "Optimal management of a coastal aquifer in southern Turkey", *Journal of Water Resources Planning and Management*, 122(4): 233-244.
- Haiso, C. T. and Chang, L. C. (2002). "Dynamic optimal groundwater management with inclusion of fixed costs", *Journal of Water Resources planning and Management*, 128(1): 57-65.
- Hamza, K. I. (2004). "Numerical analysis of saltwater upconing below a pumping well", *Proceeding of the 18<sup>th</sup> Salt Water Intrusion Meeting, Cartagena (Spain)*.

- Harne, S., Chaube, U. C., Sharma, S., Sharma, P. and Parkhya, S. (2006). "Mathematical modelling of salt water transport and its control in groundwater", *Natural and science*, 4: 32-39.
- Haupt, R. and Haupt, S. E. (1998). "Practical Genetic Algorithms", *John Wiley & Sons, Inc., Reading, New York, USA*.
- Henry, H. R. (1959). "Salt intrusion into fresh-water aquifer", *Journal of Geophys. Res.*, 64:1911-1919.
- Henry, H. R. (1964). "Effect of dispersion on salt encroachment in coastal aquifers", *U. S. Geol. Surv., Water-Supply Pap.* 1613-C, pp. 70-84.
- Herzberg, A. (1901). "Die wasserversorgung einniger nordseebader", *Journal Gasbeleuchtung U. Wasserversurg, Jahrg 44, Munich, Germany*, pp.815-819.
- Hills, R. G., Porro, I., Hudson, D. B. and Wierenga, P. J. (1989). "Modelling one-dimensional infiltration into very dry soils 1. Model development and evaluation", *Water Resources Research*, 25(6): 1259-1269.
- Holland, J. H. (1975). "Adaptation in Natural and artificial Systems", *Univ. of Mich. Press, And Arbor*.
- Hong, S., Park, N., Bhopanam, N. and Han, S. (2004). "Verification of optimal model of coastal pumping with sand-tank experiment", *Proceeding of the 18<sup>th</sup> Salt Water Intrusion Meeting, Cartagena (Spain)*.
- Hornig, J. S., Richard, C. and Peralta, C. (2005). "Optimal in situ bioremediation design by hybrid genetic algorithm-simulated Annealing", *Journal of Water Resources planning and Management*, 131(1): 67-78.
- Huang, K., Mohanty B. P. and Van Genuchten, M. T. (1996). "A new convergence criterion for the modified Picard iteration method to solve the variably saturated flow equation", *Journal of Hydrology*, 260: 69-91.

- Hubbert, M. K. (1940). "The theory of ground water motion", *Journal of Geology*, 48(8): 785-944.
- Huyakorn, P. S, Jones, E. G. and Andersen, P. F. (1986). "Finite element algorithms for simulating three dimensional groundwater flow and solute transport in multilayer systems" *Water Resources Research*, 22(3): 361-374.
- Huyakorn, P. S. Anderson, P. F., Mercer, J. W. and White, H. O. (1987). "Saltwater intrusion in aquifers: Development and testing of a three-dimensional finite element model", *Water Resources Research*, 23(2): 293-312.
- Isikh, Y. and Karahanoglu, N. (2004). "Coastal aquifer, Kocaeli- Darica Turkey", *Proceeding of the 18<sup>th</sup> Salt Water Intrusion Meeting, Cartagena (Spain)*.
- Islam, J. and Singhal, N. (2002). "A one-dimensional reactive multi-component landfill leachate transport model", *Environmental Modelling and Software*, 17: 531-543.
- Islas, A. L. and Illangasekare, T. H. (1992). "Solute Transport Under a Constant Infiltration Rate. 1- Analytical Solutions", *Abstracts of Annual American Geophysical Union, Hydrology Days, H. J. Morel-Seytoux (ed.), 57 Selby Lane, Atherton, California, USA*.
- Ismail, M. (2003). "Prospects of Water Desalination in the Gaza Strip", *MSc. Thesis, Land and Water Resources Engineering, KTH*.
- Istok, J. D. (1989). "Groundwater modelling by the finite element", *American geophysical union, USA*.
- Istok, A. L. M. (1989). "Modelling multiphase migration of organic chemicals in groundwater systems- a review and assessment", *Environmental Health Perspectives*, 83: 117-143.

- IPCC. (1996). *Climate Change 1995: The science of climate change: contribution of working group I to the second assessment report of the Intergovernmental Panel on Climate Change*. Houghton, J. T., Meira Fihlo, L. G., Callander, B. A., Harris, N., Kattenberg, A. and Maskell, K. Cambridge University Press, Cambridge, UK and New York, NY, USA.
- IPCC. (2001). *Climate Change 2001: Impacts, Adaptations, and Vulnerability: contribution of working group II to the third assessment report of the Intergovernmental Panel on Climate Change*. McCarthy, J. J., Canziani, O. F., Leary, N. A., Dokken, D. J. and White, K. S. Cambridge University Press, Cambridge, UK and New York, NY, USA.
- Izuka, S. K. and Gingrich, S. B. (1998). "Estimation of the depth of the fresh water/salt water interface from vertical head gradient in wells in coastal and inland aquifers", *Hydrology Journal*, 6(3): 365-373.
- Jaber I. S., Ahmed, M. R. (2004). "Technical and economic evaluation of brackish groundwater desalination by reverse osmosis (RO) process", *Elsevier, Desalination* , 165: 209-213.
- Jacob, C. E. (1950). "Flow in Groundwater in Engineering Hydraulics", *John Wiley and Sons, New York, USA*.
- James G., Hiebert, R., Warwood, B. and Cunningham, A. (2001). "Subsurface biofilm for controlling saltwater intrusion", *Proceeding of the 1<sup>st</sup> international conference and workshop on saltwater intrusion and coastal aquifers, monitoring, modelling, and management (Morocco)*.
- Javadi, A. A., AL-Najjar, M. M. and Elkassass, A. S. I. (2006). "Numerical modelling of contaminant transport in unsaturated soil", *Proceeding of the 5th international congress on environmental geotechnics. Cardiff University, UK*: 1177-1184.

- Javadi, A. A. and Al-Najjar, M. M. (2007). "Finite element modelling of contaminant transport in soils including the effect of chemical reactions", *Journal of Hazardous Materials*, 143(3): 690-701.
- Javadi, A. A., Al-Najjar, M. M. and Evans, B. (2008). "Numerical modeling of contaminant transport through soils: Case study", *Journal of Geotech. Geoenviron.*, 134(2): 214-230.
- Johnson, P. C., Kemblowski, M. W. and Colthart, J. D. (1990). "Quantitative analysis for the cleanup of hydrocarbon-contaminated soils by in-situ soil venting", *Groundwater*, 28(3): 413-429.
- Johnson, V. M. and Rogers L. L. (1995), "Location analysis in ground-water remediation using neural networks", *Ground Water*, 33(5): 749-758.
- Johnson, T., Reichard, E., Land, M. and Crawford, S. (2001). "Monitoring, modelling, and managing saltwater intrusion, central and west coast groundwater basins, Los Angeles country, California", *Proceeding of the 1<sup>st</sup> international conference and workshop on saltwater intrusion and coastal aquifers, monitoring, modelling, and management (Morocco)*.
- Johnson, T. and Sperry, M. (2001). "Direct potable use of intruded seawater from west coast basin aquifers, Los Angeles country, California", *Proceeding of the 1<sup>st</sup> international conference and workshop on saltwater intrusion and coastal aquifers, monitoring, modelling, and management (Morocco)*.
- Jung, B., Kim, J. and Chang, H. (2002). "Finite element modeling of density-dependent groundwater flow and solute transport in the unsaturated layered coastal aquifer system", *Proceeding of the 17<sup>th</sup> Salt Water Intrusion Meeting, Delft, the Netherlands*.
- Kacimov, A. R., Sherif, M. M., Perret J. S. and Al-Mushikhi, A. (2009). "Control of sea-water intrusion by salt-water pumping: Coast of Oman", *Hydrogeology Journal*, 17: 541–558.

- Kacur, J., Malengier, B. and Remesikova, M. (2004). "Solution of contaminant transport with equilibrium and non-equilibrium adsorption", *Journal of Computer Methods in Applied Mechanics and Engineering*, 194: 479-489.
- Karkuri, H. M. and Molenkamp, F. (1997). "Analysis of advection dispersion of pollutant transport through a layered porous media", *Proceeding of the International Conference on Geoenvironmental Engineering, Cardiff University, Wales, U.K.*
- Kashef, A. (1976). "Control of saltwater intrusion by recharge wells", *Journal of Irrigation and Drainage Division*, 102: 445-456.
- Kawatani, T. (1980). "Behaviour of seawater intrusion in layered coastal aquifer", *Proceeding of the 3<sup>rd</sup> Int. Conf. Finite Element Water Resou., Univ. of Mississippi, Oxford, Miss.*
- Kaye, G. W. C. and Laby, T. M. (1973). "Tables of physical and chemical constants", *14th edition Harlow: Longman.*
- Klaus, J. B. (1996). "Finite Element Procedures", *Prentice-Hill, Inc., New Jersey, USA.*
- Koch, M. and Starke, B. (2001). "Experimental and numerical investigation of macrodispersion of density-dependent flow and transport in stochastically heterogeneous media", *Proceeding of the 1<sup>st</sup> international conference and workshop on saltwater intrusion and coastal aquifers, monitoring, modelling, and management (Morocco).*
- Kohout, F. A. (1960a). "Cyclic flow of fresh water in the Biscayne aquifer of southeastern Florida", *Journal of Geophys. Res.*, 65: 2133-2141.
- Kohout, F. A. (1960b). "Flow pattern of fresh water and saltwater in the Biscayne aquifer of the Miami, Florida", *Int. Ass. Sci. Hydrol. Publ.* 52:440-448.

- Krischer, D. and Rohnalter, H. (1940). "Warmeleitung and Dampfdiffusion in feuchten utern", *Verein Deut, Ing-Forschungsheft*. p. 402.
- Lakfifi, L., Larabi, A., Bzioui, M., Benbibba, M. and Lahmouri, A. (2004). "Regional model for seawater intrusion in the chaouia coastal aquifer (Morocco)", *Proceeding of the 18<sup>th</sup> Salt Water Intrusion Meeting, Cartagena (Spain)*.
- Lapen, D. R., Price, J. S. and Gilbert, R. (2005). "Modelling two-dimensional steady-state groundwater flow and flow sensitivity to boundary conditions in blanket peat complex", *Hydrological processes*, 19: 371-386.
- Lazar, A., Gvirtzman, H. and Yechieli, Y. (2004). "Freshwater-salinewater interface fluctuation in coastal aquifer due to sea tide", *Proceeding of the 18<sup>th</sup> Salt Water Intrusion Meeting, Cartagena (Spain)*.
- Lecca, G., Berjamy, B., Paniconi, C. and El Hebil, A. (2001). "Numerical modelling of seawater intrusion in the Sahel region of the Atlantic coast of Morocco", *Proceeding of the 1<sup>st</sup> international conference and workshop on saltwater intrusion and coastal aquifers, monitoring, modelling, and management (Morocco)*.
- Lecca, G., Cau, P. and Ardaù, F. (2004). "Modelling study of the seawater intrusion in the muravera coastal plain (SE Sardinia, Italy)", *Proceeding of the 18<sup>th</sup> Salt Water Intrusion Meeting, Cartagena (Spain)*.
- Lee, C. H. and Cheng, R. T.-Sh. (1974). "On seawater encroachment in coastal aquifer", *Water Resources Research*, 10(5): 1039-1043.
- Lee, S. (2004). "Investigation of seawater intrusion in coastal plain and Karst Hinterland aquifer of Cape Range, Northwestern Australia", *Proceeding of the 18<sup>th</sup> Salt Water Intrusion Meeting, Cartagena (Spain)*.

- Lessoff, S.C. and Indelman, P. (2004). "Analytical model of solute transport by unsteady unsaturated gravitational infiltration", *Journal of Contaminant Hydrology*, 72: 85-107.
- Levi, E., Goldman, M., Shalem, Y., Weinstein, Y., Yechieli, Y. and Herut, B. (2010). "Combined ERT-TDEM measurements for delineating saline water intrusions from an estuarine river into the adjacent aquifer", *Proceeding of 21<sup>st</sup> SWIM, Azores, Portugal*.
- Li, X., Cescotto, S. and Thomas, H. R. (1999). "Finite element method for contaminant transport in unsaturated soils", *Journal of Hydrologic Engineering*, 4(3): 265-274.
- Liang, X., Xu, F., Lin, B., Fan Su, Schramm, K. and Kettrup, A. (2002). "Retention behavior of hydrophobic organic chemicals as a function of temperature in soil leaching column chromatography", *Geosphere*, 49: 569-474.
- Liles, M., Thomas, S. and Sovich, T. (2001). "Saltwater intrusion in orange country, California: planning for the future", *Proceeding of the 1<sup>st</sup> international conference and workshop on saltwater intrusion and coastal aquifers, monitoring, modelling, and management (Morocco)*.
- Lloret, A. and Alonso, E. E. (1980). "Consolidation of unsaturated soils including swelling and collapse behaviour", *Geotechnique*, 30(4): 449-477.
- Liu, F., Turner, I. and Anh, V. (2001). "A finite volume unstructured mesh method for modelling saltwater intrusion into aquifer systems", *Proceeding of the 1<sup>st</sup> international conference and workshop on saltwater intrusion and coastal aquifers, monitoring, modelling, and management (Morocco)*.
- Lopez-Ramirez, J. A., Oviedo M. D., Alonso J. M. (2006). "Comparative studies of reverse osmosis membranes for wastewater reclamation", *Elsevier, Desalination*, 191: 137-147.



- Mahesha, A. (1996a). "Transient Effect of Battery of Injection Wells on Seawater Intrusion", *Journal of Hydraulic Engineering, ASCE*, 122: 266-271.
- Mahesha, A. (1996b). "Steady-State Effect of Freshwater Injection on Seawater Intrusion", *Journal of Irrigation and Drainage Engineering, ASCE*, 122:149-154.
- Mahesha, A. (1996c). "Control of Seawater Intrusion through Injection-Extraction Well System", *Journal of Irrigation and Drainage Engineering, ASCE*, 122: 314-317.
- Maimone, M. and Fitzgerald, R. (2001). "Effective modelling of coastal aquifers systems", *Proceeding of the 1<sup>st</sup> international conference and workshop on saltwater intrusion and coastal aquifers, monitoring, modelling, and management (Morocco)*.
- Maimone, M. (2001). "Computer modelling and surface geophysics unravel the mystery of salt water intrusion in Long Island", *Proceeding of the 1<sup>st</sup> international conference and workshop on saltwater intrusion and coastal aquifers, monitoring, modelling, and management (Morocco)*.
- Marin, L. E., Perry, E.C., Essaid, H. I. and Steinich, B. (2001). "Hydrogeological investigations and numerical simulation of groundwater flow in karstic aquifer of northwestern Yucatan, Mexico", *Proceeding of the 1<sup>st</sup> international conference and workshop on saltwater intrusion and coastal aquifers, monitoring, modelling, and management (Morocco)*.
- Marshall, J. D., Shimada, B. W. and Jaffe, P. R. (2000). "Effect of temporal variability in infiltration on contaminant transport in the unsaturated zone", *Journal of Contaminant Hydrology*, 46: 151–161.
- Maskey, S., Jonoski, A. and Solomatine, D. P. (2002). "Ground water remediation strategy using global optimization algorithms", *Journal of Water Resources planning and Management*, 431- 439.

- Ma Tain, S., Sophocleous, M., Yu, Y. and Buddemeier, R. W. (1997). "Modelling saltwater upconing in a freshwater aquifer south-central Kansas", Elsevier, *Journal of Hydrology*, 201: 120-137.
- Matyas, E. L. and Radhakrishna, H. S. (1968). "Volume change characteristics of partially saturated soils", *Geotechnique*, 18(4): 432-448.
- McCarthy, K. A. and Johnson, R. L. (1993). "Transport of volatile organic compounds across the capillary fringe", *Water Resources Research*, 29(6): 1675-1683.
- McDonald, M. G. and Harbaugh, A. W. (1988). "A modular three-dimensional finite difference groundwater flow model", *Technical report, U.S. Geological Survey Techniques of Water Resources Investigations, Book 6, Chapter A1*.
- McGrail, B. P. (2001). "Inverse reactive transport simulator (INVERTS): an inverse model for contaminant transport with nonlinear adsorption and source terms", *Environmental Modelling and Software*, 16: 711-723.
- Mckinney, D. C. and Lin, M. D. (1994). "Genetic algorithm solution of groundwater management models", *Water Resources Research*, 30(6): 1897-1906.
- Mckinney, D. C. and Lin, M. D. (1995). "Approximate mixed-integer nonlinear programming methods for optimal aquifer remediation design", *Water Resources Research*, 31(3): 731-740.
- Mendoza, C. A. and Frind, E. O. (1990). "Advective dispersive transport of dense organic vapours in the unsaturated zone 1. model development", *Water Resources Research*, 26(3): 379-387.
- Melloul, A. J. and Goldenberg, L. C. (1997). "Monitoring of seawater intrusion in coastal aquifer: basics and local concerns", *Journal of Environmental Management*, 51:73-86.

- Michalewicz, Z. (1992). "Genetic algorithm + data structures = evolutionary programs", *Springer-Verlag, New Yourk, USA*.
- Miller, C. T., Williams, G. A., Kelley, C. T. and Tocci, M. D. (1998). "Robust solution of Richards' equation for non-uniform porous media" *Water Resources Research*, 34(10): 2599-2610.
- Mitchell, J.K. (1976). "Fundamentals of soils behaviour", *John wiley, New York*.
- Moe, H., Hossain, R., Fitzgerald, R., Banna, M., Mushtaha, A. and Yaqubi, A. (2001). "Application of a 3-dimensional coupled flow and transport model in the Gaza strip", *Proceeding of the 1<sup>st</sup> international conference and workshop on saltwater intrusion and coastal aquifers, monitoring, modelling, and management (Morocco)*.
- Moreaux, M. and Reynaud, A. (2001). "Optimal management of a coastal aquifer under saline intrusion", *Proceeding of the 1<sup>st</sup> international conference and workshop on saltwater intrusion and coastal aquifers, monitoring, modelling, and management (Morocco)*.
- Motz, L. H. (2004). "Representing the saltwater-freshwater interface in regional groundwater flow models", *Proceeding of the 18<sup>th</sup> Salt Water Intrusion Meeting, Cartagena (Spain)*.
- Mukhopadhyay, A., Al-Awadi, E., Oskui, R., Hadi, K., Al-Ruwaih, F., Turner, M. and Akber, A. (2004). "Laboratory investigations of compatibility of the Kuwait group aquifer, Kuwait, with possible injection waters", *Journal of Hydrology*, 285: 158-176.
- Mulligan, A. E. and Brown, L. C. (1998). "Genetic algorithm for calibrating water quality models", *Journal of Environmental Engineering*, 124(3): 202-211.

- Mulrennan, M. E. and Woodroffe, C. D. (1998). "Saltwater intrusion into the coastal plains of the lower Mary River, northern Territory, Australia", *Journal of Environmental Management*, 54: 169-188.
- Murphy, L. J., Simpson, A. R. and Dandy, G. C. (1993). "Design of a pipe network using genetic algorithms", *Water*, 20: 40-42.
- Naji, A., Ouazar, D. and Cheng, A. H. D. (1998). "Locating the saltwater-freshwater interface using nonlinear programming and h-adaptive BEM", *Elsevier, Engineering Analysis with Boundary Elements*, 21: 253-259.
- Narayan, K. A., Schleeberger, C., Charlesworth, P. B. and Bristow, K. L. (2002). "Modelling saltwater intrusion in the lower Burdekin Delta north Queensland, Australia", *Denver Annual Meeting, The Geological Society of America (GSA)*.
- Narayan, K. A., Schleeberger, C., Charlesworth, P. B. and Bristow, K. I. (2006). "Effects of groundwater pumping on saltwater intrusion in the lower Burdekin Delta, north Queensland", *CSIRO Land and Water, Davies Laboratory, Townsville, Australia*
- Nowroozi, A. A., Horrocks, S. B. and Henderson, P. (1999). "Saltwater intrusion into the freshwater aquifer in the eastern shore of Virginia: a reconnaissance electrical resistivity survey", *Elsevier, Journal of Applied Geophysics*, 42: 1-22.
- Nwaogazie, I. L. (1986). "Groundwater recharge estimate by numerical modelling; a case study", *Aqua*, 2: 77-80.
- Ofelia, T., Marcela P. and Monica D. (2004). "Salt water vertical upward intrusion due to intensive exploitation. Santa Fe. Argentina", *Proceeding of the 18<sup>th</sup> Salt Water Intrusion Meeting, Cartagena (Spain)*.
- Ogata, A. (1970). "Theory of Dispersion in Granular Medium", *U.S. Geological Survey Professional Paper 411-I*

- Ojeda, C. G., Gallardo, P., Hita, L. G. and Arteaga, L. M. (2004). "Saline interface of the Yucatan peninsula aquifer", *Proceeding of the 18<sup>th</sup> Salt Water Intrusion Meeting, Cartagena (Spain)*.
- Olivera, R. and Loucks, D. P. (1997). "Operating rules for multi-reservoir systems", *Water Resources Research*, 33(4): 839-852.
- Oswald, S. E., Kinzelbach, W. and Johannsen, K. (2001). "Three- dimensional modelling of seawater intrusion into an island aquifer to study water resources management", *Proceeding of the 1<sup>st</sup> international conference and workshop on saltwater intrusion and coastal aquifers, monitoring, modelling, and management (Morocco)*.
- Oude Essink, G. H. P. (1998). "MOC3D adapted to simulate 3-D density-dependant groundwater flow", *proceeding of MODFLOW-98 conference, Golden, Colorado, USA: 291-303*.
- Oude Essink, G. H. P. (2001a). "Salt water intrusion at the island of Texel, the Netherland: a numerical study", *Proceeding of the 1<sup>st</sup> international conference and workshop on saltwater intrusion and coastal aquifers, monitoring, modelling, and management (Morocco)*.
- Oude Essink, G. H. P. (2001b). "Salt water intrusion in the groundwater system of Noord-Holland, the Netherland: a numerical study", *Proceeding of the 1<sup>st</sup> international conference and workshop on saltwater intrusion and coastal aquifers, monitoring, modelling, and management (Morocco)*.
- Oude Essink, G. H. P. (2001c). "Saltwater intrusion in 3D large-scale aquifers: a Dutch case", *Elsevier, Physics and Chemistry of the Earth (B)*, 26: 337-344.
- Oude Essink, G. H. P. and Schaars, F. (2002). "Impact of climate changes on the groundwater system of the water board of the Rijnland, the Netherlands", *Proceeding of the 17<sup>th</sup> Salt Water Intrusion Meeting, Delft, the Netherlands*.

- Pan, L. and Wierenga, P. J. (1997). "Improving numerical modeling of two dimensional water flow in variably saturated, heterogeneous porous media", *Soil Science Society of America Journal*, 61(2): 335-346.
- Pandy, S. (1995). "Mathematical modelling of freshwater-saltwater system: a response to discussion of a density-dependant flow and transport analysis of the effects of groundwater development in a freshwater lens of limited areal extent: the Geneva area (Florida, USA) case study, by Pandey et al. (1993), by Motz (1995 in this issue)", *Elsevier, Journal of contaminant hydrology*, 18: 327-331
- Paniconi, C., Khalaifi, I., Lecca, G., Giacomelli, A. and Tarhouni, J. (2001). "Modelling and analysis of seawater intrusion in the coastal aquifers of eastern Cap-Bon, Tunisia", *Proceeding of the 1<sup>st</sup> international conference and workshop on saltwater intrusion and coastal aquifers, monitoring, modelling, and management (Morocco)*.
- Paniconi, C., Khlaifi, I., Lecca, G., Giacomelli, A. and Tarhouni, J. (2001). "A modelling study of seawater intrusion in the Korba plain, Tunisia", *Elsevier, Physics and Chemistry of the Earth (B)*, 26(4): 345-351.
- Papadopoulou, M. P., Karatzas, G. P., Koukadaki, M. A. AND Trichakis, Y. (2005). "Modelling the saltwater intrusion phenomenon in coastal aquifers – A case study in the industrial zone of Herakleio in Crete", *Global NEST journal*, 7(2):197-203.
- Park, C.-H and Aral, M. M. (2004). "Multi-objective optimization of pumping rates and well placement in coastal aquifers", *Journal of Hydrology*, 290: 80-99.
- Park, N., Kim, S., Shi, L. and Song, S. (2008). "Field validation of simulation-optimization model for protecting excessive pumping wells", *Proceeding of 20<sup>th</sup> SWIM, Naples, Florida, USA*.

- Partington, J. R. (1949). "Advanced treatise on physical chemistry", *vol. 1, Longmans, Green and Co., London.*
- Payne, D. F., Provost, A. M., Voss, C. I. and Clarke, J. S. (2001). "Mechanism of saltwater contamination of ground water in coastal Georgia U.S.A.: preliminary results of variable-density transport modelling", *Proceeding of the 1<sup>st</sup> international conference and workshop on saltwater intrusion and coastal aquifers, monitoring, modelling, and management (Morocco).*
- Payne, D. F. (2010). "Effects of climate change on saltwater intrusion at Hilton HeadIsland, SC. U.S.A. ", *Proceeding of 21<sup>st</sup> SWIM, Azores, Portugal.*
- Phillip, J. R. and de Vries, D. A. (1957). "Moisture movement in porous materials under temperature gradients", *Trans. amer. gephys. Union* 38(2): 222-232.
- Philip, J. R., Knight, J. H. (1991). "Redistribution from plane, line, and point sources", *Irrigation Science*. 12: 169-180.
- Philip, J. R. (1992). "Exact solutions for redistribution by nonlinear convection-diffusion", *Journal of the Australian Mathematical Society, (Series B)* , *Applied Mathematics*, 33: 363– 383.
- Pina, A. L., Gomes, A. M., Melo, M. T. C. and Silva, M .A. M. (2004). "The impact of saltwater intrusion on groundwater quality and the social and economical development of the Santiago island (Cape Verde)", *Proceeding of the 18<sup>th</sup> Salt Water Intrusion Meeting, Cartagena (Spain).*
- Pinder, G. F. and Cooper, H. H. (1970). "A numerical technique for calculating the transient position of the saltwater front", *Water Resources Research*, 6(3): 875-882.
- Pinder, G. F. and Abriola, M. L. (1986). "On the simulation of nonaqueous phase organic compounds in the subsurface", *Water Resources Research*, 22(9): 109-119.

- Pollock, D.W. (1986). "Simulation of fluid and energy transport processes associated with high-level radioactive waste disposal in unsaturated alluvium", *Water Resources Research*, 22(5): 765-775.
- Preece, R. J. (1975). "The measurement and calculation of physical properties of cable bedding sands, Parts 2: specific thermal capacity, thermal conductivity and temperature ratio across air filled pores", *CEGB. Laboratory note No.ED/L/N231/74*.
- Prieto, C., Destouni, G. and Schwarz, J. (2001). "Seawater intrusion in coastal aquifers: effects of seasonal variations in extraction and recharge rates", *Proceeding of the 1<sup>st</sup> international conference and workshop on saltwater intrusion and coastal aquifers, monitoring, modelling, and management (Morocco)*.
- Purnama, A., Al-Barwani, H. H. and Al-Lawatia, M. (2003). "Modelling dispersion of brine waste discharges from a coastal desalination plant", *Elsevier, Desalination*, 155: 41-47.
- PWA/CAMP (2000). "Coastal aquifer management program (CAMP)", *final model report (task 7)*. PWA, Palestine.
- Qahman, K. and Zhou Y. (2001). "Monitoring of seawater intrusion in the Gaza Strip, Palestine", *Proceeding of the 1<sup>st</sup> international conference and workshop on saltwater intrusion and coastal aquifers, monitoring, modelling, and management, Morocco*.
- Qahman, K. and Larabi, A. (2003a). "Identification and modeling of seawater intrusion of the Gaza Strip Aquifer-Palestine", *Proceedings of TIAC03 international conference, Alicante, Spain*, 1: 245-254.
- Qahman, K. and Larabi, A. (2003b). "Simulation of seawater intrusion using SEWAT code in Khan Yunis Area of the Gaza Strip aquifer, Palestine", *Proceedings of JMP2003 international conference, Toulouse, France*.



- Qahman, K. and Larabi, A. (2004). "Three dimensional numerical models of seawater intrusion in Gaza aquifer, Palestine", *Proceeding of the 18<sup>th</sup> Salt Water Intrusion Meeting, Cartagena (Spain)*.
- Qahman, K. (2004). "Aspects of hydrogeology, modeling and management of seawater intrusion for Gaza aquifer - Palestine", *PhD thesis, Laboratory of Identification and modeling of Natural Environment (LIMEN), Ecole Mohammadia d'Ingénieurs (EMI), Rabat-Morocco*.
- Qahman, K. and Larabi, A. (2006). "Evaluation and numerical modeling of seawater intrusion in the Gaza aquifer (Palestine) ", *Hydrology Journal*, 14(5): 713-728.
- Qurtobi, M., Bouchaou, L., IbnMajah, M., Marah, H., Gaye, C. B. and Michelot, J. L. (2004). "Origin of salinity and its impact on fresh ground water resources in the Souss-Massa Basin in the South- west of Morocco: optimisation of isotopic techniques", *Proceeding of the 18<sup>th</sup> Salt Water Intrusion Meeting, Cartagena (Spain)*.
- Ramesh, A. D. (1996). "Modelling the thermo/hydraulic/mechanical behaviour of unsaturated soil using an elasto-plastic constitutive relationship", *PhD Thesis*.
- Rao, K. L. N. and Rao, P. B. (2004). "Salinization of coastal fresh water aquifers of Andhra Pradesh, India", *Proceeding of the 18<sup>th</sup> Salt Water Intrusion Meeting, Cartagena (Spain)*.
- Rao, S. V. N., Asulu, V. S., Bhallamudi, S. M., Thandaaveswara, B. S. and Sudheer, K. P. (2004). "Planning groundwater development in coastal aquifers", *Hydrological Sciences Journal*, 49: 155-170.
- Rastogi, A. K., Choi, G. W. and Ukarande, S. K. (2004). "Diffused interface model to prevent ingress of seawater in multi-layer coastal aquifers", *Journal of Special Hydrology*, 4(2): 1-31.

- Rathfelder, K., Yeh, W.W.G. and Mackay, D. (1991). "Mathematical simulation of soil vapor extraction systems: Model development and numerical examples", *Journal of Contaminant Hydrology*, 8: 263-297.
- Reichard, E., G. and Johnson, T., A. (2005). "Assessment of regional management strategies for controlling seawater intrusion", *Journal of Water Resources Planning and Management*, 131(4): 280-291.
- Remesikova, M. (2005). "Numerical solution of contaminant transport problems with non-equilibrium adsorption in 2D", *Proceeding of the ALGORITMY Conference. Slovak University, Slovak*.
- Rifai, M. N. E., Kaufman, W. J. and Todd, D. K. (1956). "Dispersion Phenomena in Laminar Flow Through Porous Media", *University of California Institute of Engineering, Progress report No. 2*.
- Ritzel, B. J., Eheart, J. W. and Ranjitha S. (1994). "Using genetic algorithms to solve a multiple objective groundwater pollution problem", *Water Resources Research*, 30(5): 1589-1603.
- Rogers, L. L. and Dowla, F. U. (1994). "Optimization of groundwater remediation using artificial neural networks with parallel solute transport modeling", *Water Resources Research*, 30(2): 457-481.
- Rohsenow, W. M. and Chio, H. (1961). "Heat, mass and momentum transfer", *Prentice Hall Inc., New Jersey*.
- Rosenbloom, J., Mock, P. Lawson, P. Brown, J. Turin, H.J. (1993). "Application of VLEACH to vadose zone transport of VOCs at an Arizona Superfund site", *Groundwater Monitoring and Remediation*, 13(3): 159- 169.
- Rouve, G. and Stoessinger, W. (1980). "Simulation of the transient position of the saltwater intrusion in the coastal aquifer near Madras coast", *Proceeding 3<sup>rd</sup>*

*international conference, Finite Element in Water Resources, Univ. of Miss., Oxford, Miss.*

- Ru, Y., Jinno, K., Hosokawa, T. and Nakagawa, K. (2001). "Study on effect of subsurface dam in coastal seawater intrusion", *Proceeding of the 1<sup>st</sup> international conference and workshop on saltwater intrusion and coastal aquifers, monitoring, modelling, and management (Morocco)*.
- Sabi, M. A., Smedt ,F. and Larabi, A. (2001). "A generalized approach for modelling 3D transient free and moving boundaries in coastal aquifers", *Proceeding of the 1<sup>st</sup> international conference and workshop on saltwater intrusion and coastal aquifers, monitoring, modelling, and management (Morocco)*.
- Sadeg ,S. A. and Karahannoglu, N. (2001). "Numerical assessment of seawater intrusion in the Tripoli region, Libya", *Environmental Geology*, 40: 1151-1168.
- Sakr, S. A. (1999). "Validity of a sharp-interface model in a confined coastal aquifer", *Hydrology Journal*, 7: 155-160.
- Sander, G. C. and Braddock, R.D. (2005). "Analytical solutions to the transient, unsaturated transport of water and contaminants through horizontal porous media", *Advances in Water Resources*, 28: 1102-1111.
- Savic, D. A. and Walters, G. A. (1997). "Genetic algorithms for least cost design of water distribution networks", *Journal of Water Resources planning and Management, ASCE*, 123(2): 67-77.
- Sbai, M. A., Larabi, A. and De Smedt, F. (1998). "Modelling saltwater intrusion by a 3-D sharp interface finite element model", *Transactions on Ecology and the Environment*, 17: 1743-3541.
- Scholze, O. Hillmer, G. and Schneider, W. (2002). "Protection of the groundwater resources of Metropolis CEBU (Philippines) in consideration of saltwater

intrusion into the coastal aquifer", *Proceeding of the 17<sup>th</sup> Salt Water Intrusion Meeting, Delft, the Netherlands*.

Segol, G., Pinder, G. F. and Gray, W. G. (1975). "A Galerkin finite element technique for calculating the transition position of the saltwater front", *Water Resources Research*, 11(2): 343-347.

Shahalam, A. M., Al-Harthy, A. and Al-Zawahry, A. (2002). "Feed water pretreatment in RO systems: unit process in the Middle East", *Elsevier, Desalination*, 150:235-245.

Shalabey, M. E. E., Kashyap, D. and Sharma, A. (2006). "Numerical model of saltwater intrusion transport toward a pumping well", *Journal of Hydrologic Engineering (ASCI)*, 11(4): 306-318.

Shamir, U., Bear, J. and Gamliel, A. (1984). "Optimal annual operation of a coastal aquifer", *Water Resources Research*, 20: 435-444.

Sheng, D. and Smith, D. W. (2000). "Numerical modelling of competitive components transport with nonlinear adsorption", *International Journal for Numerical and Analytical Methods in Geomechanics*, 24: 47-71.

Sheng, D. and Smith, D. W. (2002). "2D finite element analysis of multi-component contaminant transport through soils", *International Journal of Geomechanics*, 2(1): 113-134.

Sherif, M. M., Singh, V. P. and Amer, A. M. (1988). "A two-dimensional finite element model for dispersion (2D-FED) in coastal aquifers", *Journal of Hydrological*, 103:11-36.

Sherif, M. M., Singh, V. P. and Amer, A. M. (1990). "A note on saltwater intrusion in coastal aquifers", *Water Resources Management*, 4: 123-134.

- Sherif, M. M. and Singh, V. P. (1999). "Effects of climate change on sea water intrusion in coastal aquifers". *Hydrological Processes Journal*, 13: 1277-1287.
- Sherif, M. M. and Hamza, K. I. (2001). "Mitigation of seawater intrusion by pumping brackish water", *Journal of Transport in Porous Media*, 43(1): 29-44.
- Sherif, M. M and Al-Rashed, M. F. (2001). "Vertical and horizontal simulation of seawater intrusion in the Nile Delta Aquifer", *Proceeding of the 1<sup>st</sup> international conference and workshop on saltwater intrusion and coastal aquifers, monitoring, modelling, and management (Morocco)*.
- Sherif, M., El Mahmoudi, A., Garamoon, H., Kacimov, A., Akram, S., Ebraheem, A. and Shetty A. (2005). "Geoelectrical and hydrogeochemical studies for delineating seawater intrusion in the outlet of Wadi Ham, UAE", *Environmental Geology*.
- Sherif, M. and Kacimov, A. (2008). "Pumping of brackish and saline water in coastal aquifers: an effective tool for alleviation of seawater intrusion", *Proceeding of 20<sup>th</sup> SWIM, Naples, Florida, USA*.
- Sherif, M., Kacimov, A., Ebraheem, A. and AlMulla, M. (2010). "Three-dimensional mapping of seawater intrusion using geophysical methods", *Proceedings of the World Environmental and Water Resources Congress 2010*.
- Simpson, A. R., Dandy, G. C. and Murphy, L. J. (1994). "Genetic algorithm compared with other techniques for pipe optimization", *Journal of Water Resources planning and Management, ASCE*, 120(4): 423-443.
- Sisson, J. B., Ferguson, A. H., Van Genuchten, M. (1980). "Simple method for predicting drainage of field plots", *Soil Science Society of America Journal*, 44: 1147– 1152.

- Sleep, B. E. and Sykes, J. F. (1993). "Compositional simulation of groundwater contamination by organic compounds.1. Model development and verification", *Water Resources Research*, 29(6): 1697-1708.
- Smalley, J. B., Minsker, B. S. and Goldberg, D. E. (2000). "Risk based in-situ bio-remediation design using a noisy genetic algorithm", *Water Resources Research*, 36(10): 3043-3052.
- Smiles, D. E., Philip, J. R., Knight, J. H. and Elrick, D. E. (1978). "Standard Methods for the Examination of Water and Wastewater", *Soil Science Society of America Journal*, 42: 229.
- Smith, D. W., Rowe, R. K and Booker, J. R. (1992). "Contaminant transport and non-equilibrium sorption", *Numerical Models in Geomechanics*, 1: 509-517.
- Snyder, I. K. and Woolhiser, D. A. (1985). "Effect of infiltration on chemical transport into overland flow" *Transactions of the American Society of Agricultural Engineers*, 28: 1450-1457.
- Sonnenborg, T. O., Roosmalen, L. and Hinsby, K. (2010). "Integrated assessment of climate change and sea level rise on the water quality of a coastal lake", *Proceeding of 21<sup>st</sup> SWIM, Azores, Portugal*.
- Sorenson, R. M., Weisman, R. N. and Lennon, G. P. (2001). "Control of erosion, inundation, and salinity intrusion caused by sea level rise". *Chapter 6, Erosion, inundation, and salinity intrusion*.
- Stasa, F. L. (1985). "Applied Finite Element Analysis for Engineers", *Holt, Rinehart and Winstone, Inc., Orlando, USA*.
- Stuyfzand, P. J., Maas, K., Kappelhof, J. and Kooiman, J. W. (2004). "Pumping brackish ground water to prepare drinking water and keep salinized wells fresh", *Proceeding of the 18<sup>th</sup> Salt Water Intrusion Meeting, Cartagena (Spain)*.

- Tasi, W. and Kou, C. (1998). "Numerical analysis of hydrological and geological effects on seawater intrusion", *Transactions on Ecology and the Environment*, 17: 1743-3541.
- Taylor, A., Hulme, P., Hughes, A. and Foot, S. (2001). "Benchmarking of variable density model codes against Henry's problem", *Proceeding of the 1<sup>st</sup> international conference and workshop on saltwater intrusion and coastal aquifers, monitoring, modelling, and management (Morocco)*.
- Teatini, P., Gambolati, G., Gonella, M., Brunone, M., Ferrante, M. and Marconi, S. (2001). "Modelling seawater intrusion in the protorecanati, Italy", *Proceeding of the 1<sup>st</sup> international conference and workshop on saltwater intrusion and coastal aquifers, monitoring, modelling, and management (Morocco)*.
- Theis, C.V. (1935). "The relationship between lowering of the piezometric surface and the rate and duration of discharge of a well using groundwater storage", *Transactions, American Geophysical Union*, 2: 519-524.
- Thomas, H. R. and Ferguson, W. J. (1999). "A fully coupled heat and mass transfer model incorporating contaminant gas transfer in an unsaturated porous medium", *Computers and Geotechnics*, 24: 65-87.
- Thomas, S. D., Liles, J. M. and Johnson, T. A. (2001). "Managing seawater intrusion in the Dominguez gap area of Los Angeles country, California, USA", *Proceeding of the 1<sup>st</sup> international conference and workshop on saltwater intrusion and coastal aquifers, monitoring, modelling, and management (Morocco)*.
- Tiruneh, N. D. and Motz, L. H. (2004). "Three dimensional modelling of saltwater intrusion coupled with the impact of climate changes and pumping", *Proceeding of World Water Congress*.
- Tocci, M. D., Kelley, C. T. and Miller, C. T. (1997). "Accurate and economical solution of the pressure-head form of Richards' equation by the method of lines. ", *Advances in Water Resources*, 20(1): 1-14.

- Todd, D. K. (1974). "Salt-water intrusion and its control", *Water technology/ resources. Journal of American Water Works Association*, 66(3): 180-187.
- Tompson, A., Davisson, M., Maxwell, R., Hudson, G., Welty, C., Carle, S. and Rosenberg, N. (2001). "On the fate of artificial recharge in a coastal aquifer", *Proceeding of the 1<sup>st</sup> international conference and workshop on saltwater intrusion and coastal aquifers, monitoring, modelling, and management (Morocco)*.
- Tracy, N. (1998). "Water-resources optimization model for Santa Barbara, California", *Journal of Water Resources Planning and Management*, 124(5): 129-139.
- Tsutsumi, A., Jinno, K. and Oheda, Y. (2001). "Changes in fresh and saltwater movement in a coastal aquifer by land surface alteration", *Proceeding of the 1<sup>st</sup> international conference and workshop on saltwater intrusion and coastal aquifers, monitoring, modelling, and management (Morocco)*.
- Tulipano, L. and Fidelibus, M. D. (2002). "Mechanisms of groundwater salinization in a coastal Karstic aquifer subject to over exploitation", *Proceeding of the 17<sup>th</sup> Salt Water Intrusion Meeting, Delft, the Netherlands*.
- Vallejos, A., Pulido, B. A. and Gisbert, A. y. (2004). "Monitoring saltwater intrusion in a Karstic aquifer", *Proceeding of the 18<sup>th</sup> Salt Water Intrusion Meeting, Cartagena (Spain)*.
- Vandenbohede, A., Lebbe L. and Houtte, E. V. (2008). "Artificial Recharge of Fresh Water in the Belgian Coastal Dunes", *Proceeding of 20<sup>th</sup> SWIM, Naples, Florida, USA*.
- Van Genuchten, M. T. (1980). "A closed-form equation for predicting the hydraulic conductivity of unsaturated soils", *Soil Science Society of America Journal*, 44: 892-898.



- Van Meir, N., Jaeggi, D., Herfort, M., Low, S., Lods, G., Pezard, Ph. and Gouze, Ph. (2004). "Development of a test site for the investigation of saltwater intrusion process in a karstified limestone aquifer (Campos Mallorca, Spain)", *Proceeding of the 18<sup>th</sup> Salt Water Intrusion Meeting, Cartagena (Spain)*.
- Vazquez, S. E., Abarca, E., Capino, B., Casamitjana, A., Gamez, D. and Carrera, J. (2004). "Groundwater flow and saltwater intrusion modelling of the low valley and Llobregat delta aquifer", *Proceeding of the 18<sup>th</sup> Salt Water Intrusion Meeting, Cartagena (Spain)*.
- Voss, C. I. (1984). "SUTRA, a finite element simulation for saturated-unsaturated fluid density-dependant groundwater flow with energy transport or chemically reactive single species solute transport", *U.S.G.S. Water-Resources Investigations Report 84:4369:409*.
- Voss, C.I. and Provost, A. M. (2001). "Three- dimensional simulation of variable-density flow and seawater intrusion using the USGS Sutra code and SutraSuite", *Proceeding of the 1<sup>st</sup> international conference and workshop on saltwater intrusion and coastal aquifers, monitoring, modelling, and management (Morocco)*.
- Voss, C. I. and Provost, A. M. (2003). "SUTRA: A model for saturated-unsaturated, variable-density ground-water flow with solute or energy transport", *U.S. Geological Survey Water-Resources Investigations Report 84-4369*
- Voudouris, K., Mandilaras, D. and Antoakos, A. (2004). "Methods to define the surface distribution of the salt intrusion zone", *Proceeding of the 18<sup>th</sup> Salt Water Intrusion Meeting, Cartagena (Spain)*.
- Wallach, R., Jury, W. A., Spencer, W. F. (1989). "The concept of convective mass transfer for prediction of surface runoff pollution by soil surface applied chemicals" *Transactions of the American Society of Agricultural Engineers*, 32: 906-912.

- Wallach, R. and Shabtai, R. (1992). "Surface runoff contamination by soil chemicals: simulations for equilibrium and first order kinetics", *Water Resources Research*, 28: 167-173.
- Wang, H. F. and Anderson, M. P. (1982). "Introduction to groundwater modeling, finite difference and finite element methods", *W. H. Freeman and company, San Francisco, USA*.
- Wang, Q. J. (1987). "The genetic algorithm and its application to calibration of conceptual rainfall-runoff models", *Water Resources Research*, 27(9):2467-2471.
- Ward, D. S. (1991). "Data input for SWIFT/386, version 2.5", *Geotrans Technical Report, Sterling, Va*.
- Ward, D. S. and Benegar (1998). "Data input guide for SWIFT-98, version 2.57", *HIS Geotrans, Inc., Sterling, Va*.
- Wardlaw, R. and Sharif, M. (1999). "Evaluation of genetic algorithms for optimal reservoir system operation", *Journal of Water Resources planning and Management, ASCE*, 251(1): 25-33.
- Warrick, A. W., Lomen, D. O. and Islas, A. (1990). "An analytical solution to Richards, equation for a draining soil profile", *Water Resources Research*. 26: 253-258.
- Watson, K. K. and Jones, M. J. (1981). "Estimation of hydrodynamic dispersion in a fine sand using a approximate analytical solution", *Australian Journal of Soil Research*, 19: 265-273.
- Weeks, E. P., Douglas E. E. and Glenn M. T. (1982). "Use of atmospheric fluorocarbons F-11 and F-12 to determine the diffusion parameters of the unsaturated zone in the southern high plains of Texas", *Water Resources Research*, 18(5): 1365-1378.

- Williams, G. A. and Miller, C. T. (1999). "An evaluation of temporally adaptive transformation approaches for solving Richards' equation", *Advances in Water Resources*, 22(8): 831-840.
- Willis, R. and Finney, B. A. (1988). "Planning model for optimal control of saltwater intrusion", *Journal of Water Resources planning and Management*, 114:333-347.
- Willert, T., Behain, D., Fulda, C. and Kessels, W. (2001). "Regional saltwater distribution in the coastal aquifer test field (CAT-Field) between Bermerhaven and Cuxhaven, Germany, by DC-geoelectric measurements", *Proceeding of the 1<sup>st</sup> international conference and workshop on saltwater intrusion and coastal aquifers, monitoring, modelling, and management (Morocco)*.
- Wilson, J. L., Gelhar, L.W. (1981). "Analysis of longitudinal dispersion in unsaturated flow 1. The analytical method", *Water Resources Research*. 17: 122-130.
- Worch, E. (2004). "Modelling the solute transport under non-equilibrium conditions on the basis of mass transfer equations", *Journal of Contaminant Hydrology*, 68: 97-120.
- Yakirevich, A., Melloul A., Sorek S. and Shaat S. (1998). "Simulation of seawater intrusion into the Khan Yunis Area of the Gaza Strip coastal aquifer", *Hydrology Journal*, 6:549-559.
- Zhang, X. and Ewen, J. (2000). "Efficient method for simulating gravity-dominated water flow in unsaturated soils", *Water Resources Research*, 36(9): 2777- 2780.
- Zhang, Z. (2002). "The alternating-direction schemes and numerical analysis for the three-dimensional seawater intrusion simulation", *Acta Mathematicae Applicatae Sinica, English Series*, 18(3): 389-404.

- Zhang, X., Bengough, A. G., Crawford, J. W. and Young, I. M. (2002). "Efficient methods for solving water flow in variably saturated soils under prescribed flux infiltration", *Journal of Hydrology*, 260: 75-87.
- Zhang, Z. and Brusseau, M. L. (2004). "Nonideal transport of reactive contaminants in heterogeneous porous media: 7. distributed-domain model incorporating immiscible-liquid dissolution and rate-limited sorption/desorption", *Journal of Contaminant Hydrology*, 74: 83–103.
- Zheng, C. and Wang, P. P. (1999). "MT3DMS, a modular three-dimensional multi-species transport model for advection, dispersion and chemical reactions of contamination and user's guide", *US. AERDCC, Report SERDP-99-1*.
- Zheng, C. and Wang P. P. (2001). "A field demonstration of a simulation-optimization approach for remediation system design", *Ground Water*.
- Zheng, C. and Bennett, G.D. (2002). "Applied Contaminant Transport Modelling", *Second edition, John Wiley and Sons, Inc., New York, USA*.
- Zhou, X., Chen, M., Liang, C. (2003). "Optimal schemes of groundwater exploitation for prevention of seawater intrusion in the Leizhou Peninsula in southern China", *Environmental geology*, 43: 978-985.
- Zhou, Y. and Rowe, R. K. (2005). "Modelling of Clay Liner Desiccation", *International Journal of Geomechanics*, 5(1): 1-9.
- Zienkiewicz, O. C. and Cheung, Y. K. (1965). "Finite elements in the solution of field problems", *Engineer*, 220: 507–510.
- Zubari, W. K. (1999). "The Dammam aquifer in Bahrain- hydrochemical characterization and alternatives for management of groundwater quality", *Hydrology Journal*, 7: 197-208.